



UNIVERSITY OF
KWAZULU-NATAL

INYUVESI
YAKWAZULU-NATALI

**The role of *Mycobacterium tuberculosis*
curli pili (MTP) and heparin-binding
hemagglutinin adhesin (HBHA) on global
in vitro bacterial transcriptomics**

TARIEN JAEL NAIDOO

**Submitted in fulfilment of the requirements for the degree of
Masters in Medical Science (Medical Microbiology)**

**Discipline of Medical Microbiology
School of Laboratory Medicine and Medical Sciences
College of Health Sciences
University of Kwa-Zulu- Natal
South Africa**

2021

MANUSCRIPT AND PLAGIARISM DECLARATION

This Masters Dissertation consists of 1 manuscript that is ready for submission. Author contributions are stipulated below.

Manuscript 1: Naidoo T, J., Senzani, S., Ravesh Singh., Pillay, B., and Pillay, M. Global transcriptomics reveals major perturbations in central carbon metabolism, cell wall biosynthesis and processes, lipid biosynthesis and virulence in the absence of *M. tuberculosis* curli pili (MTP) and heparin-binding hemagglutinin adhesin (HBHA).

Author contribution: MP conceptualized the study. MP and BP designed the study. TJN conducted experiments, analysed the data and drafted the manuscript. SS provided guidance on bioinformatics and analytical support. RS provided guidance on RT-qPCR and analytical support. All authors contributed to and approved the manuscript.

I, Tarien Jael Naidoo, declare that the work presented in this dissertation has not been submitted to the University of Kwa-Zulu- Natal or any other university for the obtainment of an academic qualification. Any work performed by individuals other than myself has been duly acknowledged and referenced in this dissertation.



Tarien Jael Naidoo

16 June 2021
Date

As the candidate's supervisor, and co-supervisor, we agree with all aspects of this Master's submission.



Supervisor: Professor Manormoney Pillay

16 June 2021
Date



Co-supervisor: Professor Balakrishna Pillay

16 June 2021
Date

PRESENTATIONS

Poster presentation

School of Laboratory Medicine and Medical Sciences Research Day, Durban, South Africa.

18 September 2020

The role of *Mycobacterium tuberculosis* curli pili (MTP) and heparin-binding hemagglutinin adhesin (HBHA) on global *in vitro* bacterial transcriptomics.

Oral presentation

The South African Society for Microbiology (SASM) Conference 2021, Virtual Conference, The Interacting Microbe.

5 May 2021.

Global transcriptomics reveals major perturbations in central carbon metabolism, cell wall biosynthesis and processes, and virulence in the absence of *Mycobacterium tuberculosis* curli pili (MTP) and heparin-binding haemagglutinin adhesin (HBHA).

DEDICATION

To my beloved parents, Chevin and Mauline Naidoo.

ACKNOWLEDGEMENTS

“I can do all things through Christ who strengthens me”, Philippians 4:13.

I would like to thank my Lord and Saviour Jesus Christ, for being my strength and guidance always.

I would like to sincerely thank my supervisor, Professor Manormoney Pillay for her guidance, continuous motivation, patience and scientific contributions throughout my masters degree. You inspired me to pursue this degree and I am truly grateful for your support and guidance. I would also like to thank my co-supervisor, Professor Balakrishna Pillay, for his advice, scientific input and support.

I would like to acknowledge the project funding provided by the National Research Foundation (Grantholder-linked and DST-NRF Innovation Masters Bursary) and the UKZN College of Health Sciences.

To my colleagues and mentors at Medical Microbiology, thank you for sharing your scientific knowledge and assisting with my training. A special thank you goes out to Dr Sibusiso Senzani, Dr Dhaneshree Bestinee Naidoo, Dr Nontobeko Eunice Mvubu, Deepika Moti, Tashmin Rampersad and Koobashnee Pillay.

Thank you to Kajal Soulakshana Reedoy and Jenine Ramruthan, for being a rock throughout this journey. I am truly grateful for your friendship. A wholehearted thank you goes out to Kynesha Moopnar, I will always be grateful for your constant support, encouragement, advice, and friendship. A special thank you to Maureen and Shinese Ashokcoomar, for your unwavering support, encouragement, friendship, and kindness. Shinese, you have been invaluable in my professional growth. Thank you for being my anchor.

Lastly and most importantly, I would like to thank my family. My beloved parents, Chevin and Mauline Naidoo, for their continuous love, support, and encouragement to follow my dreams. Dada, you have imparted knowledge, equipped me with valued life skills and pushed me to excel. Thank you for all you do, always. Mum, your prayers, advice, faith and never-ending love has enabled me to become the God-fearing strong woman I am today. I am eternally grateful to have parents who have fostered me with so much love and support. A special thank you to my brothers, Chevin Jeron Naidoo, Bryce Callen Naidoo and Chaka Naidoo, for dealing with me throughout this journey. You have made my life immeasurably better, thank you. My

aunt and her husband, Elaine and Pranesh Bhudu, and my uncle and his wife, Rennie and Seama Govender, your constant support, love, and kindness holds no bounds. I am eternally grateful for you. My grandmothers, Sylvie Naidoo and Joyce Govender, having such strong, tenacious, loving, and God-fearing women has inspired me to soar higher. My grandfathers, Samson Naidoo and Narian Govender, thank you for your encouragement, love, prayers, and continued support.

TABLE OF CONTENTS

MANUSCRIPT AND PLAGIARISM DECLARATION	i
PRESENTATIONS.....	ii
DEDICATION.....	iii
ACKNOWLEDGEMENTS.....	iv
TABLE OF CONTENTS.....	vi
LIST OF TABLES.....	ix
LIST OF FIGURES	x
LIST OF ABBREVIATIONS.....	xii
ABSTRACT.....	xvii
Introduction.....	xix
Chapter 1: Literature Review.....	1
1.1 Epidemiology of tuberculosis.....	1
1.2 Drug resistance.....	2
1.3 Characteristics of <i>Mycobacterium tuberculosis</i>	3
1.3.1 <i>Mycobacterium tuberculosis</i> cell envelope.....	4
1.4 Pathogenesis of <i>Mycobacterium tuberculosis</i>	5
1.5 Current status of tuberculosis diagnosis.....	7
1.6 Vaccine development	10
1.7 Current antibiotic treatment of tuberculosis.....	12
1.8 Biomarkers	14
1.8.1 Tuberculosis biomarkers	15
1.9 <i>Mycobacterium tuberculosis</i> adhesins	17
1.9.1 Heparin-binding hemagglutinin adhesin	22
1.9.2 <i>Mycobacterium tuberculosis</i> curli pili	24
1.10 The ‘Omics’ approach to better understand <i>Mycobacterium tuberculosis</i>	26
1.10.1 Whole genomics.....	26
1.10.2 Transcriptomics.....	27
1.10.2.1 Global transcriptomics enhances current knowledge on MTP and HBHA	28
1.10.3 Metabolomics.....	29
1.11 Significance of study	31
1.12. Research design	31
1.12.1 Aim	31
1.12.2 Objectives	31

1.13	References	32
CHAPTER 2: Global transcriptomics reveals major perturbations in central carbon metabolism, cell wall biosynthesis and processes and virulence in the absence of <i>M. tuberculosis</i> curli pili (MTP) and heparin-binding hemagglutinin adhesin (HBHA).....		
2.1	Abstract	48
2.2	Introduction	49
2.3	Materials and methods	49
2.3.1	Ethics Approval	49
2.3.2	Bacterial isolates and growth conditions	49
2.3.3	RNA isolation and sequencing.....	53
2.3.4	Read alignment and transcript assembly.....	55
2.3.5	Enrichment and statistical analysis	55
2.3.6	Real-time quantitative polymerase chain reaction (RT-qPCR) as a functional assay.....	56
2.3.7	Statistical analysis.....	57
2.3.8	Determination of bacterial bioluminescence	58
2.4	Results	58
2.4.1	Differential expression of genes induced by the deletion of MTP and HBHA.....	58
2.4.1.1	Functional categorisation of significantly up-regulated and down-regulated genes.....	60
2.4.2	Alterations in central carbon metabolism, ATP synthase, cell wall and cell processes in the absence of MTP and HBHA.....	59
2.4.3	Alterations in differential gene expression of ATP synthase.....	62
2.4.4	Alterations in the cell wall and cell wall processes	66
2.4.5	Gene expression analysis of functional RT-qPCR performed on selected genes	68
2.4.5.1	Comparison of gene expression differences between RNA sequencing and RT-qPCR.....	73
2.4.6	Luciferase assay phenotypically confirms increased ATP utilization or lower ATP production in the absence of MTP and HBHA	78
2.5	Discussion	77
2.5.1	The role of MTP and HBHA in cell wall biosynthesis.....	78
2.5.2	MTP and HBHA modulate energy production in <i>M. tuberculosis</i> by regulating central carbon metabolism.....	79
2.5.2.1	MTP and HBHA influence gluconeogenesis/glycolysis pathways linked to the TCA cycle	79
2.5.2.2	MTP influences the citric acid cycle.....	81

2.5.2.3	MTP and HBHA modulate ATP synthesis via the oxidative phosphorylation pathway.....	85
2.5.3	The role of MTP and HBHA in transport across the cell wall and cell membrane	88
2.5.4	The regulatory role of MTP and HBHA	89
2.5.4.1	The regulatory role of MTP in molybdenum cofactor biosynthesis	89
2.5.4.2	The role of HBHA in copper and iron regulation	90
2.5.4.3	The role of MTP-HBHA in regulation of DevR-DevS	90
2.5.4.4	The role of MTP-HBHA in regulation of insertion sequence element IS6110.....	88
2.5.5	The role of MTP and HBHA in virulence	89
2.6	Conclusion.....	94
2.7	References	95
Chapter 3:	Synthesis of research findings, conclusions, and recommendations.....	106
3.1	MTP and HBHA influence central carbon metabolism (CCM) and the tricarboxylic acid (TCA) cycle in <i>Mycobacterium tuberculosis</i>	107
3.2	MTP and HBHA play a role in regulation of ATP synthesis in <i>Mycobacterium tuberculosis</i>	108
3.3	MTP influences cell wall biosynthesis in <i>Mycobacterium tuberculosis</i>	108
3.4	MTP and HBHA influence transport across the cell wall and cell membrane	109
3.5	MTP and HBHA play a role in transport and regulation	109
3.6	MTP and HBHA influence virulence.....	110
3.7.	Conclusion.....	110
3.8.	Limitations	111
3.9.	Recommendations for future research.....	111
3.10	References	1121
APPENDICES	1154
Appendix A:	BREC Approval.....	1154
Appendix B:	Media, solutions and reagents.....	1165
Appendix C:	Chapter 2 Supplementary Material.....	1187
C1.	PCR confirmation of bacterial strains.....	118
C2.	Bioinformatic Analysis	126
C3.	Real time quantitative PCR (RT-qPCR) raw data	156
C4.	ATP synthase genes used in a comparison of RNA sequencing to RT-qPCR	177
C5.	Bioluminescence raw data	178
Appendix D:	Turnitin Reports.....	179

LIST OF TABLES

Table 1.1. Currently known <i>Mycobacterium tuberculosis</i> adhesins	20-21
Table 2.1. Bacterial strains used in this study	52
Table 2.2. Gene and primer sequences selected for analysis of gene expression using RT-qPCR.....	57
Table 2.3. The statistically significant up-regulated genes induced by the three <i>M. tuberculosis</i> deletion mutants relative to the WT.	59
Table 2.4. The statistically significant down-regulated genes induced by the three <i>M. tuberculosis</i> deletion mutants relative to the WT.	60

LIST OF FIGURES

Figure 1.1. Estimated global incidence rates of TB in 2019.....	2
Figure 1.2. The cell wall structure of <i>M. tuberculosis</i>	5
Figure 1.3. Active and latent <i>M. tuberculosis</i> infection.....	6
Figure 1.4. An illustration depicting the role of <i>M. tuberculosis</i> associated adhesins in host infection	19
Figure 1.5. Selected mycobacterial adhesins and the various pathways that are available for initiating host interaction and subsequent colonization	19
Figure 1.6. HBHA-mediated aggregation of <i>M. tuberculosis</i>	233
Figure 2.1. Transcriptomic analysis revealed alterations in central carbon metabolism	63
Figure 2.2. Transcriptomic analysis revealed alterations in L-valine and L-isoleucine biosynthesis.....	64
Figure 2.3. Cytochrome c oxidase and ATP synthase involved in Complex IV and V during oxidative phosphorylation.....	66
Figure 2.4. Transcriptomic analysis revealed alterations in gene regulation of cell wall maintenance, transport proteins and probable adhesion components.....	68
Figure 2.5a. Real-time quantitative PCR to assess gene expression of 5 ATP synthase genes (<i>atpB</i> , <i>atpD</i> , <i>atpE</i> , <i>atpF</i> and <i>atpH</i>) in the WT, Δmtp and <i>mtp</i> -complement strains.. ..	70
Figure 2.5b. Real-time quantitative PCR to assess gene expression of 4 genes: adhesion molecules and ABC transporters (<i>secE2</i> , <i>Rv0986</i> and <i>Rv0987</i>), and lipoprotein (<i>lpqV</i>) in the WT, Δmtp and <i>mtp</i> -complement strains.....	71
Figure 2.6a. Real-time quantitative PCR to assess gene expression of 5 ATP synthase genes (<i>atpB</i> , <i>atpD</i> , <i>atpE</i> , <i>atpF</i> and <i>atpH</i>) in the WT, $\Delta hbhA$ and <i>hbhA</i> -complement strains.....	72
Figure 2.6b. Real-time quantitative PCR to assess gene expression of 4 genes: adhesion molecules and ABC transporters (<i>secE2</i> , <i>Rv0986</i> and <i>Rv0987</i>), and lipoprotein (<i>lpqV</i>) in the WT, $\Delta hbhA$ and <i>hbhA</i> -complement strains.....	73
Figure 2.7a. Real-time quantitative PCR to assess gene expression of 5 ATP synthase genes (<i>atpB</i> , <i>atpD</i> , <i>atpE</i> , <i>atpF</i> and <i>atpH</i>) in the WT, $\Delta mtp-hbhA$ and <i>mtp-hbhA</i> -complement strains.	74
Figure 2.7b. Real-time quantitative PCR to assess gene expression of 4 genes: adhesion molecules and ABC transporters (<i>secE2</i> , <i>Rv0986</i> and <i>Rv0987</i>), and lipoprotein (<i>lpqV</i>) in the WT, $\Delta mtp-hbhA$ and <i>mtp-hbhA</i> -complement strains.	75

Figure 2.8. Comparison of RNA sequencing data and RT-qPCR for ATP synthase (*atpB*, *atpD*, *atpE*, *atpF*, *atpH*).77

Figure 2.9. Bioluminescence assay depicting lower ATP levels in Δmtp , $\Delta hbhA$, $\Delta mtp-hbhA$ in comparison to *M. tuberculosis* V9124 WT.....79

LIST OF ABBREVIATIONS

<u>Abbreviation</u>	<u>Full name</u>
ABC	Adenosine triphosphate-binding cassette
Ad	Adenovirus
ADP	Adenosine di-phosphate
AEC	Alveolar epithelial cells
AES	Allelic exchange substrate
Ag	Antigen
Ag85A	Antigen 85A
AGP	Arabinogalactan complex
AIDS	Acquired Immunodeficiency Syndrome
AMP	Adenosine monophosphate
Apa	Alanine-proline rich antigen
ATP	Adenosine triphosphate
BAM	Binary alignment files
BCG	Bacillus Calmette-Guérin
BDQ	Bedaquiline
°C	Degrees Celsius
CCM	Central carbon metabolism
cDNA	Complementary deoxyribonucleic acid
CFU	Colony forming unit
CFP	Culture filtrate protein
CFZ	Clofazimine
CI	Confidence interval
CO ₂	Carbon dioxide
Cpn	Chaperone protein
Cpn60.2	Chaperone protein 60.2
DEPC	Diethyl pyrocarbonate
DLM	Delamanid

DNA	Deoxyribonucleic acid
ECM	Extracellular matrix
EMB	Ethambutol
ESAT	Early secreted antigenic target
FBS	Fetal bovine serum
FC	Fold change
FPKM	Fragments Per Kilobase of Transcript per Million
g	G-Force/ Relative Centrifugal Force
GC	Gas chromatography
GCxGC-TOFMS	Two-dimensional gas chromatography time-of-flight mass spectrometry
G3P	Glycerol-3-phosphate
G6P/F6P	Glucose-6-phosphate/fructose-6-phosphate
GTC	Guanidine thiocyanate
GTF	Gene Transfer Format
HBHA	Heparin-binding hemagglutinin adhesin
$\Delta hbhA$	<i>hbhA</i> -knockout mutant
<i>hbhA</i> -complement	Complemented heparin-binding hemagglutinin adhesin -knockout strain
HISAT	Hierarchical Indexing for Spliced Alignment of Transcripts
HIV	Human Immunodeficiency Virus
HLA	Human leukocyte antigen
hMDM	Human monocyte-derived macrophages
Hrs	Hours
Hz	Hertz
HygR	Hygromycin-resistance
I3PS	Inositol-3-phosphate synthase
INF	Interferon
IFN- γ	Interferon gamma
Ig	Immunoglobulin
IgG	Immunoglobulin G

IGRA	IFN- γ release assay
IL	Interleukin
IM	Inner/plasma membrane
IMP	Inosine monophosphate
INH	Isoniazid
IPP	Isopentenyl diphosphate
kDa	Kilo Dalton
KEGG	Kyoto Encyclopedia of Genes and Genome
KZN	Kwa-Zulu- Natal
LAM	Lipoarabinomannan
LEFX	Levofloxacin
LJ	Lowenstein-Jensen medium
LTBI	Latent tuberculosis infection
LZD	Linezolid
MOPS	3-(N-morpholino) propane sulfonic acid
mAGP	Mycolic acid-arabinogalactan-peptidoglycan
ManLAM	Mannosylated lipoarabinomannan
Mce	Mammalian cell entry
MDR	Multidrug-resistant
MXF	Moxifloxacin
Mg ²⁺	Magnesium ions
MHC	Major histocompatibility complex
min	Minutes
mL	Millilitre
mm	Millimetre
MOI	Multiplicity of infection
MS	Mass spectrometry
<i>M. tuberculosis</i>	<i>Mycobacterium tuberculosis</i>
MTBC	<i>Mycobacterium tuberculosis</i> complex
MTP	<i>Mycobacterium tuberculosis</i> curli pili

Δmtp	<i>Mycobacterium tuberculosis curli pili</i> -knockout mutant
<i>mtp</i> -complement	Complemented <i>Mycobacterium tuberculosis curli pili</i> -knockout strain
$\Delta mtp-hbhA$	<i>Mycobacterium tuberculosis curli pili</i> -heparin binding hemagglutinin adhesin-knockout mutant
<i>mtp-hbhA</i> -complement	Complemented <i>Mycobacterium tuberculosis curli pili</i> -heparin binding hemagglutinin adhesin-knockout strain
NAD	Nicotinamide adenine dinucleotide
NADP	Nicotinamide adenine dinucleotide phosphate
NADPH	Nicotinamide adenine dinucleotide phosphate (reduced form)
Nm	Nanometres
NTM	Nontuberculous mycobacteria
OADC	Oleic acid-albumin-dextrose-catalase
OD	Optical density
OPP	Oxidative phosphorylation pathway
PBS	Phosphate buffered saline
PCR	Polymerase chain reaction
PDIM	Phthiocerol dimycocerosates
PE_PGRS	Protein family characterized by Proline-Glutamic Acid motif (PE) Polymorphic guanine-cytosine-rich repetitive sequence (PGRS)
PEP	Phosphoenolpyruvate
PGL	Phenolic glycolipids
POC	Point of care
PPP	Pentose phosphate pathway
PSP-A	Pulmonary surfactant protein- A
PZA	Pyrazinamide
QC	Quality control
RIF	Rifampicin
RNI	Reactive nitrogen intermediates
RNA	Ribonucleic acid
RNOS	Reactive nitrogen and oxygen species

ROI	Reactive oxygen intermediates
rpm	Rotations per minute
RR	Rifampicin resistant
RT-qPCR	Real time reverse transcription quantitative polymerase chain reaction
s	Second
SA	South Africa
TA	Toxin-antitoxin
TB	Tuberculosis
TCA	Tricarboxylic acid
TDR	Total drug-resistant
TLR	Toll-like receptor
TNF- α	Tumour necrosis factor alpha
TST	Tuberculin skin test
μ L	Microlitre
μ m	Micrometre
V	Volts
VAP	Virulence associated proteins
v/v	Volume/ volume
WHO	World Health Organization
WT	Wild-type
XDR	Extensively drug-resistant

ABSTRACT

Background/Aim: Tuberculosis (TB), is an infectious, airborne disease caused by *Mycobacterium tuberculosis* (*M. tuberculosis*). TB remains one of the most devastating bacterial causes of human mortality, especially in low-income countries. Surface located adhesins are crucial for *M. tuberculosis* survival, as they initiate and perpetuate host-pathogen interactions. The adhesin, *M. tuberculosis* curli pili (MTP), plays a role in adhesion and invasion of host cells and biofilm formation, whilst heparin-binding hemagglutinin adhesin (HBHA) promotes *M. tuberculosis* dissemination from the site of infection. The use of transcriptomics promises to enhance current knowledge on MTP and HBHA as virulence factors, thereby substantiating their role as biomarkers for the development of accurate TB diagnostics and therapeutics. Therefore, this study aimed to elucidate the role of MTP and HBHA in the regulation of *M. tuberculosis* transcriptome, and to identify novel biomarkers. This was achieved by analysing the transcriptomic perturbations in the strains lacking the MTP adhesin, HBHA adhesin or both MTP-HBHA adhesins and the strains containing the aforementioned adhesins.

Methods: Polymerase chain reaction (PCR) confirmed strains of *M. tuberculosis* wild-type (WT), *mtp*-deletion mutant (Δmtp), *hbhA*-deletion mutant ($\Delta hbhA$), *mtp-hbhA*-deletion mutant ($\Delta mtp-hbhA$), and the respective complemented strains, were standardized and cultured until log phase. Thereafter, the bacterial cultures were prepared for RNA extraction. RNA was extracted via an optimized TRIzol method and sequenced using the Illumina 2×150 HiSeq ×10 platform. The sequenced reads were analysed by FastQC toolkit (version 0.11.8), pre-processed using Trimmomatic (version 0.36), mapped to the custom-built *M. tuberculosis* H37Rv genome index using hierarchical indexing for spliced alignment of transcripts (HISAT version 2.1.0), assembled by Stringtie (version 1.2.1), and further annotated and assembled the transcripts into known and novel categories by Gffcompare, located within Stringtie. The output files were annotated in R (version 1.2.1578) using the Ballgown package to generate the respective fold changes (FC) between the deletion mutants and the WT, and *q*-values and *p*-values for the differential expression. The generated results were filtered using a FC cut-off value ≥ 1.3 (to indicate a 1.3-fold up-regulation) and ≤ 0.5 (to indicate a 2-fold down-regulation) to identify significant genes and pathways. Thereafter, relevant databases and literature were reviewed to categorize the genes into pathways. Real time quantitative PCR (RT-qPCR) was performed on 10 selected genes, as a genotypic method to functionally confirm

the RNA sequencing data. A bacterial bioluminescence cell viability assay was performed to elucidate the concentration of adenosine triphosphate (ATP) in the deletion mutants and complements, relative to the WT.

Results: A total of 43 genes were significantly differentially expressed amongst the deletion mutants. These genes were functionally categorized into: intermediary metabolism and respiration metabolism, cell wall biosynthesis, cell wall transport and processes, lipid metabolism, and virulence; stable RNA's; conserved hypotheticals; proline-glutamate (PE) or proline-proline-glutamate (PPE); insertion sequences and phages; and information pathways. The bioluminescence assay functionally confirmed the increased utilization of ATP in the absence of MTP and HBHA.

Discussion/Conclusion: Adhesin gene deletions caused major perturbations to the central carbon metabolism, cell wall biosynthesis, cell transport process, lipid biosynthesis, and virulence pathways, leading to potentially increased energy requirements; compensatory transport of proteins to the cell wall, altered cell wall biosynthesis and decreased virulence and pathogenicity. Additionally, deletion of these adhesins resulted in the disruption of many processes potentially attenuating growth and replication. Thus, this study further corroborates the adhesins, MTP and HBHA, and associated pathway genes as potential suitable targets for TB diagnostic/therapeutic interventions.

Introduction

Tuberculosis (TB), formerly known as “consumption”, is an infectious, airborne disease caused by *Mycobacterium tuberculosis* (*M. tuberculosis*). TB remains one of the most devastating bacterial causes of human morbidity and mortality, particularly in low-income and middle-income countries (Fogel, 2015, Pai et al., 2016). It is acquired by the inhalation of infectious aerosol particles that are released in close proximity to another individual (Comas et al., 2009, Cruz-Knight and Blake-Gumbs, 2013). In most instances, individuals who inhale the bacteria mount an effective immune response in the lungs, leading to successful inhibition of the growth of *M. tuberculosis* resulting in dormancy of the bacteria, referred to as latent TB that is consequently asymptomatic (Thillai et al., 2014).

In 2019, an estimated 1.4 million TB deaths and an additional 208 000 deaths from TB-human immunodeficiency virus (HIV) co-infected individuals (World Health Organization (WHO), 2020) were reported globally. The highest incidence rate of TB in 2019 were reported in South-East Asia (44%), Africa (25%), and Western Pacific (18%) (WHO, 2020). Approximately one third of the human population live with latent TB infection (WHO, 2016). Latent TB infection can progress into a more severe state of active TB that manifests as pulmonary disease, with symptoms that are easily identified such as fever, coughing and severe chest pains (Berry et al., 2013, Fogel, 2015). Approximately 5-10% of latent TB infection cases are at risk of progressing to active TB (Comas et al., 2009, Cruz-Knight and Blake-Gumbs, 2013). Immunocompromised individuals, such as those with cancer or HIV or currently taking immunosuppressing medication pose a higher risk of progressing to active TB (Fogel, 2015).

In 2019, approximately 10 million cases of TB were reported, and of these, 8.2% were HIV co-infected individuals (WHO, 2020). Deaths due to TB accounted for 1.21 million and 208 000 amongst HIV negative and HIV positive individuals, respectively (WHO, 2020). Between 2000 to 2015, only 49 million deaths were averted globally due to the persistent gaps in treatment and diagnostic testing (WHO, 2016). Hence, TB still poses a global health threat and remains one of the most significant and severe cause of death from an infectious disease (WHO, 2020).

In 2015, Kwa-Zulu- Natal (KZN) had the highest burden of multi-drug resistant TB (MDR-TB) and extensively drug resistant TB (XDR-TB) cases that were reported in South Africa (Heidebrecht et al., 2016). A gross underestimation of the prevalence of TB was reported in

both the Western Cape (Claassens et al, 2013) and KZN (Wallengren et al., 2011). This particular underestimation was evident despite KZN reporting the highest incidence rates of MDR and XDR-TB (Wallengren et al., 2011). Hence, rapid TB detection and treatment is imperative in order to address the global MDR and XDR-TB crisis (WHO, 2018).

The rapid increase in drug resistance, lack of an effective vaccine and efficacious drugs (Andersen and Doherty, 2005), and the growing HIV epidemic (Karim et al., 2009), are the major contributors to the high TB burden in South Africa (Hughes and Osman, 2014). The TB vaccine currently being used, developed in 1921, proves only partially effective and serves little protection to adults (Calmette and Plotz, 1929, Andersen and Doherty, 2005). The slow replication rate of *M. tuberculosis* leads to diagnostic delays as a result of slow diagnostic tests (Vaughan et al., 1989), which significantly contribute to an increase in the transmission of TB and its acquisition of drug resistance (El-Sony et al., 2002). Hence, novel TB diagnostic biomarkers that incorporate cost effective point-of-care (POC) tests, are of urgent need.

The increase in global efforts to decrease transmission of TB should focus on POC testing, followed by prompt drug administration and the subsequent TB management, especially in third world countries burdened by this disease (Wallis et al., 2013). A small number of the newly designed putative diagnostic tests, such as paper-, immune- and PCR-based diagnostics, were adopted for routine diagnosis (Parsons et al., 2011, Somoskovi, 2015). Since the current approaches, QuantiFERON[®]-TB Gold In-Tube and T-Spot, show cross-reactivity (Helmy et al., 2012), poor predictive values and are unable to distinguish between re-infections and new infections, alternative innovative approaches and increased research efforts are in urgent need for the design of novel drugs and rapid diagnostic tools for the eradication of TB, especially MDR and XDR TB.

The exploration of virulence factors, biomarker discovery and genomic evolution of *M. tuberculosis* has been facilitated by the availability of the complete genomes of *M. tuberculosis* complex (MTBC) and nontuberculous mycobacteria (NTM). In addition to the genomes being compared for identification of unique epitopes to *M. tuberculosis*, the amino acid profiles (Brosch et al., 2002) can be analysed further to identify folding and secretion characteristics and can be used for transcriptomic research that explores the host and pathogen-associated biomarker discovery (Parsons et al., 2011).

M. tuberculosis pathogenesis encompasses many processes. Understanding each stage of host-pathogen interactions allows the identification of novel biomarkers enabling the development

of various TB diagnostics and therapeutics that could potentially eradicate this disease. An important stage of TB infection is the initial adherence of *M. tuberculosis* to the host-target tissue (Pethe et al., 2001, Sia et al., 2015). *Mycobacterium tuberculosis* adhesins comprises transmembrane proteins and proteins with and without signal peptide sequence (Klemm and Schembri, 2000, Vinod et al., 2020). The host-pathogen interaction results in adhesion of the microbes to host cells, inducing immune response and aids in the pathogenesis of the disease (Niemann et al., 2004, Vinod et al., 2020). Enhancing current information on adhesins will prove to be beneficial in the development of novel therapeutic strategies, and aid in the identification of diagnostic markers, new drug targets, and vaccine candidates (Vinod et al., 2020). *Mycobacterium tuberculosis* encodes multiple adhesins, which include *M. tuberculosis* curli pili (MTP) (Alteri et al., 2007) and heparin-binding hemagglutinin adhesin (HBHA) (Pethe et al., 2001).

As a virulence factor, HBHA (*Rv0475*) is present during early stages of TB infection and is responsible for the initial interaction with epithelial cells (Pethe et al., 2001). Significant reduction in adhesion and invasion of A549 pneumocytes by *M. tuberculosis* HBHA-deficient strain, relative to the wild-type (WT), depicted HBHA as a principle *M. tuberculosis* adhesin crucial in its interaction with the host cell (Pethe et al., 2001). Additionally, HBHA was observed to play a role in the binding of the pathogen to glycoconjugates of the epithelial cells (Pethe et al., 2001). Antibody responses to HBHA, suggest it may provide additional immune protection against *M. tuberculosis* (Pethe et al., 2001). Microscopy studies (Menozzi et al., 2006), suggested that HBHA induces epithelial transcytosis, which could represent a macrophage-independent extrapulmonary dissemination mechanism, subsequently leading to *M. tuberculosis* infection. The HBHA adhesin is a noteworthy marker, distinguishing active TB from latent TB infection (LTBI) in humans, as the presence of this adhesin induces a higher level of interferon- γ (IFN- γ) in LTBI (Hougardy et al., 2007). Furthermore, the HBHA adhesin facilitates cell adhesion and bacterial aggregation, two crucial steps in TB pathogenesis (Esposito et al., 2012). Hence, HBHA may pose as useful target in TB diagnostics and therapeutics (Esposito et al., 2012).

Virulence factor and putative diagnostic/therapeutic target, MTP (*Rv3312A*) (Alteri et al., 2007), has been reported as another important target for vaccine and drug development. *Mycobacterium tuberculosis* curli pili binds to laminin and is known to react with IgG antibodies in TB patients' sera (Alteri et al., 2007). Genomic studies highlighted that the *mtp*

gene (*Rv3312A*), is a conserved gene that is unique to *M. tuberculosis* complex (MTBC) pathogens (Naidoo et al., 2014). Additionally, a synthetic MTP peptide was shown to react with IgG antibodies of patients (Naidoo et al., 2018). Functional genomics studies illuminated the role MTP plays in adhesion and invasion of THP-1 macrophages (Ramsugit and Pillay, 2014) and A549 epithelial cells (Ramsugit et al., 2016). Furthermore, MTP is known to play a role in biofilm production (Ramsugit et al., 2013), and may reduce chemokine/cytokine induction in epithelial cells as a survival mechanism (Ramsugit et al., 2016). Thus, MTP may pose as a suitable biomarker candidate for the development of a POC TB test, and TB therapeutics.

Global transcriptomic analysis provides a fundamental link between the genome and proteome by evaluation of global changes occurring in gene expression profiles of cells, tissues, organs or whole organisms (Parida and Kaufmann, 2010). Transcriptomic studies, using RNA sequencing, investigating the *in vitro* role of MTP in induction of host immune response, highlighted that *mtp* affects A549 alveolar epithelial cell gene regulation, including cell surface receptors (Dlamini, 2016).

Transcriptomic investigations on the combined effect of MTP and HBHA on adhesion and invasion in a THP-1 human macrophage model, demonstrated that, in combination, these adhesins influence transcriptional changes favouring adhesion and subsequent invasion of macrophages (Moodley et al., 2018, unpublished). This data was supported by a functional genomic study by Govender et al, 2018 in which bacterial growth and biomass formation was facilitated by the MTP and HBHA adhesins, in combination (Govender et al., 2018).

Collectively, these findings indicate the potential these adhesins may represent as TB biomarkers or novel targets for a POC diagnostic test, vaccine, and drug developments. Therefore, with the use of functional transcriptomics, real time quantitative PCR (RT-qPCR) and a phenotypic bioluminescence assay, this study aimed to determine the individual and combined effects MTP and HBHA have on the bacterial transcriptome of *M. tuberculosis*.

Dissertation outline

This dissertation comprises of 3 chapters. Chapter 1 reviews the relevant literature. Chapter 2 presents Manuscript 1, which is ready for publication, and which investigated the individual and combined roles MTP and HBHA play in regulation of *M. tuberculosis* bacterial transcriptome, using *M. tuberculosis* V9124, Δmtp , $\Delta hbhA$, and $\Delta mtp-hbhA$ deletion mutants and their respective complemented strains. Chapter 3 synthesises the eminent findings from

the literature review and manuscript, highlights limitations and provides the conclusions and recommendations for future studies.

Chapter 1: Literature Review

1.1 Epidemiology of tuberculosis

Globally, tuberculosis (TB) remains the leading cause of death from a single infectious agent, superseding human immunodeficiency virus/acquired immunodeficiency syndrome (HIV/AIDS) (WHO, 2020). In 2019, an estimated 10 million individuals contracted TB, a number that has very gradually declined in recent years (WHO, 2020). An estimated 1.4 million deaths, and an additional 208 000 deaths from TB-HIV co-infected individuals were reported in 2019 (WHO, 2020). Globally, South Africa (SA) along with India, Indonesia, Philippines, Nigeria, China, Pakistan, and Bangladesh account for two thirds of TB related deaths (WHO, 2020). The severity of TB in SA is alarming (Figure 1.1), with more than 500 new cases per 100 000 population (WHO, 2020). An estimated 36 000 TB-HIV deaths was reported in 2019 in SA (WHO, 2020). The high prevalence of HIV infected individuals in SA, 20.4% of the population (Avert, 2018), has potentially led to the increased TB incidence rates during the early 1900's, according to the National Institute For Communicable Diseases NICD, 2016). The TB-HIV co-infection rate was estimated at 63.2% in 2015 (NICD, 2016), which dropped to 60% in 2017 (WHO, 2018) and significantly increased in 2019 to almost 70% (WHO, 2020).

Approximately 1.7 billion people, estimated 23% of the world's population, have latent TB infection, and thus are at risk of developing active TB during their lifetime (WHO, 2018). Latent TB infection is a result of the hosts' immune system regulating the bacterial growth to an extent to which the bacteria becomes inactive (Zuñiga et al., 2012).

Tuberculosis incidence rate and mortality is declining globally at approximately 2% and 3% per year respectively, with 16% of TB incidents resulting in death (case fatality ratio) (WHO, 2018). To achieve the first milestone of the End TB strategy of 2020, the incidence rate should fall between 4-5% per annum, with the case fatality ratio declining to 10% (WHO, 2018).

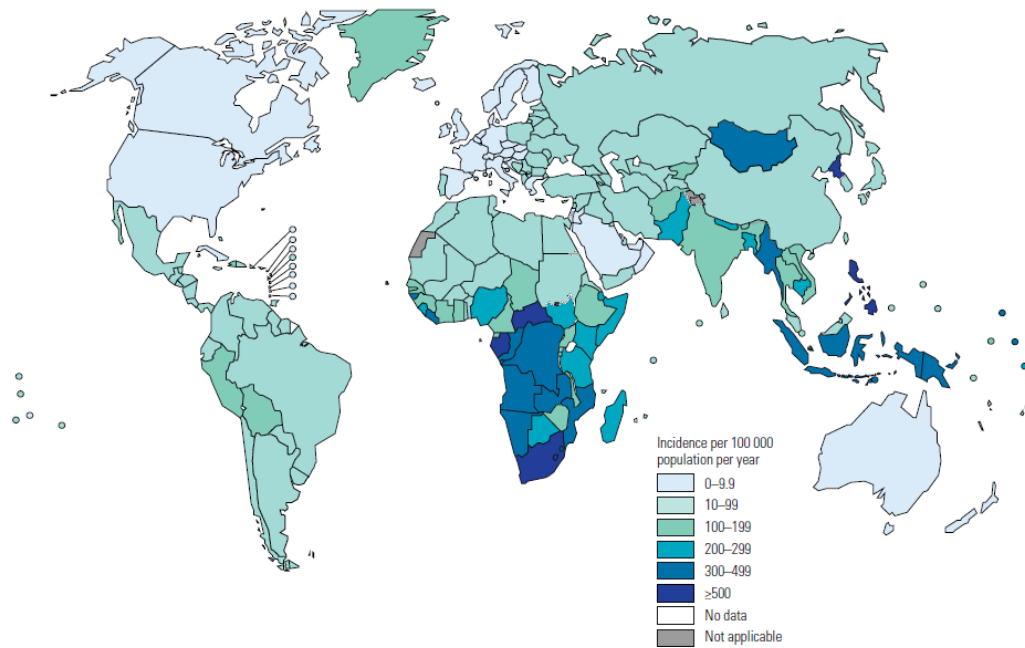


Figure 1.1. Estimated global incidence rates of TB in 2019 (WHO, 2020).

1.2 Drug resistance

The phenomenon of drug resistance was first described during the very first human TB therapy trial in 1948 (Daniels and Hill, 1952, Pai et al., 2016). The widespread emergence of resistant strains has been described, usually, within a decade of the introduction of new anti-TB drugs into clinical practices. Drug resistance in *M. tuberculosis* occurs through genetic mutations (Gillespie, 2002). Currently, no reports have been noted of resistance developed by the acquisition of new deoxyribonucleic acid (DNA) (Nebenzahl-Guimaraes et al., 2014, Pai et al., 2016).

Drug resistance continues to be a public health crisis, with approximately 465 000 individuals developing resistance to the most effective first line drug, rifampicin (R), of which 78% were multi-drug resistant TB (MDR-TB) (WHO, 2020). *Mycobacterium tuberculosis* strains that are resistant to the two most effective anti-TB drugs (rifampicin and isoniazid), are termed MDR-TB and have been reported in virtually all countries (WHO, 2020). In 2019, SA had an estimated 14 000 new MDR/RR- TB cases (WHO, 2020). In 2019, an estimated 3.3% of incidence cases and 18% of previously treated cases developed RR-TB/MDR-TB (WHO, 2020). Among these cases of MDR-TB, 12 350 incidences were estimated to have extensively drug-resistant TB (XDR-TB), caused by *M. tuberculosis* strains that are resistant to at least four of the core TB drugs including, isoniazid and rifampicin, in addition to any fluoroquinolones

and second line injectables, including, amikacin and kanamycin (WHO, 2020). Approximately 619 new cases, of these 12 350 XDR-TB incidences, were reported in Africa (WHO, 2020).

Totally drug resistant TB (TDR-TB) refers to those strains of *M. tuberculosis* resistant to all first- and second-line TB drugs (Parida et al., 2015). In 2012, there were 12 reported cases of TDR-TB in Mumbai, India, that were found to be resistant to 12 TB drugs (WHO, 2013). A study by Klopper et al., (2013), found that 93% of atypical XDR Beijing isolates from SA, had mutations that conferred resistance to 10 anti-TB drugs, with some isolates resistant to *para*-aminosalicylic acid, suggesting the emergence of TDR-TB in SA (Klopper et al., 2013).

1.3 Characteristics of *Mycobacterium tuberculosis*

Mycobacterium tuberculosis is a facultative anaerobic intracellular pathogen (Ducati et al., 2006). The non-motile, capsulated (Daffe and Reyrat, 2008), non-sporing pathogen (Ducati et al., 2006) is able to infect and persist in humans for decades despite the presence of functioning immune cells (Kalscheuer et al., 2019). The slender rod shaped bacteria (Kumar et al., 2013), range between 1 - 4 μm in length and 0.3 - 0.6 μm in width (Ducati et al., 2006). *Mycobacterium tuberculosis* optimally grows at 35 - 37°C, with the optimal pH ranging between 6.4 to 7 (Kannan, 2016). The slow growing pathogen has an average generation time of 15 to 24 hours in synthetic media and infected tissue (Cole et al., 1998, Kannan, 2016). In laboratories, *M. tuberculosis* is grown in either Middlebrook 7H9 broth or on Middlebrook 7H11 agar plates or Lowenstein-Jensen solid media (Kannan, 2016). *Mycobacterium tuberculosis* colonies on solid media start to appear at two weeks of incubation and could take up to eight weeks to grow (Kannan, 2016). Colonies appear creamy white with a raised elevation, irregular shape, and a wrinkled, dry surface on Middlebrook 7H11 plates, after an incubation period of three to four weeks (Bloom and Murray, 1992, Kannan, 2016). *Mycobacterium tuberculosis* is an acid-fast, Gram-positive bacteria (Kannan, 2016). The acid-fast bacteria stain bright red through the Ziehl-Neelsen stain, which makes the cording appearance of the pathogen more prominent under a microscope (Kannan, 2016). Additionally, this pathogen is resistant to drying, which significantly contributes to the ease of its transmission. Although *M. tuberculosis* is Gram-positive, their highly impermeable cell walls make them difficult to stain (Kannan, 2016).

1.3.1 *Mycobacterium tuberculosis* cell envelope

A hallmark of *M. tuberculosis* survival is the complexity of its cell envelope (Kalscheuer et al., 2019). The cell envelope is abundant with polysaccharides and lipids and has a unique chemical structure (Angala et al., 2014, Jankute et al., 2015). The intrinsically highly impermeable nature of the *M. tuberculosis* cell wall is due to the presence of mycolic acids (Kannan, 2016) and the intricate organization of its components (Brennan and Crick, 2007). Mycobacterial cell envelopes consist of four layers, which include: the plasma/inner membrane (IM), a peptidoglycan-arabinogalactan complex (AGP), an asymmetrical outer mycomembrane covalently bonded via mycolic acids to AGP, and the outer capsule (Daffe and Reyrat, 2008). The mycobacterial capsule has a weak bond to the cell wall and can be dispensed to the growth medium whilst retaining similar physicochemical characteristics (Lemassu et al., 1996).

Mycobacterium tuberculosis has a distinct cell wall that consists of lipids, polysaccharides, and proteins (Kumar, 2015). A major part of the cell wall is comprised of lipids (60%) (Kumar, 2015). The distinct layers of *M. tuberculosis* comprise: arabinogalactan, mycolic acids, peptidoglycan, and mycoside (Figure 1.2) (Kumar, 2015). Mycosides comprise phenolic glycolipids or peptidoglycolipids, and form the outermost cell layer consisting of agglutinin antigens (Kumar, 2015). A fundamental component of the *M. tuberculosis* cell wall is the mycolic acid layer (Kumar, 2015). The mycolic layer lies beneath the outermost mycoside layer (Kumar, 2015), and comprises long α -alkyl and β -hydroxy fatty acids, bonded to arabinose terminal units of arabinogalactan via ester bonds (Kumar, 2015). The mycobacterial cell envelope comprises 50% of mycolic acids, that are hydrophobic in nature (Todar, 2012). The ester bonded molecules form a lipid shell that protects the extracellular mycobacteria from deposition in the serum, by disturbing cell surface permeability (Todar, 2012). Additionally, mycolic acids were observed to form a protective layer within the phagocytic granule, protecting the cell against oxygen radicals, cationic proteins and lysozymes (Todar, 2012). Arabinogalactan is located external to the innermost peptidoglycan layer and is responsible for maintaining the cell shape and rigidity of the pathogen (Kumar, 2015).

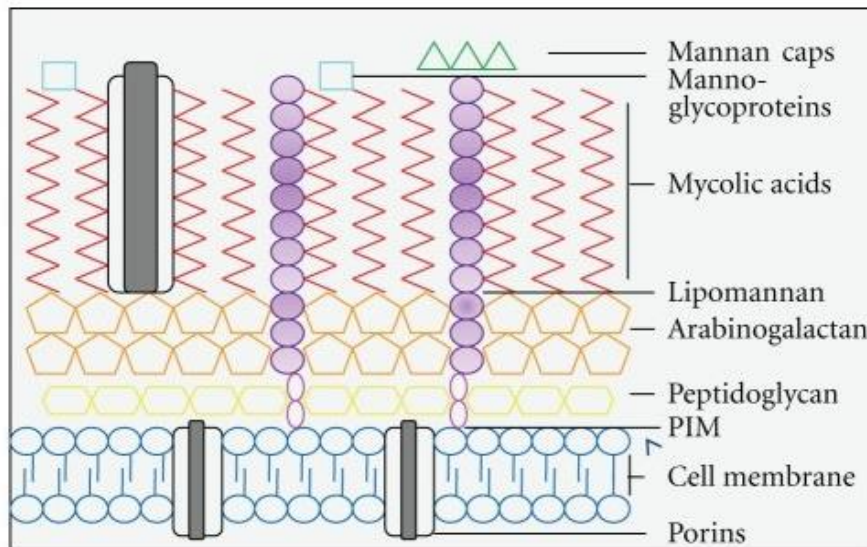


Figure 1.2. The cell wall structure of *M. tuberculosis* (Kleinnijenhuis et al., 2011).

1.4 Pathogenesis of *Mycobacterium tuberculosis*

Mycobacterium tuberculosis has no known environmental reservoir except humans (host); thus, it is both a symbiont and a pathogen (Comas et al., 2013, Pai et al., 2016). This presents many implications in the understanding of host-pathogen interactions (Comas et al., 2013, Pai et al., 2016). Therefore, investigation of host-pathogen interactions may enhance current knowledge and aid in eradication of TB.

Pathogenesis of *M. tuberculosis* comprises four distinct stages which include: inhalation of the bacilli, recruitment of the inflammatory cells, control of the pathogen's growth and the reactivation of *M. tuberculosis* (Zuñiga et al., 2012).

Mycobacterium tuberculosis infection is initiated by the inhalation of the bacilli into the alveoli (Hestvik et al., 2005, Bruns and Stenger, 2014, Ryndak et al., 2015), where it encounters resident macrophages serving as the first line of defence. If the macrophages fail to eliminate it, *M. tuberculosis* initiates the invasion of lung interstitial tissue, either by direct bacterial infection of the alveolar epithelium or migration of the infected macrophages to the lung parenchyma epithelium (Lin et al., 2014, Pai et al., 2016) (Figure 1.3a). The pathogen is then transported, by either inflammatory monocytes or dendritic cells, to the pulmonary lymph nodes for T-cell priming (Lin et al., 2014, Pai et al., 2016). Cell priming then leads to

recruitment of immune cells, which include the B- and T-cells, to the lung parenchyma forming a granuloma (Lin et al., 2014, Pai et al., 2016). Replication of the bacteria then occurs within the growing granuloma, and once the bacterial load becomes too great, the granuloma fails to contain the infection (Figure 1.3b), subsequently leading to dissemination to the local lymph nodes and other organs, including the brain (Lin et al., 2014, Pai et al., 2016). At this phase in the infection, the bacteria can re-enter the respiratory tracts to be released or enter the bloodstream, thereby making the host infectious and symptomatic allowing for progression to active TB (Lin et al., 2014, Pai et al., 2016).

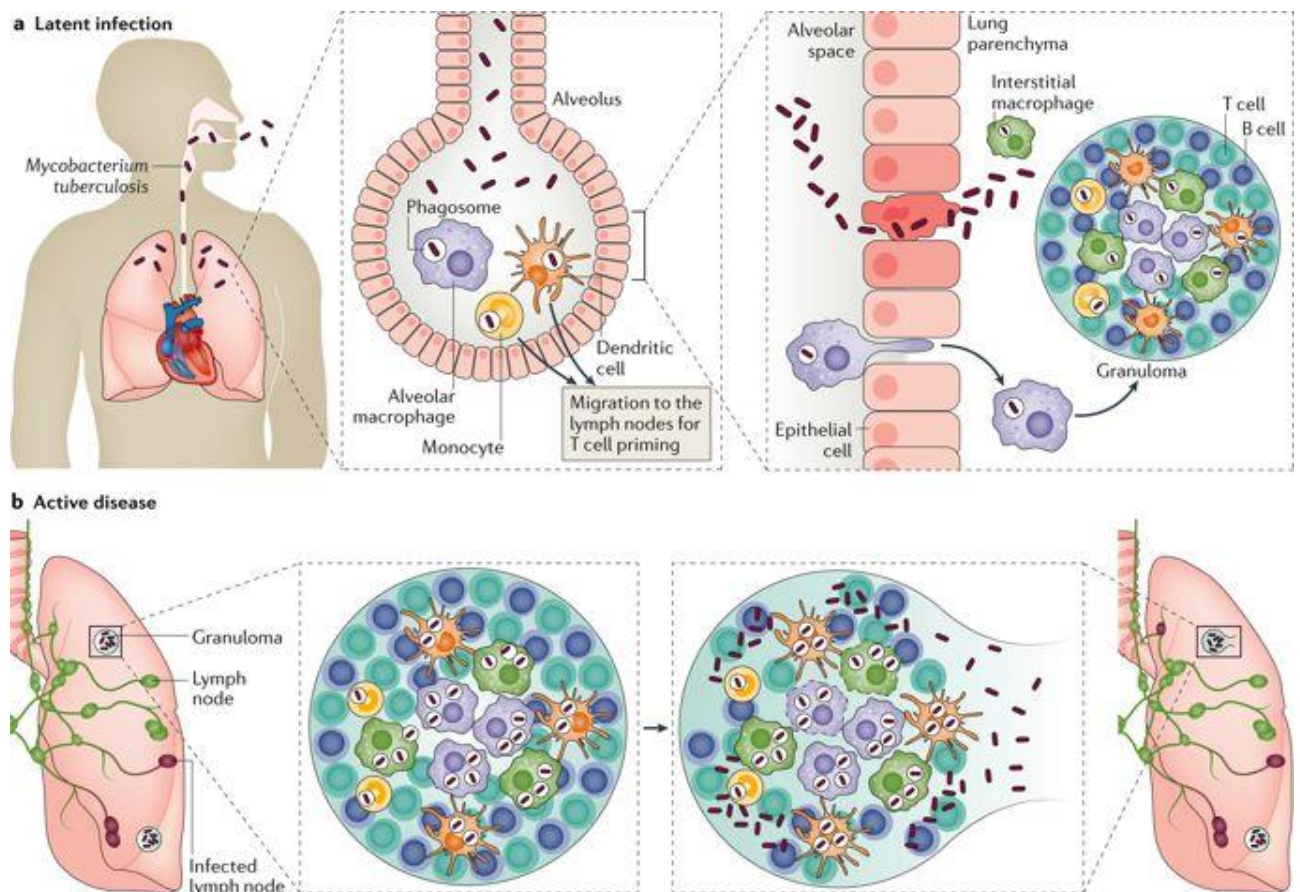


Figure 1.3. Active and latent *M. tuberculosis* infection (Pai et al., 2016).

Studies on the lungs of aerosol-infected mice have provided evidence for the extensive replication of *M. tuberculosis* in non-migrating, non-antigen-presenting-cells in the alveoli during the first 2-3 weeks post-infection (Wolf et al., 2008). The alveoli are lined by two types of alveolar epithelial cells (AEC), namely, Type I and Type II, which outnumber alveolar macrophages (Crandall et al., 1991, Schneeberger, 1991). *Mycobacterium tuberculosis* DNA and viable *M. tuberculosis* have been observed in AEC as well as other non-macrophage cells of the spleen, kidney and liver in autopsied tissues obtained from latently infected subjects from TB-endemic regions, indicative of systemic bacterial dissemination during the primary infection (Ryndak et al., 2015). *M. tuberculosis* has been observed to rapidly replicate in A549 cells (Type II AEC line) and acquire an increased invasiveness for endothelial cells (Ryndak et al., 2015). These findings suggest that AEC could provide an important niche for bacterial development and expansion of a phenotype that will promote dissemination during the primary infection (Ryndak et al., 2015).

1.5 Current status of tuberculosis diagnosis

Despite recent insights gained on the transmission, diagnosis and the treatment of TB, much remains unknown in understanding ways to eradicate it (WHO, 2020). Understanding the mechanisms that this organism utilizes to cause an infection in its host, offers a novel perspective and may define new targets that will enable the design and development of drugs that could prove effective against both sensitive and resistant organisms (Ginsberg and Spigelman, 2007, Govender et al., 2014), as well as provide novel perspectives in the design and development of much needed rapid and cheap POC tests (Simmons et al., 2018). The limited number of suitable biomarkers that have been identified hampers the design and development of novel drugs as well as rapid TB diagnostic tools and vaccines (Simmons et al., 2018).

The current active TB diagnosis methods relies mostly on smear microscopy, chest X-rays as well as culture-based methods and molecular tests (Pai et al., 2016). Currently the typical diagnostic algorithm takes approximately two weeks, during which the infected individual can infect around 10 to 15 people before they begin treatment (Shen et al., 2019). Current conventional methods used to diagnose active TB include the isolation of *M. tuberculosis* in bacteriological culture and sputum smear (Tiwari et al., 2007, Tucci et al., 2014, WHO, 2016), which is currently the most cost-effective option. However, sputum smear has many limitations

including the false negative results in children and in adults co-infected with HIV due to paucibacillary TB (Nicol and Zar, 2011), as well as low specificity and sensitivity (Nakiyingi et al., 2013). A potential POC test recommended by the WHO is the lipoarabinomannan (LAM) antigen detection, for use on HIV-co-infected individuals who are diagnosed sputum smear negative (Pai et al., 2016).

The interferon gamma release assay (IGRA), through QuantiFERON[®]-TB Gold In-Tube (Qiagen, Hilden, Germany) and T-Spot (Oxford Immunotec, Abingdon, United Kingdom) and the Mantoux tuberculin skin test (TST) (Sanofi Pasteur, Lyon, France), remain TB infection detection methods. However, QuantiFERON[®]-TB Gold In-Tube (Qiagen, Hilden, Germany), T-Spot (Oxford Immunotec, Abingdon, United Kingdom) and the Mantoux tuberculin skin test (TST) (Sanofi Pasteur, Lyon, France) fail to distinguish between the active and the latent form of the TB infection (Pai et al., 2016). The QuantiFERON[®]-TB Gold diagnostic test (Qiagen, Hilden, Germany) quantifies IGRA production in response to the early secreted antigenic target (ESAT-6) and culture filtrate protein (CFP)-10 (Helmy et al., 2012). Although it is cost effective, easy to use and quick, the QuantiFERON[®]-TB Gold (Qiagen, Hilden, Germany) displays cross-reactivity to other *Mycobacterial* species including *M. marinum*, *M. sulzgai*, and *M. kansasii* (Helmy et al., 2012). Unfortunately, QuantiFERON[®]-TB Gold In-Tube (Qiagen, Hilden, Germany) and T-Spot (Oxford Immunotec, Abingdon, United Kingdom) exhibit poor predictive values and prove unable to distinguish between re-infections and new infections (Rangaka et al., 2012, Sia and Rengarajan, 2019).

The main concern regarding the detection of this devastating disease remains to be the slow generation time of the *M. tuberculosis* bacilli (approximately two to six weeks in liquid media), which leads to consequent diagnostic delays (Asmar et al., 2015, Sulis et al., 2016). Hence, this results in the impediment of the more accurate diagnostic methods (Hasegawa et al., 2002, Asmar et al., 2015, Sulis et al., 2016).

There has been significant progress in the development of new diagnostic methods for TB, resulting in the expansion of the pipeline of new diagnostic technique. Currently, various serological, genotypic, and phenotypic methods are used in TB diagnosis. These include, the rapid test GeneXpert MTB/RIF Ultra (Cepheid, California, USA), an automated molecular assay, which was recommended by the WHO for diagnosis of TB due to its superior level of accuracy (WHO, 2019). The GeneXpert MTB/RIF Ultra (Cepheid, California, USA), near-patient cartridge-based assay, utilizes RT-qPCR to detect both TB and Rifampicin-resistant

tuberculosis (RR-TB), within two hours (WHO, 2019). Novel DNA-based diagnostic tests identifying genetic mutations in MDR-TB yielded results between 24 to 48 hours (WHO, 2016). This is a significant decrease in turn-around time from the lead time of three months. Faster detection of MDR-TB allows infected individuals to begin treatment with appropriate second-line drugs earlier (WHO, 2016).

The Determine TB-LAM diagnostic assay (Alere Incorporated, California, USA) is an attractive POC option due to its cost effectiveness, user friendliness and rapid turnaround time (Lawn et al., 2013). This diagnostic assay detects the presence of *M. tuberculosis* antigen LAM in urine samples to diagnose TB (Lawn et al., 2013). However, it displays a lower sensitivity in comparison to the GeneXpert MTB/RIF Ultra (Cepheid, California, USA) molecular diagnostic assay (Lawn et al., 2013).

The GenoType[®] MTBDR plus strip test (Hain Life Science), a nucleic acid amplification test, enables the detection of TB, as well as mutations on genes such as catalase peroxidase (*katG*), RNA polymerase (*rpoB*) and enoyl reductase (*inhA*) that define infection with *M. tuberculosis* strains resistant to isoniazid and rifampicin (Hillemann et al., 2007, Barnard et al., 2008). Furthermore, the rapid DNA-based test, GenoType[®] MTBDRs1, facilitates the detection of specific mutations that are linked to resistance of fluoroquinolones and the second-line injectable drugs, amikacin and kanamycin (Theron et al., 2016). A study by Abanda et al., 2018 recommended the GenoType[®] MTBDR plus assay (Hain Life Science) to assume RR-TB based on the failure to hybridize to the *rpoB* wild-type probe allowing identification of crucial rifampicin resistant isolates, of which approximately 20% could be missed by relying on the standard minimum inhibitory concentration (MIC) test (Abanda et al., 2018). Studies comparing the GenoType[®] MTBDR plus assay (Hain Life Science) and the gold standard phenotypic Lowenstein Jenson proportion method to detect MDR-TB reported that the GenoType[®] MTBDR plus assay (Hain Life Science) performed well in the detection of drug resistance to rifampicin, isoniazid, and MDR-TB, therefore, it is an efficient and rapid tool to diagnose MDR-TB (Amunda et al., 2020).

Recent studies investigated biomarkers present in blood to discriminate active TB from latent TB (Riou et al., 2017, Sia and Rengarajan, 2019). The human leukocyte antigen (HLA)-DR is expressed on *M. tuberculosis*-specific CD4 T cells, and is anticipated to be a pertinent marker that is able to distinguish active TB from latent TB in TB-HIV co-infected individuals (Riou et al., 2017). A better understanding of antigen-specific responses to *M. tuberculosis* during

TB infection can be utilized in developing diagnostics to monitor infection and therapeutic responses (Sia and Rengarajan, 2019).

Although research and development in POC tools and novel diagnostic targets have substantially taken off, most of the current POC TB diagnostic tests lack desirable WHO target profiles that allow its implementation (García-Basteiro et al., 2018). Innovative technologies that enable effective, timeous, and cost-effective detection of TB for low-income settings remain limited. However, current commercial POC tests offer a better understanding of *M. tuberculosis* infection and control, thus enabling the development of more effective tools within a high-burden setting (García-Basteiro et al., 2018).

1.6 Vaccine development

Developed in 1921, the BCG vaccine remains the only licensed vaccine available for protection against *M. tuberculosis* infections (Calmette, 1931, Behr et al., 1999). However, this vaccine is not reliable against pulmonary TB in adults and adolescent children (Mangtani et al., 2014, Roy et al., 2014). Furthermore, the BCG vaccine is not recommended for use by individuals infected with HIV and is also known to cause disseminated BCG disease in approximately 88% of neonates (Wilkie and McShane, 2015). Currently, the pipeline for TB vaccine candidates includes various platforms such as recombinant subunit vector vaccines, adjuvanted proteins and whole cell vaccines (WHO, 2020). Currently the candidate vaccines; such as Ag85A (Smaill and Xing, 2014, WHO, 2020), AEC/BC02 (Lu et al., 2015, WHO, 2020), ChAdOx185A (Wilkie et al., 2020, WHO, 2020), MVA85A (Tameris et al., 2013), VPM100 (Grode et al., 2013), MTBVAC (Aguilo et al., 2016), that have been developed are being investigated for prevention of primary and recurrent TB in adolescents and adults, reducing the duration of treatment, and for BCG boosters and replacements (WHO, 2020). The goal of TB vaccine development is to prevent TB infections and ultimately eradicate the disease (WHO, 2020).

The different stages that each vaccine needs to complete include the first-in-human Phase I, followed by Phase II and Phase III clinical trials (Martin et al., 2020). Currently, there are three vaccine candidates in phase I trials, namely; Ad5 Ag85A, AEC/BC02, and ChAdOx185A-MCA85A, and 11 in phase II/III trials (WHO, 2020). Adenovirus serotype 5 vector, Ad5 Ag85A, expressing antigen 85 A (Ag85A) has been evaluated for safety and immunogenicity in previously BCG-immunized and BCG-naïve individuals (Smaill and Xing, 2014, WHO, 2020). A more potent immunogenicity was displayed in volunteers that had been previously

vaccinated with BCG (Smaill and Xing, 2014, WHO, 2020). Freeze-dried recombinant vaccine, AEC/BC02, expresses Ag85B and an alum salt-based adjuvant, a fusion protein CFP-10 and ESAT-6 with CpG, from BCG (Lu et al., 2015, WHO, 2020). Simian adenovirus, ChAdOx185A, and recombinant pox virus, MVA85A, express antigen 85A (Wilkie et al., 2020, WHO, 2020). These candidates are being investigated with the aim of developing a joint heterologous prime-boost regime delivered through mucosal and systemic routes (Wilkie et al., 2020, WHO, 2020).

Recently, the recombinant fusion protein, M72/AS01_E, was investigated in phase IIb trials (WHO, 2020). The fusion protein is derived from *M. tuberculosis* 32A (Mtb32A) and Mtb39A antigens fused to AS01_E adjuvant system (Tait et al., 2019). This vaccine candidate displayed significant protection against TB, in individuals exhibiting latent TB in Zambia, SA, and Kenya (Tait et al., 2019). Final analysis of this candidate showed a 50% vaccine efficacy over a three-year period (Tait et al., 2019, WHO, 2020). The clinical significance and strength of this evidence is unparalleled in decades of research for TB vaccines (WHO, 2020).

Protein vaccine candidates currently investigated include; ID93/GLA-SE (Baldwin et al., 2016) H56:IC31 (Luabeya et al., 2015), and H4:IC31 (Geldenhuys et al., 2015). Adjuvanted subunit vaccine, H56:IC31, comprises three *M. tuberculosis* antigens, ESAT-6, Rv2660c, and Ag85A (Luabeya et al., 2015). Analysis of phase Ib trials showed that the vaccine was immunogenic, at all doses being investigated, and displayed an acceptable safety profile (Bekker et al., 2020, WHO, 2020).

Currently, the viral vector vaccine candidates investigated include; MVA85A (Tameris et al., 2013), VPM100 (Grode et al., 2013), and MTBVAC (Aguilo et al., 2016). Phase IIb clinical trials on MVA85A vaccine candidate displayed a heightened antigen-specific CD4 T-cells response, and no additional protection in infants, against TB (Tameris et al., 2013). Live recombinant vaccine candidate, VPM1002, aims to improve BCG immunogenicity and vaccine potential (Grode et al., 2013, WHO, 2020). To accomplish this, BCG was designed to evade the phagosome by expression of lysteriolysin and enable perforation of the phagosomal membrane, thereby enhancing major histocompatibility complex class I antigen presentation to CD8-T-cells (Grode et al., 2013, WHO, 2020). Phase II trials of VPM1002, investigating safety and immunogenicity were successful (WHO, 2020). Genetically attenuated *M. tuberculosis* strain, MTBVAC, lacks *fadD26* and *phoP* genes, restricts the synthesis of several surface lipids (Aguilo et al., 2016). Currently, phase IIa trials investigating MTBVAC as a BCG replacement

vaccine (in neonates) and booster vaccine (in adults) are ongoing (WHO, 2020). The last two decades have reported significant breakthroughs in TB vaccinology. Thousands of potential vaccine candidates were identified in the discovery phase during this period, of which hundreds passed to preclinical trials and evaluation in animal models, and only a little more than a dozen were tested in early clinical trials in humans (Martin et al., 2020). Although these vaccine candidates display great promise, they could fall short during the ongoing clinical trials. Hence, there is a need for the discovery of novel biomarkers.

1.7 Current antibiotic treatment of tuberculosis

The severe difficulty in TB treatment lies in the global and rapid evolution of drug resistance as well as the predominance of drug resistant phenotypes (Mazel and Davies, 1999; Pillay and Sturm, 2007; WHO, 2014). The current effective anti-TB strategy uses a rigorous combination of antimicrobial drugs including, ethambutol (EMB), rifampicin (RIF) as well as pyrazinamide (PZA) and isoniazid (INH) in an intensive two-month initial phase, followed by a maintenance phase (four months) consisting of only INH and RIF (Nahid et al., 2016, WHO, 2019). Active TB that is drug susceptible can be treated and cured with the four mentioned antibiotics (WHO, 2020). Additionally, patients that are at risk of neuropathy (HIV-positive patients, diabetics, pregnant woman, and individuals with chronic renal failure) are given pyridoxine, and vitamin B6, in conjunction with INH (Nahid et al., 2016, WHO, 2019).

Drug resistant TB is treated with a combination of antimicrobial drugs, including fluoroquinolones, and injectable medication, such as kanamycin, amikacin, and capreomycin (Garcia-Prats et al., 2016). Treatment for drug resistant TB usually lasts 20 to 30 months (Garcia-Prats et al., 2016, WHO, 2018). Currently, there are a small number of new drugs being investigated as add-on therapy to the current treatment for drug resistance. These include; delamanid (DLM), linezolid (LZD), and bedaquiline (BDQ) (WHO, 2018). Although these antimicrobial drugs show great promise, they are accompanied by various side effects such as nausea, hepatitis, neurotoxicity, vestibular toxicity and jaundice (Garcia-Prats et al., 2016).

Currently, there are two treatment regimens to treat MDR-TB. The first regimen comprises a short injectable-free option of nine to 11 months (WHO, 2019). The second regimen comprise a long injectable-free option of 18 to 20 months (WHO, 2019). Patients are able to switch from the initial short regimen to the longer regimen, once further relevant diagnostic information becomes available (WHO, 2019).

The initial shorter regimen comprises a four-month intensive phase, potentially extending to six months if sputum results are positive at the end of month four (WHO, 2019). This regimen has a fixed continuation phase at five months (WHO, 2019). Superior to injectables regarding efficacy and treatment of RR-TB and MDR-TB, BDQ, is a key anti-TB drug in the shorter regimen (Ahmad et al., 2018, WHO, 2018, WHO, 2019). Only administered in the initial two-month period, LZD, is likely to be effective against RR-TB and MDR-TB at the start of the treatment (Ahmad et al., 2018, WHO, 2018, WHO, 2019). Clofazimine (CFZ) and levofloxacin (LFX), which replaces moxifloxacin (MFX), are also used in the shorter regimen (Ahmad et al., 2018, WHO, 2018). In children younger than six years, *para*-aminosalicylic acid is used as a substitute for injectables (WHO, 2019). In children aged six to 12, DLM is preferred as a replacement for injectables (WHO, 2019). The intensive phase of this regimen encompasses a high dose of INH, EMB, and PZA (WHO, 2019). Treatment of RR-TB/MDR-TB includes the use of rifabutin and rifamycin, administered for six months with possible side effects such as neutropenia and uveitis, and RIF, which cannot be co-administered with BDQ (WHO, 2019).

The longer regimen comprises five drugs administered during the intensive phase and three during the continuation phase (WHO, 2018). A six month intensive phase is required, which can be extended to eight months if patients display delayed culture conversion, slow clinical responses to treatment, and extensive cavitation of bilateral pulmonary disease (WHO, 2018). This regimen has the fixed continuation phase at 12 months (WHO, 2018). The treatment regimen is divided into group A, group B, and group C. In group A, the anti-microbials prioritized are MFX/LFX, LZD and BDQ (WHO, 2018). Group B comprises terizidone/cycloserine and CFZ (WHO, 2018). Capreomycin and kanamycin are not recommended because of the high risk of relapse and treatment failure (WHO, 2019). Priority is given to oral drugs, as injectables often cause pain, distress and adverse reactions in patients leading to treatment interruption (WHO, 2019).

To eradicate the TB epidemic, development of effective TB treatment should be paralleled with the development of accessible, affordable and rapid POC tests for diagnosis (WHO, 2020). Thus, the discovery and the characterization of novel biomarkers is imperative in the design of such diagnostic methods (Abebe et al., 2007, Wallis et al., 2013, Naidoo et al., 2014), as well as effective vaccine and drugs (Wilkie and McShane, 2015).

1.8 Biomarkers

A biomarker refers to any characteristic objectively measured and evaluated for the identification of a particular pathogenic disease, response to pharmacological events or biological processes (Working, 2001, Wallis et al., 2013). A biomarker candidate is considered valid if it can be reproduced and measured accurately. There are four types of biomarkers, which include; predictive, prognostic, diagnostic, and predisposition biomarkers (Simon, 2011, Simon, 2014). Biomarkers such as molecules, genetic materials or epitopes have been incorporated into assays that are able to identify active TB inexpensively and rapidly, as well as distinguish an appropriate response to anti-TB drugs, and evaluate individuals at risk for disease progression (Nyendak et al., 2009).

Development of effective biomarkers comprises four steps; discovery, analytical validation, evaluating the clinical efficacy, and clinical use (Quezada et al., 2017). The initial step, discovery of a biomarker, is characterized by the analysis of various specimens that derive from cell lines, archived samples or animal models, which highlight potential candidate biomarkers (Vargas and Harris, 2016). Additionally, the discovery phase provides valuable insight on molecular mechanisms contributing to the pathological state as well as potential therapeutic targets (Goossens et al., 2015). Information obtained from this step must be deduced in the context ensuring the most accurate and promising biomarkers are selected. The analytical validation step is required to assess the efficacy of potential biomarkers with laboratory tools (Goossens et al., 2015). Reproducibility of tests performed in this step is crucial (Goossens et al., 2015).

Although numerous single biomarkers have been successfully implemented in diagnostic prognosis, there lies a dawn of ‘omics’ technology that highlights the prospect of biosignatures, a combination of biomarker profiles, to achieve the same goal (Du Preez et al., 2017). Biosignatures may be valuable when single biomarkers do not exist or cannot be identified (Du Preez et al., 2017). An interplay of several molecules, including RNA, DNA and proteins, determine pathological state, hence the use of multilevel biomarkers are a desirable option (Quezada et al., 2017). A biomarker’s ability to diagnose a specific clinical condition must be enhanced in trials before clinical use. Once a candidate biomarker demonstrates usefulness in retrospective or prospective studies, it can be approved for clinical use and commercialized (Quezada et al., 2017).

1.8.1 Tuberculosis biomarkers

Biomarkers used for diagnosis of TB originate from the pathogen and host (Goletti et al., 2016). Unlike diagnostics, which describe an individual's condition at a point in time, it is hoped that TB biomarkers might provide prognostic information, that will allow the differentiation of TB infection, disease, and latency (Wallis et al., 2013). There is an urgent need for biomarkers for the three forms of TB, namely, active disease, prediction of durable success of the treatment; latent TB, indicating risk of reactivation; and prediction of vaccine efficacy, indicative of protection from TB with the use of vaccines (Wallis et al., 2013, Naidoo et al., 2014).

Numerous TB biomarkers have been identified and tested for diagnosis of TB, some showing great potential whilst others have notable drawbacks. Solid and liquid culture proves a more accurate approach in comparison to sputum smear, however, it requires sample preparation and growth of *M. tuberculosis* in liquid and on solid culture takes 3-6 weeks and 14 days, respectively (Wallis et al., 2013).

Antigen specific biomarkers, including secretory proteins like CFP10 and ESAT6, are specific to *M. tuberculosis* complex (MTBC) and prove capable of diagnosing latent TB infection (Munk et al., 2001, Hopprich et al., 2012). However, in order to improve the accuracy of the putative diagnostic tests, epitopes are required to be well characterized (Munk et al., 2001, Hopprich et al., 2012). The interferon- γ (IFN- γ) response to specific antigens, a type of immunological biomarker, was reported to have a high specificity, but remains discouraged by the WHO due to its cross reactivity with nontuberculous mycobacteria (NTM) (Pai et al., 2004). The inducible protein biomarker IFN- γ (IP10), was detected in increased concentrations in patients with active TB (Azzurri et al., 2005, Lighter et al., 2009, Chegou et al., 2013, Petrone et al., 2015). *Mycobacterium tuberculosis* Ag85 complex is a family of enzymatic proteins with mycolyl transferase activity (Ronning et al., 2000, Cannas et al., 2008, Minion et al., 2011). In comparison to LAM, detected in urine samples, Ag85 complex is detected in urine and blood samples of individuals with pulmonary TB (Ronning et al., 2000, Cannas et al., 2008, Minion et al., 2011).

Expression of Ki-67 (proliferation marker), HLA-DR, and CD38 on *M. tuberculosis* CD4⁺ T-cells are related to *M. tuberculosis* load (Adekambi et al., 2012). Modulation of these specific markers distinguishes both active and latent forms of TB infection, with a high specificity and sensitivity (Adekambi et al., 2012, Goletti et al., 2016). Moreover, patients that successfully completed TB therapy were accurately classified with the use of these markers (Adekambi et

al., 2012). Proteomic fingerprinting of sera is used to identify potential diagnostic biomarker candidates. Using this method, C-reactive protein, neopterin, and transthyretin were analysed (Agranoff et al., 2006). Analysis revealed that these proteins might discriminate subjects with other inflammatory and infectious conditions from those with TB, with 84% accuracy (Agranoff et al., 2006).

Subjects infected with *M. africanum* and *M. tuberculosis* were evaluated, using metabolic and transcriptomic profiling. Evaluations were performed before and after anti-TB therapy to determine host factors that are associated with pathology of disease and treatment responses and/or variations in biological processes (Tientcheu et al., 2015). No differences were observed in gene expression profiles of peripheral blood between *M. tuberculosis*-infected and *M. africanum*-infected patients before treatment, however, significant differences were observed post-treatment (Tientcheu et al., 2015). Results indicated that the upstream regulator hepatocyte nuclear factor 4- α , is capable of differentially regulating approximately 15% of the genes between the two groups (Tientcheu et al., 2015). Furthermore, analysis on serum metabolic profiles of the infected patients displayed similarities before treatment, however, significant differences in profiles were observed post-treatment (Tientcheu et al., 2015).

Although there is much research on TB biomarkers (Ronning et al., 2000, Munk et al., 2001, Azzurri et al., 2005, Agranoff et al., 2006, Cannas et al., 2008, Adekambi et al., 2012, Hopprich et al., 2012, Chegou et al., 2013, Petrone et al., 2015), a cost effective, accurate POC diagnostic marker is not available. The challenges associated with biomarker studies encompass those applicable to many infectious diseases. These include, the concentration of the biomarker, in the specimen type, that is practical in settings with limited resources and technology platforms and the biological limitation of the biomarker (Kunnath-Velayudhan and Gennaro, 2011).

The only licensed vaccine for TB prevention is the BCG vaccine, hence, novel biomarkers are urgently needed in the development of new effective TB vaccines. To control TB, novel and more efficacious vaccines are required. Biomarkers can aid in developing novel TB vaccines through many platforms, which include: identifying individuals with a high risk of disease progression for recruitment into targeted, smaller efficacy trials, and vaccine intake or the early assessment of vaccine immunogenicity (Fletcher and Dockrell, 2016). The first efficacy trial of MVA85A, a candidate vaccine for TB prevention, has displayed no significant protective efficacy in infants vaccinated with BCG in SA (Tameris et al., 2013). Hence, there is an urgent

need for novel biomarker identification in the design of further efficacious vaccine development.

Although the discovery and characterization of biomarkers proves a time consuming and expensive process, the benefits far outweigh its limitations, especially in the case of TB, with its associated challenges including those of diagnostic, therapeutic and preventive platforms (Pai et al., 2016). The use of a panel of biomarkers, instead of a single biomarker, was recommended to increase both diagnostic specificity and sensitivity (Nagler et al., 2006). Despite the increasing evidence showing that *M. tuberculosis* adhesins, heparin-binding hemagglutinin adhesin (Menozzi et al., 2006, Shin et al., 2006, Esposito et al., 2011, Lebrun et al., 2012, Chiacchio et al., 2017, Govender et al., 2018) and *M. tuberculosis* curli pili (MTP) (Kline et al., 2009, Govender et al., 2014, Ramsugit and Pillay, 2016), may be suitable candidates for diagnostic targets, vaccines and therapeutics, their role in regulating the bacterial transcriptome of *M. tuberculosis* has not been elucidated. Knowledge on this aspect would be pertinent in supporting the validation of these adhesins, and identify novel molecular signatures, as vaccine and diagnostic candidates.

1.9 *Mycobacterium tuberculosis* adhesins

Initial contact between the pathogen and its target cell is imperative for host cell entry during infection (Krachler and Orth, 2013). Weak, non-specific forces that are induced by physiochemical properties, induce the initial binding of the pathogen to its host (Krachler and Orth, 2013). Subsequently, specific and transient receptor interactions allow a stronger anchorage between pathogen and host (Krachler and Orth, 2013).

Adherence molecules (adhesins), due to their surface localization and role in host-pathogen interaction, are potential novel targets for rapid TB diagnosis, antimicrobial drugs and vaccine development (Kumar et al., 2013). Adhesins are structures or molecules that are present extracellularly on the surface of the bacterial cell (Fronzes et al., 2008), and serve to fulfil a basic role which is to initiate close contact between itself and a receptor like domain on the host cell. This results in the formation of a fundamental link between the bacterium and host (Gerlach and Hensel, 2007). Figure 1.4 illustrates the role that adhesins play in the infection of their host cell. The adhesins that are present on the surface of the bacterial cell, bind to the molecules present on the host cell (in this instance, *M. tuberculosis* binding to the macrophage) (Govender et al., 2014). This results in the invasion of the bacterial cells and thereafter, its ability to survive as well as replicate within its host cell (Govender et al., 2014). Bacterial

adhesion allows the pathogen to manipulate host signalling, thereby promoting dissemination of the pathogen and evasion of host immune responses (Stones and Krachler, 2015). Adhesins have also been shown to prevent stress removal of the microorganism from the colonized host (Stones and Krachler, 2015).

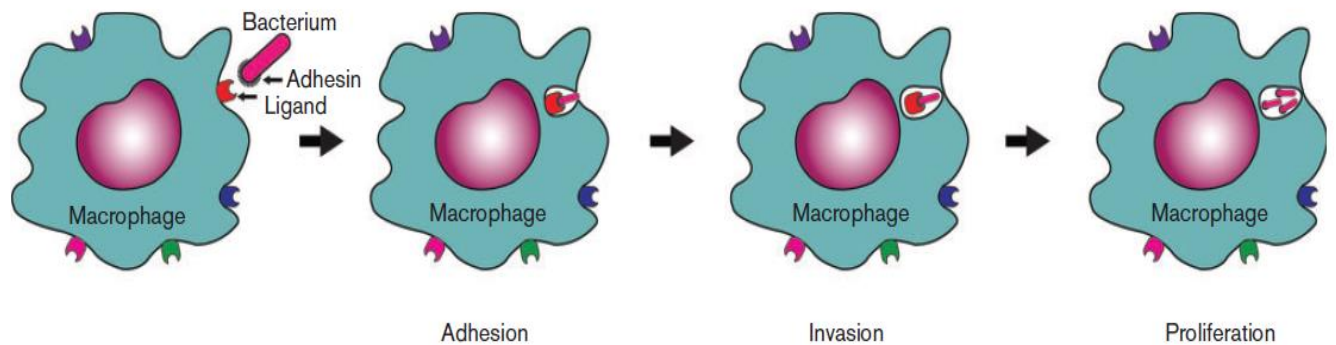


Figure 1.4. An illustration depicting the role of *M. tuberculosis* associated adhesins in host infection (Govender et al., 2014).

Mycobacterium tuberculosis has a few potential adhesins that are central to its pathogenesis (Figure 1.5 and Table 1.1). Mycobacterial adhesins refers to *M. tuberculosis* proteins that are able to form interactions with host cell receptors in order to facilitate binding to the mammalian components (Kumar et al., 2013, Govender et al., 2014). Malate synthase, is able bind to human extracellular matrix (ECM) proteins, laminin and fibronectin, via an unknown mechanism of attachment to the cell wall (Kinhikar et al., 2006). Therefore, it is characterized as an anchorless adhesin (Kumar et al., 2013). Additionally, malate synthase is also essential for glyoxylate detoxification in *M. tuberculosis* (Puckett et al., 2017). *Mycobacterium tuberculosis* chaperone protein, Cpn60.2 (GroEL2 and Hsp65), is an abundant lipoprotein (Kong et al., 1993) and acts as a CD43-dependant adhesin of the pathogen for macrophage binding (Hickey et al., 2010). Recent studies revealed an association of Cpn60.2 secretion and *M. tuberculosis* virulence (Vargas-Romero et al., 2016), and promotes *M. tuberculosis* survival in the macrophage environment (Joseph et al., 2017).

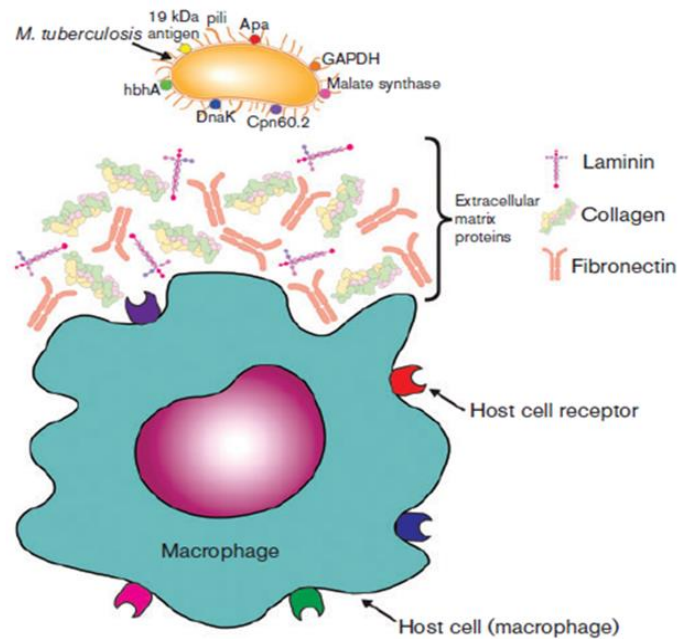


Figure 1.5. Selected mycobacterial adhesins and the various pathways that are available for initiating host interaction and subsequent colonization (Govender et al., 2014).

The alanine-proline rich antigen (Apa) mycobacterial glycoprotein, a mycobacterial adhesin, was initially considered to be a secretory molecule, but subsequent studies demonstrated it to be transiently associated with the cell wall in order to allow the attachment to the pulmonary surfactant protein- A (PSP-A) (Ragas et al., 2007, Kuo et al., 2019). Additionally, it is considered to play a central role in stimulation of immune responses and adhesion to host cells (Ragas et al., 2007, Kuo et al., 2019). A mycolyl-transferase enzyme belonging to the fibronectin-binding family or antigen 85 complex, has the ability to bind to the extracellular matrix protein fibronectin *in vitro* (Ronning et al., 2000, Kruh-Garcia et al., 2014). The properties of these adhesins provide a mechanism for colonization of tissue cells. Proline-glutamic acid, polymorphic guanine-cytosine-rich repetitive sequence (PE_PGRS) proteins have also been observed to display these fibronectin-binding properties and are part of the subfamily of glycine rich and polymorphic acidic proteins (Delogu et al., 2008).

Table 1.1. Currently known *Mycobacterium tuberculosis* adhesins (Ramsugit and Pillay, 2016)

Adhesin	Gene (s)	Mediates adhesion to	References
19-kDa antigen	<i>Rv3763</i>	Monocytes and macrophages	(Diaz-Silvestre et al., 2005, Esparza et al., 2015)
Alanine- and proline-rich antigen (Apa)	<i>Rv1860</i>	Pulmonary surfactant protein A and macrophages	(Ragas et al., 2007, Esparza et al., 2015)
Antigen 85 complex	<i>Rv0129c</i> , <i>Rv1886c</i> , <i>Rv3803c</i> , and <i>Rv3804c</i>	Fibronectin and macrophages	(Abou-Zeid et al., 1988, Esparza et al., 2015)
Cpn60.2 molecular chaperone	<i>Rv0440</i>	Macrophages	(Hickey et al., 2009, Hickey et al., 2010)
Curli pili (MTP)	<i>Rv3312A/mtp</i>	Laminin, macrophages and epithelial cells	(Alteri et al., 2007, Ramsugit et al., 2013, Ramsugit and Pillay, 2014, Ramsugit et al., 2016)
DnaK molecular chaperone	<i>Rv0350</i>	Macrophages	(Hickey et al., 2010)
Early secreted antigen ESAT-6	<i>Rv3875</i>	Laminin	(Kinhikar et al., 2006)
Glyceraldehyde-3-phosphate dehydrogenase	<i>Rv1436</i>	Possibly fibronectin (as occurs in group A streptococci)	(Pancholi and Fischetti, 1992)
Heparin-binding hemagglutinin adhesin	<i>Rv0475</i>	Epithelial cells	(Menozzi et al., 1998, Pethe et al., 2001)

Table 1.2. Currently known *Mycobacterium tuberculosis* adhesins (Ramsugit and Pillay, 2016) (continued)

Adhesin	Gene (s)	Mediates adhesion to	References
Laminin-binding protein	<i>Rv2986c</i>	Laminin	(Pethe et al., 2001)
L, D-transpeptidase	<i>Rv0309</i>	Fibronectin and laminin	(Kumar et al., 2013)
Malate synthase	<i>Rv1837c</i>	Fibronectin, laminin, and epithelial cells	(Kinhikar et al., 2006)
Membrane protein	<i>Rv2599</i>	Collagen, fibronectin, and laminin	(Kumar et al., 2013)
<i>Mycobacterium</i> cell entry-1 protein	<i>Rv0169</i>	Epithelial cells	(Chitale et al., 2001)
N-acetylmuramoyl-L-alanine amidase	<i>Rv3717</i>	Fibronectin and laminin	(Kumar et al., 2013)
PE-PGRS proteins	<i>Rv1759c</i> and <i>Rv1818c</i>	Fibronectin and macrophages	(Espitia et al., 1999, Brennan et al., 2001)
Protein kinase D	<i>Rv0931c</i>	Brain endothelia and laminin	(Brennan et al., 2001, Nicholas et al., 2012)
Type IV pili	<i>Rv3654c-Rv3660c</i>	Possibly macrophages and epithelial cells	(Alteri, 2005)

To develop accurate and effective TB therapeutics that target the initial pathogen-host interaction, appropriate proteins involved have to be identified, characterized and classified, and their role in pathogenesis established. Mycobacteria comprises various surface proteins that display primary and secondary adhesin functions that interact with host receptor cells (Table 1.2) (Menozzi et al., 2006). Amongst several *M. tuberculosis* adhesins, HBHA (Menozzi et al., 2006, Hougardy et al., 2007, Esposito et al., 2011, Esposito et al., 2012, Lebrun et al., 2012, Chiacchio et al., 2017, Govender et al., 2018) and MTP (Alteri et al., 2007, Ramsugit et al., 2013, Naidoo et al., 2014, Ramsugit and Pillay, 2014, Ramsugit et al., 2016, Govender et al., 2018) significantly emerge as potential biomarkers that may pose a target for intervention strategies.

1.9.1 Heparin-binding hemagglutinin adhesin

The most characterized mycobacterial adhesin is the 28kDa heparin-binding hemagglutinin adhesin (HBHA), a surface exposed protein (Menozzi et al., 1998, Esposito et al., 2011, Esposito et al., 2012). As a virulence factor, HBHA aids in the dissemination of *M. tuberculosis* from the site of primary infection (Pethe et al., 2001), by initiating an interaction with the host epithelial cells (Menozzi et al., 1998, Esposito et al., 2011, Esposito et al., 2012). This protein is known to facilitate the two crucial steps in TB pathogenesis, namely cell adhesion and bacterial aggregation (Figure 1.6) (Menozzi et al., 1998, Esposito et al., 2011, Esposito et al., 2012). Since it induces mycobacterial aggregation, this suggests that it would mediate bacterium-bacterium interactions as well (Menozzi et al., 1998, Esposito et al., 2011, Esposito et al., 2012). This novel adhesin is also known to promote the agglutination of rabbit erythrocytes which is known to be specifically inhibited by sulphated carbohydrates (Menozzi et al., 1996). This protein also allows the attachment to the epithelial cells that are specifically inhibited in the presence of anti-HBHA antibodies (Menozzi et al., 1998, Esposito et al., 2011, Esposito et al., 2012). An immunoblot analysis using antigen specific antibodies performed by Menozzi et al. (1996), indicated that HBHA is significantly different from the fibronectin-binding proteins of the antigen 85 complex. The comparison of the NH₂-terminal amino acid sequence of the HBHA that was purified with the data base of the protein sequence did not show any significant similarity to other known proteins (Menozzi et al., 1998).

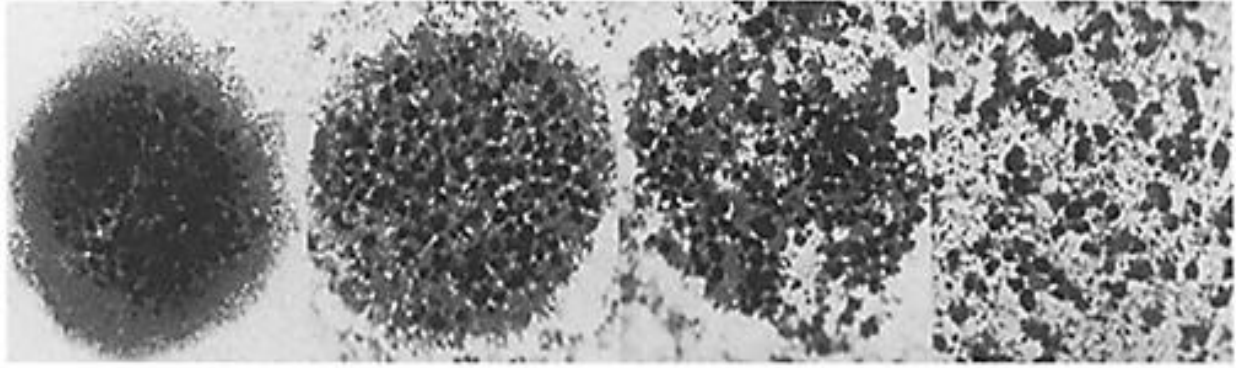


Figure 1.6. HBHA-mediated aggregation of *M. tuberculosis*. Aggregation of *M. tuberculosis* H37Ra was induced by incubating 10^8 bacteria/ mL with 5, 1.25, 0.15, or 0 μg protein/ mL final concentration (left to right) of HBHA purified from *M. tuberculosis* H37Ra. This was visualized on a 912 electron microscope (Carl Zeiss Inc., Thornwood, NY) (Menozzi et al., 1996).

Bacterial aggregation mediated by HBHA is instrumental in the formation of bacterial clumps, which allow for a more effective adherence and subsequent invasion (Esposito et al., 2012, Lebrun et al., 2012). A study by Menozzi et al. (1996) demonstrated that *M. tuberculosis* can be aggregated in a dose-dependent manner with the addition of HBHA. Maximum aggregation was observed at a starting concentration of 0.5 μg HBHA per mL (Menozzi et al., 1996).

Menozzi et al. (1996), showed a definitive role that HBHA played in facilitating host adherence whereby, antibodies that were directed against HBHA inhibited the attachment of the *Mycobacteria* to the epithelial cells. In support of this, patients that exhibit active TB have been observed to produce anti-HBHA antibodies, which suggests HBHA expression during human infection (Menozzi et al., 1998). This adhesin contains a carboxy-terminal domain that is rich in lysine, and functions to recognize heparin sulphate-containing receptors that are present on the epithelial cells (Delogu and Brennan, 1999, Pethe et al., 2001). Pethe et al. (2001) showed that the colonization of a *M. tuberculosis hbhA* mutant strain in the lungs of mice displayed an equivalence to that of the wild-type (WT) strain. However, a significant difference was observed in the reduced capacity of the mutant to disseminate from the lungs to other regions in the body, which suggests the role of HBHA in extrapulmonary spread (Pethe et al., 2001). The study also showed that an antibody against the carboxyl-terminal domain of HBHA would serve to block the binding of the bacteria to the epithelial cell receptors, and thus impede the extrapulmonary spread of *M. tuberculosis* in the mouse model (Pethe et al., 2001). This suggests that the humoral immune

response to HBHA, and possibly other mycobacterial adhesins, could potentially play a fundamental protective role in blocking dissemination from the lungs (Pethe et al., 2001).

A study by Mueller-Ortiz et al. (2002), reported a significant decrease in the infectivity despite having an unaltered human complement C3 binding by a $\Delta hbhA$ mutant of *M. tuberculosis*. This study entailed the use of a HBHA mutant strain to determine if this protein's C3-binding activity could play a role in *M. tuberculosis* pathogenesis (Mueller-Ortiz et al., 2002). The results indicated that the $\Delta hbhA$ mutation did not significantly reduce *M. tuberculosis* binding to the human C3 cell or to J774 (Mueller-Ortiz et al., 2002). Additionally, in the absence of HBHA, and other molecules, such as a C3-binding protein HupB, would serve as a C3-binding molecule of *M. tuberculosis* (Mueller-Ortiz et al., 2002). This data depicts the importance of HBHA in the infectivity of *M. tuberculosis*. However, its ability to bind to C3 is not crucial for the adherence of *M. tuberculosis* to macrophage-like cells (Mueller-Ortiz et al., 2002).

1.9.2 *Mycobacterium tuberculosis curli pili*

Bacterial pili or fimbriae, due to their ability to serve as extensions on the cell surface and not integrate within the cell, are potentially a more cost-effective option for the design of diagnostic tests (Proft and Baker, 2009). Expressed by many pathogenic bacteria as a filamentous appendage, pili are known to function in many bacterial processes which include locomotion, uptake of DNA, mediating the bacterial interaction, and colonizing the host (Kline et al., 2009). Pili are regarded as important virulence factors for many diseases that include genital, gastrointestinal and urinary infections (Proft and Baker, 2009). These appendages have been reported to play a role in various virulence-associated functions including, colonization of mucosal surfaces, biofilm formation, bacterial aggregation as well as agglutination of both animal and human erythrocytes (Strom and Lory, 1993, Finlay and Falkow, 1997, Alteri et al., 2007).

Pili, the first point of contact to the host cell, are used to overcome the net repulsive forces existing on the surface of the pathogen and host (Proft and Baker, 2009). Contact with the pili adhesins result in the induction of the host signalling cascade and activates immune response (Sauer et al., 2000, Craig et al., 2004). Pili, which are polymeric, proteinaceous, hydrophobic adhesive organelles that are produced by many pathogenic bacteria, are composed of pilin, a major repeating subunit and in some instances a minor tip associated adhesin subunit (Kline et al., 2009). Biogenesis of Gram-negative pili involves the non-covalent homopolymerization of the major pilin

to generate the pilus shaft (Proft and Baker, 2009). Four general assembly pathways distinguish Gram-negative pili. These include the, type IV pili, chaperone-usher pathway, the alternate chaperone-usher pathway, and extracellular nucleation or precipitation pathway, responsible for curli pili assembly (Proft and Baker, 2009).

Two types of pili are observed in *M. tuberculosis*, namely, Type IV pili and *M. tuberculosis* curli pili (MTP) (Alteri, 2005). Type IV pili, observed in Gram-negative and Gram-positive bacteria as well as archaeal bacteria, are surface exposed flexible filaments that tend to form bundles (Alteri et al., 2007, Berry and Pelicic, 2015). Encoded by *Rv3312A (mtp)* (Alteri, 2005), MTP was first observed in *M. lepraemurium* by negative-staining microscopy (Draper and Rees, 1970), and characterized by Alteri et al., (2007). Additionally, three different operons were found to encode type IV pili, namely; *pil*, *tad* and *com* operons (Imam et al., 2011). Type IV pili, in Gram-negative bacteria, have been observed to function in host cell adhesion, microcolony formation, twitching motility, secretion of proteins, and gliding (Aas et al., 2002, Mattick, 2002, Kirn et al., 2003, Burrows, 2005, Han et al., 2007, Burrows, 2012).

Analysis by electron microscopy revealed the various types of pili *M. tuberculosis* produces, namely; aggregative pili, fine pili and flexible pili (Alteri et al., 2007). Classified as a curli amyloid, MTP is insoluble in sodium dodecyl sulphate and characteristically binds to Congo red dye (Alteri et al., 2007). Subunits of MTP are observed to lack the typical β -sheet secondary structure of curlins and do not display any primary sequence homology to curli amyloids (Alteri et al., 2007, Ramsugit et al., 2013, Ramsugit and Pillay, 2015). Electron microscopy revealed pili exist as bundles of long filaments resembling a rope like structure (Alteri et al., 2007). Flexible pili were reported to be recognized by anti-MTP IgG antibodies contained in patient sera that tested positive for active TB, indicating that the bacilli produce pili organelles, or a pili associated antigen during the initiation of human infection (Alteri et al., 2007).

The hydrophobic nature of MTP, due to its hydrophobic amino terminal, aids in overcoming the existing net repulsive force between eukaryote and bacteria (Finlay and Falkow, 1997, Alteri, 2005). It was postulated that pili arose in *Mycobacteria* through horizontal gene transfer, possibly from *Caulobacter crescentens* and *Pseudomonas aeruginosa* (Alteri, 2005), that was supported by evidence of the direct repeats flanking the operon (Alteri et al., 2007). Curli pili, also present in pathogens such as *Salmonella typhimurium* and *Escherichia coli*, are estimated to be

approximately 2-5 nm wide (Alteri, 2005). The curli pili are coiled, highly aggregative, adhesive fibres that are assembled using the nucleation pathway that requires both the major and minor pili subunits (Pohlschroder et al., 2011). Adherence of MTP to epithelial cells, present in the lung and other tissues, are due to the adhesin's great affinity to laminin (Alteri, 2005).

Previous studies showed that surface located adhesin, MTP, is encoded by a conserved gene that is present only in *M. tuberculosis* strains (Naidoo et al., 2014) and sera of active patients are known to contain IgG antibodies against this adhesin (Alteri et al., 2007). Thus, MTP, may be a suitable biomarker candidate for the development of a POC TB test.

1.10 The 'Omics' approach to better understand *Mycobacterium tuberculosis*

Discovery of novel biomarkers can be accomplished with the use of 'omics' technologies which involves high-throughput processes (Quezada et al., 2017). Combinations of research methodologies can aid scientists to enhance current knowledge on infection processes and pathogenesis of *M. tuberculosis* (Quezada et al., 2017). Together, these methods can aid in achieving a holistic understanding of *M. tuberculosis* pathogenicity (Hasin et al., 2017). A systems biology approach that includes functional genomics, global transcriptomics and metabolomics focussing on host-pathogen interactions would contribute significantly to the discovery of potential novel biomarkers for the design of rapid diagnostic and therapeutic options.

1.10.1 Whole genomics

A study by Defelipe et al. (2016), focused on a whole genome bioinformatic approach to be used to determine the potential latent specific targets in *M. tuberculosis*. Analysis on the *M. tuberculosis* metabolic network of the whole proteome of potential reactive nitrogen and oxygen species (RNOS) sensitive as well as relevant targets was performed, which included criteria of essentiality and drug target ability. These results revealed new potential TB targets, that include inositol-3-phosphate synthase (I3PS), depicting the essentiality of transcriptomic analysis (Defelipe et al., 2016).

Functional genomics studies confirmed that *mtp* is crucial for piliation and facilitates biofilm formation (Ramsugit et al., 2013). Further studies clarified the involvement of MTP in both adhesion and invasion of THP-1 macrophages (Ramsugit and Pillay, 2014) and A549 epithelial cells (Ramsugit et al., 2016), ascertained by the differences in levels of adhesion and invasion of

MTP-deficient and MTP-proficient strains of *M. tuberculosis* V9124, obtained from a clinical drug susceptible strain of F15/LAM4/KZN family (Ramsugit and Pillay, 2014, Ramsugit et al., 2016). Furthermore, MTP minimally modulates the immune responses of the host cell in A549 pulmonary epithelial cells (Ramsugit et al., 2016), in comparison to other bacterial pili (Hedges et al., 1992, Berin et al., 2002, Xicohtencatl-Cortes et al., 2006, Ledesma et al., 2010). Although the mechanism of interaction between MTP and THP-1 macrophages is currently unknown, it is suggested that MTP indirectly adheres to the macrophage by the formation of molecular bridge via a direct reaction, using membrane-bound ligands, or indirectly, with the help of host proteins (Ramsugit and Pillay, 2014). Additionally, it was suggested that MTP reduces cytokine/chemokine induction in epithelial cells as a survival strategy (Ramsugit et al., 2016). Furthermore, a functional genomics study using MTP-proficient, MTP-deficient, HBHA-deficient, HBHA-proficient and MTP-HBHA-deficient *M. tuberculosis* V9124 strains revealed the significance of MTP and HBHA in facilitating bacterial growth and biomass formation, with no impact on the metabolic viability of *M. tuberculosis* (Govender et al., 2018).

1.10.2 Transcriptomics

Transcriptome analysis provides a dynamic link between the genome and the proteome by evaluating the global changes that occur in gene expression profiles in tissue, organs, cells or whole organisms (Parida and Kaufmann, 2010). Mvubu et al. (2016b), demonstrated the use of transcriptomics to identify differential gene expression and strain specific molecular signatures in the pulmonary epithelial cells that were induced by different strains of *M. tuberculosis*, including LAM4/F15/KZN, F28, Beijing and F11 and unique genotypes that were analysed by RNA sequencing. The results indicated that the gene expression among the strains varied and a subset of 292 genes was commonly induced by all the strains (Mvubu et al., 2016b). Approximately 240 of these 292 commonly induced were up-regulated, whilst 52 genes down-regulated (Mvubu et al., 2016b). This study provided the evidence to confirm that epithelial cells play a significant role in the innate and adaptive immune response (Mvubu et al., 2016b). Additionally, the diversity on a genetic basis of the virulent strains stimulates strain-specific and differential immune host response that potentially could impact clinical outcome, granuloma formation and downstream changes (Mvubu et al., 2016b). The molecular signatures that this study identified can potentially be used

in the design of adjunctive immunotherapies for TB infection and host-associated biomarkers (Mvubu et al., 2016b).

A further study by Mvubu et al. (2016a), used the Ingenuity Pathway Analysis (IPA) software to quantitatively analyse the enrichment of the canonical pathways as well as the networks and transcriptional factor regulation that was induced by different dominant clinical strains of *M. tuberculosis*, in Kwa-Zulu- Natal, SA, on pulmonary epithelial cells at a post infection of 48 hours. This was achieved with the use of ribonucleic acid (RNA) sequencing and bioinformatic analysis to identify differentially expressed genes. The hepatic fibrosis/hepatic satellite cell activation and the IFN signalling pathway were among the top five canonical pathways for all strains (Mvubu et al., 2016a). This study demonstrated the networks as well as the strain-specific molecular pathways in epithelial cells that were induced by the clinical strains that represent major strain families in SA and provided further evidence to support that the hyper virulent strains, such as the Beijing strain, invoke a much lower protective host response. This was displayed by the low enrichment of the immune related pathways in comparison to the LAM4/KZN/F15, F28 and the F11 genotypes (Mvubu et al., 2016a).

The phenotypic adjustments of *M. tuberculosis* are frequently inferred from the analysis of transcript abundance. Whilst there has been extensive analysis on the transcriptional regulation of *Mycobacteria*, much remains unknown about the mechanisms regulating RNA decay rates that shape the transcriptome. A study by Płociński et al. (2019), aimed to identify core components of *M. tuberculosis* RNA degradosome and analyse its function in RNA metabolism with the use of an approach involving cross-linking to 4-thiouridine-labelled RNA. The engineering and the transcriptional profiling of the strains observed to have a reduced expression level of core degradosome ribonucleases provided crucial evidence that suggested the important pleiotropic roles these enzymes play in the RNA metabolism of *Mycobacteria*, and highlights its potential vulnerability as a drug target (Płociński et al., 2019).

1.10.2.1 Global transcriptomics enhances current knowledge on MTP and HBHA

A global transcriptomic study, in a mouse model of infection, investigated the role MTP plays in pathogenesis, by evaluating its role in host-pathogen interactions and host immune responses, using MTP-proficient and MTP-deficient *M. tuberculosis* V9124 strains (Nyawo, 2016). Growth

assays revealed that the MTP-deficient strain displayed a significantly decreased growth rate, relative to the WT, suggesting that MTP facilitates the growth rate of the pathogen (Nyawo, 2016). Additionally, MTP plays a significant role in host-pathogen interactions leading to infection, resulting in host immune response crucial to the host defence by triggering inflammatory and innate immune response (Nyawo, 2016). Moreover, MTP is associated with regulation of immune response, by cytokines and transcriptional factors (Nyawo, 2016). This study demonstrated MTP to be a robust immunogen (Nyawo, 2016).

Investigations on the *in vitro* role of MTP in induction of host immune response was performed by RNA sequencing of pulmonary A549 epithelial cells infected by MTP-proficient and MTP-deficient *M. tuberculosis* V9124 strains (Dlamini, 2016). The findings suggested that *mtp* affects gene regulation of A549 alveolar epithelial cells and its presence allows an increased expression of host immune response associated genes such as cell surface receptors (Dlamini, 2016).

Previous studies investigated the combined effect of HBHA and MTP on adhesion and invasion in a THP-1 human macrophage model (Moodley et al., 2018, unpublished). A lower bacillary load was observed in the MTP-deficient strain, relative to the WT, at examined intervals which include a four-hour post infection (Moodley et al., 2018, unpublished). The results suggested that these combined adhesins influence transcriptional changes to favour adhesion and subsequent invasion of macrophages (Moodley et al., 2018, unpublished).

1.10.3 Metabolomics

Metabolomics has proved to be an effective tool, over the last decade, in the pursuit to identify both novel prognostic and diagnostic markers and risk factors (Dunn and Ellis, 2005). Defined as the unbiased identification and quantification of all metabolic intermediates in a biological system, metabolomics encompass the use of both analytical techniques and mathematical and biostatistical analysis (Schoeman and Du Preez, 2012, de Villiers and Du Loots, 2013). A study performed by Olivier and Loots (2012), focused on the use of a gas chromatography and mass spectrometry (GC-MS) metabolomics approach to characterize and differentiate various infectious *Mycobacterium* species, that included *M. bovis*, *M. tuberculosis*, *M. avium* and *M. kansasii*, on the basis of their characteristic lipid profiles. The study led to the identification of 12 lipid biomarkers that were

used to build a multivariate discriminate model that could correctly assign an unknown sample to its respective species group with a probability ranging from 72-100% (Olivier, 2012).

A similar approach was used in a study by Che et al. (2013), to find diagnostic markers for active TB that was not influenced by TB treatment. This was achieved by comparing the serum samples that were collected from healthy controls and TB patients before and after they started TB therapy (Che et al., 2013). This study demonstrated a total of nine potential diagnostic TB markers that remained unaffected by first line TB therapy, including 5-oxoproline (Che et al., 2013). A further study was then performed by Luies et al. (2017), to predict tuberculosis treatment outcomes with the use of metabolomics. This was achieved by analysing urine samples that were collected at baseline from TB-positive patients that had both successful and unsuccessful treatment outcome. Two possible predictors were identified, which were associated with the gut microbiota imbalance (Che et al., 2013). Hence, the findings demonstrated the capacity of metabolomics to be used to predict TB treatment failure at the time of diagnosis which potentially offers a significant benefit for use in individualized patient care and new drug development clinical trials (Luies et al., 2017). These studies indicated the capacity of metabolomics to identify novel, useful biomarkers that can be used for early prediction of a treatment outcome as well as to differentiate *M. tuberculosis* from other *Mycobacterium* strains and its possible use in the development of new TB drugs (Luies et al., 2017).

A metabolomics study investigating the role of MTP in modulation of *M. tuberculosis* metabolism was performed using MTP-proficient and MTP-deficient *M. tuberculosis* V9124 strains (Ashokcoomar et al., 2020). Two-dimensional gas chromatography time-of-flight mass spectrometry and bioinformatic tools were used to analyse *M. tuberculosis* metabolites (Ashokcoomar et al., 2020). The results revealed a total of 28 metabolites which were significantly altered in the MTP-deficient strain, relative to the WT, associated with cell wall biogenesis, reduction in amino acid synthesis and fatty acid hydrolysis (Ashokcoomar et al., 2020). This suggests that the absence of MTP results in cell wall alterations and associated metabolic perturbations, thus, highlighting the importance of this adhesin as a virulence factor and suitable biomarker candidate (Ashokcoomar et al., 2020). Furthermore, a subsequent study investigated the role of MTP in modulation of host-pathogen metabolic pathways in a A549 pulmonary epithelial model of infection, using MTP proficient and deficient strains of *M. tuberculosis* V9124 (Reedoy

et al., 2020). Significantly lower concentrations of 46 metabolites were observed in the MTP-deficient strain, relative to the WT (Ashokcoomar et al., 2020). This indicates a significant reduction in peptidoglycan, nucleic acid synthesis, oxidative stress, glutathione and amino acid metabolism, highlighting the significance of this adhesin in *M. tuberculosis* pathogenicity (Reedoy et al., 2020). Metabolomic investigations in a THP-1 macrophage infection model, using MTP proficient and deficient strains of *M. tuberculosis* V9124, revealed significantly elevated concentrations of nine metabolites in the MTP-deficient infection model (Ashokcoomar et al., 2021). These observations indicated that in the absence of MTP, amino acid, carbon and fatty acid metabolism are altered during host infection, suggesting the pertinent role of MTP in TB pathogenesis by modulation of host metabolic activity (Ashokcoomar et al., 2021).

1.11 Significance of study

Collectively the above-mentioned studies indicate the potential of MTP and HBHA as suitable TB biomarkers or targets for novel vaccine and drug development. However, understanding the individual and combined role these adhesins play in the regulation of *M. tuberculosis* transcriptome is yet to be deciphered. Therefore, using global transcriptomics, RT-qPCR and a phenotypic assay, this study assessed the influence that MTP and HBHA have on the bacterial transcriptome, alone and combined, thereby, further substantiating their potential as suitable candidates for intervention therapies against TB.

1.12. Research design

1.12.1 Aim

To determine the effect of MTP and HBHA on global *in vitro* bacterial transcriptomics using RNA sequencing and *mtp* and *hbhA* gene knockout and complemented mutants of *M. tuberculosis*.

1.12.2 Objectives

1. To culture Δmtp -*hbhA*, Δmtp and $\Delta hbhA$ gene deletion mutants, complements and WT strains of *M. tuberculosis* in liquid media
2. To confirm the gene knockout mutants using PCR
3. To perform bacterial RNA extraction on all strains from broth culture

4. To submit RNA extracted from broth cultures for sequencing
5. To conduct bioinformatic analysis on the RNA sequencing data
6. To use RT-qPCR to validate RNA sequencing results and to determine bacterial gene expression of selected genes involved in cellular respiration and metabolism, and cell wall processes in *M. tuberculosis*
7. To perform statistical analysis to identify any significant differences between strains using GraphPad prism to perform unpaired, parametric *t*-tests
8. To phenotypically validate RNA sequencing and RT-qPCR data by performing a bacterial bioluminescent cell viability assay and statistically analyse results using GraphPad prism to perform unpaired, parametric *t*-tests

1.13 References

- Aas, F. E., Wolfgang, M., Frye, S., Dunham, S., Løvold, C. & Koomey, M. 2002. Competence for natural transformation in *Neisseria gonorrhoeae*: components of DNA binding and uptake linked to type IV pilus expression. *Molecular Microbiology*, 46, 749-760.
- Abanda, N. N., Djieugoue, J. Y., Khadka, V. S., Pefura-Yone, E. W., Mbacham, W. F., Vernet, G., Penlap, V. M., Deng, Y., Eyangoh, S. I., Taylor, D. W. & Leke, R. G. F. 2018. Absence of hybridization with the wild-type and mutant *rpoB* probes in the Genotype MTBDRplus assays detects 'disputed' rifampicin mutations. *Clinical Microbiology and Infection*, 24, 781-e1.
- Abebe, F., Holm-Hansen, C., Wiker, H. & Bjune, G. 2007. Progress in serodiagnosis of *Mycobacterium tuberculosis* infection. *Scandinavian Journal of Immunology*, 66, 176-191.
- Abou-Zeid, C., Ratliff, T., Wiker, H., Harboe, M., Bennedsen, J. & Rook, G. 1988. Characterization of fibronectin-binding antigens released by *Mycobacterium tuberculosis* and *Mycobacterium bovis* BCG. *Infection and Immunity*, 56, 3046-3051.
- Adekambi, T., Ibegbu, C. C., Kalokhe, A. S., Yu, T., Ray, S. M. & Rengarajan, J. 2012. Distinct effector memory CD4⁺ T cell signatures in latent *Mycobacterium tuberculosis* infection, BCG vaccination and clinically resolved tuberculosis. *PLoS One*, 7, e36046.
- Agranoff, D., Fernandez-Reyes, D., Papadopoulos, M. C., Rojas, S. A., Herbst, M., Loosemore, A., Tarelli, E., Sheldon, J., Schwenk, A. & Pollok, R. 2006. Identification of diagnostic markers for tuberculosis by proteomic fingerprinting of serum. *The Lancet*, 368, 1012-1021.
- Aguilo, N., Uranga, S., Marinova, D., Monzon, M., Badiola, J. & Martin, C. 2016. MTBVAC vaccine is safe, immunogenic and confers protective efficacy against *Mycobacterium tuberculosis* in newborn mice. *Tuberculosis*, 96, 71-74.
- Ahmad, N., Ahuja, S., Akkerman, O., Alffenaar, J., Anderson, L. & Baghaei, P. 2018. Collaborative Group for the Meta-Analysis of Individual Patient Data in MDR-TB treatment–2017. Treatment correlates of successful outcomes in pulmonary multidrug-resistant tuberculosis: an individual patient data meta-analysis. *The Lancet*, 392, 821-34.

- Alteri, C. 2005. Novel pili of *Mycobacterium tuberculosis*. PhD thesis. University of Arizona, Arizona, United States of America.
- Alteri, C. J., Xicohténcatl-Cortes, J., Hess, S., Caballero-Olín, G., Girón, J. A. & Friedman, R. L. 2007. *Mycobacterium tuberculosis* produces pili during human infection. *Proceedings of the National Academy of Sciences*, 104, 5145-5150.
- Amunda, B. O., Oduyebo, O. O. & Abutu, P. 2020. Detection of Multi-Drug Resistant Tuberculosis using the Genotype MTBDR DNA strip Assay and Lowenstein Jenson Proportion method. *Asian Journal of Research in Infectious Diseases*, 11-22.
- Andersen, P. & Doherty, T. M. 2005. The success and failure of BCG—implications for a novel tuberculosis vaccine. *Nature Reviews Microbiology*, 3, 656-662.
- Angala, S. K., Belardinelli, J. M., Huc-Claustre, E., Wheat, W. H. & Jackson, M. 2014. The cell envelope glycoconjugates of *Mycobacterium tuberculosis*. *Critical Reviews in Biochemistry and Molecular Biology*, 49, 361-399.
- Asmar, S., Chatellier, S., Mirande, C., van Belkum, A., Canard, I., Raoult, D. & Drancourt, M. 2015. A novel solid medium for culturing *Mycobacterium tuberculosis* isolates from clinical specimens. *Journal of Clinical Microbiology*, 53, 2566-2569.
- Ashokcoomar, S., Reedoy, K., Senzani, S., Loots, D., Beukes, D., van Reenen, M., Pillay, B. & Pillay, M. 2020. *Mycobacterium tuberculosis* curli pili (MTP) deficiency is associated with alterations in cell wall biogenesis, fatty acid metabolism and amino acid synthesis. *Metabolomics*, 16, 1-15.
- Ashokcoomar, S., Beukes, D., van Reenen, M., Pillay, B. and Pillay, M., 2021. *M. tuberculosis* curli pili (MTP) is associated with alterations in carbon, fatty acid and amino acid metabolism in a THP-1 macrophage infection model. *Microbial Pathogenesis*, 154, 104806.
- Avert. 2018. *HIV and AIDS in South Africa [Online]* [Online]. Available: <https://www.avert.org/professionals/hiv-around-world/sub-saharan-africa/south-africa> [Accessed].
- Azzurri, A., Sow, O. Y., Amedei, A., Bah, B., Diallo, S., Peri, G., Benagiano, M., D'elios, M. M., Mantovani, A. & Del Prete, G. 2005. IFN-gamma-inducible protein 10 and pentraxin 3 plasma levels are tools for monitoring inflammation and disease activity in *Mycobacterium tuberculosis* infection. *Microbes and Infection*, 7, 1-8.
- Baldwin, S. L., Reese, V. A., Po-wei, D. H., Beebe, E. A., Podell, B. K., Reed, S. G. & Coler, R. N. 2016. Protection and long-lived immunity induced by the ID93/GLA-SE vaccine candidate against a clinical *Mycobacterium tuberculosis* isolate. *Clinical and Vaccine Immunology*, 23, 137-147.
- Barnard, M., Albert, H., Coetzee, G., O'Brien, R. & Bosman, M. E. 2008. Rapid molecular screening for multidrug-resistant tuberculosis in a high-volume public health laboratory in South Africa. *American Journal of Respiratory and Critical Care Medicine*, 177, 787-792.
- Behr, M., Wilson, M., Gill, W., Salamon, H., Schoolnik, G., Rane, S. & Small, P. 1999. Comparative genomics of BCG vaccines by whole-genome DNA microarray. *Science*, 284, 1520-1523.
- Bekker, L.-G., Dintwe, O., Fiore-Gartland, A., Middelkoop, K., Hutter, J., Williams, A., Randhawa, A. K., Ruhwald, M., Kromann, I. & Andersen, P. L. 2020. A phase 1b randomized study of the safety and immunological responses to vaccination with H4: IC31, H56: IC31, and BCG revaccination in *Mycobacterium tuberculosis*-uninfected adolescents in Cape Town, South Africa. *EClinicalMedicine*, 100313.

- Berin, M. C., Darfeuille-Michaud, A., Egan, L. J., Miyamoto, Y. & Kagnoff, M. F. 2002. Role of EHEC O157: H7 virulence factors in the activation of intestinal epithelial cell NF- κ B and MAP kinase pathways and the upregulated expression of interleukin 8. *Cellular Microbiology*, 4, 635-648.
- Berry, J.-L. & Pelicic, V. 2015. Exceptionally widespread nanomachines composed of type IV pilins: the prokaryotic Swiss Army knives. *Federation of European Microbiological Societies Microbiology Reviews*, 39, 134-154.
- Berry, M. P. R., Blankley, S., Graham, C. M., Bloom, C. I. & O'Garra, A. 2013. Systems approaches to studying the immune response in tuberculosis. *Current Opinion in Immunology*, 25, 579-587.
- Bloom, B. R. & Murray, C. J. 1992. Tuberculosis: commentary on a reemergent killer. *Science*, 257, 1055-64.
- Brennan, M. J., Delogu, G., Chen, Y., Bardarov, S., Kriakov, J., Alavi, M. & Jacobs, W. R. 2001. Evidence that mycobacterial PE_PGRS proteins are cell surface constituents that influence interactions with other cells. *Infection and Immunity*, 69, 7326-7333.
- Brennan, P. J. & Crick, D. C. 2007. The cell-wall core of *Mycobacterium tuberculosis* in the context of drug discovery. *Current Topics in Medicinal Chemistry*, 7, 475-488.
- Brosch, R., Gordon, S. V., Marmiesse, M., Brodin, P., Buchrieser, C., Eiglmeier, K., Garnier, T., Gutierrez, C., Hewinson, G. & Kremer, K. 2002. A new evolutionary scenario for the *Mycobacterium tuberculosis* complex. *Proceedings of the National Academy of Sciences*, 99, 3684-3689.
- Bruns, H. & Stenger, S. 2014. New insights into the interaction of *Mycobacterium tuberculosis* and human macrophages. *Future Microbiology*, 9, 327-341.
- Burrows, L. L. 2005. Weapons of mass retraction. *Molecular Microbiology*, 57, 878-888.
- Burrows, L. L. 2012. Prime time for minor subunits of the type II secretion and type IV pilus systems. *Molecular Microbiology*, 86, 765-769.
- Calmette, A. & Plotz, H. 1929. Protective inoculation against tuberculosis with BCG. *American Review of Tuberculosis*, 19, 567-572.
- Calmette, A. 1931. Preventive Vaccination Against Tuberculosis with BCG. *Proceedings of the Royal Society of Medicine*, 24, 1481-90.
- Cannas, A., Goletti, D., Girardi, E., Chiacchio, T., Calvo, L., Cuzzi, G., Piacentini, M., Melkonyan, H., Umansky, S. & Lauria, F. 2008. *Mycobacterium tuberculosis* DNA detection in soluble fraction of urine from pulmonary tuberculosis patients. *The International Journal of Tuberculosis and Lung Disease*, 12, 146-151.
- Che, N., Cheng, J., Li, H., Zhang, Z., Zhang, X., Ding, Z., Dong, F. & Li, C. 2013. Decreased serum 5-oxoproline in TB patients is associated with pathological damage of the lung. *Clinica Chimica Acta*, 423, 5-9.
- Chegou, N. N., Detjen, A. K., Thiart, L., Walters, E., Mandalakas, A. M., Hesselning, A. C. & Walzl, G. 2013. Utility of host markers detected in Quantiferon supernatants for the diagnosis of tuberculosis in children in a high-burden setting. *PLoS One*, 8, e64226.
- Chiacchio, T., Delogu, G., Vanini, V., Cuzzi, G., De Maio, F., Pinnetti, C., Sampaolesi, A., Antinori, A. & Goletti, D. 2017. Immune characterization of the HBHA-specific response in *Mycobacterium tuberculosis*-infected patients with or without HIV infection. *PLoS One*, 12, e0183846.

- Chitale, S., Ehrh, S., Kawamura, I., Fujimura, T., Shimono, N., Anand, N., Lu, S., Cohen-Gould, L. & Riley, L. W. 2001. Recombinant *Mycobacterium tuberculosis* protein associated with mammalian cell entry. *Cellular Microbiology*, 3, 247-254.
- Claassens, M., Van Schalkwyk, C., Den Haan, L., Floyd, S., Dunbar, R., Van Helden, P., Godfrey-Faussett, P., Ayles, H., Borgdorff, M. & Enarson, D. 2013. High prevalence of tuberculosis and insufficient case detection in two communities in the Western Cape, South Africa. *Plos One*, 8, E58689.
- Cole, S. T., Brosch, R., Parkhill, J., Garnier, T., Churcher, C., Harris, D., Gordon, S. V., Eiglmeier, K., Gas, S., Barry, C. E., 3rd, Tekaia, F., Badcock, K., Basham, D., Brown, D., Chillingworth, T., Connor, R., Davies, R., Devlin, K., Feltwell, T., Gentles, S., Hamlin, N., Holroyd, S., Hornsby, T., Jagels, K., Krogh, A., Mclean, J., Moule, S., Murphy, L., Oliver, K., Osborne, J., Quail, M. A., Rajandream, M. A., Rogers, J., Rutter, S., Seeger, K., Skelton, J., Squares, R., Squares, S., Sulston, J. E., Taylor, K., Whitehead, S. & Barrell, B. G. 1998. Deciphering the biology of *Mycobacterium tuberculosis* from the complete genome sequence. *Nature*, 393, 537-44.
- Comas, I., Homolka, S., Niemann, S. & Gagneux, S. 2009. Genotyping of genetically monomorphic bacteria: DNA sequencing in *Mycobacterium tuberculosis* highlights the limitations of current methodologies. *PLoS One*, 4, e7815.
- Comas, I., Coscolla, M., Luo, T., Borrell, S., Holt, K. E., Kato-Maeda, M., Parkhill, J., Malla, B., Berg, S. & Thwaites, G. 2013. Out-of-Africa migration and Neolithic coexpansion of *Mycobacterium tuberculosis* with modern humans. *Nature Genetics*, 45, 1176-1182.
- Craig, L., Pique, M. E. & Tainer, J. A. 2004. Type IV pilus structure and bacterial pathogenicity. *Nature Reviews Microbiology*, 2, 363-378.
- Crandall, E.D. and Kim, K.J., 1991. Alveolar epithelial barrier properties. *The Lung: Scientific Foundation*, 273-287.
- Cruz-Knight, W. & Blake-Gumbs, L. 2013. Tuberculosis: an overview. *Primary Care: Clinics in Office Practice*, 40, 743-756.
- Daffe, M. & Reyrat, J.-M. 2008. The mycobacterial cell envelope, *ASM Press*.
- Daniels, M. & Hill, A. B. 1952. Chemotherapy of pulmonary tuberculosis in young adults. *British Medical Journal*, 1, 1162.
- de Villiers, L. & Du Loots, T. 2013. Using metabolomics for elucidating the mechanisms related to tuberculosis treatment failure. *Current Metabolomics*, 1, 306-317.
- Defelipe, L. A., Do Porto, D. F., Ramos, P. I. P., Nicolás, M. F., Sosa, E., Radusky, L., Lanzarotti, E., Turjanski, A. G. & Marti, M. A. 2016. A whole genome bioinformatic approach to determine potential latent phase specific targets in *Mycobacterium tuberculosis*. *Tuberculosis*, 97, 181-192.
- Delogu, G. & Brennan, M. J. 1999. Functional domains present in the mycobacterial hemagglutinin, HBHA. *Journal of Bacteriology*, 181, 7464-7469.
- Delogu, G., Cole, S. T. & Brosch, R. 2008. The PE and PPE protein families of *Mycobacterium tuberculosis*. *Handbook of Tuberculosis*, 131-150.
- Diaz-Silvestre, H., Espinosa-Cueto, P., Sanchez-Gonzalez, A., Esparza-Ceron, M. A., Pereira-Suarez, A. L., Bernal-Fernandez, G., Espitia, C. & Mancilla, R. 2005. The 19-kDa antigen of *Mycobacterium tuberculosis* is a major adhesin that binds the mannose receptor of THP-1 monocytic cells and promotes phagocytosis of mycobacteria. *Microbial Pathogenesis*, 39, 97-107.

- Dlamini, M. T. 2016. 'Whole transcriptome analysis to elucidate the role of *mtp* in gene regulation of pulmonary epithelial cells infected with *Mycobacterium tuberculosis*.' Unpublished Masters thesis. University of KwaZulu-Natal, Durban, South Africa.
- Draper, P. & Rees, R. 1970. Electron-transparent zone of mycobacteria may be a defence mechanism. *Nature*, 228, 860-861.
- Du Preez, I., Luies, L. & Loots, D. T. 2017. Metabolomics biomarkers for tuberculosis diagnostics: Current Status and Future Objectives. *Biomarkers in Medicine*, 11(2), 179-194.
- Ducati, R. G., Ruffino-Netto, A., Basso, L. A. & Santos, D. S. 2006. The resumption of consumption: a review on tuberculosis. *Memórias do Instituto Oswaldo Cruz*, 101, 697-714.
- Dunn, W. B. & Ellis, D. I. 2005. Metabolomics: current analytical platforms and methodologies. *TrAC Trends in Analytical Chemistry*, 24, 285-294.
- El-Sony, A., Enarson, D., Khamis, A., Baraka, O. & Bjune, G. 2002. Relation of grading of sputum smears with clinical features of tuberculosis patients in routine practice in Sudan. *The International Journal of Tuberculosis and Lung Disease*, 6, 91-97.
- Esparza, M., Palomares, B., García, T., Espinosa, P., Zenteno, E. & Mancilla, R. 2015. PstS-1, the 38-kDa *Mycobacterium tuberculosis* Glycoprotein, is an Adhesin, Which Binds the Macrophage Mannose Receptor and Promotes Phagocytosis. *Scandinavian Journal of Immunology*, 81, 46-55.
- Espitia, C., Laclette, J. P., Mondragón-Palomino, M., Amador, A., Campuzano, J., Martens, A., Singh, M., Cicero, R., Zhang, Y. & Moreno, C. 1999. The PE-PGRS glycine-rich proteins of *Mycobacterium tuberculosis*: a new family of fibronectin-binding proteins? The GenBank accession number for the sequence reported in this paper is AF071081. *Microbiology*, 145, 3487-3495.
- Esposito, C., Marasco, D., Delogu, G., Pedone, E. & Berisio, R. 2011. Heparin-binding hemagglutinin HBHA from *Mycobacterium tuberculosis* affects actin polymerisation. *Biochemical and Biophysical Research Communications*, 410, 339-344.
- Esposito, C., Cantisani, M., D'Auria, G., Falcigno, L., Pedone, E., Galdiero, S. & Berisio, R. 2012. Mapping key interactions in the dimerization process of HBHA from *Mycobacterium tuberculosis*, insights into bacterial agglutination. *Federation of European Biochemical Societies Letters*, 586, 659-667.
- Finlay, B. B. & Falkow, S. 1997. Common themes in microbial pathogenicity revisited. *Microbiology and Molecular Biology Reviews*, 61, 136-69.
- Fletcher, H.A. and Dockrell, H.M., 2016. Human biomarkers: Can they help us to develop a new tuberculosis vaccine? *Future Microbiology*, 11(6), pp.781-787.
- Fogel, N. 2015. Tuberculosis: a disease without boundaries. *Tuberculosis*, 95, 527-531.
- Fronzes, R., Remaut, H. & Waksman, G. 2008. Architectures and biogenesis of non-flagellar protein appendages in Gram-negative bacteria. *The EMBO journal*, 27, 2271-2280.
- García-Basteiro, A. L., DiNardo, A., Saavedra, B., Silva, D. R., Palmero, D., Gegia, M., Migliori, G. B., Duarte, R., Mambuque, E. & Centis, R. 2018. Point of care diagnostics for tuberculosis. *Pulmonology*, 24, 73-85.
- Garcia-Prats, A. J., Schaaf, H. S. & Hesselning, A. C. 2016. The safety and tolerability of the second-line injectable antituberculosis drugs in children. *Expert Opinion on Drug Safety*, 15, 1491-1500.
- Goldenhuis, H., Mearns, H., Miles, D. J., Tameris, M., Hokey, D., Shi, Z., Bennett, S., Andersen, P., Kromann, I., Hoff, S. T., Hanekom, W. A., Mahomed, H., Hatherill, M., Scriba, T. J.,

- Van Rooyen, M., Bruce McClain, J., Ryall, R. & De Bruyn, G. 2015. The tuberculosis vaccine H4:IC31 is safe and induces a persistent polyfunctional CD4 T cell response in South African adults: A randomized controlled trial. *Vaccine*, 33, 3592-9.
- Gerlach, R. G. & Hensel, M. 2007. Protein secretion systems and adhesins: the molecular armory of Gram-negative pathogens. *International Journal of Medical Microbiology*, 297, 401-415.
- Gillespie, S. H. 2002. Evolution of drug resistance in *Mycobacterium tuberculosis*: clinical and molecular perspective. *Antimicrobial Agents and Chemotherapy*, 46, 267-274.
- Ginsberg, A. M. & Spigelman, M. 2007. Challenges in tuberculosis drug research and development. *Nature Medicine*, 13, 290-294.
- Goletti, D., Petruccioli, E., Joosten, S. A. & Ottenhoff, T. H. 2016. Tuberculosis biomarkers: from diagnosis to protection. *Infectious Disease Reports*, 8.
- Goossens, N., Nakagawa, S., Sun, X. & Hoshida, Y. 2015. Cancer biomarker discovery and validation. *Translational Cancer Research*, 4, 256-269.
- Govender, V. S., Ramsugit, S. & Pillay, M. 2014. *Mycobacterium tuberculosis* adhesins: potential biomarkers as anti-tuberculosis therapeutic and diagnostic targets. *Microbiology*, 160, 1821-1831.
- Govender, V. S., Jain, P., Larsen, M. H. & Pillay, M. 2018. '*Mycobacterium tuberculosis* heparin binding hemagglutinin adhesin (HBHA) and curli pili (MTP) are essential for in vitro growth, but not viability and biofilm production.' Unpublished Manuscript from the PhD thesis. University of Kwa-Zulu- Natal, Durban, South Africa.
- Grode, L., Ganoza, C. A., Brohm, C., Weiner, J., 3rd, Eisele, B. & Kaufmann, S. H. 2013. Safety and immunogenicity of the recombinant BCG vaccine VPM1002 in a phase 1 open-label randomized clinical trial. *Vaccine*, 31, 1340-8.
- Han, X., Kennan, R. M., Parker, D., Davies, J. K. & Rood, J. I. 2007. Type IV fimbrial biogenesis is required for protease secretion and natural transformation in *Dichelobacter nodosus*. *Journal of Bacteriology*, 189, 5022-5033.
- Hasegawa, N., Miura, T., Ishii, K., Yamaguchi, K., Lindner, T. H., Merritt, S., Matthews, J. D. & Siddiqi, S. H. 2002. New simple and rapid test for culture confirmation of *Mycobacterium tuberculosis* complex: a multicenter study. *Journal of Clinical Microbiology*, 40, 908-912.
- Hasin, Y., Seldin, M. & Lusic, A. 2017. Multi-omics approaches to disease. *Genome biology*, 18, 1-15.
- Hedges, S., Svensson, M. & Svanborg, C. 1992. Interleukin-6 response of epithelial cell lines to bacterial stimulation in vitro. *Infection and Immunity*, 60, 1295-1301.
- Heidebrecht, C. L., Podewils, L. J., Pym, A., Mthiyane, T. & Cohen, T. 2016. Assessing local risk of rifampicin-resistant tuberculosis in Kwa-Zulu- Natal, South Africa using lot quality assurance sampling. *PLoS One*, 11, e0153143.
- Helmy, N., Kamel, M., Ashour, W. & El Kattan, E. 2012. Role of Quantiferon TB gold assays in monitoring the efficacy of antituberculosis therapy. *Egyptian Journal of Chest Diseases and Tuberculosis*, 61, 329-336.
- Hestvik, A. L. K., Hmama, Z. & Av-Gay, Y. 2005. Mycobacterial manipulation of the host cell. *Federation of European Microbiological Societies Microbiology Reviews*, 29, 1041-1050.
- Hickey, T. B., Thorson, L. M., Speert, D. P., Daffé, M. & Stokes, R. W. 2009. *Mycobacterium tuberculosis* Cpn60. 2 and DnaK are located on the bacterial surface, where Cpn60. 2 facilitates efficient bacterial association with macrophages. *Infection and Immunity*, 77, 3389-3401.

- Hickey, T. B., Ziltener, H. J., Speert, D. P. & Stokes, R. W. 2010. *Mycobacterium tuberculosis* employs Cpn60. 2 as an adhesin that binds CD43 on the macrophage surface. *Cellular Microbiology*, 12, 1634-1647.
- Hillemann, D., Rüscher-Gerdes, S. & Richter, E. 2007. Evaluation of the GenoType MTBDRplus assay for rifampin and isoniazid susceptibility testing of *Mycobacterium tuberculosis* strains and clinical specimens. *Journal of Clinical Microbiology*, 45, 2635-2640.
- Hopprich, R., Shephard, L., Taing, B., Kralj, S., Smith, A. & Lumb, R. 2012. Evaluation of (SD) MPT64 antigen rapid test, for fast and accurate identification of *Mycobacterium tuberculosis* complex. *Pathology*, 44, 642-643.
- Hougardy, J.-M., Schepers, K., Place, S., Drowart, A., Lechevin, V., Verscheure, V., Debrie, A.-S., Doherty, T. M., Van Vooren, J.-P. & Loch, C. 2007. Heparin-binding-hemagglutinin - induced IFN- γ release as a diagnostic tool for latent tuberculosis. *PLoS One*, 2, e926.
- Hughes, J. & Osman, M. 2014. Diagnosis and management of drug-resistant tuberculosis in South African adults. *South African Medical Journal*, 104, 894.
- Imam, S., Chen, Z., Roos, D. S. & Pohlschröder, M. 2011. Identification of surprisingly diverse type IV pili, across a broad range of gram-positive bacteria. *PLoS One*, 6, e28919.
- Jankute, M., Cox, J. A., Harrison, J. & Besra, G. S. 2015. Assembly of the mycobacterial cell wall. *Annual Review of Microbiology*, 69, 405-423.
- Joseph, S., Yuen, A., Singh, V. & Hmama, Z. 2017. *Mycobacterium tuberculosis* Cpn60. 2 (GroEL2) blocks macrophage apoptosis via interaction with mitochondrial mortalin. *Biology Open*, 6, 481-488.
- Kalscheuer, R., Palacios, A., Anso, I., Cifuentes, J., Anguita, J., Jacobs Jr, W. R., Guerin, M. E. & Prados-Rosales, R. 2019. The *Mycobacterium tuberculosis* capsule: a cell structure with key implications in pathogenesis. *Biochemical Journal*, 476, 1995-2016.
- Kannan, I. D. 2016. *Essentials of Microbiology for Nurses*, -Ebook, Elsevier Health Sciences.
- Karim, S. S. A., Churchyard, G. J., Karim, Q. A. & Lawn, S. D. 2009. HIV infection and tuberculosis in South Africa: an urgent need to escalate the public health response. *The Lancet*, 374, 921-933.
- Kinhikar, A. G., Vargas, D., Li, H., Mahaffey, S. B., Hinds, L., Belisle, J. T. & Laal, S. 2006. *Mycobacterium tuberculosis* malate synthase is a laminin-binding adhesin. *Molecular Microbiology*, 60, 999-1013.
- Kirn, T. J., Bose, N. & Taylor, R. K. 2003. Secretion of a soluble colonization factor by the TCP type 4 pilus biogenesis pathway in *Vibrio cholerae*. *Molecular Microbiology*, 49, 81-92.
- Kleinnijenhuis, J., Oosting, M., Joosten, L. A., Netea, M. G. & Van Crevel, R. 2011. Innate immune recognition of *Mycobacterium tuberculosis*. *Clinical and Developmental Immunology*, 2011,405310.
- Klemm, P. & Schembri, M. A. 2000. Bacterial adhesins: function and structure. *International Journal of Medical Microbiology*, 290, 27-35.
- Kline, K. A., Fälker, S., Dahlberg, S., Normark, S. & Henriques-Normark, B. 2009. Bacterial adhesins in host-microbe interactions. *Cell Host & Microbe*, 5, 580-592.
- Klopper, M., Warren, R. M., Hayes, C., van Pittius, N. C. G., Streicher, E. M., Müller, B., Sirgel, F. A., Chabula-Nxiweni, M., Hoosain, E. & Coetzee, G. 2013. Emergence and spread of extensively and totally drug-resistant tuberculosis, South Africa. *Emerging Infectious Diseases*, 19, 449.

- Kong, T. H., Coates, A., Butcher, P., Hickman, C. & Shinnick, T. 1993. *Mycobacterium tuberculosis* expresses two chaperonin-60 homologs. *Proceedings of the National Academy of Sciences*, 90, 2608-2612.
- Krachler, A.-M. & Orth, K. 2013. Made to stick: anti-adhesion therapy for bacterial infections. *Microbe*, 8, 286-290.
- Kruh-Garcia, N. A., Murray, M., Prucha, J. G. & Dobos, K. M. 2014. Antigen 85 variation across lineages of *Mycobacterium tuberculosis*—Implications for vaccine and biomarker success. *Journal of Proteomics*, 97, 141-150.
- Kumar, S., Puniya, B. L., Parween, S., Nahar, P. & Ramachandran, S. 2013. Identification of novel adhesins of *M. tuberculosis* H37Rv using integrated approach of multiple computational algorithms and experimental analysis. *PLoS One*, 8, 69790.
- Kumar, S. 2015. *Essentials of Microbiology*, JP Medical Ltd.
- Kunnath-Velayudhan, S. & Gennaro, M. L. 2011. Immunodiagnosis of tuberculosis: a dynamic view of biomarker discovery. *Clinical Microbiology Reviews*, 24, 792-805.
- Kuo, C.-J., Gao, J., Huang, J.-W., Ko, T.-P., Zhai, C., Ma, L., Liu, W., Dai, L., Chang, Y.-F. & Chen, T.-H. 2019. Functional and structural investigations of fibronectin-binding protein Apa from *Mycobacterium tuberculosis*. *Biochimica et Biophysica Acta (BBA)-General Subjects*, 1863, 1351-1359.
- Lawn, S. D., Dheda, K., Kerkhoff, A. D., Peter, J. G., Dorman, S., Boehme, C. C. & Nicol, M. P. 2013. Determine TB-LAM lateral flow urine antigen assay for HIV-associated tuberculosis: recommendations on the design and reporting of clinical studies. *BMC Infectious Diseases*, 13, 407.
- Lebrun, P., Raze, D., Fritzing, B., Wieruszkeski, J.-M., Biet, F., Dose, A., Carpentier, M., Schwarzer, D., Allain, F. & Lippens, G. 2012. Differential contribution of the repeats to heparin binding of HBHA, a major adhesin of *Mycobacterium tuberculosis*. *PLoS One*, 7, e32421.
- Ledesma, M. A., Ochoa, S. A., Cruz, A., Rocha-Ramírez, L. M., Mas-Oliva, J., Eslava, C. A., Giron, J. A. & Xicohtencatl-Cortes, J. 2010. The hemorrhagic coli pilus (HCP) of *Escherichia coli* O157: H7 is an inducer of proinflammatory cytokine secretion in intestinal epithelial cells. *PLoS One*, 5, e12127.
- Lemassu, A., Ortalo-Magne, A., Bardou, F., Silve, G., Lanéelle, M.-A. & Daffé, M. 1996. Extracellular and surface-exposed polysaccharides of non-tuberculous mycobacteria. *Microbiology*, 142, 1513-1520.
- Lighter, J., Rigaud, M., Huie, M., Peng, C. & Pollack, H. 2009. Chemokine IP-10: an adjunct marker for latent tuberculosis infection in children. *The International Journal of Tuberculosis and Lung Disease*, 13, 731-736.
- Lin, P. L., Ford, C. B., Coleman, M. T., Myers, A. J., Gawande, R., Ioerger, T., Sacchettini, J., Fortune, S. M. & Flynn, J. L. 2014. Sterilization of granulomas is common in active and latent tuberculosis despite within-host variability in bacterial killing. *Nature Medicine*, 20, 75-79.
- Lu, J.-b., Chen, B.-w., Wang, G.-z., Fu, L.-l., Shen, X.-b., Su, C., Du, W.-x., Yang, L. & Xu, M. 2015. Recombinant tuberculosis vaccine AEC/BC02 induces antigen-specific cellular responses in mice and protects guinea pigs in a model of latent infection. *Journal of Microbiology, Immunology and Infection*, 48, 597-603.
- Luabeya, A. K., Kagina, B. M., Tameris, M. D., Geldenhuys, H., Hoff, S. T., Shi, Z., Kromann, I., Hatherill, M., Mahomed, H., Hanekom, W. A., Andersen, P., Scriba, T. J., Schoeman, E.,

- Krohn, C., Day, C. L., Africa, H., Makhetha, L., Smit, E., Brown, Y., Suliman, S., Hughes, E. J., Bang, P., Snowden, M. A., McClain, B. & Hussey, G. D. 2015. First-in-human trial of the post-exposure tuberculosis vaccine H56:IC31 in *Mycobacterium tuberculosis* infected and non-infected healthy adults. *Vaccine*, 33, 4130-40.
- Luies, L., Reenen, M. v., Ronacher, K., Walzl, G. & Loots, D. T. 2017. Predicting tuberculosis treatment outcome using metabolomics. *Biomarkers in Medicine*, 11, 1057-1067.
- Mangtani, P., Abubakar, I., Ariti, C., Beynon, R., Pimpin, L., Fine, P. E., Rodrigues, L. C., Smith, P. G., Lipman, M. & Whiting, P. F. 2014. Protection by BCG vaccine against tuberculosis: a systematic review of randomized controlled trials. *Clinical Infectious Diseases*, 58, 470-480.
- Martin, C., Aguilo, N., Marinova, D. & Gonzalo-Asensio, J. 2020. Update on TB vaccine pipeline. *Applied Sciences*, 10, 2632.
- Mattick, J. S. 2002. Type IV pili and twitching motility. *Annual Reviews in Microbiology*, 56, 289-314.
- Mazel, D. & Davies, J. 1999. Antibiotic resistance in microbes. *Cellular and Molecular Life Sciences CMLS*, 56, 742-754.
- Menziozi, F. D., Rouse, J. H., Alavi, M., Laude-Sharp, M., Muller, J., Bischoff, R., Brennan, M. J. & Locht, C. 1996. Identification of a heparin-binding hemagglutinin present in mycobacteria. *The Journal of Experimental Medicine*, 184, 993-1001.
- Menziozi, F. D., Bischoff, R., Fort, E., Brennan, M. J. & Locht, C. 1998. Molecular characterization of the mycobacterial heparin-binding hemagglutinin, a mycobacterial adhesin. *Proceedings of the National Academy of Sciences*, 95, 12625-12630.
- Menziozi, F. D., Reddy, V. M., Cayet, D., Raze, D., Debrie, A.-S., Dehouck, M. P., Cecchelli, R. & Locht, C. 2006. *Mycobacterium tuberculosis* heparin-binding hemagglutinin adhesin (HBHA) triggers receptor-mediated transcytosis without altering the integrity of tight junctions. *Microbes and Infection*, 8, 1-9.
- Minion, J., Leung, E., Talbot, E., Dheda, K., Pai, M. & Menzies, D. 2011. Diagnosing tuberculosis with urine lipoarabinomannan: systematic review and meta-analysis. *European Respiratory Journal*, 38, 1398-1405.
- Moodley, S. 2018. "The role of heparin binding haemagglutinin adhesin and curli pili on the pathogenicity of *Mycobacterium tuberculosis*." Unpublished PhD thesis, University of Kwa-Zulu- Natal, Durban, South Africa.
- Mueller-Ortiz, S. L., Sepulveda, E., Olsen, M. R., Jagannath, C., Wanger, A. R. & Norris, S. J. 2002. Decreased infectivity despite unaltered C3 binding by a $\Delta hbhA$ mutant of *Mycobacterium tuberculosis*. *Infection and Immunity*, 70, 6751-6760.
- Munk, M. E., Arend, S. M., Brock, I., Ottenhoff, T. H. & Andersen, P. 2001. Use of ESAT-6 and CFP-10 antigens for diagnosis of extrapulmonary tuberculosis. *The Journal of Infectious Diseases*, 183, 175-176.
- Mvubu, N. E., Pillay, B., Gamielidien, J., Bishai, W. & Pillay, M. 2016a. Canonical pathways, networks and transcriptional factor regulation by clinical strains of *Mycobacterium tuberculosis* in pulmonary alveolar epithelial cells. *Tuberculosis*, 97, 73-85.
- Mvubu, N. E., Pillay, B., Gamielidien, J., Bishai, W. & Pillay, M. 2016b. *Mycobacterium tuberculosis* strains exhibit differential and strain-specific molecular signatures in pulmonary epithelial cells. *Developmental & Comparative Immunology*, 65, 321-329.
- Nagler, R., Bahar, G., Shpitzer, T. & Feinmesser, R. 2006. Concomitant analysis of salivary tumor markers—a new diagnostic tool for oral cancer. *Clinical Cancer Research*, 12, 3979-3984.

- Nahid, P., Dorman, S. E., Alipanah, N., Barry, P. M., Brozek, J. L., Cattamanchi, A., Chaisson, L. H., Chaisson, R. E., Daley, C. L., Grzemska, M., Higashi, J. M., Ho, C. S., Hopewell, P. C., Keshavjee, S. A., Lienhardt, C., Menzies, R., Merrifield, C., Narita, M., O'Brien, R., Peloquin, C. A., Raftery, A., Saukkonen, J., Schaaf, H. S., Sotgiu, G., Starke, J. R., Migliori, G. B. & Vernon, A. 2016. Official American Thoracic Society/Centers for Disease Control and Prevention/Infectious Diseases Society of America Clinical Practice Guidelines: Treatment of Drug-Susceptible Tuberculosis. *Clinical Infectious Diseases*, 63, e147-e195.
- Naidoo, N., Ramsugit, S. & Pillay, M. 2014. *Mycobacterium tuberculosis pili* (MTP), a putative biomarker for a tuberculosis diagnostic test. *Tuberculosis*, 94, 338-345.
- Naidoo, N., Pillay, B., Bubb, M., Pym, A., Chiliza, T., Naidoo, K., Ndung'u, T., Kasprovicz, V. O. & Pillay, M. 2018. Evaluation of a synthetic peptide for the detection of anti-*Mycobacterium tuberculosis* curli pili IgG antibodies in patients with pulmonary tuberculosis. *Tuberculosis*, 109, 80-84.
- Nakiyingi, L., Bwanika, J. M., Kirenga, B., Nakanjako, D., Katabira, C., Lubega, G., Sempa, J., Nyesiga, B., Albert, H. & Manabe, Y. C. 2013. Clinical predictors and accuracy of empiric tuberculosis treatment among sputum smear-negative HIV-infected adult TB suspects in Uganda. *PLoS One*, 8, e74023.
- Nebenzahl-Guimaraes, H., Borgdorff, M. W., Murray, M. B. & van Soolingen, D. 2014. A novel approach-the propensity to propagate (PTP) method for controlling for host factors in studying the transmission of *Mycobacterium tuberculosis*. *PLoS One*, 9, e97816.
- NICD. 2016. *Drug Resistance Survey Full Report [Online]. National Institute for Communicable Diseases.* [Online]. Available: http://www.nicd.ac.za/assets/files/DRS_Executive%20Summary.pdf [Accessed 2020]. [Accessed].
- Nicholas, A. B., Bishai, W. R. & Jain, S. K. 2012. Role of *Mycobacterium tuberculosis* pknD in the pathogenesis of central nervous system tuberculosis. *BMC Microbiology*, 12, 7.
- Nicol, M. P. & Zar, H. J. 2011. New specimens and laboratory diagnostics for childhood pulmonary TB: progress and prospects. *Paediatric Respiratory Reviews*, 12, 16-21.
- Niemann, H. H., Schubert, W.-D. & Heinz, D. W. 2004. Adhesins and invasins of pathogenic bacteria: a structural view. *Microbes and Infection*, 6, 101-112.
- Nyawo, G. R. 2016. 'The role of *Mycobacterium tuberculosis pili* in pathogenesis: growth and survival kinetics, gene regulation and host immune response, and in vitro growth kinetics.' Masters dissertation. University of KwaZulu- Natal, Durban, South Africa.
- Nyendak, M., Lewinsohn, D. & Lewinsohn, D. 2009. New diagnostic methods for tuberculosis. *Current Opinion in Infectious Diseases*, 22(2), 174.
- Olivier, I. 2012. A metabolomics approach to characterise and identify various *Mycobacterium* species. *Journal of Microbiological Methods*, 88, 419-426.
- Pai, M., Riley, L. W. & Colford Jr, J. M. 2004. Interferon- γ assays in the immunodiagnosis of tuberculosis: a systematic review. *The Lancet Infectious Diseases*, 4, 761-776.
- Pai, M., Behr, M. A., Dowdy, D., Dheda, K., Divangahi, M., Boehme, C. C., Ginsberg, A., Swaminathan, S., Spigelman, M. & Getahun, H. 2016. Tuberculosis. *Nature reviews. Disease Primers*, 2, 16076.
- Pancholi, V. & Fischetti, V. A. 1992. A major surface protein on group A streptococci is a glyceraldehyde-3-phosphate-dehydrogenase with multiple binding activity. *The Journal of Experimental Medicine*, 176, 415-426.

- Parida, S., Axelsson-Robertson, R., Rao, M., Singh, N., Master, I., Lutckii, A., Keshavjee, S., Andersson, J., Zumla, A. & Maeurer, M. 2015. Totally drug-resistant tuberculosis and adjunct therapies. *Journal of Internal Medicine*, 277, 388-405.
- Parida, S. K. & Kaufmann, S. H. 2010. The quest for biomarkers in tuberculosis. *Drug Discovery Today*, 15, 148-157.
- Parsons, L. M., Somoskövi, Á., Gutierrez, C., Lee, E., Paramasivan, C., Abimiku, A. I., Spector, S., Roscigno, G. & Nkengasong, J. 2011. Laboratory diagnosis of tuberculosis in resource-poor countries: challenges and opportunities. *Clinical Microbiology Reviews*, 24, 314-350.
- Pethe, K., Alonso, S., Biet, F., Delogu, G., Brennan, M. J., Locht, C. & Menozzi, F. D. 2001. The heparin-binding hemagglutinin of *M. tuberculosis* is required for extrapulmonary dissemination. *Nature*, 412, 190-194.
- Petrone, L., Cannas, A., Aloï, F., Nsubuga, M., Sserumkuma, J., Nazziwa, R. A., Jugheli, L., Lukindo, T., Girardi, E. & Reither, K. 2015. Blood or urine IP-10 cannot discriminate between active tuberculosis and respiratory diseases different from tuberculosis in children. *BioMedical Research International*, 2015, 589471.
- Pillay, M. & Sturm, A. W. 2007. Evolution of the extensively drug-resistant F15/LAM4/KZN strain of *Mycobacterium tuberculosis* in Kwa-Zulu- Natal, South Africa. *Clinical Infectious Diseases*, 45, 1409-1414.
- Płociński, P., Macios, M., Houghton, J., Niemiec, E., Płocińska, R., Brzostek, A., Słomka, M., Dziadek, J., Young, D. & Dziembowski, A. 2019. Proteomic and transcriptomic experiments reveal an essential role of RNA degradosome complexes in shaping the transcriptome of *Mycobacterium tuberculosis*. *Nucleic Acids Research*, 47, 5892-5905.
- Pohlschroder, M., Ghosh, A., Tripepi, M. & Albers, S.-V. 2011. Archaeal type IV pilus-like structures—evolutionarily conserved prokaryotic surface organelles. *Current Opinion in Microbiology*, 14, 357-363.
- Proft, T. & Baker, E. 2009. Pili in Gram-negative and Gram-positive bacteria—structure, assembly and their role in disease. *Cellular and Molecular Life Sciences*, 66, 613.
- Puckett, S., Trujillo, C., Wang, Z., Eoh, H., Ioerger, T. R., Krieger, I., Sacchettini, J., Schnappinger, D., Rhee, K. Y. & Ehrt, S. 2017. Glyoxylate detoxification is an essential function of malate synthase required for carbon assimilation in *Mycobacterium tuberculosis*. *Proceedings of the National Academy of Sciences*, 114, E2225-E2232.
- Quezada, H., Guzmán-Ortiz, A. L., Díaz-Sánchez, H., Valle-Rios, R. & Aguirre-Hernández, J. 2017. Omics-based biomarkers: current status and potential use in the clinic. *Boletín Médico Del Hospital Infantil de México (English Edition)*, 74, 219-226.
- Ragas, A., Roussel, L., Puzo, G. & Rivière, M. 2007. The *Mycobacterium tuberculosis* cell-surface glycoprotein apa as a potential adhesin to colonize target cells via the innate immune system pulmonary C-type lectin surfactant protein A. *Journal of Biological Chemistry*, 282, 5133-5142.
- Ramsugit, S., Guma, S., Pillay, B., Jain, P., Larsen, M. H., Danaviah, S. & Pillay, M. 2013. Pili contribute to biofilm formation in vitro in *Mycobacterium tuberculosis*. *Antonie Van Leeuwenhoek*, 104, 725-735.
- Ramsugit, S. & Pillay, M. 2014. *Mycobacterium tuberculosis* pili promote adhesion to and invasion of THP-1 macrophages. *Japanese Journal of Infectious Diseases*, 67, 476-478.
- Ramsugit, S. & Pillay, M. 2015. Pili of *Mycobacterium tuberculosis*: current knowledge and future prospects. *Archives of Microbiology*, 197, 737-744.

- Ramsugit, S., Pillay, B. & Pillay, M. 2016. Evaluation of the role of *Mycobacterium tuberculosis* pili (MTP) as an adhesin, invasin, and cytokine inducer of epithelial cells. *The Brazilian Journal of Infectious Diseases*, 20, 160-165.
- Ramsugit, S. & Pillay, M. 2016. Identification of *Mycobacterium tuberculosis* adherence-mediating components: a review of key methods to confirm adhesin function. *Iranian Journal of Basic Medical Sciences*, 19, 579-84.
- Rangaka, M. X., Wilkinson, K. A., Glynn, J. R., Ling, D., Menzies, D., Mwansa-Kambafwile, J., Fielding, K., Wilkinson, R. J. & Pai, M. 2012. Predictive value of interferon- γ release assays for incident active tuberculosis: a systematic review and meta-analysis. *The Lancet Infectious Diseases*, 12, 45-55.
- Reedoy, K., Loots, D., Beukes, D., Van Reenen, M., Pillay, B. & Pillay, M. 2020. *Mycobacterium tuberculosis* curli pili (MTP) is associated with significant host metabolic pathways in an A549 epithelial cell infection model and contributes to the pathogenicity of *Mycobacterium tuberculosis*. *Metabolomics*, 16, 1-14.
- Riou, C., Berkowitz, N., Goliath, R., Burgers, W. A. & Wilkinson, R. J. 2017. Analysis of the phenotype of *Mycobacterium tuberculosis*-specific CD4⁺ T cells to discriminate latent from active tuberculosis in HIV-uninfected and HIV-infected individuals. *Frontiers in Immunology*, 8, 968.
- Ronning, D. R., Klabunde, T., Besra, G. S., Vissa, V. D., Belisle, J. T. & Sacchettini, J. C. 2000. Crystal structure of the secreted form of antigen 85C reveals potential targets for mycobacterial drugs and vaccines. *Nature Structural Biology*, 7, 141-146.
- Roy, A., Eisenhut, M., Harris, R., Rodrigues, L., Sridhar, S., Habermann, S., Snell, L., Mangtani, P., Adetifa, I. & Lalvani, A. 2014. Effect of BCG vaccination against *Mycobacterium tuberculosis* infection in children: systematic review and meta-analysis. *British Medical Journal*, 349, g4643.
- Ryndak, M. B., Singh, K. K., Peng, Z. & Laal, S. 2015. Transcriptional profile of *Mycobacterium tuberculosis* replicating in type II alveolar epithelial cells. *PLoS One*, 10, e0123745.
- Sauer, F. G., Mulvey, M. A., Schilling, J. D., Martinez, J. J. & Hultgren, S. J. 2000. Bacterial pili: molecular mechanisms of pathogenesis. *Current Opinion in Microbiology*, 3, 65-72.
- Schneeberger, E.E., 1991. Alveolar type I cells. *The Lung, Scientific Foundations*, 229-234.
- Schoeman, J. C. & Du Preez, I. 2012. A comparison of four sputum pre-extraction preparation methods for identifying and characterising *Mycobacterium tuberculosis* using GCxGC-TOFMS metabolomics. *Journal of Microbiological Methods*, 91, 301-311.
- Shen, Y., Yu, G., Zhong, F. & Kong, X. 2019. Diagnostic accuracy of the Xpert MTB/RIF assay for bone and joint tuberculosis: A meta-analysis. *PLoS One*, 14, e0221427.
- Shin, A.-R., Lee, K.-S., Lee, J.-S., Kim, S.-Y., Song, C.-H., Jung, S.-B., Yang, C.-S., Jo, E.-K., Park, J.-K. & Paik, T.-H. 2006. *Mycobacterium tuberculosis* HBHA protein reacts strongly with the serum immunoglobulin M of tuberculosis patients. *Clinical and Vaccine Immunology*, 13, 869-875.
- Sia, J. K., Georgieva, M. & Rengarajan, J. 2015. Innate immune defenses in human tuberculosis: an overview of the interactions between *Mycobacterium tuberculosis* and innate immune cells. *Journal of Immunology Research*, 2015.
- Sia, J. K. & Rengarajan, J. 2019. Immunology of *Mycobacterium tuberculosis* infections. *Gram-Positive Pathogens*, 1056-1086.
- Simmons, J. D., Stein, C. M., Seshadri, C., Campo, M., Alter, G., Fortune, S., Schurr, E., Wallis, R. S., Churchyard, G. & Mayanja-Kizza, H. 2018. Immunological mechanisms of human

- resistance to persistent *Mycobacterium tuberculosis* infection. *Nature Reviews Immunology*, 18, 575-589.
- Simon, R. 2011. Genomic biomarkers in predictive medicine. An interim analysis. *European Molecular Biology Organization Molecular Medicine*, 3, 429-435.
- Simon, R. 2014. Biomarker based clinical trial design. *Chinese Clinical Oncology*, 3, 39.
- Smaill, F. & Xing, Z. 2014. Human type 5 adenovirus-based tuberculosis vaccine: is the respiratory route of delivery the future? *Expert review of vaccines*, 13, 927-930.
- Somoskovi, A. 2015. Novel laboratory diagnostic tests for tuberculosis and their potential role in an integrated and tiered laboratory network. *Tuberculosis*, 95, S197-S199.
- Stones, D. H. & Krachler, A.-M. 2015. Fatal attraction: how bacterial adhesins affect host signaling and what we can learn from them. *International Journal of Molecular Sciences*, 16, 2626-2640.
- Strom, M. S. & Lory, S. 1993. Structure-function and biogenesis of the type IV pili. *Annual review of Microbiology*, 47, 565-597.
- Sulis, G., Centis, R., Sotgiu, D'Ambrosia, L., Pontali, E., Spanevello, A., Matteelli, A., Zumla, A. & Migliori, G. B. 2016. Recent developments in the diagnosis and management of tuberculosis. *NPJ Primary Care Respiratory Medicine*, 26, 1-8.
- Tait, D. R., Hatherill, M., Van Der Meeren, O., Ginsberg, A. M., Van Brakel, E., Salaun, B., Scriba, T. J., Akite, E. J., Ayles, H. M., Bollaerts, A., Demoitié, M.-A., Diacon, A., Evans, T. G., Gillard, P., Hellström, E., Innes, J. C., Lempicki, M., Malahleha, M., Martinson, N., Mesia Vela, D., Muyoyeta, M., Nduba, V., Pascal, T. G., Tameris, M., Thienemann, F., Wilkinson, R. J. & Roman, F. 2019. Final Analysis of a Trial of M72/AS01E Vaccine to Prevent Tuberculosis. *New England Journal of Medicine*, 381, 2429-2439.
- Tameris, M. D., Hatherill, M., Landry, B. S., Scriba, T. J., Snowden, M. A., Lockhart, S., Shea, J. E., McClain, J. B., Hussey, G. D., Hanekom, W. A., Mahomed, H. & Mcshane, H. 2013. Safety and efficacy of MVA85A, a new tuberculosis vaccine, in infants previously vaccinated with BCG: a randomised, placebo-controlled phase 2b trial. *Lancet*, 381, 1021-8.
- Theron, G., Peter, J., Richardson, M., Warren, R., Dheda, K. & Steingart, K. R. 2016. GenoType® MTBDRsl assay for resistance to second-line anti-tuberculosis drugs. *Cochrane Database of Systematic Reviews*, 9.
- Thillai, M., Pollock, K., Pareek, M. & Lalvani, A. 2014. Interferon-gamma release assays for tuberculosis: current and future applications. *Expert review of respiratory medicine*, 8, 67-78.
- Tientcheu, L. D., Maertzdorf, J., Weiner, J., Adetifa, I. M., Mollenkopf, H.-J., Sutherland, J. S., Donkor, S., Kampmann, B., Kaufmann, S. H. & Dockrell, H. M. 2015. Differential transcriptomic and metabolic profiles of *M. africanum*-and *M. tuberculosis*-infected patients after, but not before, drug treatment. *Genes & Immunity*, 16, 347-355.
- Tiwari, R. P., Hattikudur, N. S., Bharmal, R. N., Kartikeyan, S., Deshmukh, N. M. & Bisen, P. S. 2007. Modern approaches to a rapid diagnosis of tuberculosis: promises and challenges ahead. *Tuberculosis*, 87, 193-201.
- Todar, K. 2012. *Tuberculosis- Online Book of Bacteriology* [Online]. Available: <http://textbookofbacteriology.net/tuberculosis.html> [Accessed 2020] [Accessed].
- Tucci, P., González-Sapienza, G. & Marin, M. 2014. Pathogen-derived biomarkers for active tuberculosis diagnosis. *Frontiers in Microbiology*, 5, 549.

- Vargas-Romero, F., Guitierrez-Najera, N., Mendoza-Hernández, G., Ortega-Bernal, D., Hernández-Pando, R. & Castañón-Arreola, M. 2016. Secretome profile analysis of hypervirulent *Mycobacterium tuberculosis* CPT31 reveals increased production of EsxB and proteins involved in adaptation to intracellular lifestyle. *Pathogens and Disease*, 2, 74.
- Vargas, A. J. & Harris, C. C. 2016. Biomarker development in the precision medicine era: lung cancer as a case study. *Nature Reviews Cancer*, 16, 525.
- Vaughan, J. P., Morrow, R. H. & Organization, W. H. 1989. *Manual of Epidemiology for District Health Management*, World Health Organization.
- Vinod, V., Vijayrajratnam, S., Vasudevan, A.K. and Biswas, R., 2020. The cell surface adhesins of *Mycobacterium tuberculosis*. *Microbiological Research*, 232, 126392.
- Wallengren, K., Scano, F., Nunn, P., Margot, B., Buthelezi, S. S., Williams, B., Pym, A., Samuel, E. Y., Mirzayev, F. & Nkhoma, W. 2011. Drug-resistant tuberculosis, Kwa-Zulu- Natal, South Africa, 2001–2007. *Emerging Infectious Diseases*, 17, 1913.
- Wallis, R. S., Kim, P., Cole, S., Hanna, D., Andrade, B. B., Maeurer, M., Schito, M. & Zumla, A. 2013. Tuberculosis biomarkers discovery: developments, needs, and challenges. *The Lancet Infectious Diseases*, 13, 362-372.
- Wolf, A.J., Desvignes, L., Linas, B., Banaiee, N., Tamura, T., Takatsu, K. and Ernst, J.D. 2008. Initiation of the adaptive immune response to *Mycobacterium tuberculosis* depends on antigen production in the local lymph node, not the lungs. *The Journal of Experimental Medicine*, 205,105-115.
- WHO. 2013. *Global tuberculosis report 2012* [Online]. Available: [www.who.int › publications › global_report › gtbr12_main](http://www.who.int/publications/global_report/gtbr12_main) [Accessed].
- WHO. 2014. *Global tuberculosis report 2014* [Online]. Available: https://www.who.int/tb/publications/global_report/gtbr14_main_text.pdf [Accessed May 2021].
- WHO. 2016. *Global tuberculosis report 2015* [Online]. Available: https://www.who.int/tb/publications/global_report/gtbr2016_executive_summary.pdf?ua [Accessed].
- WHO. 2018. *Global tuberculosis report 2018* [Online]. Available: https://www.who.int/tb/publications/global_report/en/ [Accessed November 2020].
- WHO. 2019. *Global tuberculosis report 2018* [Online]. Available: <https://www.who.int/teams/global-tuberculosis-programme/tb-reports/global-report-2019> [Accessed].
- WHO. 2020. *Global tuberculosis report 2020* [Online]. Available: https://www.who.int/tb/publications/global_report/en/ [Accessed November 2020].
- Wilkie, M. E. & McShane, H. 2015. TB vaccine development: where are we and why is it so difficult? *Thorax*, 70, 299-301.
- Wilkie, M., Satti, I., Minhinnick, A., Harris, S., Riste, M., Ramon, R. L., Sheehan, S., Thomas, Z.-R. M., Wright, D. & Stockdale, L. 2020. A phase I trial evaluating the safety and immunogenicity of a candidate tuberculosis vaccination regimen, ChAdOx1 85A prime–MVA85A boost in healthy UK adults. *Vaccine*, 38, 779-789.
- Working, G. B. D. 2001. Biomarkers and surrogate endpoints: preferred definitions and conceptual framework. *Clinical Pharmacology and Therapeutics*, 69, 89-95.
- Xicohtencatl-Cortes, J., Lyons, S., Chaparro, A. P., Hernandez, D. R., Saldaña, Z., Ledesma, M. A., Rendón, M. A., Gewirtz, A. T., Klose, K. E. & Girón, J. A. 2006. Identification of

proinflammatory flagellin proteins in supernatants of *Vibrio cholerae* O1 by proteomics analysis. *Molecular & Cellular Proteomics*, 5, 2374-2383.

Zuñiga, J., Torres-García, D., Santos-Mendoza, T., Rodríguez-Reyna, T. S., Granados, J. & Yunis, E. J. 2012. Cellular and humoral mechanisms involved in the control of tuberculosis. *Clinical and Developmental Immunology*, 2012, 193923.

Chapter 1 delved into the current literature exploring TB epidemiology, *M. tuberculosis* pathogenesis, characteristics, current therapeutics and intervention strategies against TB/LTB infection, novel biomarkers and adhesins with the focus on HBHA and MTP and their significance in TB research. Chapter 2 investigated the role of MTP and HBHA in regulation of respiration and metabolism, cell wall biosynthesis, membrane transport, lipid biosynthesis and virulence pathways in *M. tuberculosis* V9124, the Δmtp , $\Delta hbhA$, and $\Delta mtp-hbhA$ deletion mutants and their respective complements.

CHAPTER 2: Global transcriptomics reveals major perturbations in central carbon metabolism, cell wall biosynthesis and processes, and virulence in the absence of *M. tuberculosis* curli pili (MTP) and heparin-binding hemagglutinin adhesin (HBHA)

*Naidoo T, J¹., Senzani, S¹., Ravesh Singh²., Pillay, B³., and Pillay, M¹**.

¹Medical Microbiology, School of Laboratory Medicine and Medical Sciences, College of Health Sciences, University of Kwa-Zulu- Natal, 1st floor, Doris Duke Medical Research Institute, Congella, Private Bag 7, Durban, 4013, South Africa.

²Department of Medical Microbiology/National Health Laboratory Service, College of Health Sciences, University of Kwa-Zulu-Natal, 1st Floor, George Campbell Building, Congella, Private Bag 7, Durban, 4013, South Africa.

³Microbiology, School of Life Sciences, College of Agriculture, Engineering and Science, University of Kwa-Zulu- Natal, Westville Campus, Private Bag X54001, Durban, 4000, South Africa.

*Corresponding author

Prof. Manormoney Pillay, PhD.

Medical Microbiology, School of Laboratory Medicine and Medical Sciences, College of Health Sciences, University of Kwa-Zulu- Natal, 1st floor Doris Duke Medical Research Institute, Congella, Private Bag 7, Durban, 4013, South Africa.

Tel: +2731 260 4059

E-mail addresses: tarienjael@gmail.com (Naidoo, TJ); senzanis@ukzn.ac.za (Senzani, S); singhra@ukzn.ac.za (Singh, R); Pillayb1@ukzn.ac.za (Pillay, B); pillayc@ukzn.ac.za (Pillay, M).

2.1 Abstract

Tuberculosis (TB) remains the most devastating bacterial cause of human mortality globally. Surface located adhesins are crucial for *Mycobacterium tuberculosis* (*M. tuberculosis*) survival, as they initiate and perpetuate host-pathogen interactions. Functional genomics, transcriptomics, proteomics, and metabolomics analyses have identified *M. tuberculosis* heparin binding hemagglutinin adhesin (HBHA) and curli pili (MTP) as significant potential targets for intervention strategies. MTP adhesin plays a role in adhesion and invasion of host cells as well as biofilm formation, whilst heparin-binding HBHA promotes *M. tuberculosis* dissemination from the site of infection. The current study aimed to identify novel biomarkers via global transcriptomic analyses using gene proficient and deficient *M. tuberculosis* strains. RNA sequencing was performed on *M. tuberculosis* RNA extracted from wild-type V9124 (WT), single and double deletion HBHA and MTP mutants, and their respective complemented strains. Validation of RNA sequencing data and functional confirmation were conducted by RT-qPCR of selected differentially regulated genes. A bacterial bioluminescence assay was performed to determine the concentration of adenosine triphosphate (ATP) in the deletion mutants and complements, relative to the WT. A total of 43 genes were significantly differentially expressed amongst the deletion mutants. The biologically significant genes were functionally categorized into: central carbon

metabolism, cell wall biosynthesis, cell wall transport and processes, lipid metabolism, and virulence. The RT-qPCR genotypically confirmed expression levels of genes associated with ATP synthase and cell wall transport and biosynthesis pathways. The bioluminescence assay functionally confirmed the increased utilization of ATP in the absence of MTP and HBHA. Adhesin gene deletions caused major perturbations to the respiration and metabolism, cell wall and cell process, and virulence pathways. These perturbations lead to increased energy requirements, compensatory transport of proteins to the cell wall and decreased virulence and pathogenicity. Thus, this study further substantiates *mtp* and *hbhA* and associated pathway genes as potential important targets for TB diagnostic/therapeutic interventions.

2.2 Introduction

Tuberculosis (TB), is an infectious, airborne disease caused by *Mycobacterium tuberculosis*, and remains one of the most devastating bacterial causes of human morbidity and mortality, particularly in low/middle-income countries (Fogel, 2015, Pai et al., 2016). In 2019, there was an estimated 1.4 million TB deaths and which included 208 000 deaths from TB-human immunodeficiency virus (HIV), co-infected individuals (WHO, 2020). The slow replication rate of *M. tuberculosis* leads to diagnostic delays that significantly impede treatment initiation which contributes to increased transmission of TB (El-Sony et al., 2002), including multi-drug resistant TB (MDR-TB) and extensive drug resistant TB (XDR-TB) which is virtually untreatable with the current drugs. Drug resistance continues to be a public health crisis. Rifampicin remains the most effective first line drug against TB, nonetheless, approximately 500 000 individuals developed rifampicin resistant TB (RR-TB) in 2019 (WHO, 2020). Approximately 78% of the 500 000 RR-TB individuals developed MDR-TB (WHO, 2020). In 2017, South Africa had an estimated 3.4% of new MDR/RR- TB cases (WHO, 2018).

Development of more rapid diagnostic tools, drugs, and vaccines are still inadequate due to the lack of suitable, accurate biomarkers. The strategy of specifically targeting the initial interaction between pathogen and host, in the hope of preventing infection, holds great promise in the identification of novel biomarkers. Hence, there is a need to fully characterize the function of the proteins and putative proteins, identified to play a role in this initial interaction (Díaz-Silvestre et al., 2002, Kinhikar et al., 2006, Alteri et al., 2007, Ragas et al., 2007, Hickey et al., 2010, Kumar et al., 2013, Esparza et al., 2015), and the effect they have on the bacterial transcriptome.

Adhesins have been identified as potential novel targets for rapid TB diagnosis and vaccine development, due to their surface localization and role in host-pathogen interaction (Solanki et al., 2018). *M. tuberculosis* encodes multiple adhesins, including the 28-kDa heparin-binding hemagglutinin adhesin (HBHA) (Pethe et al., 2001) and 4-kDa *M. tuberculosis* curli pili (MTP) (Alteri et al., 2007). As a virulence factor, HBHA (*Rv0475*) is present during early stages of infection and is responsible for the initial interaction with epithelial cells, subsequently, facilitating the dissemination of *M. tuberculosis* from the site of infection (Menozzi et al., 2006, Esposito et al., 2011). This was evidenced by infection studies using a mouse model (Pethe et al., 2001) and THP-1 macrophage model (Menozzi et al., 2006).

Previous studies showed that the surface located adhesin, MTP encoded by *mtp* (*Rv3312A*), is a conserved gene that is present only in *M. tuberculosis* strains (Naidoo et al., 2014). In addition, sera of active TB patients are known to contain IgG antibodies against MTP (Alteri et al., 2007, Naidoo et al., 2018). The involvement of MTP in biofilm production (Ramsugit et al., 2013) as well as in adhesion and invasion of THP-1 macrophages (Ramsugit and Pillay, 2014) and A549 epithelial cells (Ramsugit et al., 2016) was previously elucidated. Additionally, it was suggested that MTP reduces cytokine/chemokine induction in epithelial cells as a survival strategy (Ramsugit et al., 2016). Thus, HBHA (Masungi et al., 2002), and MTP may be suitable biomarker candidates for the development of a point-of-care (POC) TB test.

Transcriptome analysis provides a dynamic link between the genome and the proteome by evaluating the global changes that occur in gene expression profiles of tissue, organs, cells or whole organisms (Parida and Kaufmann, 2010). The *in vitro* role of MTP in inducing the host immune response of A549 alveolar epithelial cells, was previously investigated in a transcriptomic study (Dlamini, 2016). This study reported an increased expression of the host immune response associated genes such as cell surface receptors (Dlamini, 2016). Transcriptome investigations in a mouse model, further evaluated the role of MTP in host defence by triggering both inflammatory and innate immune responses (Nyawo, 2016). The MTP adhesin was associated with regulating immune responses by transcriptional factors and cytokines (Nyawo, 2016). In addition, growth assays showed that MTP-deficient strains displayed a significantly decreased growth rate, relative to the *M. tuberculosis* V9124 wild-type (WT) (Nyawo, 2016). Transcriptome studies, in a THP-1 human macrophage model infected with the *mtp-hbhA* deletion mutant of *M. tuberculosis*,

suggested that the combined effect of HBHA and MTP influence transcriptional changes to favour adhesion and subsequent invasion of macrophages (Moodley, 2018, unpublished). This correlated with a functional genomics study that demonstrated the significance of these two adhesins in facilitating bacterial growth and biomass formation (Govender et al., 2018). Collectively, these findings indicate the potential of MTP and HBHA when combined as a suitable TB biomarker or a target for novel vaccine and drug development. Therefore, using functional transcriptomics, real time quantitative PCR (RT-qPCR) and a bioluminescence assay, the present study aimed to determine the individual and combined effects of these adhesins, MTP and HBHA, on the bacterial transcriptome of *M. tuberculosis*, as well as identify novel pathogen biomarkers.

2.3 Materials and methods

2.3.1 Ethics Approval

The study was approved by the Biomedical Research Ethics Committee (BE383/18).

2.3.2 Bacterial isolates and growth conditions

The bacterial strains (Table 2.1) included *M. tuberculosis* wild-type (WT) V9124, a clinical isolate of the F15/LAM4/KZN family previously isolated in Medical Microbiology, University of Kwa-Zulu- Natal, from Tugela Ferry (Kwa-Zulu- Natal, South Africa) (Gandhi et al., 2006), *mtp* deletion mutant (Δmtp), *mtp*-complemented strain (*mtp*-complement), *hbhA* deletion mutant ($\Delta hbhA$), *hbhA*-complemented strain (*hbhA*-complement), *mtp-hbhA* deletion mutant ($\Delta mtp-hbhA$) and *mtp-hbhA* complemented strain (*mtp-hbhA*-complement).

Table 2.1. The seven bacterial strains used in this study

Strains	Genetic information	Reference
WT	Wild-type V9124 (F15/LAM4/KZN), expressing MTP	(Gandhi et al., 2006)
Δmtp	<i>mtp</i> deletion mutant, MTP adhesin deficient	(Ramsugit et al., 2013)
<i>mtp</i> -complement	<i>mtp</i> complemented strain, MTP overexpressing	(Govender et al., 2018, unpublished)
$\Delta hbhA$	<i>hbhA</i> deletion mutant, HBHA adhesin deficient	(Govender et al., 2018, unpublished)
<i>hbhA</i> -complement	<i>hbhA</i> complemented strain, HBHA overexpressing	(Govender et al., 2018, unpublished)
$\Delta mtp-hbhA$	<i>mtp-hbhA</i> double deletion mutant, MTP and HBHA deficient	(Govender et al., 2018, unpublished)
<i>mtp-hbhA</i> -complement	<i>mtp-hbhA</i> complemented strain, MTP-HBHA overexpressing	(Muniram, 2018. unpublished)

WT: wild-type; Δmtp : *mtp*-gene knockout mutant; $\Delta hbhA$: *hbhA*-gene knockout mutant; $\Delta mtp-hbhA$: *mtp-hbhA* gene knockout mutant.

Briefly, the Δmtp (Ramsugit et al., 2013) and $\Delta hbhA$ (Govender et al., 2018, unpublished) strains were constructed from *M. tuberculosis* V9124 via specialized transduction, whereby, an allelic exchange substrate (AES) replaced specific genes with a hygromycin-resistance (HygR)-*sacB* cassette (Bardarov et al., 2002). The *mtp*-complemented (Ramsugit et al., 2013) and *hbhA*-complemented (Govender et al., 2018, unpublished) strains were constructed via electrotransformation by insertion of the non-integrating pMV261 plasmids (Bardarov et al., 2002) containing either *mtp* or *hbhA* genes, respectively. The $\Delta mtp-hbhA$ (Govender et al., 2018, unpublished) was constructed by specialized transduction using the unmarked $\Delta hbhA$ single

deletion mutant and *mtp* high-titre phage containing the targeted gene-specific AES (Bardarov et al., 2002). The *mtp-hbhA* complemented strain (Muniram, 2018. unpublished) was constructed via electrotransformation using electrocompetent cells and the pMV261-*hbhA* and pMV261-*mtp* plasmids (Bardarov et al., 2002). The strains were confirmed by polymerase chain reaction (PCR) using genomic deoxyribonucleic acid (DNA) extracted via InstaGene Matrix (Bio-Rad Laboratories, Hercules, California, USA) (Appendix C1).

Three technical replicates of each of the seven *M. tuberculosis* strains (*M. tuberculosis* WT V9124, Δmtp , *mtp*-complement, $\Delta hbhA$, *hbhA*-complement, $\Delta mtp-hbhA$, and *mtp-hbhA*-complement) were cultured for RNA extraction for three biological assays. All strains were retrieved from storage at -80°C and cultured in 10 mL of Middlebrook 7H9 medium (Difco, Becton-Dickinson, Franklin Lake, New Jersey, USA) supplemented with 10% (v/v) oleic albumin dextrose catalase (OADC) (Difco, Becton-Dickinson, Franklin Lake, New Jersey, USA), 0.5% (v/v) glycerol (Sigma-Aldrich, Missouri, USA), and 0.05% (v/v) tween-80 (Sigma-Aldrich, Missouri, USA). The strains were cultured in a shaking incubator (I-26 Shaking Incubator, New Brunswick Scientific, Canada) at $1 \times g$ for 7-8 days at 37°C to an $\text{OD}_{600\text{nm}}$ of 1.0, equivalent to approximately 1×10^8 colony forming units (CFU)/mL (Larsen et al., 2007). The OD was determined using the Lightwave II Spectrophotometer (Biochrom Ltd, Cambridge, United Kingdom). The deletion mutants and WT strains did not grow at the same rate. The strains were first grown to an $\text{OD}_{600\text{nm}}$ of 1, thereafter the strains were back-diluted to an $\text{OD}_{600\text{nm}}$ of 0.015 to standardize all replicates. Thereafter, the strains were monitored until an OD of 1 was achieved and the cultures were subjected to RNA extraction.

2.3.3 RNA isolation and sequencing

Prior to RNA extraction, the samples were treated with 4 M guanidine thiocyanate (GTC) (Thermo Fisher Scientific, Massachusetts, USA) solution equal to the sample volume to prevent any alterations in transcription and to acquire accurate mRNA representation (Stewart et al., 2002, Butcher, 2004, Larsen et al., 2007). The samples were then centrifuged (Mikro 200R, Hettich Zentrifugen, Tuttlingen, Germany) at $2000 \times g$ for 10 minutes at 4°C (Larsen et al., 2007) and the pellets resuspended in 1 mL of TRIzol reagent (Ambion, Life Technologies, California, USA). A modified TRIzol method of RNA extraction was used, which comprised an additional wash step to increase the purity of the RNA. The samples were mechanically lysed with 0.1 mm zirconia

beads (BioSpec Products, Oklahoma, USA) in a Precellys tissue homogenizer (Bertin Technologies, Montigny-le-Bretonneux, France) under continuous cooling at 2°C. Following lysis, the samples were cooled and a volume of 300 µL of ≥99.5% chloroform (Sigma-Aldrich, Missouri, USA) was added. The samples were mixed by inversion and incubated at room temperature (25°C ± 5°C) following centrifugation (Heraeus Fresco™ 21, Thermo Fisher Scientific, Massachusetts, USA) at 27 670 × g for 15 minutes at 4°C. The aqueous layer was collected and 500 µL of ice-cold ≥99.5% isopropanol (Sigma-Aldrich, Missouri, USA) was added and the samples mixed by inversion. Samples were centrifuged (Heraeus Fresco™ 21, Thermo Fisher Scientific, Massachusetts, USA) at 27 670 × g for 10 minutes at 4°C and the supernatants discarded. Subsequently, the 75% ethanol (Sigma-Aldrich, Missouri, USA) wash step was performed twice followed by the addition of 30 µL diethyl pyrocarbonate (DEPC) water (Thermo Fisher Scientific, Massachusetts, USA) to resuspend the RNA pellet.

The concentrations (ng/ µL), purities (260/280 and 260/230 ratio) and integrities (presence of two distinct bands on MOPS gel electrophoresis) of the RNA samples were assessed using the Nanodrop 2000 (Thermo Fisher Scientific, Massachusetts, USA) and 3-(N-morpholino) propane sulfonic acid (MOPS) (Sigma-Aldrich, Missouri, USA) gel electrophoresis. A single replicate of the *Δmtp*, *ΔhbhA*, *Δmtp-hbhA* and WT showing the best concentration (≥ 500 ng/µL), integrity (presence of two distinct bands on MOPS gel electrophoresis) and purity (260/280 and 260/230 ratio $1.9 \leq x \leq 2.3$) was selected from each of the three biological assays to be sent to Omega Bioservices (Norcross, USA) for RNA sequencing. Hence, a total of twelve RNA samples [Biological assay 1: *Δmtp2*, *ΔhbhA2*, *Δmtp-hbhA2* and WT2 (Table C1.2, Appendix C1), Biological assay 2: *Δmtp2*, *ΔhbhA3*, *Δmtp-hbhA2* and WT2 (Table C1.3, Appendix C1), Biological assay 3: *Δmtp3*, *ΔhbhA2*, *Δmtp-hbhA3* and WT2 (Table C1.4, Appendix C1)], were selected for sequencing. The RNA was stored at -80°C in single use aliquots until shipment on dry ice. After spectrophotometric quantification (≥ 500 ng/µL) (Nanodrop 2000, Thermo Fisher Scientific, Massachusetts, USA) and sample purity assessment [RNA integrity value (RIN) $6 \leq x \leq 8$] using the Nanodrop and RNA screen tape (Omega Bioservices, Norcross, USA), the sequencing library was prepared using the Illumina TruSeq Stranded Total RNA Library Prep Kit with RiboMinus Transcriptome Isolation kit 2000 (Thermo Fisher Scientific, Massachusetts, USA) for removal of

ribosomal RNA. The Illumina 2×150 HiSeq×10 platform (Illumina Incorporated, San Diego, USA) was used to sequence 34 - 70 million, 125 bp paired-end reads of bacterial RNA.

2.3.4 Read alignment and transcript assembly

The quality of the generated reads was assessed using the FastQC toolkit (version 0.11.8; Babraham Bioinformatics, Cambridge, UK), and pre-processed using Trimmomatic (version 0.36) to remove low quality reads and adapter sequences (Bolger et al., 2014). The remaining clean reads were subsequently mapped to the custom-built *M. tuberculosis* H37Rv genome index using Hierarchical Indexing for Spliced Alignment of Transcripts (HISAT version 2.1.0) to generate 12 different Binary Alignment Files (BAM) (Kim et al., 2015, Pertea et al., 2016). Mapping rates to the reference genome ranged from 83.5 - 92.5%. The aligned reads were assembled using the Stringtie (version 1.2.1) assembler against the *M. tuberculosis* H37Rv annotations as a reference. Gffcompare, found in the Stringtie package, was used to further quantify, and annotate the assembled transcripts into known and novel categories (Pertea et al., 2016, Sreenivasamurthy et al., 2017). To determine the expressed transcripts as a Gene Transfer Format (GTF) file, the Stringtie-merge option was used to merge the Stringtie assemblies built for the WT and the deletion mutant replicates (ie. Δmtp replicate 1, Δmtp replicate 2, Δmtp replicate 3, WT replicate 1, WT replicate 2, and WT replicate 3 were merged into one GTF file). The merged Stringtie assemblies of the Δmtp , $\Delta hbhA$, and $\Delta mtp-hbhA$ deletion mutants were compared to the annotated transcript of the *M. tuberculosis* H37Rv genome index to generate novel isoforms and intergenic transcripts (Frazee et al., 2015, Pertea et al., 2016, Sreenivasamurthy et al., 2017, Das et al., 2018). The merged output files were annotated in R (version 1.2.1578) using the Ballgown package (Frazee et al., 2015, Das et al., 2018), to obtain Fragments Per Kilobase of Transcript per Million (FPKM) reads sequenced values (Frazee et al., 2015, Das et al., 2018). To stabilize the variance, due to the FPKM values attached to each transcript being typically skewed, Ballgown's incorporated functions apply a log transformation and then fit the standard linear models to be used to test for differential expression (Pertea et al., 2016).

2.3.5 Enrichment and statistical analysis

Further analysis was performed on Ballgown at the gene and transcript level to generate *q*-values and *p*-values for the differential expression and the fold changes (FC) between the deletion mutants

and the WT. The generated results were filtered using a FC cut-off value ≥ 1.3 (to indicate a 1.3-fold up-regulation) and ≤ 0.5 (to indicate a 2-fold down-regulation) to identify significant genes for pathway analysis through databases such as Kyoto Encyclopaedia of Genes and Genomes (KEGG) (Kanehisa and Goto, 2000, Kanehisa, 2019) and BioCyc databases (Caspi et al., 2016, Karp et al., 2019).

2.3.6 Real-time quantitative polymerase chain reaction (RT-qPCR) as a functional assay

The validation and functional confirmation of the RNA sequencing data using a genotypic assay, RT-qPCR, was conducted on seven bacterial strains (Δmtp , mtp -complement, $\Delta hbhA$, $hbhA$ -complement, $\Delta mtp-hbhA$, $mtp-hbhA$ -complement, and WT) and used to assess gene expression levels as a result of the $hbhA$, mtp , and $mtp-hbhA$ gene deletion. Using the RNA sequencing data, 10 genes which were significantly up-regulated were selected, based on differential expression in the ATP synthesis and cell wall biosynthesis and transport pathways, for RT-qPCR analysis, using the primers listed in Table 2.2. The 16S rRNA was included as the housekeeping gene with the primers listed in Table 2.2. The FASTA format for each gene was obtained from MycoBrowser (Kapopoulou et al., 2011) and inserted into Primer3Plus (Untergasser et al., 2007) to select the best primer set for each gene. The RNA (Δmtp , $\Delta hbhA$, $\Delta mtp-hbhA$, and WT) used for the subsequent cDNA synthesis was derived from the same sample sent for sequencing. The complemented strains (Δmtp -complement, $\Delta hbhA$ -complement, and $\Delta mtp-hbhA$ -complement) were not sequenced; however, RNA concentration and integrity were used to select samples from each biological assay for RT-qPCR. Prior to DNase treatment, as per the manufacturer's instruction (Thermo Fisher Scientific, Massachusetts, USA), the RNA concentrations for each sample were standardized to 1 μg . The High-Capacity cDNA Reverse Transcription Kit (Roche Applied Sciences, Penzberg, Germany) was used to perform the cDNA conversion as per Manufacturer's instructions. Prior to RT-qPCR, the primer efficiency for each primer set was tested. The RT-qPCR was conducted using the Ssoadvanced Universal SYBR Green Supermix kit (Bio-Rad Laboratories, Hercules, California, USA) in a 10 μL total reaction volume, in a QuantStudio Real-Time PCR System (Applied Biosystems, California, USA). Cycling conditions were as follows; holding stage at 95°C for 3 min, PCR stage of 40 cycles which include, 95°C for

30 s, 60°C for 30 s and 75°C for 30 s. The melt curve analysis was determined at continuous fluorescence set at 90 °C for 1 min, 60°C for 30 s and 95°C for 15 s.

Table 2.2. Gene and primer sequences selected for analysis of gene expression using RT-qPCR

Gene	Primer sequence (5' - 3')
<i>atpB</i>	Forward primer: gccacctggctcggtatgac Reverse primer: gcgcatctgaatggtgatcg
<i>atpD</i>	Forward primer: atccccgagctgttcaatgc Reverse primer: aagacgtggcccttcacacc
<i>atpF</i>	Forward primer: tgaagtgagcgcgattgtcc Reverse primer: gtcacgttcccgaagacct
<i>atpE</i>	Forward primer: ctcatcggcggtggactgat Reverse primer: tatgccgcctcaaccaaacc
<i>atpH</i>	Forward primer: ttatctggtgtggcgattt Reverse primer: cctgggcctctagtgttct
<i>lpqV</i>	Forward primer: ctgtcgcgaatggttttg Reverse primer: tactcctctcggtcgattc
<i>secE2</i>	Forward primer: caaggtgatcgacatcatcg Reverse primer: agcttgatgcggttaggtgat
<i>Rv2477c</i>	Forward primer: atgggggacatcaagatcaa Reverse primer: acaacagcagtttgacacgc
<i>Rv0987</i>	Forward primer: ccgacacgggtacgattttt Reverse primer: actgtgtaggcgcaccttt
<i>Rv0986</i>	Forward primer: accacatcaccttcgatttc Reverse primer: gtgggaatcaggtgaaaaa
<i>16S rRNA</i>	Forward primer: cctacgggaggcagcagt Reverse primer: cgtttacggcgtggactac

2.3.7 Statistical analysis

The gene expression data was normalized using 16S rRNA and analysed using the relative quantification method. Three biological replicates and three technical replicates were performed for each strain for each gene. GraphPad Prism (version 8) (GraphPad Software, La Jolla,

California, USA) was used to perform the parametric, unpaired *t*-test analysis to determine the significance values. All *p*-values ≤ 0.05 were considered as statistically significant.

2.3.8 Determination of bacterial bioluminescence

Functional confirmation of increased ATP synthase was performed using a BacTiter-Glo™ Microbial Cell Viability Assay (Promega, Madison, Wisconsin, USA), as per manufacturer's instructions. Briefly, an opaque walled multi-well plate with equal volume (100 μ L each) of microbial cells (OD_{600nm} of 1.0) in supplemented 7H9 broth (as described previously) and BacTiter-Glo™ Reagent was prepared. The contents were briefly mixed and incubated (I-26 Shaking Incubator, New Brunswick Scientific, Canada) for five minutes at 37°C. Thereafter, luminescence was recorded using the Glomax®-Multi+ Detection System (Promega, Madison, Wisconsin, USA). The expression levels were recorded and analysed using GraphPad Prism (version 8) (GraphPad Software, La Jolla, California, USA) to perform parametric, unpaired *t*-tests to determine significance. The bioluminescence assay was performed in triplicate for each of the three biological assays.

2.4 Results

2.4.1 Differential expression of genes induced by the deletion of MTP and HBHA

The genes were shortlisted in R using the Ballgown package, using FC and *p*-value (≤ 0.05) as selection criteria. Additionally, due to the very low number of significant regulated transcripts a FC ≥ 1.30 for up-regulated genes and ≤ 0.75 for down-regulated genes were selected. A total of 43 genes were significantly differentially expressed amongst the deletion mutants. Relative to the WT, the Δmtp displayed a significant up- and down-regulation of 13 and six genes, respectively (Table 2.3 and 2.4). A total of eight significantly up-regulated, and eight down-regulated genes were observed in the $\Delta hbhA$, relative the WT (Table 2.3 and 2.4). The $\Delta mtp-hbhA$ displayed four significantly up-regulated genes, and six significantly down-regulated genes, relative to the WT (Table 2.3 and 2.4).

Table 2.3. The statistically significant up-regulated genes induced by the three *M. tuberculosis* deletion mutants relative to the WT.

Δmtp			$\Delta hbhA$			$\Delta mtp-hbhA$		
Gene	FC	<i>p</i> -value	Gene	FC	<i>p</i> -value	Gene	FC	<i>p</i> -value
<i>lpqV</i>	1.927	0.014	<i>fdxA</i>	3.152	0.044	<i>ASdes</i>	1.706	0.015
<i>ctaC</i>	1.690	0.009	<i>TB31.7</i>	2.248	0.006	<i>PPE59</i>	1.694	0.021
<i>Rv3377c</i>	1.562	0.028	<i>pfkB</i>	2.088	0.005	<i>moaA1</i>	1.502	0.010
<i>ppdK</i>	1.562	0.028	<i>secE2</i>	1.708	0.028	<i>lpdA</i>	1.495	0.022
<i>Rv0986</i>	1.552	0.039	<i>devS</i>	2.224	0.002			
<i>atpF</i>	1.434	0.041	<i>devR</i>	2.130	0.010			
<i>secE2</i>	1.403	0.006	<i>csoR</i>	1.519	0.034			
<i>atpE</i>	1.320	0.010	<i>Rv3128c</i>	1.633	0.046			
<i>ilvC</i>	1.318	< 0.001						
<i>icd1</i>	1.300	0.006						
<i>Rv0988</i>	1.552	0.039						
<i>Rv3857c</i>	1.327	0.042						
<i>Rv1303</i>	1.375	0.006						

WT: wild-type; Δmtp : *mtp*-gene knockout mutant; $\Delta hbhA$: *hbhA*-gene knockout mutant; $\Delta mtp-hbhA$: *mtp-hbhA* gene knockout mutant; FC: fold change (FC \geq 1.3); *p* \leq 0.05.

Table 2.4. The statistically significant down-regulated genes induced by the three *M. tuberculosis* deletion mutants relative to the WT.

<i>Δmtp</i>			<i>ΔhbhA</i>			<i>Δmtp-hbhA</i>		
Gene	FC	<i>p</i> -value	Gene	FC	<i>p</i> -value	Gene	FC	<i>p</i> -value
<i>mtp</i>	0.041	0.004	<i>hbhA</i>	0.062	0.002	<i>hbhA</i>	0.042	< 0.001
<i>Rv2814c</i>	0.558	0.041	<i>mtp</i>	0.533	0.001	<i>mtp</i>	0.471	0.019
<i>serA2</i>	0.730	0.028	<i>Rv2642c</i>	0.644	0.038	<i>Rv3326</i>	0.599	0.016
<i>trpD</i>	0.731	0.005	<i>purA</i>	0.654	0.030	<i>Rv2815c</i>	0.600	0.008
<i>moeX</i>	0.740	0.027	<i>Rv0224c</i>	0.705	0.027	<i>Rv3475</i>	0.634	0.036
<i>mmuM</i>	0.739	0.022	<i>vapC5</i>	0.733	0.034	<i>Rv2042c</i>	0.642	0.027
			<i>cfp2</i>	0.747	0.018			
			<i>Rv1082</i>	0.494	0.044			

WT: wild-type; *Δmtp*: *mtp*-gene knockout mutant; *ΔhbhA*: *hbhA*-gene knockout mutant; *Δmtp-hbhA*: *mtp-hbhA* gene knockout mutant; FC: fold change (FC ≥ 1.3); *p* ≤ 0.05.

2.4.1.1 Functional categorisation of significantly up-regulated and down-regulated genes

The genes which displayed significant up-regulation between *Δmtp* and the WT were functionally categorized. The *ppdK*, *icd1*, and *ilvC* genes are involved in intermediary metabolism and respiration, while *Rv1303*, *atpE*, *atpF*, and *ctaC* were associated with the oxidative phosphorylation pathway (OPP) and adenosine triphosphate (ATP) synthesis (Table 2.3). The genes, *Rv0986*, *Rv0988*, *secE2*, *Rv3377c* and *lpqV* were categorized into cell wall processes, and *Rv3857c* into hypothetical proteins (Table 2.3). Significant down-regulation was observed in genes involved in several functional groups including: *mmuM*, *moeX*, *trpD*, and *serA2* (intermediary metabolism and respiration); *Rv2814c* (insertion sequences and phages); and *mtp* (*Rv3312A*) (cell wall and cell processes) (Table 2.4).

Significant up-regulation between $\Delta hbhA$ and the WT was observed in genes involved in the following functional groups: *secE2* (cell wall and cell process); *fdxA*, and *csor* (intermediary metabolism and respiration), *pfkB* (pentose phosphate pathway); *TB31.7* (virulence, detoxification and adaptation); *devS* and *devR* (regulatory proteins) and *Rv3128c* (conserved hypotheticals) (Table 2.3). A significant down regulation was noted in the following genes and their related pathways: *hbhA*, *mtp*, *cfp2* (cell wall and cell process); *purA*, and *Rv0224c* (intermediary metabolism and respiration); *vapC5* and *Rv1082* (virulence, detoxification and adaptation); and *Rv2642c* (regulatory proteins) (Table 2.4).

Genes that displayed significant up-regulation between $\Delta mtp-hbhA$ and the WT were: *moaA1* and *lpdA* (intermediary metabolism and cell respiration); *ASdes* (conserved hypotheticals); and *PPE59* family (proline-glutamate and proline-proline-glutamate [PE/PPE]) (Table 2.3). Significant down-regulation was observed in: *mtp* and *hbhA* (cell wall and cell process); *Rv2042c* (conserved hypotheticals); *Rv3475*, *Rv2815c* and *Rv3326* (insertion sequences and phages) (Table 2.4).

Alterations in the central carbon metabolism (CCM), ATP synthase, and cell wall transport and processes were observed in the absence of the adhesins. Significant up-regulation of the ATP synthase was observed in the absence of MTP, whilst significant perturbations in cell wall and transport, virulence and regulation or proteins were observed in the absence of HBHA. In addition, genes associated with respiration and metabolism were up-regulated in the absence of both MTP and HBHA.

2.4.2 Alterations in central carbon metabolism, ATP synthase, cell wall and cell processes in the absence of MTP and HBHA

Alterations in expression levels of genes associated with CCM in the absence of MTP and HBHA might subsequently affect production and utilization of ATP. The Δmtp deletion mutant displayed significant up-regulation of *ppdK*, *icd1*, *ilvC* involved in CCM, and a significant down-regulation of genes responsible for the biosynthesis of essential amino acids, tryptophan (*trpD*), and methionine (*mmuM*). Pyruvate phosphate dikinase (PPDK) is responsible for the reversible conversion of phosphoenolpyruvate (PEP) into pyruvate and adenosine 5'-monophosphate (AMP), or ATP (Sauer and Eikmanns, 2005, Beste et al., 2013, Basu et al., 2018) (Figure 2.1). The significant up-regulation of *ppdK*, might indicate an increase in pyruvate and AMP or an increase

in ATP. Pyruvate is then converted to acetyl Coenzyme A (acetyl CoA), which enters the tricarboxylic cycle (TCA) (Sauer and Eikmanns, 2005, Beste et al., 2013, Basu et al., 2018). Probable isocitrate dehydrogenase, *icd1*, is responsible for the conversion of isocitrate into α -ketoglutarate and CO₂ in the TCA cycle (Stryer et al., 1981, Banerjee et al., 2005). This rate-limiting step is the initial NADH yielding reaction of this cycle (Stryer et al., 1981, Banerjee et al., 2005). The increased expression of *icd1* suggests an enhancement of the carbon flux through the TCA cycle. The ketol-acid reductoisomerase, *ilvC*, is involved in the biosynthesis of essential amino acids, valine and isoleucine (Figure 2.2), and is the second enzyme involved in the essential branched-chain amino acid (BCAA) biosynthesis (Armstrong and Wagner, 1961, Amorim Franco and Blanchard, 2017). Significant up-regulation of this second enzyme involved in the BCAA biosynthesis, suggests an increase in 2,3-dihydroxy-3-methylbutanoate and 2,3-dihydroxy-3-methylpentanoate, precursors of valine and isoleucine (Armstrong and Wagner, 1961, Amorim Franco and Blanchard, 2017).

The $\Delta hbhA$ deletion mutant displayed significant up-regulation of *pfkB* and a significant down-regulation of *purA* (Figure 2.1). The up-regulation of *pfkB* suggests an enhancement of the carbon flux through the glycolysis pathway. The gene *purA* (Table 2.4 and Figure 2.1), involved in the purine salvage pathway, encodes an adenylosuccinate synthase which is responsible for catalysing inosine monophosphate (IMP) to AMP (Stayton et al., 1983, Ducati et al., 2011, Kapopoulou et al., 2011). Significant down-regulation of *purA* suggests a decrease in the demand for purines, essential compounds required for replication (Stayton et al., 1983, Ducati et al., 2011). This suggests that in the absence of HBHA, glycolysis is potentially enhanced, thus affecting ATP concentrations within the cell.

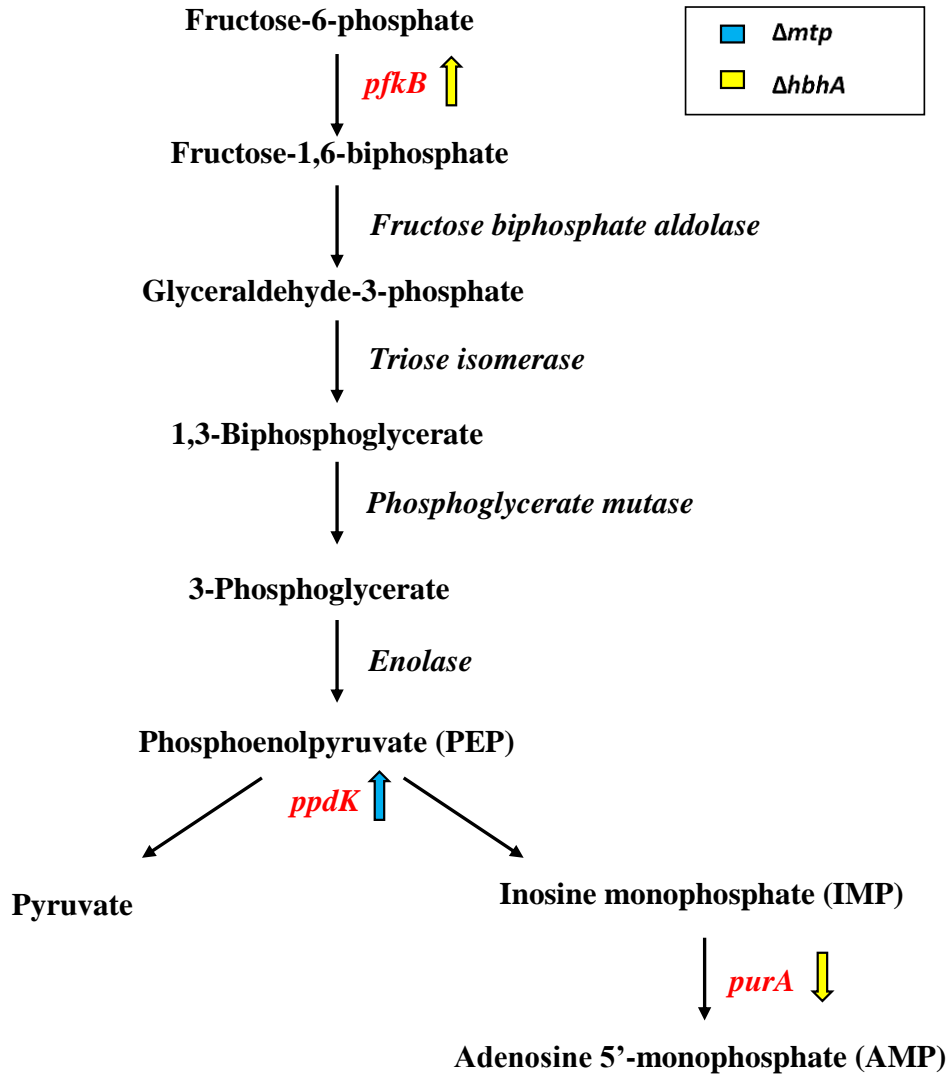


Figure 2.1. Transcriptomic analysis revealed alterations in central carbon metabolism. Significant up-regulation of *pfkB* and *ppdK* is involved in production of pyruvate during glycolysis. Down-regulation of *purA* indicates a decrease in AMP generation. Alterations in the *Δmtp* and *ΔhbhA* deletion mutants relative to the WT are depicted by blue and yellow arrows, respectively. The genes altered in this study are depicted in red. Up- or down-regulation of genes are depicted by direction of the arrows.

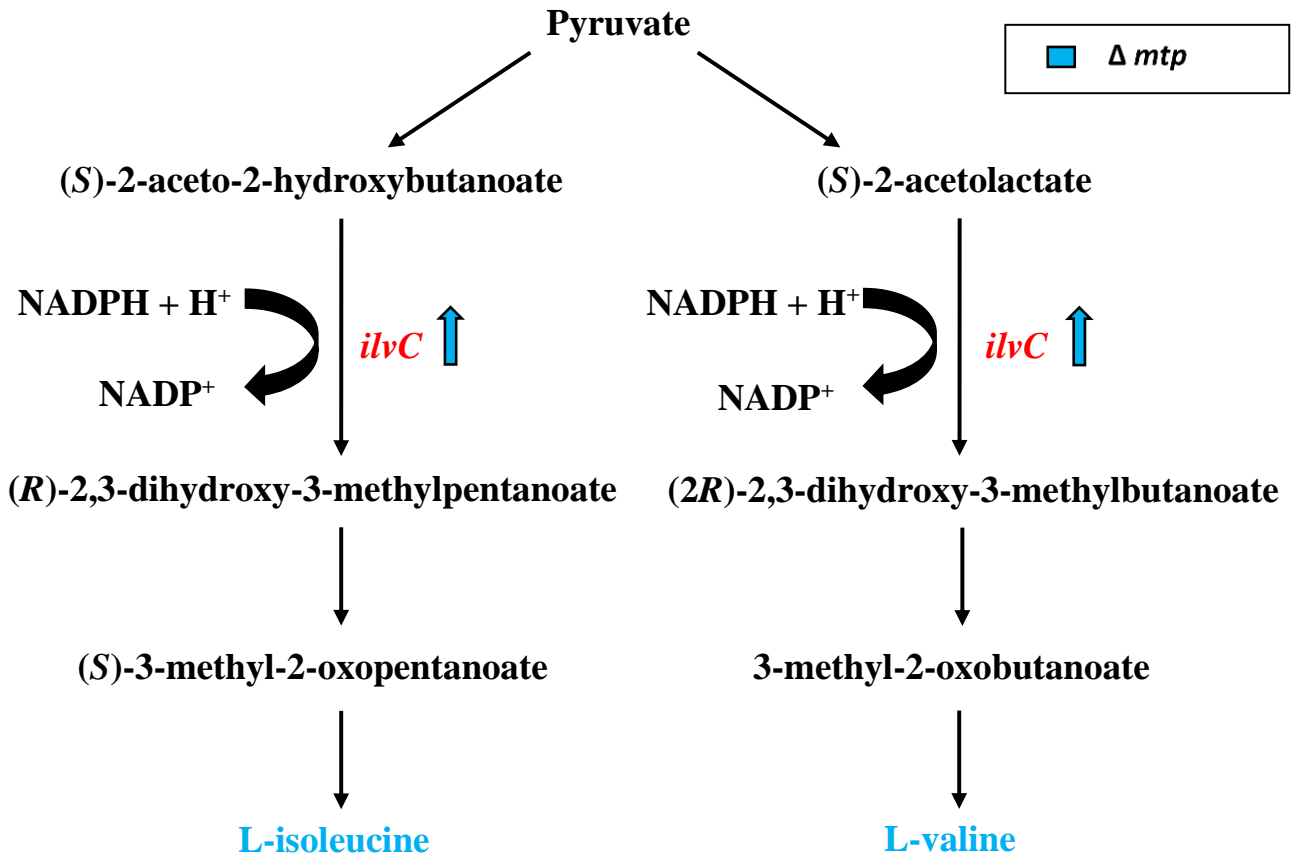


Figure 2.2. Transcriptomic analysis revealed alterations in L-valine and L-isoleucine biosynthesis. Transcriptomic analysis revealed a significant up-regulation of ketol-acid reductoisomerase (*ilvC*) responsible for the conversion of 2-aceto-2-hydroxybutanoate to 2,3-dihydroxy-3-methylpentanoate, involved in the production of L-isoleucine. The reductoisomerase regulates the conversion of 2-acetolactate to 2,3-dihydroxy-3-methylbutanoate, involved in the production of L-valine. This indicates a potential increase in essential amino acids, valine and isoleucine (blue), reported in the Δmtp deletion mutant, relative to WT. Up- or down-regulation of genes are depicted by direction of the arrows. The genes altered in this study are depicted in red.

2.4.3 Alterations in differential gene expression of ATP synthase

The OPP comprises five complexes of which complex IV and V depicted significant up-regulation of the genes encoding the following: Cytochrome *c* oxidase (*ctaC*), ATP synthase (*atpB*, *atpD*, *atpE*, *atpF*, *atpH*) and ATP synthase promoter (*Rv1303*) (Table 2.3; Figures 2.3 and 2.5-2.7), in the Δmtp . Cytochrome *c* oxidase encoded by *ctaC*, *ctaD* and *ctaE* plays a role in complex IV of OPP and feeds into complex V to generate ATP (Figure 2.3) (Sasseti et al., 2003, Rowland and Niederweis, 2012). The mycobacterial F₀-F₁-ATP synthase is encoded by the *Rv1303-atpBEFGHDC-Rv1312* operon (Black et al., 2014). The *Rv1303* gene is located upstream of ATP synthase operon with a 7-bp overlap with *atpB* (Verma et al., 2014). The promoter for the ATP synthase operon is located upstream of *Rv1303* and co-transcribes the genes encoding the different ATP synthase subunits (*atpB*) (Verma et al., 2014). Analysis of RNA sequencing revealed significant up-regulation of ATP synthase promoter and synthase genes, induced in Δmtp (Table 2.3). This significant up-regulation warranted genotypic confirmation to determine if the deletion of *mtp* increased expression of the ATP synthase. Therefore, five ATP synthase genes, *atpB*, *atpD*, *atpE*, *atpF*, and *atpH* were selected for investigation using RT-qPCR. This was also investigated in the $\Delta hbhA$ and $\Delta mtp-hbhA$, to determine if a more significant effect on ATP synthase was observed in the absence of MTP alone or in combination with HBHA. Although there was no significant up-regulation observed in the $\Delta hbhA$ and $\Delta mtp-hbhA$, reported by RNA sequencing, a noteworthy FC of a few ATP synthase genes (*atpB*, *atpC*, *atpF*) was observed (Figure 2.3, Appendix C2.2, C2.3 and C2.4). RT-qPCR demonstrated an overall increased expression of ATP synthase genes in all deletion mutants, Δmtp ($p \leq 0.05$), $\Delta hbhA$ ($p \leq 0.05$), and $\Delta mtp-hbhA$ ($p \leq 0.05$), relative to the WT (Figure 2.5-2.7). However, the genes; *atpB*, *atpD*, *atpH* displayed statistical significance ($p \leq 0.05$) in all complements relative to the WT, which could be attributed to the construction of the complements via non-integrating over-expressing plasmids (Figure 2.5-2.7).

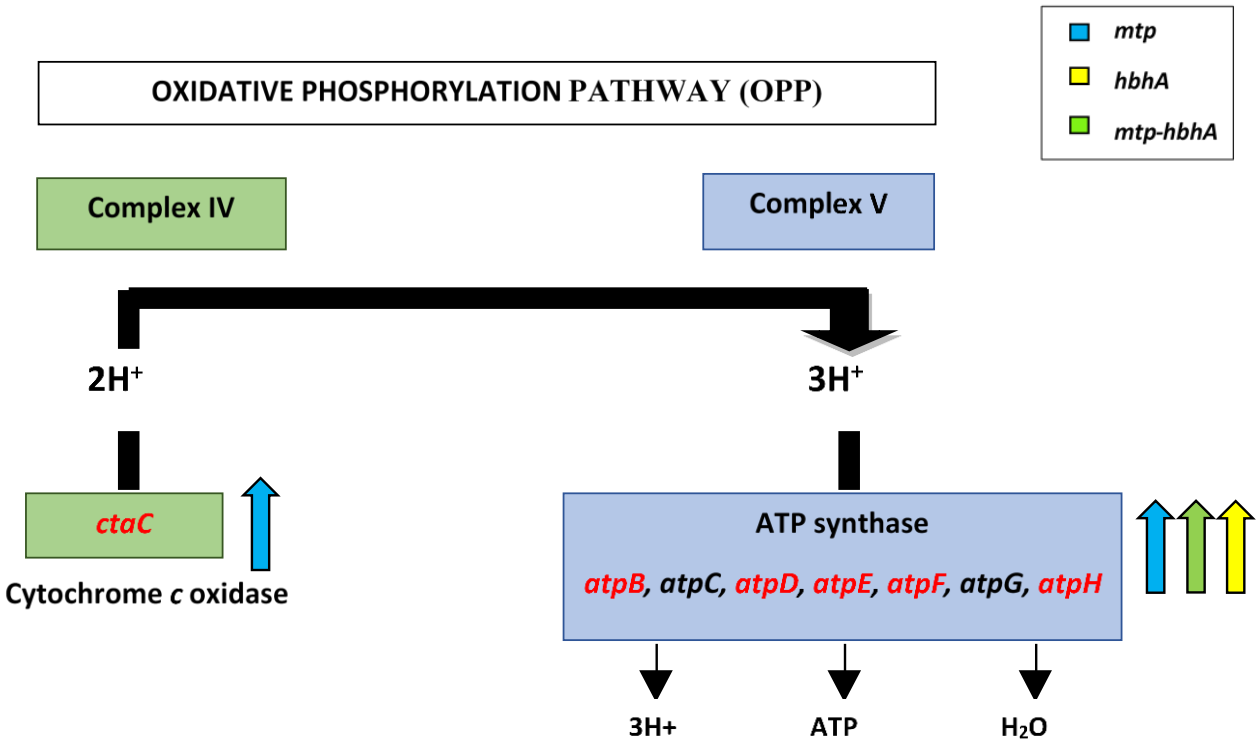


Figure 2.3. Cytochrome *c* oxidase and ATP synthase involved in Complex IV and V during oxidative phosphorylation. Cytochrome *c* oxidase encoded by *ctaC* plays a role in complex IV (green) which feeds into complex V (blue) of the OPP. ATP is generated by ATP synthase encoded by *atpB*, *atpD*, *atpE*, *atpF*, *atpH* involved in complex V. Transcriptomic analysis revealed a significant up-regulation of *ctaC*, *atpE* and *atpF* in the Δmtp deletion mutant, relative to WT. Gene expression analysis revealed significant up-regulation of *atpB*, *atpD*, *atpE*, *atpF*, and *atpH* in Δmtp , $\Delta hbhA$, and $\Delta mtp-hbhA$ relative to the WT. Alterations in the Δmtp , $\Delta hbhA$, and $\Delta mtp-hbhA$ deletion mutants relative to the WT are depicted by blue, yellow and green arrows, respectively. Up- or down-regulation of genes are depicted by direction of the arrows. The genes altered in this study are depicted in red.

2.4.4 Alterations in the cell wall and cell wall processes

Transcriptomic analysis revealed a significant up-regulation of ABC transporter, *secE2*, probable adhesion components, *Rv0986*, and a probable exported protein, *Rv0988* (Pethe et al., 2004), in the Δmtp (Table 2.3, Figure 2.4). The *Rv0986* gene forms part of the ABC transporter along with *Rv0987* and *secE2* (Daniel et al., 2018). Moreover, a non-significant up-regulation of *Rv0987* was observed in the Δmtp (Appendix C2.2). The $\Delta hbhA$ displayed a significant up-regulation of *secE2* (Table 2.3). Furthermore, *Rv0986*, *Rv0987* and *secE2* displayed up-regulation in the $\Delta mtp-hbhA$, however it was statistically non-significant (Appendix C2.2, C2.3 and C2.4). To determine if the

deletion of *mtp* and *hbhA* affected the regulation of the ATP-binding ABC transporters, *Rv0986*, *Rv0987* and *secE2* were investigated by analysing the gene expression determined by RT-qPCR. These genes were also investigated in the $\Delta mtp-hbhA$ to identify if the deletion of both adhesins affected the expression of the transporter to a greater extent. The RT-qPCR showed a significant up-regulation of transport proteins and probable adhesion components in the absence of MTP and HBHA, as observed by the increased gene expression of *Rv0987* ($p \leq 0.05$), *Rv0986* ($p \leq 0.05$), and *secE2* ($p \leq 0.05$) in all mutant strains, relative to the WT (Figure 2.5-2.8). Additionally, *lpqV*, encoding a possible membrane lipoprotein (Kapopoulou et al., 2011), was significantly up-regulated in the absence of MTP (Table 2.3). RT-qPCR showed higher gene expression levels of *lpqV*, in the absence of MTP-HBHA (Figure 2.4 and 2.5-2.7). However, there is a large variance observed in the expression of *lpqV* by the WT, possibly accounting for the non-significance between the WT and Δmtp and $\Delta hbhA$ (Figure 2.5b and 2.6b; Table C3.8). A significant up-regulation of *Rv3377c*, a membrane permeable terpene nucleoside (Layre et al., 2014, Buter et al., 2019), was reported in the Δmtp . The terpene nucleoside is a naturally abundant compound in *M. tuberculosis* (Layre et al., 2014, Buter et al., 2019). Significant down-regulation of the putative secreted protein, *cfp2* (*Rv2376c*), was observed in the $\Delta hbhA$. The secreted protein is an early secreted component of the pathogen that may play a role in the protective immune responses (Webb et al., 1998). The significant down-regulation of this gene suggests perturbations to this pathway. These findings suggest that the absence of the MTP and HBHA adhesins increases the expression of the above-mentioned ABC transporters to the cell wall. The depletion of the HBHA and both MTP-HBHA adhesins, increases expression of a lipoprotein. The depletion of only the MTP adhesin increased expression of a membrane nucleoside, whilst the depletion of only the HBHA adhesin decreased expression of a putative protein involved in protective immune response. These perturbations could be a compensatory mechanism for the lack of the adhesins.

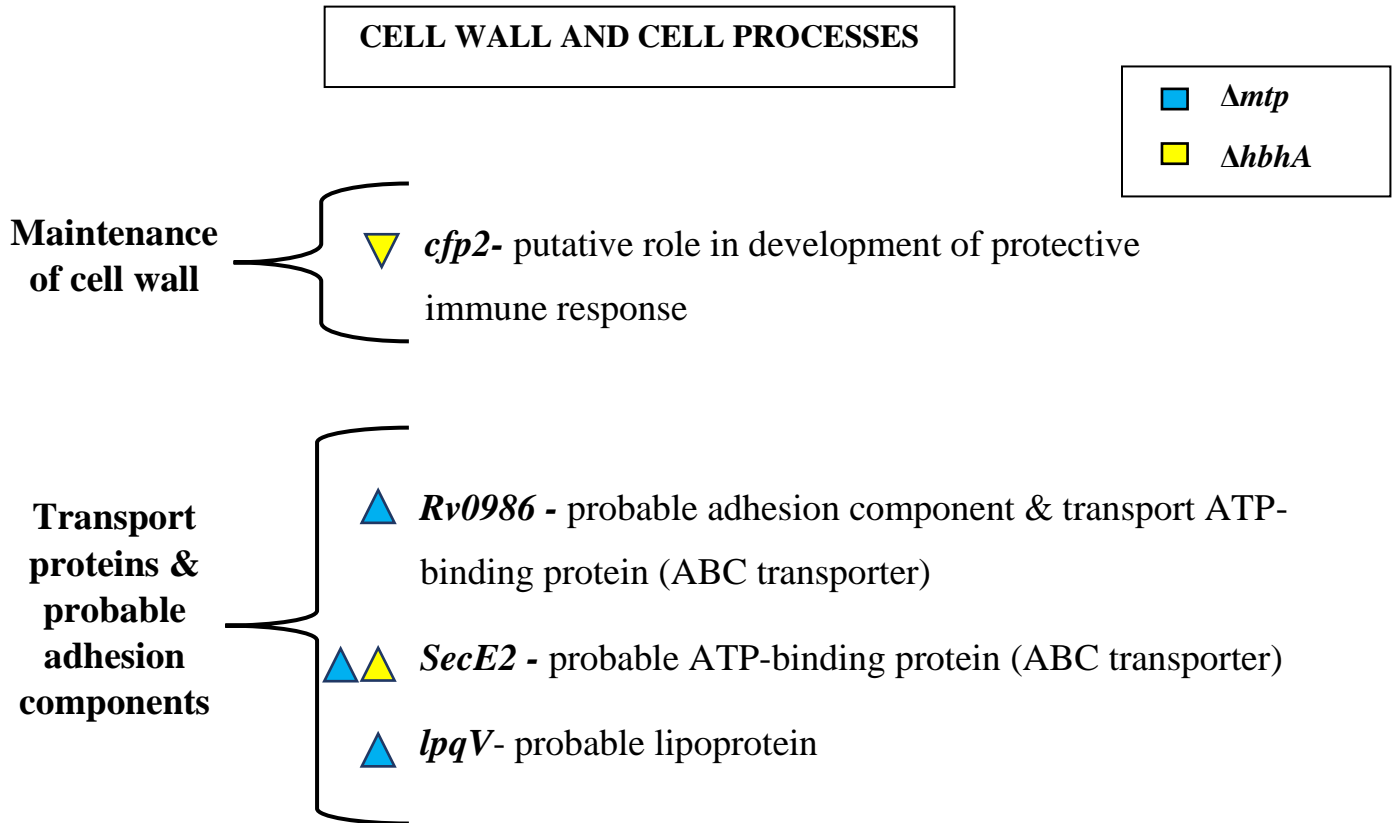


Figure 2.4. Transcriptomic analysis revealed alterations in gene regulation of cell wall maintenance, transport proteins and probable adhesion components. Significant down-regulation of *cfp2*, involved in the maintenance of the cell wall, was reported in the $\Delta hbhA$ deletion mutant. Significant up-regulation of *lpqV*, encoding a possible membrane lipoprotein was reported in Δmtp . The genes, *Rv0986*, and *secE2* form part of an ABC transporter. The gene *Rv0986* is a probable adhesion component and was significantly up-regulated in the Δmtp deletion mutant. The gene *secE2* was significantly up-regulated in the Δmtp and $\Delta hbhA$ deletion mutants. Genes altered in the Δmtp and $\Delta hbhA$ relative to the WT are depicted in blue and yellow, respectively. Up- or down-regulation of genes are depicted by direction of the arrows.

2.4.5 Gene expression analysis of functional RT-qPCR performed on selected genes

RNA sequencing data revealed an up-regulation of the ATP synthase complex (Δmtp) (Appendix C3), and cell wall transport and structural proteins (Δmtp and $\Delta hbhA$). Therefore, 9 genes (*atpB*, *atpD*, *atpE*, *atpF*, *atpH*, *lpqV*, *Rv0986*, *Rv0987*, and *secE2*) were selected to functionally confirm this data by RT-qPCR using the WT, deletion mutants, and complemented strains. The RT-qPCR

data analysis demonstrated a cycle threshold (C_t) value below 29 for all genes, indicating a strong positive reaction (Appendix C3). An ideal standard curve regression (R^2) ranges from 0.980 to 0.999 (Wittwer and Garling, 1991, Pfaffl et al., 2009, Pfaffl, 2012). In this study, the standard curves generated for each reaction showed R^2 values ranging from 0.9670-0.9970 (Appendix C3, Figures C13-23), which was acceptable. Furthermore, the majority of the data points for each standard curve falls on the regression line. The primer efficiencies for all genes ranged from 96.9-116.5% (Appendix C3, Figures C13-23), indicative of good primer qualities, thus ensuring efficient doubling of the template after subsequent cycles. The melt curves for all genes displayed a single peak, indicative of the absence of nonspecific products in the reaction (Appendix C3, Figures C13-23).

The Δmtp strain induced a significantly higher level of gene expression ($p \leq 0.05$) for all genes, except *lpqV*, in comparison to the *mtp*-complement and WT (Figure 2.5a-b). A significantly higher gene expression of *atpB* and *atpH* was observed in all the deletion mutants relative to the WT (Figure 2.5-2.7). Amongst the deletion mutants, $\Delta mtp-hbhA$, induced the highest level of gene expression of *atpD*, *atpF*, *lpqV*, *Rv0986*, *Rv0987*, and *secE2* that was significant when compared to the WT (Figure 2.5-2.7). Overall, the $\Delta mtp-hbhA$ and $\Delta hbhA$ induced a significantly ($p \leq 0.05$) higher level of gene expression for all genes in comparison to their respective complements and the WT strain. The expression means (Table C3.8) of the complements fall closer to the WT, than their respective deletion mutants for all genes. However, between the WT and *mtp*-complement, five genes displayed statistically significant difference. Relative to the WT, the *hbhA*-complement displayed statistical significance of four genes, and the *mtp-hbhA*-complement displayed statistical significance of six genes (Figure 2.5-2.7). The significance observed in all complements, relative to the WT, could be attributed to the construction of the complements via non-integrating over-expressing plasmids.

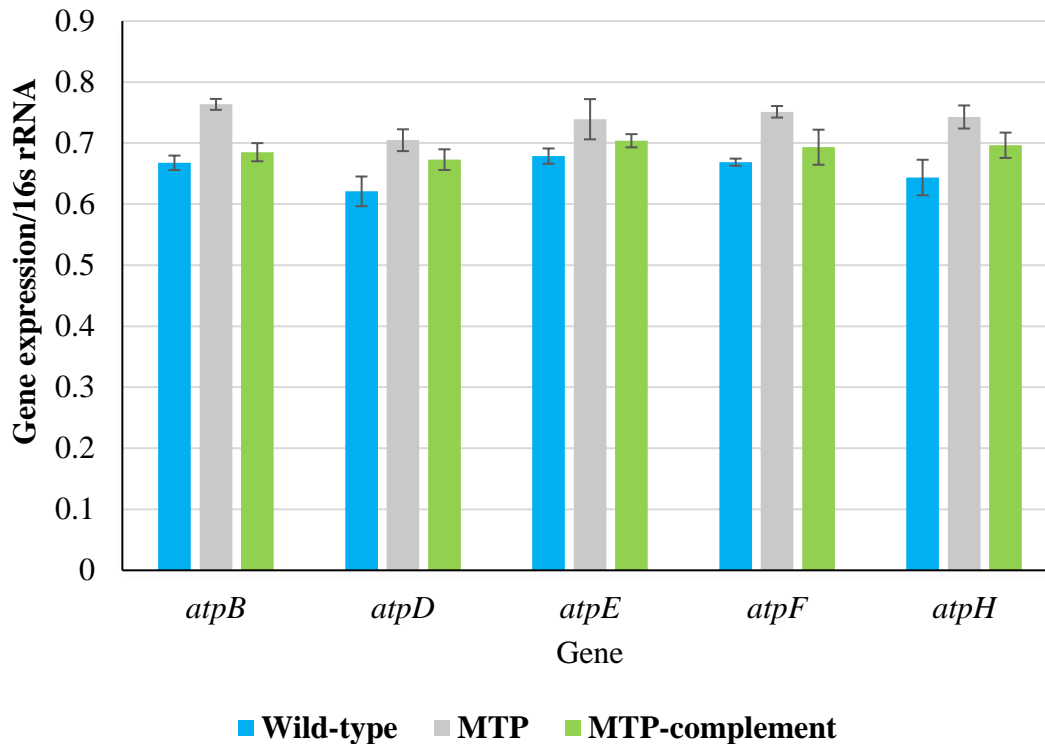


Figure 2.5a. Real-time quantitative PCR to assess gene expression of five ATP synthase genes (*atpB*, *atpD*, *atpE*, *atpF* and *atpH*) in the WT, Δmtp and *mtp*-complement strains. Relative quantification method of interpretation was used to assess the RT-qPCR data. The gene expression levels were analysed relative to 16S rRNA for each gene of interest. Significance levels were established using an unpaired, parametric *t*-test for data between WT and Δmtp strains, and for the WT and *mtp*-complement strains. Between the WT and Δmtp , all of the genes displayed statistical significance: *atpB* ($p < 0.001$), *atpD* ($p < 0.001$), *atpE* ($p = 0.002$), *atpF* ($p < 0.001$), and *atpH* ($p < 0.001$). Between the WT and the *mtp*-complement, four of the genes displayed statistical significance; *atpB* ($p = 0.049$), *atpD* ($p = 0.002$), *atpE* ($p = 0.004$), *atpH* ($p = 0.005$). The gene that displayed no statistical significance was *atpF* ($p = 0.068$).

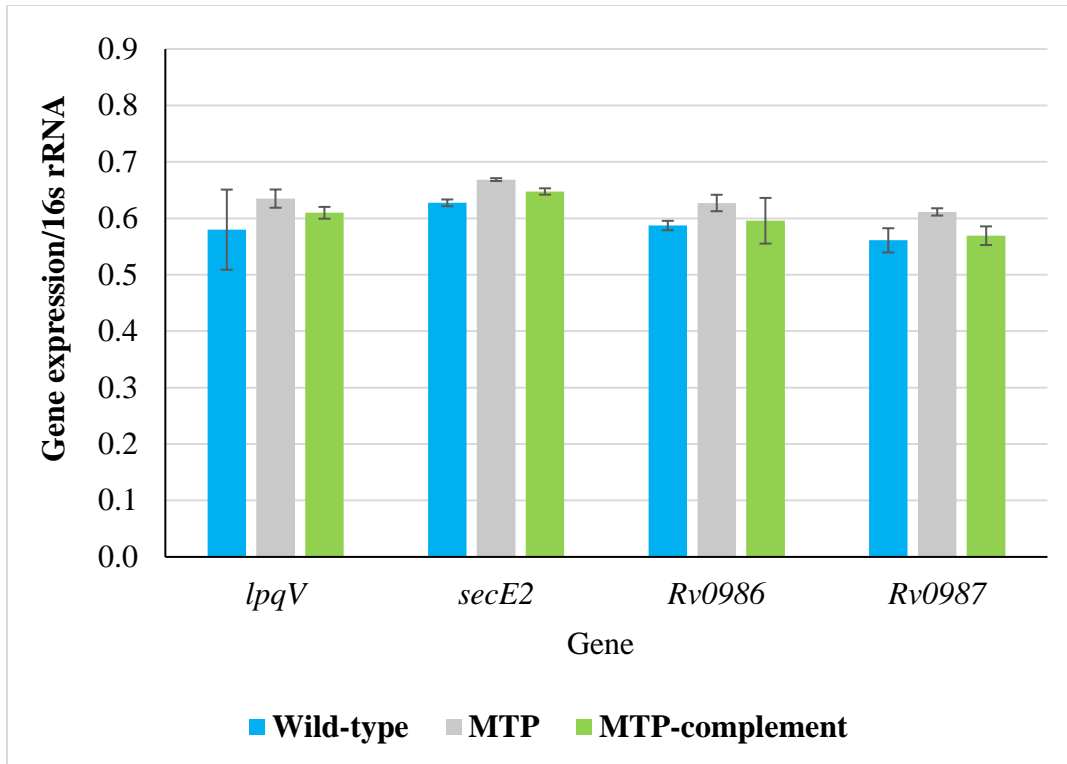


Figure 2.5b. Real-time quantitative PCR to assess gene expression of four genes: adhesion molecules and ABC transporters (*secE2*, *Rv0986* and *Rv0987*), and lipoprotein (*lpqV*) in the WT, Δmtp and *mtp*-complement strains. Relative quantification method of interpretation was used to assess the RT-qPCR data. The gene expression levels were analysed relative to 16S rRNA for each gene of interest. Significance levels were established using an unpaired, parametric *t*-test for data between WT and Δmtp strains, and for the WT and *mtp*-complement strains. Between the WT and Δmtp , three genes displayed statistical significance: *secE2* ($p < 0.001$), *Rv0986* ($p < 0.001$), and *Rv0987* ($p < 0.001$). The gene *lpqV* was not significant ($p = 0.094$). Between the WT and the *mtp*-complement, one gene displayed statistical significance, *secE2* ($p < 0.001$). The genes that were restored to the WT genotype: *lpqV* ($p = 0.332$), *Rv0986* ($p = 0.630$), and *Rv0987* ($p = 0.450$).

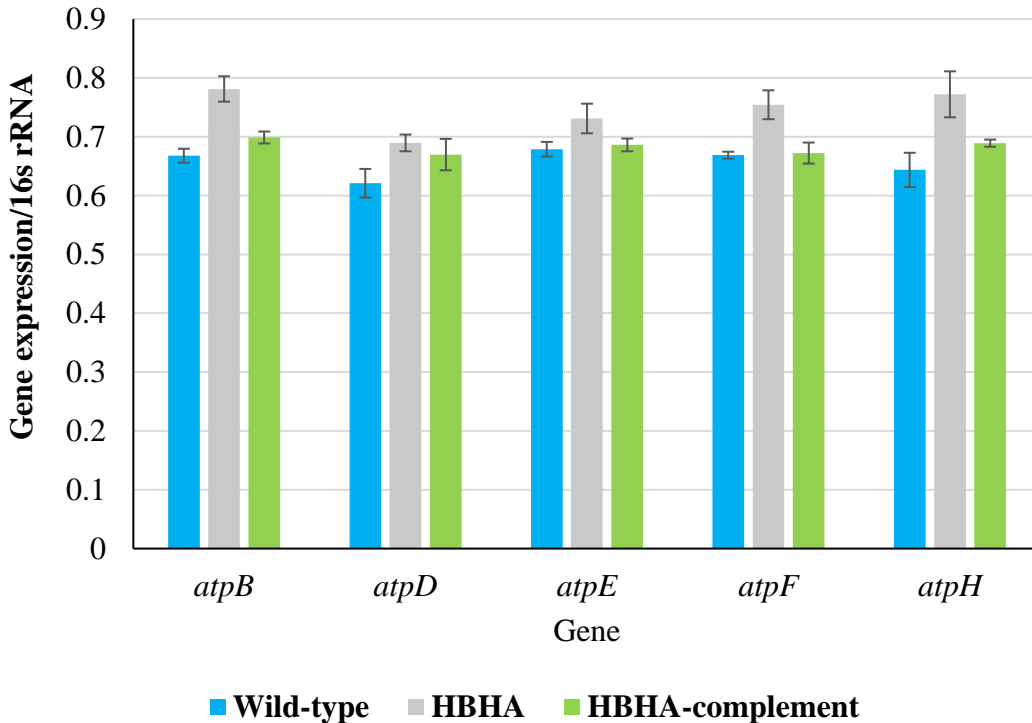


Figure 2.6a. Real-time quantitative PCR to assess gene expression of five ATP synthase genes (*atpB*, *atpD*, *atpE*, *atpF* and *atpH*) in the WT, $\Delta hbhA$ and *hbhA*-complement strains. Relative quantification method of interpretation was used to assess the RT-qPCR data. The gene expression levels were analysed relative to 16S rRNA for each gene of interest. Significance levels were established using an unpaired, parametric *t*-test for data between WT and $\Delta hbhA$ strains, and for the WT and *hbhA*-complement strains. Between the WT and $\Delta hbhA$, all the genes displayed statistical significance; *atpB* ($p < 0.001$), *atpD* ($p < 0.001$), *atpE* ($p = 0.001$), *atpF* ($p < 0.001$) and *atpH* ($p < 0.001$). Between the WT and the *hbhA*-complement, three gene displayed statistical significance: *atpB* ($p < 0.001$), *atpD* ($p = 0.008$), and *atpH* ($p = 0.004$). The genes that were restored to the WT levels: *atpE* ($p = 0.300$), and *atpF* ($p = 0.656$).

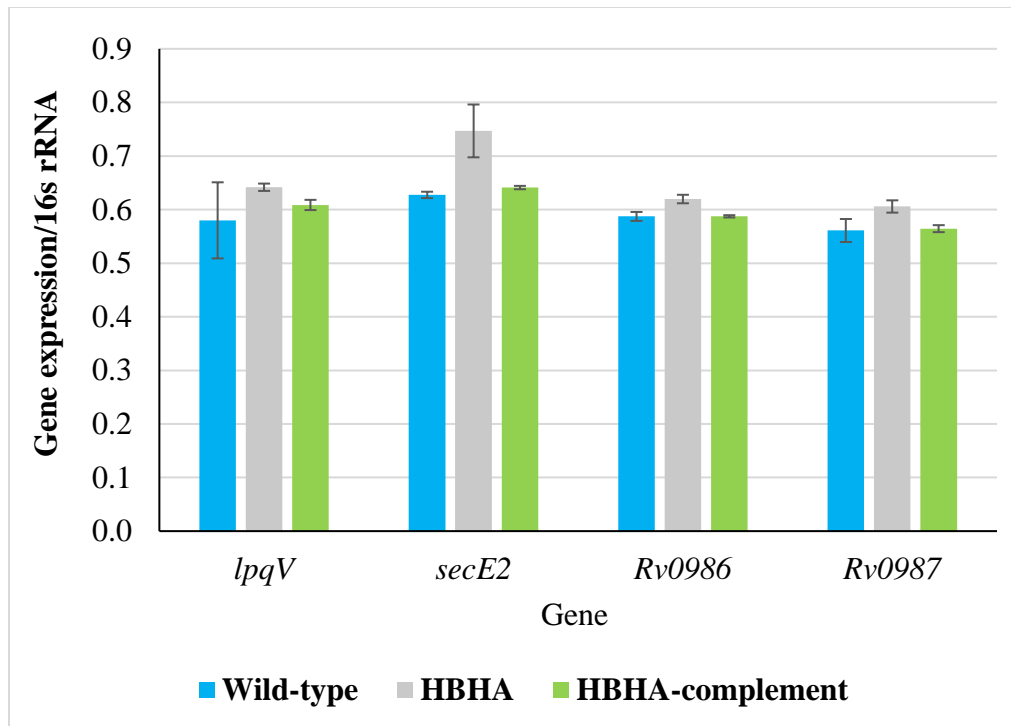


Figure 2.6b. Real-time quantitative PCR to assess gene expression of four genes: adhesion molecules and ABC transporters (*secE2*, *Rv0986* and *Rv0987*), and lipoprotein (*lpqV*) in the WT, Δ *hbhA*, and *hbhA*-complement strains. Relative quantification method of interpretation was used to assess the RT-qPCR data. The gene expression levels were analysed relative to 16S rRNA for each gene of interest. Significance levels were established using an unpaired, parametric *t*-test for data between WT and Δ *hbhA* strains, and for the WT and *hbhA*-complement strains. Between the WT and Δ *hbhA*, three genes displayed statistical significance: *secE2* ($p < 0.001$), *Rv0986* ($p < 0.001$), and *Rv0987* ($p = 0.001$). The gene *lpqV* was not statistically significant ($p = 0.060$). Between the WT and *hbhA*-complement, one gene displayed statistical significance: *secE2* ($p < 0.010$). The genes that displayed non-statistical significance were *lpqV* ($p = 0.349$), *Rv0986* ($p = 0.960$), and *Rv0987* ($p = 0.710$).

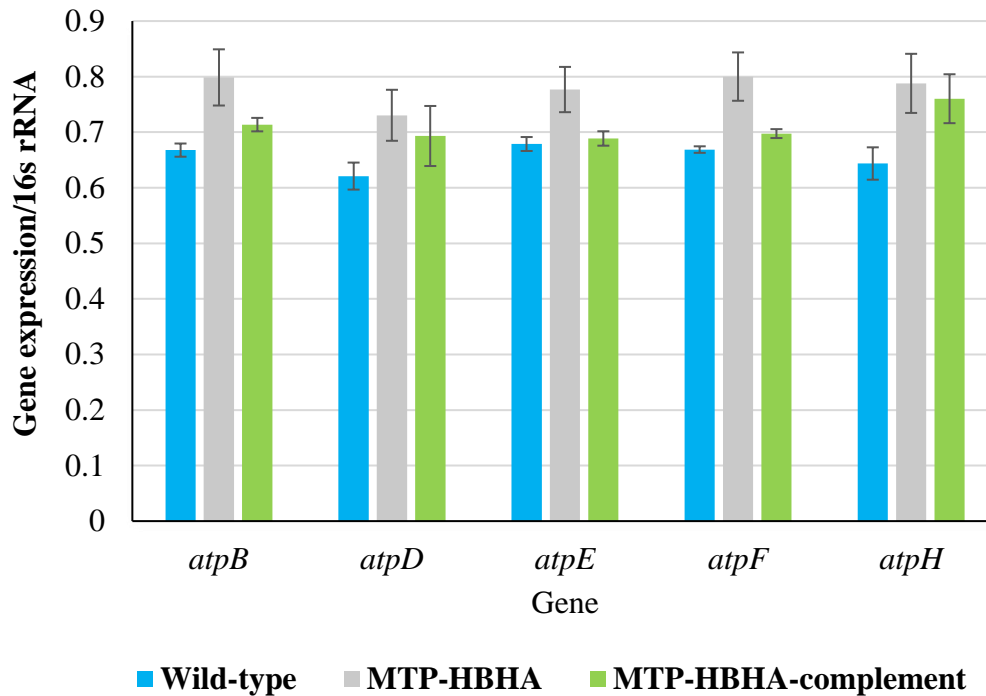


Figure 2.7a. Real-time quantitative PCR to assess gene expression of five ATP synthase genes (*atpB*, *atpD*, *atpE*, *atpF* and *atpH*) in the WT, $\Delta mtp-hbhA$ and *mtp-hbhA*-complement strains. Relative quantification method of interpretation was used to assess the RT-qPCR data. The gene expression levels were analysed relative to 16S rRNA for each gene of interest. Significance levels were established using an unpaired, parametric *t*-test for data between WT and $\Delta mtp-hbhA$ strains, and for the WT and *mtp-hbhA*-complement strains. Between the WT and $\Delta mtp-hbhA$, all the genes displayed statistically significant differences: *atpB* ($p < 0.001$), *atpD* ($p < 0.001$), *atpE* ($p < 0.001$), *atpF* ($p < 0.001$), and *atpH* ($p < 0.001$). Between the WT and *mtp-hbhA*-complement, four genes displayed statistical significance: *atpB* ($p < 0.001$), *atpD* ($p = 0.010$), *atpF* ($p < 0.001$), and *atpH* ($p < 0.001$). The gene that displayed no statistical significance was *atpE* ($p = 0.210$).

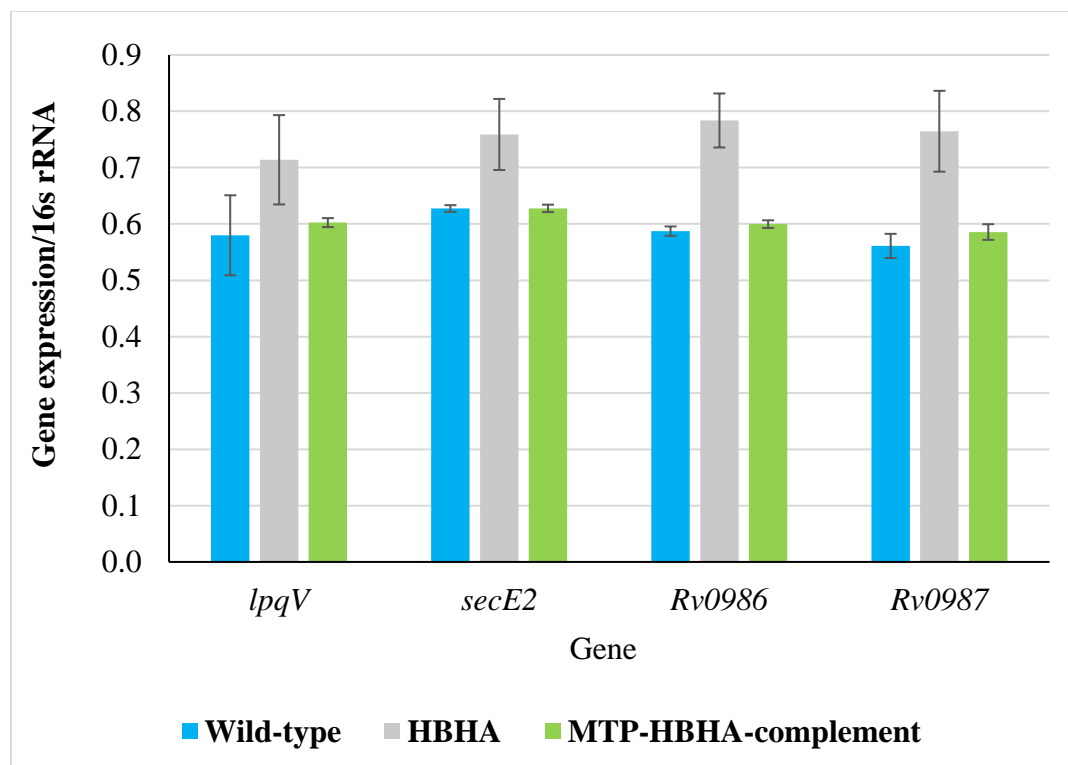


Figure 2.7b. Real-time quantitative PCR to assess gene expression of four genes: adhesion molecules and ABC transporters (*secE2*, *Rv0986* and *Rv0987*), and lipoprotein (*lpqV*) in the WT, $\Delta mtp-hbhA$, and *mtp-hbhA*-complement strains. Relative quantification method of interpretation was used to assess the RT-qPCR data. The gene expression levels were analysed relative to 16S rRNA for each gene of interest. Significance levels were established using an unpaired, parametric *t*-test for data between WT and $\Delta mtp-hbhA$ strains, and for the WT and *mtp-hbhA*-complement strains. Between the WT and $\Delta mtp-hbhA$, all genes displayed statistical significance: *lpqV* ($p = 0.011$), *secE2* ($p < 0.001$), *Rv0986* ($p < 0.001$), and *Rv0987* ($p < 0.001$). Between the WT and *mtp-hbhA*-complement, two genes displayed statistical significance: *Rv0986* ($p = 0.020$), and *Rv0987* ($p = 0.040$). The genes that displayed no statistical significance were *lpqV* ($p = 0.460$) and *secE2* ($p = 0.950$).

2.4.5.1 Comparison of gene expression differences between RNA sequencing and RT-qPCR

A comparison between the expression obtained from the RNA-sequencing and RT-qPCR was performed using the fold-changes of the ATP synthase genes. A parametric unpaired *t*-test was used to determine the significance between the techniques. Keeping in mind that the statistical analysis was performed using a sample mean test, which compares the mean value of each sample group (Yim et al., 2010), the statistical non-significance can be explained by the inconsistent expression values of each gene between the two techniques (the up- and down-regulation of *atpD*, *atpE*, *atpF* and *atpH* in $\Delta hbhA$ and *atpD*, *atpE* and *atpF* in $\Delta mtp-hbhA$), as observed in Figure 2.8. Although the expression is inconsistent, there is no radical difference between the fold-changes of the two techniques. Therefore, there is no statistically significant difference between the techniques. The comparison between the techniques provides a valuable understanding of the two technologies and the possible drawbacks. The RNA sequencing was unable to provide statistically meaningful outcomes for the ATP synthase genes, whilst RT-qPCR repeatedly generated reliable statistically significant gene expression of the synthase. The comparison figure, along with the expression data show that RT-qPCR was the more accurate technique at detecting the subtle changes in gene expression. Therefore, while RNA sequencing is still relatively in its infancy, it has value in broadly elucidating global gene expression in *M. tuberculosis*, and should be supported where necessary, by RT-qPCR data that may be viewed as a more accurate representation of the altered transcriptome.

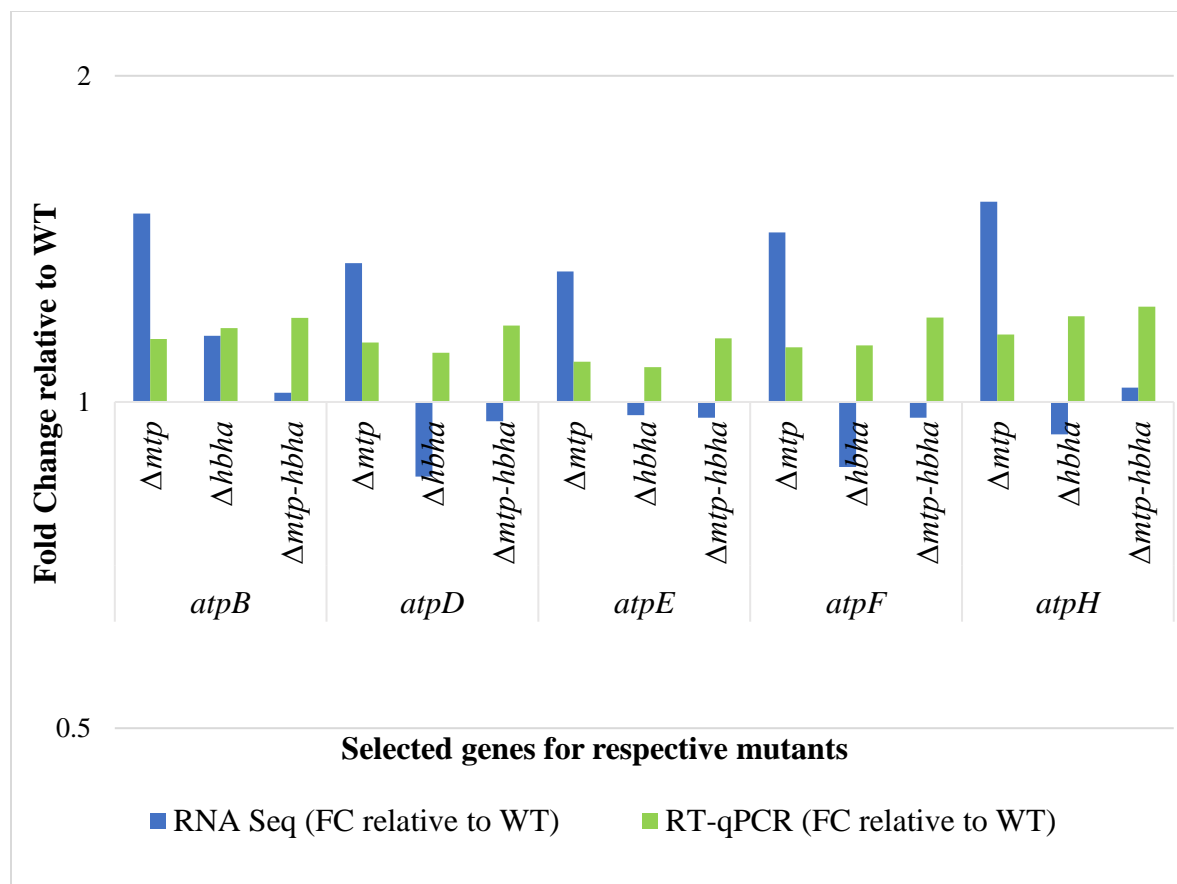


Figure 2.8. Comparison of RNA sequencing data and RT-qPCR for ATP synthase (*atpB*, *atpD*, *atpE*, *atpF*, *atpH*). Real time quantitative PCR was performed on RNA from Δmtp , $\Delta hbhA$, and $\Delta mtp-hbhA$ deletion mutants and WT strains using a QuantStudio Real-Time PCR System (Applied Biosystems, California, USA) and Ssoadvanced universal SYBR green supermix (Bio-Rad Laboratories, Hercules, California, USA). Relative quantification method of interpretation was used to assess the RT-qPCR data. The gene expression levels were analysed relative to 16S rRNA for each gene of interest. The RT-qPCR expression results and the RNA sequencing expression results for three biological assays in triplicate are represented as fold change, relative to the WT. Parametric unpaired *t*-tests showed no statistically significant difference between RNA sequencing and RT-qPCR ($p = 0.6521$), due to the fold-changes displaying a slight deviation from 1 between the techniques, despite the visual differences in the bars depicting up-regulation or down-regulation for the two techniques.

2.4.6 The luciferase assay phenotypically confirms increased ATP utilization or lower ATP production in the absence of MTP and HBHA

The bioluminescence assay revealed a significantly decreased concentration of ATP in the deletion mutants, relative to the WT (Figure 2.9). The RNA sequencing analysis and RT-qPCR expression analysis showed an increased expression of ATP synthase genes in the absence of the adhesins. Collectively, this is suggestive of either a higher ATP consumption in the mutants, or a lower ATP production via alternative pathways, such as a reduced proton motive gradient (Rao et al., 2008, Black et al., 2014). Although the RT-qPCR data suggested that the respective complements relative to the WT showed no statistically significant difference in expression of ATP synthase, the increased level of ATP in the cell could possibly be attributed to the construction of the complements via non-integrating over-expressing plasmids. Additionally, if the deletion of the adhesins potentially resulted in a reduced proton motive gradient, it is postulated that the over-expressing complements, viz., the non-integrating pMV261 plasmids, will potentially increase the proton motive gradient, thereby, explaining the increased concentration of ATP in the complements.

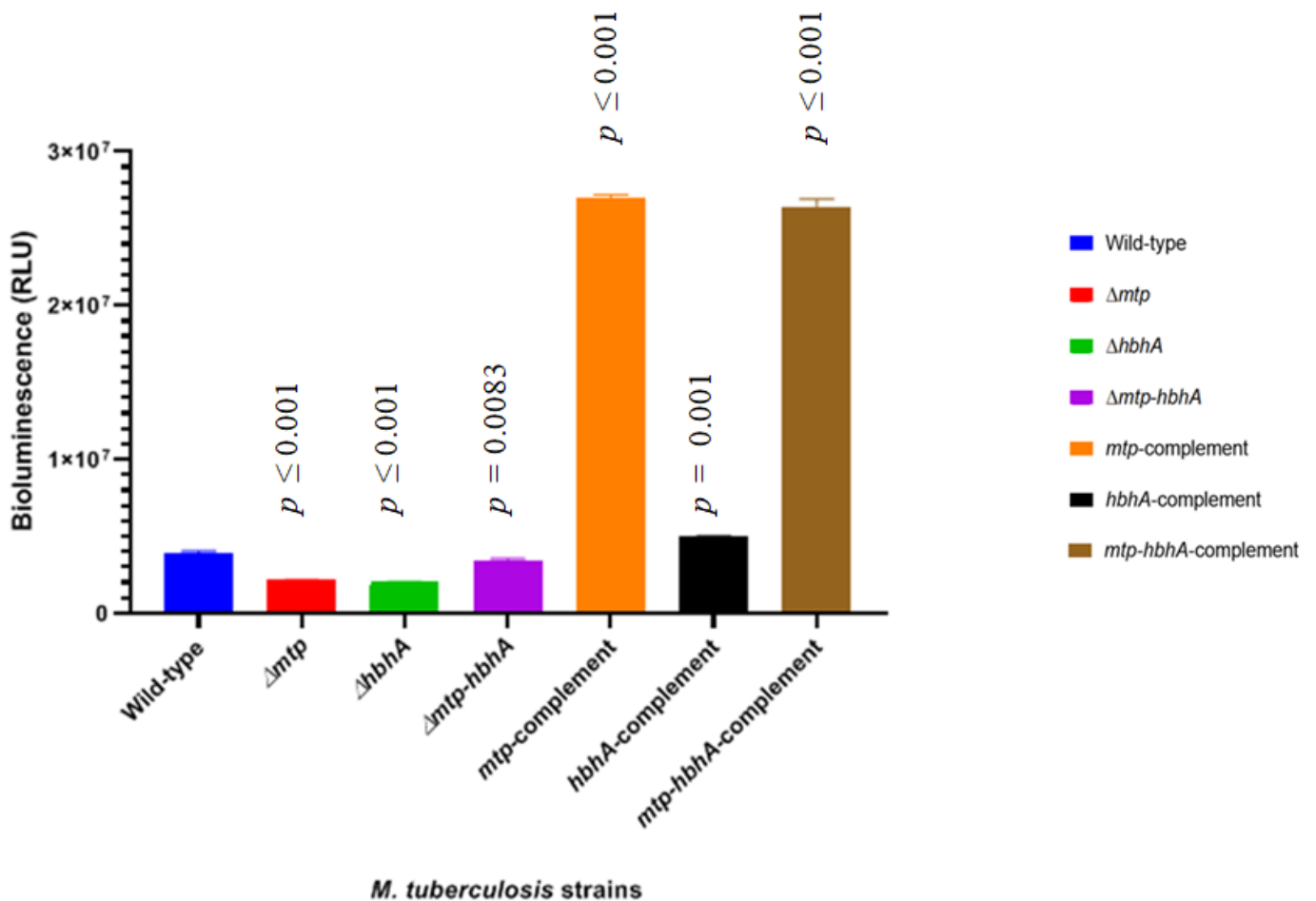


Figure 2.9. Bioluminescence assay depicting lower ATP levels in Δmtp , $\Delta hbhA$, $\Delta mtp-hbhA$ in comparison to *M. tuberculosis* V9124 WT. Significance levels were established using an unpaired, parametric *t*-test for comparison of WT to mutants and their respective complements. The results were statistically different between the mutants and wild type; Δmtp ($p \leq 0.0001$), $\Delta hbhA$ ($p \leq 0.0001$), $\Delta mtp-hbhA$ ($p = 0.0083$) as well as between the complemented strains and WT; *mtp*-complement ($p \leq 0.0001$), *hbhA*-complement ($p \leq 0.0001$), *mtp-hbhA*-complement ($p \leq 0.0001$).

2.5 Discussion

Global “omics” approaches in previous studies highlighted the importance of the surface located adhesins as putative biomarkers and potential targets for therapeutic interventions. Several studies involving transcriptomics (Dlamini, 2016, Nyawo, 2016), functional genomics (Ramsugit and Pillay, 2014, Ramsugit et al., 2016, Govender et al., 2018), and metabolomics (Ashokcoomar et al., 2020, Reedoy et al., 2020, Ashokcoomar et al 2021) highlighted the role of the MTP adhesin in TB pathogenesis. Furthermore, functional genomics (Menozzi et al., 2006), proteomics (Shin et al., 2006, Esposito et al., 2011), and immunological (Chiacchio et al., 2017) studies provided evidence that the HBHA adhesin plays a role in TB pathogenicity. Functional genomics and transcriptomic studies investigating the combined effect of HBHA and MTP demonstrated the impact of these two adhesins in facilitating bacterial growth and biomass formation (Govender et al., 2018) and influencing transcriptional changes to favour adhesion and subsequent invasion of macrophages (Moodley, 2018, unpublished). Collectively, these studies indicated the potential of MTP and HBHA in combination, as suitable TB biomarkers or targets for novel vaccine and drug development. Therefore, using functional transcriptomics, this study aimed to determine the individual, as well as the combined effects, of these adhesins on the bacterial transcriptome of *M. tuberculosis*.

In the current study, RNA sequencing revealed a total of 43 genes to be significantly differentially expressed among the Δmtp , $\Delta hbhA$, and $\Delta mtp-hbhA$ strains, relative to the WT strain. Previous RNA sequencing studies (Aguilar-Ayala et al., 2017, Gomez-Gonzalez et al., 2019, Płociński et al., 2019) focusing on the *M. tuberculosis* transcriptome detected more than 100 significantly differentially expressed genes when compared to their respective reference strains. In the current study, the lower number of significantly differentially expressed genes in the deletion mutants relative to the WT may be due to the use of a relatively new sequencing analysis platform (HISAT), which is a more efficient, user-friendly platform that requires fewer resources (Kim et al., 2015, Pertea et al., 2016). Only a portion of the significant genes are of known function and have been annotated on currently available databases. This exposes the dire need for further *M. tuberculosis* transcriptome studies. Moreover, the significant perturbations observed in the absence of these adhesins indicates the relevance of MTP and HBHA in *M. tuberculosis* pathogenicity, which could be further elucidated in future host infection studies. In contrast to the mutants, the majority of the

selected genes displayed non-significant expression between the WT and complemented strains through RT-qPCR assays. These findings suggest that differential expression of several *M. tuberculosis* genes were due to the deletion of *mtp* and *hbhA*, individually or in combination. The biologically significant genes identified in the mutants compared to the WT strain were demonstrated to play a functional role in CCM, cell wall biosynthesis, cell wall transport and processes, regulation and virulence.

A comparison of the two technologies, RNA sequencing and RT-qPCR, revealed the differences in detection of gene expression. Although various transcriptomics (Parida and Kaufmann, 2010, Mvubu et al., 2016, Płociński et al., 2019) elucidated the urgent need of this technology to understand pathogen and host cell types, this study observed the discrepancies in this technology in detecting subtle fold changes. Holistically, the data obtained from this study, point toward RT-qPCR being the more accurate technique to detect the more subtle gene expression changes in the altered bacterial transcriptome.

2.5.1 The role of MTP and HBHA in cell wall biosynthesis

M. tuberculosis has a distinct cell wall consisting of a highly impermeable lipid-rich outer layer aiding in its success as a pathogen (Minnikin, 1982). Alterations in various cell wall associated pathways were observed in the deletion mutants relative to the WT. There was significant down regulation of *cfp2* (*Rv376c*) observed in $\Delta hbhA$ (Table 2.4; Figure 2.3). Significant up-regulation of *lpqV* (*Rv1064c*) was evident in Δmtp while *ASdes* was significantly upregulated in $\Delta mtp-hbhA$. The N-terminal sequence of the putative membrane lipoprotein, *lpqV*, is postulated to be involved in the lipid attachment site (Kapopoulou et al., 2011). This 19kD lipoprotein is hypothesized to be a probable toll-like receptor 2 (TLR-2) ligand and plays a role in the development of the immune response (Gehring et al., 2004). In order to determine whether this gene displayed a significantly increased gene expression in the absence of MTP, HBHA and MTP-HBHA, RT-qPCR was performed on the WT, deletion mutants and complemented strains. Gene expression analysis revealed a significantly increased expression of *lpqV* in the $\Delta mtp-hbhA$, relative to the WT. However, Δmtp and $\Delta hbhA$ displayed a non-significant increased expression relative to the WT. The majority of the complements displayed no significant differential expression relative to the WT, indicating that they were partially restored back to the WT genotype. This data suggests that

both the *hbhA* and *mtp-hbhA* alter synthesis of a membrane protein in order to compensate for the lack of the deleted adhesins.

The small regulatory RNA, *ASdes*, is involved in mycolic acid biosynthesis and postulated to play a role in regulation of lipid metabolism (Singh et al., 2016). Significant up-regulation suggests a putative role for MTP and HBHA, in combination, in increasing lipid biosynthesis in the cell membrane. Putative secreted protein, *cfp2* (*Rv2376c*), is an early secreted component of the pathogen that may play a role in the protective immune responses (Webb et al., 1998). A study that investigated the profile of CFP-2-induced cytokines in early TB patients and healthy controls, in comparison to those induced by the 30-kDa antigen, reported that the CFP-2 protein plays a vital role in proinflammatory responses through mitogen-activated protein kinase (MAPK) pathway during the early stages of infection in humans (Lee et al., 2006). However, the T-cell immunoreactivity of the CFP-2 protein is weaker than that of the 30-kDa (Lee et al., 2006). The significant down-regulation of this gene suggests a down-regulation of CFP-2 pathogen-associated molecular patterns (PAMPs), which stimulate the production of proinflammatory molecules in recipient macrophages (Lee et al., 2006, Bhatnagar and Schorey, 2007, Smith et al., 2017, Wang et al., 2019). The deletion of both *mtp* and *hbhA*, in combination, results in perturbations to lipoprotein biosynthesis, potentially increasing membrane lipoproteins to accommodate for the lack of adhesins. Additionally, the deletion of *hbhA* confers perturbations potentially resulting in a decreased immune response.

2.5.2 MTP and HBHA modulate energy production in M. tuberculosis by regulating central carbon metabolism

The CCM is defined as the enzymatic repurposing of carbon substrates through various pathways which include: gluconeogenesis, tricarboxylic acid (TCA) cycle, glycolysis and the pentose phosphate shunt (Rhee et al., 2011). In the present study, alterations in several pathways of CCM were observed in the absence of the adhesins.

2.5.2.1 MTP and HBHA influence gluconeogenesis/glycolysis pathways linked to the TCA cycle

The genes involved in glycolysis/gluconeogenesis such as *ppdK*, *ilvC*, and *icd1* were up-regulated in the absence of *mtp* (Table 2.3; Appendix C2.2- C2.4; Figure 2.1). The $\Delta hbhA$ deletion mutant

displayed significant up-regulation of *pfkB* and a significant down-regulation of *purA* (Table 2.3 and 2.4; Appendix C2.2- C2.4; Figure 2.1).

Fructose-6-phosphate, by way of fructose-1,6-biphosphate, is converted into either glyceraldehyde-3-phosphate (which undergoes glycolysis/gluconeogenesis), or dihydroxyacetone phosphate (which utilizes nicotinamide adenine dinucleotide hydrogen (NADH) to produce glycerol-3-phosphate (G3P) (Kapopoulou et al., 2011, Phong et al., 2013). Since *pfkB* is the enzyme responsible for the rate determining step of the glycolysis pathway (Kapopoulou et al., 2011, Phong et al., 2013), the significant up-regulation of this gene in the absence of HBHA, indicates an enhancement in the carbon flux increasing production of pyruvate. The conversion of glyceraldehyde-3-phosphate to 1,3-biphosphoglycerate to phosphoenolpyruvate (PEP) is catalysed by triose phosphate isomerase, phosphoglycerate mutase and enolases, respectively (Rhee et al., 2011). Pyruvate phosphate dikinase (PPDK), is the enzyme that drives both gluconeogenesis and glycolysis (Kayne, 1973, Noy et al., 2016). Under conditions of low oxygen levels, PPDK drives the glycolysis pathway towards pyruvate production with the release of ATP, and under conditions of higher oxygen levels PPDK drives the gluconeogenesis pathway towards PEP production with the release of adenosine 5'-monophosphate (AMP) (Kayne, 1973, Noy et al., 2016). Apart from PPDK, pyruvate kinase (PK) is one of the rate-limiting steps of glycolysis, therefore, potentially controlling the flux through and out of glycolysis (Kayne, 1973, Noy et al., 2016). Pyruvate and PEP can either serve as precursors for anabolism or enter the TCA cycle via acetyl Co-A (Sauer and Eikmanns, 2005, Beste et al., 2013, Basu et al., 2018). The significant up-regulation of *ppdK*, along with the up-regulation in the TCA cycle suggests an enhancement of the carbon flux through glycolysis and indicates the pathogens preference toward carbohydrate consumption to produce ATP, in the absence of *mtp*.

Adenylosuccinate synthase (ADSS), *purA*, is responsible for the first committed step in the conversion of IMP to AMP in the purine salvage pathway (Stayton et al., 1983, Ducati et al., 2011, Kapopoulou et al., 2011). The significant down-regulation of *purA* suggests a reduced need for purine synthesis, due to the deletion of HBHA potentially suppressing replication. Thus, in the absence of MTP and HBHA individually, the pathogen favours carbohydrate metabolism by enhancing glycolysis to compensate for the lower lipid metabolism through the TCA cycle, resulting in less efficient ATP synthesis.

2.5.2.2 MTP influences the citric acid cycle

Significant alterations in the citric acid cycle (TCA) were observed in Δmtp , including an up-regulation of *ilvC* and *icd1* and down-regulation of *serA2* and *mmuM*. Pyruvate enters the TCA cycle for energy generation (Sauer and Eikmanns, 2005, Beste et al., 2013, Basu et al., 2018). Pyruvate is involved in the generation of serine, an essential amino acid for bacterial growth (Chattopadhyay et al., 2007, Ågren et al., 2008). Synthesis of 3-phosphoglycerate, precursors of L-serine, is catalysed by *serA2* (*Rv0728c*), and *serC* (Chattopadhyay et al., 2007, Ågren et al., 2008). The deletion of the MTP adhesin results in perturbations in metabolism that slow down replication, potentially decreasing the requirement of proteins, thereby decreasing expression of genes responsible for synthesis of amino acids like serine, from the intermediates of carbohydrate or lipid metabolism. Pyruvate is converted to either hydroxybutanoate or acetolactate which is converted to methylpentanoate or methylbutanoate, respectively, by a probable isocitrate dehydrogenase (*ilvC*) (Figure 2.2) (Banerjee et al., 2005, Stryer et al., 1981). Increased expression of this ketol-acid reductoisomerase suggests an increase in precursors involved in the biosynthesis of the essential branched-chain amino acids (BCAAs), valine and isoleucine (Armstrong and Wagner, 1961, Amorim Franco and Blanchard, 2017). Microorganisms produce signalling molecules called alarmones (Hauryliuk et al., 2015, Fang and Bauer, 2018), which are regulated by alarmone synthetase/hydrolase, Rel (Shivers and Sonenshein, 2004, Hauryliuk et al., 2015). This enzyme contains an ACT domain that plays a probable role in controlling amino acid metabolism (Shivers and Sonenshein, 2004, Hauryliuk et al., 2015). Studies on *Rhodobacter capsulatus* observed that the ACT domain in the Rel alarmone synthase hydrolase binds to BCAAs, valine and isoleucine (Fang and Bauer, 2018). This study indicated that the cellular concentrations of these BCAAs directly affect the alarmone activity (Fang and Bauer, 2018). Thus, the significant up-regulation of the BCAAs, valine and isoleucine, potentially suggest stimulation of the pathogens alarmone signalling the pathogen is in stress, in the absence of *mtp*.

The conversion of isocitrate into α -ketoglutarate and CO_2 , catalysed by a probable NAD^+ -dependant isocitrate dehydrogenase (*icd1*), is a vital rate-limiting step in the TCA cycle (Banerjee et al., 2005, Stryer et al., 1981). Significant up-regulation of *icd1* indicates an increase in the flux through this pathway. *M. tuberculosis* has a B12-independent methionine synthase responsible for the synthesis of L-methionine from L-homocysteine. Methionine is a precursor for succinyl-coA,

component of the citric acid cycle (Warner et al., 2007). Synthesis of L-methionine can also be catalysed by *mmuM*, a homocysteine *S*-methyltransferase (Warner et al., 2007). Studies have reported that *MmuM* is absent in rapid growing mycobacteria, however, it is conserved in the reduced genome of *M. leprae* (Pejchal and Ludwig, 2004, Young et al., 2015). Since L-methionine initiates the synthesis of most proteins (Pejchal and Ludwig, 2004, Warner et al., 2007, Young et al., 2015), the significant down-regulation of *mmuM* suggests a decrease in the pathogens' replication in the absence of the adhesin. Therefore, the deletion of *mtp* potentially results in an increased flux through the TCA pathway and stimulation of alarmones, which decreases replication resulting in a general decreased synthesis of amino acids such as serine and methionine.

2.5.2.3 MTP and HBHA modulate ATP synthesis via the oxidative phosphorylation pathway

Substrate-level phosphorylation encompasses ATP generation via utilization of free energy produced during various processes in metabolic pathways (Butlin et al., 1971, Black et al., 2014). It also provides a fast source of ATP through a process that is not dependant on electron acceptors (Butlin et al., 1971, Black et al., 2014). During OPP, ATP is generated via the F₁F₀-ATP synthase enzyme, coupled to the proton motive force (PMF) (Butlin et al., 1971, Black et al., 2014). Classified as a facultative anaerobe, *M. tuberculosis* is dependent on OPP for growth and survival during pathogenesis (Butlin et al., 1971, Black et al., 2014). The mycobacterial F₁-F₀-ATP synthase is encoded by the *Rv1303-atpBEFGHDC-Rv1312* operon (Black et al., 2014). The cf (0) subunit, of the ATP synthase, is involved in translocation of protons across the membrane and cf (1), which is the catalytic portion, is responsible for conversion of adenosine di-phosphate (ADP) to ATP (Kapopoulou et al., 2011). The PMF is important for the final generation of ATP through the F₁-F₀-ATP synthase (Rao et al., 2008, Black et al., 2014), and is established through the development of the transmembrane proton gradient (Rao et al., 2008, Black et al., 2014). The proton gradient occurs when electrons move through the electron transport chain resulting in the establishment of membrane potential (Rao et al., 2008, Black et al., 2014). The electron transport chain and PMF are vital components for the generation of ATP, a crucial requirement for metabolic processes. The proton gradient is responsible for the conversion of electrochemical potential energy produced by PMF into chemical energy, ATP (Kuroda and Tsuchiya, 2009, Black et al., 2014). The OPP is the predominant source of energy production in mycobacteria and ATP synthase

represents the pivotal enzyme in ATP generation in mycobacteria (Black et al., 2014). *M. tuberculosis* is known to survive at low PMF (- 110 mV) (Rao et al., 2008), therefore the ATP synthase needs to be adapted to allow efficient energy usage at this low PMF for ATP synthesis (Lu et al., 2014). It was previously hypothesized that *M. tuberculosis* ATP synthase may be active at a lower PMF, in comparison to other organisms or mitochondria (Bald and Koul, 2010). Furthermore, with the deletion of the surface located adhesin and increased expression of the ATP synthase, it is postulated that the proton gradient may be altered, potentially resulting in a decreased ATP production via this pathway. Subsequently, this decrease may potentially signal attempts to increased ATP synthesis via ATP synthase.

The synthesis of ATP via OPP is fed by cytochrome *c* oxidase (*ctaC*) located in Complex IV, (Shi et al., 2005, Rowland and Niederweis, 2012), and is largely mediated by ATP synthase of Complex V (Iino and Noji, 2013) (Figure 2.3). The F₁-F₀-ATP synthase is encoded by ATP synthase genes such as *atpB* (*Rv1304*), *atpC* (*Rv1311*), *atpD* (*Rv1310*), *atpE* (*Rv1305*), *atpF* (*Rv1306*), *atpG* (*Rv1309*), and *atpH* (*Rv1307*). The *Rv1303* gene is located upstream of the ATP synthase operon with a 7-bp overlap with *atpB* (Verma et al., 2014). The promoter for the ATP synthase operon is located upstream of *Rv1303* and co-transcribes the genes encoding the different ATP synthase subunits, such as *atpB* (Verma et al., 2014). The probable A-chain (*atpB*), has been postulated to play a direct role in the translocation of protons across the membrane, whilst probable lipid-binding protein C-chain (*atpE*) and B-chain (*atpF*) make up parts of the three non-enzymatic chain components (Kapopoulou et al., 2011). Linking cf (0) to cf (1), is the probable δ -chain (*atpH*) which is implicated in proton conduction (Kapopoulou et al., 2011). Lastly, the probable β -chain (*atpD*) is predicted to produce ATP from ADP in the presence of a proton gradient (Kapopoulou et al., 2011).

In the current study, genes involved in Complex IV (*ctaC*) and V (*atpE* and *atpF*) and ATP synthase promoter (*Rv1303*) of the OPP (Table 2.3; Figure 2.3 and 2.5-2.7) were significantly up-regulated in Δmtp , relative to the WT, suggesting a *Mycobacterium* that attempts to increase synthesis of ATP via this pathway under low PMF conditions created by the adhesin depletions. Alterations in complex V were observed in $\Delta mtp-hbhA$ (statistically non-significant up-regulation of *atpB*, *atpC* and *atpH*) and $\Delta hbhA$ (statistically non-significant up-regulation of *atpB*). In order to determine whether ATP synthase and ATP generation were perturbed via OPP in the absence

of MTP, HBHA and MTP-HBHA, a few genes (*atpB*, *atpD*, *atpE*, *atpF*, and *atpH*) were investigated further by RT-qPCR in all three deletion mutants. Gene expression analysis demonstrated a significantly increased expression of ATP synthase in Δmtp , with few genes displaying statistical significance between the WT and complement, suggesting the complement was partially restored to the WT genotype. The significance between the complements and WT could be attributed to the construction of the complements via non-integrating over-expressing plasmids.

The expression analysis conferred an increased expression of ATP synthase in all deletion mutants, suggesting attempted increase in ATP generation via this pathway. The $\Delta mtp-hbhA$ and $\Delta hbhA$ displayed a significantly increased expression of ATP synthase relative to the WT via RT-qPCR, whilst the RNA sequencing demonstrated a statistically non-significant down-regulation of these genes. Furthermore, their respective complements showed no significant differences relative to the WT. The contradicting RNA sequencing and RT-qPCR observations may be attributed to the use of only one housekeeping gene for normalization of gene expression, and limitations of the mapping strategies as a result of the dearth in *M. tuberculosis* annotated transcriptomic data. The RNA-sequencing analysis revealed up-regulation and down-regulation (statistically non-significant) of a few ATP synthase genes in $\Delta mtp-hbhA$ and $\Delta hbhA$, which are co-transcribed by the synthase promoter. Since the synthase is encoded by *Rv1303-atpBEFGHDC-Rv1312* operon, the up/down-regulation within the synthase could be attributed to the mapping strategy used. Since RNA sequencing broadly elucidates *M. tuberculosis* global gene expression, it should be aided when needed by a more accurate representation of the alterations such as RT-qPCR.

The functional ATP assay showed a significantly decreased concentration of ATP in the deletion mutants, relative to the WT. This decrease could be attributed to either a decrease in ATP generation via PMF or an increase in ATP consumption via ATP-dependant ABC transporters and adhesion molecules. The percentage of ATP generated by each cellular pathway (PMF, OPP, glycolysis) may be determined by further bioenergetics studies in future research. A significantly increased concentration of ATP was observed in the complements, relative to the WT. This could be attributed to either a higher energy storage observed in the complements, particularly Δmtp - and $\Delta mtp-hbhA$ -complements, relative to the WT, or an increase in ATP generation via PMF. Collectively, the data suggests that MTP and HBHA perturb ATP synthase potentially increasing

ATP synthesis, which may potentially be signalled by perturbations in the proton gradient resulting in a decreased ATP generation via PMF. The decreased concentration of ATP in the deletion mutants could be the result of a decrease in ATP via PMF or increased ATP consumption via ATP-dependant ABC transporters.

Moreover, significant up-regulation of *lpdA* (*Rv3303c*), a lipoamide dehydrogenase (Akhtar et al., 2006), was evident in Δmtp -*hbhA*. The *lpdA* gene is predicted to manage oxidative stress in pathogenic bacteria (Argyrou and Blanchard, 2001, Argyrou et al., 2004, Leung et al., 2017). Although the effect of *lpdA* on drug resistance in *M. tuberculosis* remains unknown, its involvement in regulation of the redox equilibrium suggests a potential association with drugs that require bacterial catalase activation (Leung et al., 2017). Taken together, the perturbation of OPP pathways and oxidative stress management in the absence of MTP-HBHA, suggests the potential effect of these two adhesins in combination, on the regulation of the OPP.

2.5.3 The role of MTP and HBHA in transport across the cell wall and cell membrane

M. tuberculosis has numerous cell wall transport proteins that aid in its survival and persistence (Youm and Saier Jr, 2012). In the current study, alterations to various transport proteins and operons were observed suggesting an increase in cell wall transport in the absence of the adhesins. *Rv0986*, *Rv0988*, and *secE2* (*Rv0379*) in Δmtp , and *secE2* in $\Delta hbhA$ were significantly up-regulated in the current study (Table 2.3 and 2.4; Appendix C2.2- C2.4; Figure 2.1). In *M. tuberculosis*, *Rv0986*, *Rv0987* and *secE2* encode an ATP-binding cassette (ABC) transporters which are involved in energy coupling to the transport system (Pethe et al., 2004, Rosas-Magallanes et al., 2006). The ABC transporters require ATP for transport of adhesion molecules, *Rv0987*, and are dependent on energy production in the cell (Kuroda and Tsuchiya, 2009, Black et al., 2014). The genes *Rv0986* and *Rv0987* are predicted to be involved in active transport of adhesion components across the membrane and attachment (Pethe et al., 2004, Rosas-Magallanes et al., 2006). Moreover, *secE2* (*Rv0379*), encodes possible ABC transport protein of the subfamily F (Kapopoulou et al., 2011) and displays a strong ATPase activity (Daniel et al., 2018). Gene expression analysis was performed on *Rv0986*, *Rv0987* and *secE2* of the ATP-binding cassette (ABC) transporters due to the significant up-regulation of the different ABC transport genes in the deletion mutants. The expression of these genes was significantly increased in Δmtp , $\Delta hbhA$ and

Δmtp-hbhA, relative to the WT. The *mtp*- and *hbhA*-complemented strains displayed no significant expression of *Rv0986* and *Rv0987* relative to the WT, whilst the *mtp-hbhA*-complement displayed no significant expression of *secE2* relative to the WT. Overall up-regulation of these genes points toward increased transport of proteins to the cell membrane/wall via ATP utilization in the absence of MTP and HBHA. Additionally, *Rv0988*, a probable exported protein (Pethe et al., 2004, Rosas-Magallanes et al., 2006) was significantly up-regulated in *Δmtp*, suggesting alterations in membrane associated proteins in the absence of the pili.

2.5.4 The regulatory role of MTP and HBHA

2.5.4.1 The regulatory role of MTP in molybdenum cofactor biosynthesis

Molybdenum is an essential trace element central to many large enzymes including nitrate reductase, xanthine oxidoreductases, sulphite oxidase and nitrogenases (Schwarz et al., 2009). Molybdopterins are a class of co-factors that bind to active metals found in most molybdenum enzymes (Schwarz et al., 2009). The molybdopterin and molybdenum complex is regarded as the molybdenum cofactor (Schwarz et al., 2009). *M. tuberculosis* expresses *moaA1* (*Rv1309*), *moaB1*, *moaC1* and *moaD1* that encode key enzymes involved in the synthesis of molybdopterin, a pterin based molybdenum cofactor (Schwarz et al., 2009, Lopez et al., 2010). The initial step in molybdopterin synthesis is predicted to start with the conversion of guanosine triphosphate (GTP) into cyclic pyranopterin monophosphate (cPMP) catalysed by *moaA1* and *moaAC1* (Schwarz et al., 2009, Lopez et al., 2010). Subsequently, molybdopterin synthase converts cPMP to meta binding pterin dithiolate (Schwarz et al., 2009, Lopez et al., 2010). The insertion of molybdenum into molybdopterin is predicted to be catalysed by *moaB1* (Schwarz et al., 2009, Lopez et al., 2010). Significant up-regulation of *moaA1* in the *Δmtp-hbhA* suggests an increase in molybdenum cofactor precursors. Moreover, a significant down-regulation of *moeX* (*Rv1681*) was observed in *Δmtp*. The *moeX* is a possible molybdopterin biosynthesis protein involved in molybdenum cofactor biosynthesis (Schwarz et al., 2009, Lopez et al., 2010). Therefore, significant down-regulation of *moeX* suggests a decrease in molybdenum cofactor biosynthesis. The deletion of MTP and MTP-HBHA alters molybdenum cofactor biosynthesis, indicative of the possible effect MTP could have on this process.

2.5.4.2 The role of HBHA in copper and iron regulation

Copper and iron are essential nutrients in bacteria (Arredondo and Núñez, 2005). Excess or deficiencies of these nutrients causes impaired cellular functions and cell death (Arredondo and Núñez, 2005). A systemic deficiency in copper generates cellular iron deficiency (Arredondo and Núñez, 2005). Copper is required for the function of several proteins, including metalloenzymes such as cytochrome *c* oxidase (*ctaC*) (Spagnolo et al., 2004). Iron is required for numerous proteins and electron chain transport and microsomal electron transport proteins (Arredondo and Núñez, 2005). The genes *fdxA* and *csor* were significantly upregulated in $\Delta hbhA$. The CsoR regulon was elucidated to be a copper responsive transcriptional repressor (Liu et al., 2007, Marcus et al., 2016). However, the CsoR regulon, rather than copper sensitive operon repressor *csor* (*Rv0967*), are primarily responsible for the direct mitigation of the harmful effects of copper stress (Liu et al., 2007, Marcus et al., 2016). The significant increased expression of *csor* could be attributed to an increase in *ctaC* expression, which in turn, may lead to an increased expression of ATP synthase (complex V of the OPP). The induction of *csor* could potentially indicate a harmful concentration of copper, which causes impaired cellular functions. The *fdxA* (*Rv2007c*) encodes an orthologue ferredoxin iron-sulphur protein that acts as an electron carrier (Kapopoulou et al., 2011). The significant up-regulation of *fdxA* suggests an increase in electron transfer, possibly involved in electron transfer chain. Therefore, the deletion of HBHA significantly alters *csor* regulation possibly induced by increased expression of *ctaC* (displayed non-significant up-regulation; Appendix C2.3) and increases expression of electron carriers.

2.5.4.3 The role of MTP-HBHA in regulation of DevR-DevS

The DevR-DevS is a two-component system that permits bacteria to sense and adapt to diverse environmental conditions (Gao and Stock, 2009). The DevR-DevS system is one of the most characterized two component systems in *M. tuberculosis* and is induced by various gaseous stresses such as hypoxia (Bretl et al., 2011), and vitamin C (Taneja et al., 2010). The DevR regulon induces expression of approximately 48 genes involved in dormancy (Gao and Stock, 2009). Under the inducing conditions mentioned, DevR is activated by the transfer of phosphosignals from both DevS and DosT (Roberts et al., 2004). Studies investigating the aerobic expression of this regulon in laboratory-manipulated overexpression strains reported that overexpression of DevR circumvents DevS and DosT sensor kinase-mediated or small molecule phosphodonar-dependant

activation (Sharma and Tyagi, 2016). Moreover, it was suggested that aerobic overexpression of DevR increases the concentration of $\alpha 10$ helix-mediated active dimer species above the threshold level, as during induction by hypoxia, enabling expression of the regulon (Sharma and Tyagi, 2016). Infection studies in a mouse model reported that the deletion and reduced expression of *devR*, in comparison to the *M. tuberculosis* H37Rv WT strain, resulted in a hypervirulent strain of *M. tuberculosis* that grew more rapidly in the acute stage of infection in immunocompetent mice and in IFN- γ activated macrophages (Parish et al., 2003). The significant up-regulation of only *devS* and *devR*, no significant up-regulation of *dosT*, in the $\Delta hbhA$ suggests overexpression of *devR* under aerobic conditions. Additionally, up-regulation of the OPP further corroborates the overexpression of *devR* under aerobic conditions. Thus, in the absence of HBHA, the alterations in DevR regulation could potentially affect the pathogens virulence *in vivo*.

2.5.4.4 *The role of MTP-HBHA in regulation of insertion sequence element IS6110*

The $\Delta mtp-hbhA$ demonstrated a significant down-regulation of several genes (*Rv3326*, *Rv2815c*, and *Rv3475*) involved in the transposition of insertion sequence element IS6110 (Cloete et al., 2016). Insertion element IS6110, identified as a repeated sequence, is crucial in deciphering the transmission dynamics of this pathogen and was reported to play a role in pathogenicity (Cloete et al., 2016). Although there is limited understanding of these genes, they are postulated to be probable transposases required for the transposition of IS6110 (Cloete et al., 2016). A significant decreased expression of these genes may alter the transposition of this insertion element and related pathways in the absence of MTP and HBHA.

Interestingly, a significant down-regulation of *mtp* (*Rv3312A*) was observed in the $\Delta hbhA$. Since these two adhesins are located at different loci (Kapopoulou et al., 2011), the deletion of *hbhA* was not expected to affect *mtp* during the construction of the $\Delta hbhA$. Given that these genes encode surface located proteins responsible for adhesion, hypothetically the organism may compensate for a single deletion by expressing more proteins with a similar function. However, the opposite was observed from the transcriptomic analysis in this study. Therefore, it is postulated that *hbhA* could play a role in regulation of a promoter/regulator for other adhesins such as *mtp*. Since there is a vast number of unannotated hypothetical genes in the *M. tuberculosis* transcriptome, one of

these adhesin promoters could be unannotated. Hence, there is a need to further understand the transcriptome so that these adhesins and their potential regulatory roles can be elucidated.

2.5.5 The role of MTP and HBHA in virulence

M. tuberculosis has various proteins that enhance its virulence such as, virulence associated proteins (Vap) BC toxin-antitoxin (TA) systems and chaperonin proteins (Kong et al., 1993, Hu et al., 2008). The VapB, of VapBC, is the inhibitor and VapC is the PilT N-terminal domain ribonuclease toxin (Gerdes et al., 2002, Van Melderen and De Bast, 2009). Additionally, VapBC operons were found to be associated with repetitive elements, virulence factors and transposases which suggest they play a role in maintenance of virulence factors (Arcus et al., 2005). It was postulated that the various subsets of VapBC TA systems could be activated in response to various stressors enabling the organism to adapt to different environmental conditions (Arcus et al., 2005, Arcus et al., 2011). The significant down-regulation of VapC5 (*Rv0627*) observed in the $\Delta hbhA$, suggests a significant disruption in overall mRNA cleavage and maintenance of stress induced peptides and attenuation of efficient macrophage binding. Hence, the deletion of the HBHA adhesin could potentially render the pathogen more susceptible to environmental stressors and disrupt efficient macrophage binding.

The Δmtp displayed a significant down-regulation of *trpD* (*Rv2192c*), a probable anthranilate phosphoribosyltransferase involved in tryptophan biosynthesis (Smith et al., 2001, Lott, 2020). Infection studies using *M. tuberculosis trpD* deletion mutants and murine bone marrow-derived macrophages and mice reported that over 90% of *trpD* mutants were killed during a 10-day period (Smith et al., 2001, Lott, 2020). The *trpD* mutant was essentially avirulent in an immunocompromised mouse host (Smith et al., 2001, Lott, 2020). Vaccine studies in which mice were pre-treated with the *trpD* mutant revealed better protection than BCG against *M. tuberculosis* H37Rv (Smith et al., 2001, Lott, 2020). The *trpD* is essential for *M. tuberculosis* virulence, and strains that exhibit a disruption of *trpD* show strong potential as a vaccine candidate (Smith et al., 2001, Lott, 2020). Thus, the significant down-regulation of *trpD* results in alterations in tryptophan biosynthesis potentially decreasing virulence in the absence of MTP.

The PPE and PE are highly conserved N-terminal domains (Phelan et al., 2016) and are predicted to be virulence factors involved in host-pathogen interactions (Sampson, 2011). *M. tuberculosis* encodes the protein PPE59 (*Rv3429*), ascribed to elicit low T-cell immune response in comparison

to other inducers (Al-Attayah and Mustafa, 2008), and have a low homology in the C-terminal regions with other mycobacterial species (Chen et al., 2009). This protein was predicted to be an inducer of cell-mediated response by interleukin-1 and IFN- γ (Al-Attayah and Mustafa, 2008). The significant up-regulation of PPE59 reported in $\Delta mtp-hbhA$ suggests a role for increased induction of cell mediated response thereby, potentially decreasing the response to T-cells *in vivo* thus making the pathogen susceptible to death. Collectively, these findings are suggestive of the role that MTP and HBHA play in modulation of the host immune response to ensure establishment of early infection as a survival mechanism.

A limitation of the present study is that the impact of MTP and HBHA was elucidated in a bacterial transcriptome model and cannot be directly extrapolated to an infection model. Moreover, only one housekeeping gene was included for normalization. Although numerous studies (Patel, 2013, Herricks et al., 2020, Gani et al., 2021) performed the bioluminescence assay as per manufacturer's instructions on various *M. tuberculosis* strains, future studies could include an additional lysing step to ensure the cells are exhaustively lysed, thus detecting the most accurate levels of ATP. Future studies could include a secondary housekeeping gene, such as *recA* or *sigA* to provide a stronger representation of differential expression. In addition, future bioenergetic studies should provide the percentage of ATP generated by each cellular pathway (PMF, OPP, glycolysis) in order to determine alterations in ATP generation. Moreover, alterations in the ATP synthase only were further investigated via RT-qPCR and a bioluminescence assay. Future studies could investigate the alterations observed in the CCM to determine which specific pathways are altered in the absence of MTP and HBHA. Dual RNA-sequencing in *in vitro* and *in vivo* infection models would provide a more holistic view of the role these adhesins play during host-pathogen interactions. Moreover, additional functional protein studies could provide more insights into their role and impact on the transcriptome. This study was limited to one clinical strain which may not be representative of other clinical strains. Therefore, future research could make use of infection models analysing the impact of these two adhesins on the host and bacterial transcriptomes during infection, and further protein studies could confirm alterations made to the end-products of the perturbed pathways. Furthermore, *in vivo* investigations on survival kinetics in mice could be performed to determine whether the deletion of MTP potentially attenuates virulence of the

pathogen. Despite the above limitations, this study provides a novel and valuable insight on the roles that MTP and HBHA play in the regulation of the *M. tuberculosis* transcriptome.

2.6 Conclusion

Bioinformatic analysis coupled with gene expression and a bioluminescence assay revealed perturbations to the bacterial transcriptome caused by the deletion of the *mtp* and *hbhA* genes in *M. tuberculosis*. The major perturbations were associated with respiration and metabolism, cell wall and cell process, and virulence. An overall increased expression of ATP synthase was reported in Δmtp suggesting attempts of the adhesin depleted mutant bacteria towards increasing the generation of ATP via this pathway which could possibly be attributed to alterations in the PMF. The bioluminescence assay displayed reduced concentrations of ATP in all mutants, relative to the WT, suggestive of either increased ATP consumption or decreased ATP generation via PMF. The perturbations reported may disrupt many processes, increase flux through the TCA pathway and stimulate alarmones, which decrease replication subsequently resulting in a general decreased synthesis of amino acids such as serine and methionine, which may be exacerbated by alterations to CCM. Moreover, the distinct alterations in expression levels of genes associated with cell wall biosynthesis and structure in strains lacking MTP, is indicative of the potential role this adhesin plays in the regulation of the cell wall. The observed decreased expression of specific virulence genes could potentially indicate that the deletion of the adhesins attenuates virulence and decreases pathogenicity. In the absence of HBHA, alterations in iron and copper regulation were observed, thus indicating the potential role the adhesin plays in regulation of these elements. The deletion of both adhesin genes ($\Delta mtp-hbhA$) displayed a greater impact on cell wall biosynthesis and transport, ATP consumption and virulence, in comparison to the single deletion of each adhesin gene (Δmtp and $\Delta hbhA$). Additionally, the alterations in regulation of virulence associated genes suggest that MTP and HBHA potentially modulate host immune response as a survival mechanism. Therefore, this study further supports the use of MTP and HBHA in combination as an important target for TB diagnostics and therapeutic interventions.

Funding

This study was funded by a DST-NRF Innovation Master's Scholarship, Prof. M. Pillay's South African National Research Foundation CPRR grant (105841) for Grantholder-linked bursary and project running costs, and UKZN College of Health Sciences scholarship.

Authors Conflict of Interest Statement

The authors of this study declare no conflicts of interest.

Authors Contribution Statement

MP conceptualized the study. MP and BP designed the study. TJN conducted experiments, analysed the data and drafted the manuscript. SS provided guidance on bioinformatics and analytical support. RS provided guidance on RT-qPCR and analytical support. All authors contributed to and approved the manuscript.

2.7 References

- Ågren, D., Schnell, R., Oehlmann, W., Singh, M. & Schneider, G. 2008. Cysteine synthase (CysM) of *Mycobacterium tuberculosis* is an O-phosphoserine sulfhydrylase: evidence for an alternative cysteine biosynthesis pathway in mycobacteria. *Journal of Biological Chemistry*, 283, 31567-31574.
- Aguilar-Ayala, D. A., Tilleman, L., Van Nieuwerburgh, F., Deforce, D., Palomino, J. C., Vandamme, P., Gonzalez-Y-Merchand, J. A. & Martin, A. 2017. The transcriptome of *Mycobacterium tuberculosis* in a lipid-rich dormancy model through RNAseq analysis. *Scientific Reports*, 7, 1-13.
- Akhtar, P., Srivastava, S., Srivastava, A., Srivastava, M., Srivastava, B. S. & Srivastava, R. 2006. *Rv3303c* of *Mycobacterium tuberculosis* protects tubercle bacilli against oxidative stress *in vivo* and contributes to virulence in mice. *Microbes and Infection*, 8, 2855-2862.
- Al-Attayah, R. & Mustafa, A. 2008. Characterization of human cellular immune responses to novel *Mycobacterium tuberculosis* antigens encoded by genomic regions absent in *Mycobacterium bovis* BCG. *Infection and Immunity*, 76, 4190-4198.
- Alteri, C. J., Xicohténcatl-Cortes, J., Hess, S., Caballero-Olín, G., Girón, J. A. & Friedman, R. L. 2007. *Mycobacterium tuberculosis* produces pili during human infection. *Proceedings of the National Academy of Sciences*, 104, 5145-5150.
- Amorim Franco, T. M. & Blanchard, J. S. 2017. Bacterial branched-chain amino acid biosynthesis: structures, mechanisms, and drugability. *Biochemistry*, 56, 5849-5865.
- Arcus, V. L., Rainey, P. B. & Turner, S. J. 2005. The PIN-domain toxin-antitoxin array in mycobacteria. *Trends in Microbiology*, 13, 360-365.

- Arcus, V. L., McKenzie, J. L., Robson, J. & Cook, G. M. 2011. The PIN-domain ribonucleases and the prokaryotic VapBC toxin–antitoxin array. *Protein Engineering, Design & Selection*, 24, 33-40.
- Argyrou, A. & Blanchard, J. S. 2001. *Mycobacterium tuberculosis* lipoamide dehydrogenase is encoded by *Rv0462* and not by the *lpdA* or *lpdB* genes. *Biochemistry*, 40, 11353-11363.
- Argyrou, A., Vetting, M. W. & Blanchard, J. S. 2004. Characterization of a new member of the flavoprotein disulfide reductase family of enzymes from *Mycobacterium tuberculosis*. *Journal of Biological Chemistry*, 279, 52694-52702.
- Armstrong, F. & Wagner, R. 1961. Biosynthesis of Valine and Isoleucine: IV. α -Hydroxy- β -keto acid reductoisomerase of salmonella. *Journal of Biological Chemistry*, 236, 2027-2032.
- Arredondo, M. & Núñez, M. T. 2005. Iron and copper metabolism. *Molecular Aspects of Medicine*, 26, 313-327.
- Ashokcoomar, S., Reedoy, K., Senzani, S., Loots, D., Beukes, D., van Reenen, M., Pillay, B. & Pillay, M. 2020. *Mycobacterium tuberculosis* curli pili (MTP) deficiency is associated with alterations in cell wall biogenesis, fatty acid metabolism and amino acid synthesis. *Metabolomics*, 16, 1-15.
- Ashokcoomar, S., Beukes, D., Van Reenen, M., Pillay, B. & Pillay, M. 2021. *M. tuberculosis* curli pili (MTP) is associated with alterations in carbon, fatty acid and amino acid metabolism in a THP-1 macrophage infection model. *Microbial Pathogenesis*, 104806.
- Azuma, I., Ajisaka, M. & Yamamura, Y. 1970. Polysaccharides of *Mycobacterium bovis Ushi 10*, *Mycobacterium smegmatis*, *Mycobacterium phlei*, and atypical *Mycobacterium P1*. *Infection and Immunity*, 2, 347-349.
- Baddam, R., Kumar, N., Wieler, L. H., Lankapalli, A. K., Ahmed, N., Peacock, S. J. & Semmler, T. 2018. Analysis of mutations in *pncA* reveals non-overlapping patterns among various lineages of *Mycobacterium tuberculosis*. *Scientific Reports*, 8, 1-9.
- Bald, D. & Koul, A. 2010. Respiratory ATP synthesis: the new generation of mycobacterial drug targets? *Federation of European Microbiological Societies Microbiology letters*, 308, 1-7.
- Banerjee, S., Farhana, A., Ehtesham, N. Z. & Hasnain, S. E. 2011. Iron acquisition, assimilation and regulation in mycobacteria. *Infection, Genetics and Evolution*, 11, 825-838.
- Bardarov, S., Bardarov Jr, S., Pavelka Jr, M. S., Sambandamurthy, V., Larsen, M., Tufariello, J., Chan, J., Hatfull, G. & Jacobs Jr, W. R. 2002. Specialized transduction: An efficient method for generating marked and unmarked targeted gene disruptions in *Mycobacterium tuberculosis*, *M. bovis* BCG and *M. smegmatis*. *Microbiology*, 148, 3007-3017.
- Basu, P., Sandhu, N., Bhatt, A., Singh, A., Balhana, R., Gobe, I., Crowhurst, N. A., Mendum, T. A., Gao, L. & Ward, J. L. 2018. The anaplerotic node is essential for the intracellular survival of *Mycobacterium tuberculosis*. *Journal of Biological Chemistry*, 293, 5695-5704.
- Beste, D. J., Nöh, K., Niefenführ, S., Mendum, T. A., Hawkins, N. D., Ward, J. L., Beale, M. H., Wiechert, W. & McFadden, J. 2013. ¹³C-flux spectral analysis of host-pathogen metabolism reveals a mixed diet for intracellular *Mycobacterium tuberculosis*. *Chemistry & Biology*, 20, 1012-1021.
- Bhatnagar, S. & Schorey, J. S. 2007. Exosomes released from infected macrophages contain *Mycobacterium avium* glycopeptidolipids and are proinflammatory. *Journal of Biological Chemistry*, 282, 25779-25789.
- Black, P. A., Warren, R. M., Louw, G. E., Van Helden, P. D., Victor, T. C. & Kana, B. D. 2014. Energy metabolism and drug efflux in *Mycobacterium tuberculosis*. *Antimicrobial agents and chemotherapy*, 58, 2491-2503.

- Bolger, A. M., Lohse, M. & Usadel, B. 2014. Trimmomatic: A flexible trimmer for Illumina sequence data. *Bioinformatics*, 30, 2114-2120.
- Bretl, D. J., Demetriadou, C. & Zahrt, T. C. 2011. Adaptation to environmental stimuli within the host: two-component signal transduction systems of *Mycobacterium tuberculosis*. *Microbiology and Molecular Biology Reviews*, 75, 566-582.
- Butcher, P. D. 2004. Microarrays for *Mycobacterium tuberculosis*. *Tuberculosis*, 84, 131-137.
- Buter, J., Cheng, T.-Y., Ghanem, M., Grootemaat, A. E., Raman, S., Feng, X., Plantijn, A. R., Ennis, T., Wang, J. & Cotton, R. N. 2019. *Mycobacterium tuberculosis* releases an antacid that remodels phagosomes. *Nature chemical biology*, 15, 889-899.
- Butlin, J. D., Cox, G. B. & Gibson, F. 1971. Oxidative phosphorylation in *Escherichia coli* K 12. Mutations affecting magnesium ion-or calcium ion-stimulated adenosine triphosphatase. *Biochemical Journal*, 124, 75-81.
- Caspi, R., Billington, R., Ferrer, L., Foerster, H., Fulcher, C. A., Keseler, I. M., Kothari, A., Krummenacker, M., Latendresse, M. & Mueller, L. A. 2016. The MetaCyc database of metabolic pathways and enzymes and the BioCyc collection of pathway/genome databases. *Nucleic Acids Research*, 44, D471-D480.
- Chattopadhyay, A., Meier, M., Ivaninskii, S., Burkhard, P., Speroni, F., Campanini, B., Bettati, S., Mozzarelli, A., Rabeh, W. M. & Li, L. 2007. Structure, mechanism, and conformational dynamics of O-acetylserine sulphydrylase from *Salmonella typhimurium*: comparison of A and B isozymes. *Biochemistry*, 46, 8315-8330.
- Chen, J., Su, X., Zhang, Y., Wang, S., Shao, L., Wu, J., Wang, F., Zhang, S., Wang, J. & Weng, X. 2009. Novel recombinant RD2-and RD11-encoded *Mycobacterium tuberculosis* antigens are potential candidates for diagnosis of tuberculosis infections in BCG-vaccinated individuals. *Microbes and Infection*, 11, 876-885.
- Chiacchio, T., Delogu, G., Vanini, V., Cuzzi, G., De Maio, F., Pinnetti, C., Sampaolesi, A., Antinori, A. & Goletti, D. 2017. Immune characterization of the HBHA-specific response in *Mycobacterium tuberculosis*-infected patients with or without HIV infection. *PLoS One*, 12, e0183846.
- Cloete, R., Oppon, E., Murungi, E., Schubert, W.-D. & Christoffels, A. 2016. Resistance related metabolic pathways for drug target identification in *Mycobacterium tuberculosis*. *BioMed Central Bioinformatics*, 17, 75.
- Daniel, J., Abraham, L., Martin, A., Pablo, X. & Reyes, S. 2018. Rv2477c is an antibiotic-sensitive manganese-dependent ABC-F ATPase in *Mycobacterium tuberculosis*. *Biochemical And Biophysical Research Communications*, 495, 35-40.
- Das, M. K., Ray, A. A., Cai, Y., Singhanian, A., Graham, C., Liao, M., Fountain, J. J., Pearl, J. E., Pareek, M. & Haldar, P. 2018. Differential expression of an alternative splice variant of IL-12R β 1 impacts early dissemination in the mouse and associates with disease outcome in both mouse and humans exposed to tuberculosis. *BioRxiv*, 271627.
- Díaz-Silvestre, H., Espinosa-Cueto, P., Bernal, G., Espitia, C. & Mancilla, R. 2002. The 19 kDa glycolipoprotein of *Mycobacterium tuberculosis* is a major adhesin for THP-1 and monocyte derived-human macrophages. *Revista VacciMonitor (Vacunología y Temas Afines)*, 11.
- Dlamini, M. T. 2016. 'Whole transcriptome analysis to elucidate the role of mtp in gene regulation of pulmonary epithelial cells infected with *Mycobacterium tuberculosis*.' Unpublished Masters dissertation. University of Kwa-Zulu- Natal, Durban, South Africa.

- Ducati, R. G., Breda, A., Basso, L. & Santos, D. 2011. Purine salvage pathway in *Mycobacterium tuberculosis*. *Current Medicinal Chemistry*, 18, 1258-1275.
- El-Sony, A., Enarson, D., Khamis, A., Baraka, O. & Bjune, G. 2002. Relation of grading of sputum smears with clinical features of tuberculosis patients in routine practice in Sudan. *The International Journal of Tuberculosis and Lung Disease*, 6, 91-97.
- Esparza, M., Palomares, B., García, T., Espinosa, P., Zenteno, E. & Mancilla, R. 2015. PstS-1, the 38-kDa *Mycobacterium tuberculosis* glycoprotein, is an adhesin, which binds the macrophage mannose receptor and promotes phagocytosis. *Scandinavian Journal of Immunology*, 81, 46-55.
- Esposito, C., Marasco, D., Delogu, G., Pedone, E. & Berisio, R. 2011. Heparin-binding hemagglutinin HBHA from *Mycobacterium tuberculosis* affects actin polymerisation. *Biochemical and Biophysical Research Communications*, 410, 339-344.
- Fang, M. & Bauer, C. E. 2018. Regulation of stringent factor by branched-chain amino acids. *Proceedings of the National Academy of Sciences*, 115, 6446-6451.
- Fogel, N. 2015. Tuberculosis: A disease without boundaries. *Tuberculosis*, 95, 527-531.
- Frazeo, A. C., Perteu, G., Jaffe, A. E., Langmead, B., Salzberg, S. L. & Leek, J. T. 2015. Ballgown bridges the gap between transcriptome assembly and expression analysis. *Nature Biotechnology*, 33, 243.
- Gandhi, N. R., Moll, A., Sturm, A. W., Pawinski, R., Govender, T., Lalloo, U., Zeller, K., Andrews, J. & Friedland, G. 2006. Extensively drug-resistant tuberculosis as a cause of death in patients co-infected with tuberculosis and HIV in a rural area of South Africa. *The Lancet*, 368, 1575-1580.
- Gani, Z., Boradia, V. M., Kumar, A., Patidar, A., Talukdar, S., Choudhary, E., Singh, R., Agarwal, N., Raje, M. & Iyengar Raje, C. 2021. *Mycobacterium tuberculosis* glyceraldehyde-3-phosphate dehydrogenase plays a dual role—As an adhesin and as a receptor for plasmin (ogen). *Cellular Microbiology*, 23, e13311.
- Gao, R. & Stock, A. M. 2009. Biological insights from structures of two-component proteins. *Annual Review of Microbiology*, 8, 63.
- Gerdes, S. Y., Scholle, M. D., D'Souza, M., Bernal, A., Baev, M. V., Farrell, M., Kurnasov, O. V., Daugherty, M. D., Mseeh, F. & Polanuyer, B. M. 2002. From genetic footprinting to antimicrobial drug targets: Examples in cofactor biosynthetic pathways. *Journal of Bacteriology*, 184, 4555-4572.
- Gehring, A. J., Dobos, K. M., Belisle, J. T., Harding, C. V. & Boom, W. H. 2004. *Mycobacterium tuberculosis* LprG (*Rv1411c*): A novel TLR-2 ligand that inhibits human macrophage class II MHC antigen processing. *The Journal of Immunology*, 173, 2660-2668.
- Gomez-Gonzalez, P. J., Andreu, N., Phelan, J. E., De Sessions, P. F., Glynn, J. R., Crampin, A. C., Campino, S., Butcher, P. D., Hibberd, M. L. & Clark, T. G. 2019. An integrated whole genome analysis of *Mycobacterium tuberculosis* reveals insights into relationship between its genome, transcriptome and methylome. *Scientific Reports*, 9, 1-11.
- Govender, V. S., Jain, P., Larsen, M. H. & Pillay, M. 2018. '*Mycobacterium tuberculosis* heparin binding hemagglutinin adhesin (HBHA) and curli pili (MTP) are essential for in vitro growth, but not viability and biofilm production.' Unpublished manuscript from the PhD thesis. University of Kwa-Zulu- Natal, Durban, South Africa.

- Hauryliuk, V., Atkinson, G. C., Murakami, K. S., Tenson, T. & Gerdes, K. 2015. Recent functional insights into the role of (p) ppGpp in bacterial physiology. *Nature Reviews Microbiology*, 13, 298-309.
- Herricks, T., Donczew, M., Mast, F., Rustad, T., Morrison, R., Sterling, T. R., Sherman, D. & Aitchison, J. D. 2020. ODELAM: Rapid sequence-independent detection of drug resistance in clinical isolates of *Mycobacterium tuberculosis*. *Elife*, 9, p.e56613.v.
- Hickey, T. B., Ziltener, H. J., Speert, D. P. & Stokes, R. W. 2010. *Mycobacterium tuberculosis* employs Cpn60. 2 as an adhesin that binds CD43 on the macrophage surface. *Cellular Microbiology*, 12, 1634-1647.
- Hu, Y., Henderson, B., Lund, P. A., Tormay, P., Ahmed, M. T., Gurcha, S. S., Besra, G. S. & Coates, A. R. 2008. A *Mycobacterium tuberculosis* mutant lacking the *groEL* homologue *cpn60. 1* is viable but fails to induce an inflammatory response in animal models of infection. *Infection and Immunity*, 76, 1535-1546.
- Iino, R. & Noji, H. 2013. Operation mechanism of FoF1-adenosine triphosphate synthase revealed by its structure and dynamics. *Lubmb Life*, 65, 238-246.
- Kanehisa, M. & Goto, S. 2000. KEGG: Kyoto Encyclopedia of Genes and Genomes. *Nucleic Acids Research*, 28, 27-30.
- Kanehisa, M. 2019. Toward understanding the origin and evolution of cellular organisms. *Protein Science*, 28, 1947-1951.
- Kang, C.-M., Abbott, D. W., Park, S. T., Dascher, C. C., Cantley, L. C. & Husson, R. N. 2005. The *Mycobacterium tuberculosis* serine/threonine kinases PknA and PknB: Substrate identification and regulation of cell shape. *Genes & Development*, 19, 1692-1704.
- Kang, C.-M., Nyayapathy, S., Lee, J.-Y., Suh, J.-W. & Husson, R. N. 2008. Wag31, a homologue of the cell division protein DivIVA, regulates growth, morphology and polar cell wall synthesis in mycobacteria. *Microbiology*, 154, 725-735.
- Kapopoulou, A., Lew, J. M. & Cole, S. T. 2011. The MycoBrowser portal: A comprehensive and manually annotated resource for mycobacterial genomes. *Tuberculosis*, 91, 8-13.
- Karp, P. D., Billington, R., Caspi, R., Fulcher, C. A., Latendresse, M., Kothari, A., Keseler, I. M., Krummenacker, M., Midford, P. E. & Ong, Q. 2019. The BioCyc collection of microbial genomes and metabolic pathways. *Briefings in Bioinformatics*, 20, 1085-1093.
- Kayne, F. 1973. 11 Pyruvate kinase. *The Enzymes*, 8, 358-382.
- Kim, D., Langmead, B. & Salzberg, S. L. 2015. HISAT: A fast spliced aligner with low memory requirements. *Nature Methods*, 12, 357-360.
- Kinhikar, A. G., Vargas, D., Li, H., Mahaffey, S. B., Hinds, L., Belisle, J. T. & Laal, S. 2006. *Mycobacterium tuberculosis* malate synthase is a laminin-binding adhesin. *Molecular Microbiology*, 60, 999-1013.
- Kong, T. H., Coates, A., Butcher, P., Hickman, C. & Shinnick, T. 1993. *Mycobacterium tuberculosis* expresses two chaperonin-60 homologs. *Proceedings of the National Academy of Sciences*, 90, 2608-2612.
- Kumar, S., Puniya, B. L., Parween, S., Nahar, P. & Ramachandran, S. 2013. Identification of novel adhesins of *M. tuberculosis* H37Rv using integrated approach of multiple computational algorithms and experimental analysis. *PLoS One*, 8.
- Kuroda, T. & Tsuchiya, T. 2009. Multidrug efflux transporters in the MATE family. *Biochimica et Biophysica Acta (BBA)-Proteins and Proteomics*, 1794, 763-768.
- Larsen, M. H., Biermann, K. & Jacobs Jr, W. R. 2007. Laboratory maintenance of *Mycobacterium tuberculosis*. *Current Protocols in Microbiology*, 6, 10A. 1.1-10A. 1.8.

- Layre, E., Lee, H. J., Young, D. C., Martinot, A. J., Buter, J., Minnaard, A. J., Annand, J. W., Fortune, S. M., Snider, B. B. & Matsunaga, I. 2014. Molecular profiling of *Mycobacterium tuberculosis* identifies tuberculosinyl nucleoside products of the virulence-associated enzyme Rv3378c. *Proceedings of the National Academy of Sciences*, 111, 2978-2983.
- Lee, W. L., Gold, B., Darby, C., Brot, N., Jiang, X., De Carvalho, L. P. S., Wellner, D., St. John, G., Jacobs Jr, W. R. & Nathan, C. 2009. *Mycobacterium tuberculosis* expresses methionine sulphoxide reductases A and B that protect from killing by nitrite and hypochlorite. *Molecular Microbiology*, 71, 583-593.
- Lee, J. S., Son, J., Jung, S. B., Kwon, Y. M., Yang, C. S., Oh, J. H., Song, C. H., Kim, H. J., Park, J. K. & Paik, T. H. 2006. *Ex vivo* responses for interferon-gamma and proinflammatory cytokine secretion to low-molecular-weight antigen MTB12 of *Mycobacterium tuberculosis* during human tuberculosis. *Scandinavian Journal of Immunology*, 64, 145-154.
- Leung, K. S.-S., Siu, G. K.-H., Tam, K. K.-G., To, S. W.-C., Rajwani, R., Ho, P.-L., Wong, S. S.-Y., Zhao, W. W., Ma, O. C.-K. & Yam, W.-C. 2017. Comparative genomic analysis of two clonally related multidrug resistant mycobacterium tuberculosis by single molecule real time sequencing. *Frontiers in Cellular and Infection Microbiology*, 7, 478.
- Liu, T., Ramesh, A., Ma, Z., Ward, S. K., Zhang, L., George, G. N., Talaat, A. M., Sacchetti, J. C. & Giedroc, D. P. 2007. CsoR is a novel *Mycobacterium tuberculosis* copper-sensing transcriptional regulator. *Nature Chemical Biology*, 3, 60-68.
- Lopez, P. M., Golby, P., Wooff, E., Garcia, J. N., Pelayo, M. C. G., Conlon, K., Camacho, A. G., Hewinson, R. G., Polaina, J. & García, A. S. 2010. Characterization of the transcriptional regulator Rv3124 of *Mycobacterium tuberculosis* identifies it as a positive regulator of molybdopterin biosynthesis and defines the functional consequences of a non-synonymous SNP in the *Mycobacterium bovis* BCG orthologue. *Microbiology*, 156, 2112.
- Lott, J. S. 2020. The tryptophan biosynthetic pathway is essential for *Mycobacterium tuberculosis* to cause disease. *Biochemical Society Transactions*, 48, 2029-2037.
- Lu, P., Lill, H. & Bald, D. 2014. ATP synthase in mycobacteria: Special features and implications for a function as drug target. *Biochimica et Biophysica Acta (BBA)-Bioenergetics*, 1837, 1208-1218.
- Marcus, S. A., Sidiropoulos, S. W., Steinberg, H. & Talaat, A. M. 2016. CsoR is essential for maintaining copper homeostasis in *Mycobacterium tuberculosis*. *PloS one*, 11, e0151816.
- Masungi, C., Temmerman, S., Van Vooren, J.-P., Drowart, A., Pethe, K., Menozzi, F. D., Locht, C. & Mascart, F. 2002. Differential T and B cell responses against *Mycobacterium tuberculosis* heparin-binding hemagglutinin adhesin in infected healthy individuals and patients with tuberculosis. *The Journal of infectious Diseases*, 185, 513-520.
- Menozzi, F. D., Reddy, V. M., Cayet, D., Raze, D., Debrie, A.-S., Dehouck, M.-P., Cecchelli, R. & Locht, C. 2006. *Mycobacterium tuberculosis* heparin-binding hemagglutinin adhesin (HBHA) triggers receptor-mediated transcytosis without altering the integrity of tight junctions. *Microbes and Infection*, 8, 1-9.
- Minnikin, D. E. 1982. Complex lipids, their chemistry biosynthesis and roles. *The Biology of Mycobacteria*, 1, 95-184.
- Moodley, S. 2018. "The role of heparin binding haemagglutinin adhesin and curli pili on the pathogenicity of *Mycobacterium tuberculosis*." Unpublished PhD thesis, University of Kwa-Zulu- Natal, Durban, South Africa.

- Muniram, S. 2018. "The role of *Mycobacterium tuberculosis* L,D-transpeptidase (Rv0309) in biofilm formation, growth kinetics and cellular morphology". unpublished Masters dissertation. University of Kwa-Zulu- Natal, Durban, South Africa.
- Naidoo, N., Ramsugit, S. & Pillay, M. 2014. *Mycobacterium tuberculosis* pili (MTP), a putative biomarker for a tuberculosis diagnostic test. *Tuberculosis*, 94, 338-345.
- Naidoo, N., Pillay, B., Bubb, M., Pym, A., Chiliza, T., Naidoo, K., Ndung'u, T., Kasprovicz, V. O. & Pillay, M. 2018. Evaluation of a synthetic peptide for the detection of anti-*Mycobacterium tuberculosis* curli pili IgG antibodies in patients with pulmonary tuberculosis. *Tuberculosis*, 109, 80-84.
- Noy, T., Vergnolle, O., Hartman, T. E., Rhee, K. Y., Jacobs Jr, W. R., Berney, M. & Blanchard, J. S. 2016. Central role of pyruvate kinase in carbon co-catabolism of *Mycobacterium tuberculosis*. *Journal of Biological Chemistry*, 291, 7060-7069.
- Mvubu, N. E., Pillay, B., Gamiendien, J., Bishai, W. & Pillay, M. 2016. *Mycobacterium tuberculosis* strains exhibit differential and strain-specific molecular signatures in pulmonary epithelial cells. *Developmental & Comparative Immunology*, 65, 321-329.
- Naidoo, N., Ramsugit, S. & Pillay, M. 2014. *Mycobacterium tuberculosis* pili (MTP), a putative biomarker for a tuberculosis diagnostic test. *Tuberculosis*, 94, 338-345.
- Nyawo, G. R. 2016. *The role of Mycobacterium tuberculosis pili in pathogenesis: Growth and survival kinetics, gene regulation and host immune response, and in vitro growth kinetics*. Masters dissertation. University of Kwa-Zulu Natal.
- Pai, M., Behr, M. A., Dowdy, D., Dheda, K., Divangahi, M., Boehme, C. C., Ginsberg, A., Swaminathan, S., Spigelman, M. & Getahun, H. 2016. Tuberculosis. *Nature Reviews. Disease Primers*, 2, 16076.
- Parida, S. K. & Kaufmann, S. H. 2010. The quest for biomarkers in tuberculosis. *Drug Discovery Today*, 15, 148-157.
- Parish, T., Smith, D. A., Kendall, S., Casali, N., Bancroft, G. J. & Stoker, N. G. 2003. Deletion of two-component regulatory systems increases the virulence of *Mycobacterium tuberculosis*. *Infection and Immunity*, 71, 1134-1140.
- Patel, N. 2013. The Effects of Glutathione and Its Derivatives on the Survival of *Mycobacterium bovis*-BCG Vegetative and Persistent Organisms. Honors College Thesis, Pace University, United States of America.
- Pejchal, R. & Ludwig, M. L. 2004. Cobalamin-independent methionine synthase (MetE): a face-to-face double barrel that evolved by gene duplication. *PLoS Biology*, 3, e31.
- Pertea, M., Kim, D., Pertea, G. M., Leek, J. T. & Salzberg, S. L. 2016. Transcript-level expression analysis of RNA-seq experiments with HISAT, StringTie and Ballgown. *Nature Protocols*, 11, 1650.
- Pethe, K., Alonso, S., Biet, F., Delogu, G., Brennan, M. J., Locht, C. & Menozzi, F. D. 2001. The heparin-binding hemagglutinin of *M. tuberculosis* is required for extrapulmonary dissemination. *Nature*, 412, 190-194.
- Pethe, K., Swenson, D. L., Alonso, S., Anderson, J., Wang, C. & Russell, D. G. 2004. Isolation of *Mycobacterium tuberculosis* mutants defective in the arrest of phagosome maturation. *Proceedings of the National Academy of Sciences*, 101, 13642-13647.
- Pfaffl, M., Vandesompele, J. & Kubista, M. 2009. Real-time PCR: Current technology and applications. *Data Analysis Softw.*; Logan, J., Edwards, K., Saunders, N., Eds, 65-83.
- Pfaffl, M. W. 2012. Quantification strategies in real-time polymerase chain reaction. *Quantitative real-time PCR Appl Microbiol*, 53-62.

- Phelan, J. E., Coll, F., Bergval, I., Anthony, R. M., Warren, R., Sampson, S. L., van Pittius, N. C. G., Glynn, J. R., Crampin, A. C. & Alves, A. 2016. Recombination in pe/ppe genes contributes to genetic variation in *Mycobacterium tuberculosis* lineages. *BMC Genomics*, 17, 151.
- Phong, W., Lin, W., Rao, S., Dick, T. & Alonso, S. 2013. Characterization of phosphofructokinase activity in *Mycobacterium tuberculosis* reveals that a functional glycolytic carbon flow is necessary to limit the accumulation of toxic metabolic intermediates under hypoxia. *PLoS One*, 8(2), e56037.
- Płociński, P., Macios, M., Houghton, J., Niemiec, E., Płocińska, R., Brzostek, A., Słomka, M., Dziadek, J., Young, D. & Dziembowski, A. 2019. Proteomic and transcriptomic experiments reveal an essential role of RNA degradosome complexes in shaping the transcriptome of *Mycobacterium tuberculosis*. *Nucleic Acids Research*, 47, 5892-5905.
- Ragas, A., Roussel, L., Puzo, G. & Rivière, M. 2007. The *Mycobacterium tuberculosis* cell-surface glycoprotein apa as a potential adhesin to colonize target cells via the innate immune system pulmonary C-type lectin surfactant protein A. *Journal of Biological Chemistry*, 282, 5133-5142.
- Ramsugit, S., Guma, S., Pillay, B., Jain, P., Larsen, M. H., Danaviah, S. & Pillay, M. 2013. Pili contribute to biofilm formation *in vitro* in *Mycobacterium tuberculosis*. *Antonie Van Leeuwenhoek*, 104, 725-735.
- Ramsugit, S., Pillay, B. & Pillay, M. 2016. Evaluation of the role of *Mycobacterium tuberculosis* pili (MTP) as an adhesin, invasin, and cytokine inducer of epithelial cells. *The Brazilian Journal of Infectious Diseases*, 20, 160-165.
- Ramsugit, S. & Pillay, M. 2014. *Mycobacterium tuberculosis* pili promote adhesion to and invasion of THP-1 macrophages. *Japanese Journal of Infectious Diseases*, 67, 476-478.
- Rao, A. & Ranganathan, A. 2004. Interaction studies on proteins encoded by the phthiocerol dimycocerosate locus of *Mycobacterium tuberculosis*. *Molecular Genetics and Genomics*, 272, 571-579.
- Rao, S. P., Alonso, S., Rand, L., Dick, T. & Pethe, K. 2008. The protonmotive force is required for maintaining ATP homeostasis and viability of hypoxic, nonreplicating *Mycobacterium tuberculosis*. *Proceedings of the National Academy of Sciences*, 105 (33), 11945-11950.
- Reedoy, K., Loots, D., Beukes, D., Van Reenen, M., Pillay, B. & Pillay, M. 2020. *Mycobacterium tuberculosis* curli pili (MTP) is associated with significant host metabolic pathways in an A549 epithelial cell infection model and contributes to the pathogenicity of *Mycobacterium tuberculosis*. *Metabolomics*, 16, 1-14.
- Rhee, K. Y., de Carvalho, L. P. S., Bryk, R., Ehrt, S., Marrero, J., Park, S. W., Schnappinger, D., Venugopal, A. & Nathan, C. 2011. Central carbon metabolism in *Mycobacterium tuberculosis*: An unexpected frontier. *Trends in Microbiology*, 19, 307-314.
- Roberts, D. M., Liao, R. P., Wisedchaisri, G., Hol, W. G. & Sherman, D. R. 2004. Two sensor kinases contribute to the hypoxic response of *Mycobacterium tuberculosis*. *Journal of Biological Chemistry*, 279, 23082-23087.
- Rosas-Magallanes, V., Deschavanne, P., Quintana-Murci, L., Brosch, R., Gicquel, B. & Neyrolles, O. 2006. Horizontal transfer of a virulence operon to the ancestor of *Mycobacterium tuberculosis*. *Molecular Biology and Evolution*, 23, 1129-1135.
- Rowland, J. L. & Niederweis, M. 2012. Resistance mechanisms of *Mycobacterium tuberculosis* against phagosomal copper overload. *Tuberculosis*, 92, 202-210.

- Sampson, S. L. 2011. Mycobacterial PE/PPE proteins at the host-pathogen interface. *Clinical and Developmental Immunology*, 2011, 497203.
- Sasseti, C. M., Boyd, D. H. & Rubin, E. J. 2003. Genes required for mycobacterial growth defined by high density mutagenesis. *Molecular Microbiology*, 48, 77-84.
- Sauer, U. & Eikmanns, B. J. 2005. The PEP—pyruvate—oxaloacetate node as the switch point for carbon flux distribution in bacteria: We dedicate this paper to Rudolf K. Thauer, Director of the Max-Planck-Institute for Terrestrial Microbiology in Marburg, Germany, on the occasion of his 65th birthday. *Federation of European Microbiological Societies, Microbiology Reviews*, 29, 765-794.
- Schwarz, G., Mendel, R. R. & Ribbe, M. W. 2009. Molybdenum cofactors, enzymes and pathways. *Nature*, 460, 839-847.
- Sharma, S. & Tyagi, J. S. 2016. *Mycobacterium tuberculosis* DevR/DosR dormancy regulator activation mechanism: Dispensability of phosphorylation, cooperativity and essentiality of α 10 Helix. *PloS one*, 11, e0160723.
- Shi, L., Sohaskey, C. D., Kana, B. D., Dawes, S., North, R. J., Mizrahi, V. & Gennaro, M. L. 2005. Changes in energy metabolism of *Mycobacterium tuberculosis* in mouse lung and under *in vitro* conditions affecting aerobic respiration. *Proceedings of the National Academy of Sciences*, 102, 15629-15634.
- Shin, A.-R., Lee, K.-S., Lee, J.-S., Kim, S.-Y., Song, C.-H., Jung, S.-B., Yang, C.-S., Jo, E.-K., Park, J.-K. & Paik, T.-H. 2006. *Mycobacterium tuberculosis* HBHA protein reacts strongly with the serum immunoglobulin M of tuberculosis patients. *Clinical and Vaccine Immunology*, 13, 869-875.
- Singh, A., Varela, C., Bhatt, K., Veerapen, N., Lee, O. Y., Wu, H. H., Besra, G. S., Minnikin, D. E., Fujiwara, N. & Teramoto, K. 2016. Identification of a desaturase involved in mycolic acid biosynthesis in *Mycobacterium smegmatis*. *PLoS One*, 11, e0164253.
- Shivers, R. P. & Sonenshein, A. L. 2004. Activation of the *Bacillus subtilis* global regulator CodY by direct interaction with branched-chain amino acids. *Molecular Microbiology*, 53, 599-611.
- Smith, V., Cheng, Y., Bryant, B. & Schorey, J. 2017. Exosomes function in antigen presentation during an *in vivo* *Mycobacterium tuberculosis* infection. *Scientific Reports*, 7, 43578.
- Smith, D. A., Parish, T., Stoker, N. G. & Bancroft, G. J. 2001. Characterization of Auxotrophic Mutants of *Mycobacterium tuberculosis* and Their Potential as Vaccine Candidates. *Infection and Immunity*, 69, 1142-1150.
- Solanki, V., Tiwari, M. & Tiwari, V. 2018. Host-bacteria interaction and adhesin study for development of therapeutics. *International Journal of Biological Macromolecules*, 112, 54-64.
- Spagnolo, L., Törö, I., D'orazio, M., O'Neill, P., Pedersen, J. Z., Carugo, O., Rotilio, G., Battistoni, A. & Djinović-Carugo, K. 2004. Unique features of the sodC-encoded superoxide dismutase from *Mycobacterium tuberculosis*, a fully functional copper-containing enzyme lacking zinc in the active site. *Journal of Biological Chemistry*, 279, 33447-33455.
- Sreenivasamurthy, S. K., Madugundu, A. K., Patil, A. H., Dey, G., Mohanty, A. K., Kumar, M., Patel, K., Wang, C., Kumar, A. & Pandey, A. 2017. Mosquito-borne diseases and omics: Tissue-restricted expression and alternative splicing revealed by transcriptome profiling of *Anopheles stephensi*. *Omics: A Journal of Integrative Biology*, 21, 488-497.
- Stayton, M. M., Rudolph, F. B. & Fromm, H. J. 1983. Regulation, genetics, and properties of adenylosuccinate synthetase: A review. *Current Topics in Cellular Regulation*. Elsevier.

- Stewart, G. R., Wernisch, L., Stabler, R., Mangan, J. A., Hinds, J., Laing, K. G., Young, D. B. & Butcher, P. D. 2002. Dissection of the heat-shock response in *Mycobacterium tuberculosis* using mutants and microarrays. *Microbiology*, 148, 3129-3138.
- Stryer, L., Reginald, H. & Garrett, C. M. G. 1981. *Biochemistry* (Volume 1), WH Freeman and Company, USA, 4.
- Taneja, N. K., Dhingra, S., Mittal, A., Naresh, M. & Tyagi, J. S. 2010. *Mycobacterium tuberculosis* transcriptional adaptation, growth arrest and dormancy phenotype development is triggered by vitamin C. *PLoS one*, 5, e10860.
- Untergasser, A., Nijveen, H., Rao, X., Bisseling, T., Geurts, R. & Leunissen, J. A. 2007. Primer3Plus, an enhanced web interface to Primer3. *Nucleic Acids Research*, 35, W71-W74.
- Van Melderren, L. & De Bast, M. S. 2009. Bacterial toxin–antitoxin systems: more than selfish entities? *PLoS Genet*, 5, e1000437.
- Verma, S. C., Venugopal, U., Khan, S. R., Akhtar, M. S. & Krishnan, M. Y. 2014. Coupling reporter expression to respiration detects active as well as dormant mycobacteria in vitro and in mouse tissues. *International Journal of Mycobacteriology*, 3, 25-35.
- Warner, D. F., Savvi, S., Mizrahi, V. & Dawes, S. S. 2007. A riboswitch regulates expression of the coenzyme B12-independent methionine synthase in *Mycobacterium tuberculosis*: implications for differential methionine synthase function in strains H37Rv and CDC1551. *Journal of Bacteriology*, 189, 3655-3659.
- Wang, J., Wang, Y., Tang, L. & Garcia, R. C. 2019. Extracellular vesicles in mycobacterial infections: their potential as molecule transfer vectors. *Frontiers in Immunology*, 10, 1929.
- Webb, J. R., Vedvick, T. S., Alderson, M. R., Guderian, J. A., Jen, S. S., Owendale, P. J., Johnson, S. M., Reed, S. G. & Skeiky, Y. A. 1998. Molecular Cloning, Expression, and Immunogenicity of MTB12, a Novel Low-Molecular-Weight Antigen Secreted by *Mycobacterium tuberculosis*. *Infection and Immunity*, 66, 4208-4214.
- WHO. 2018. World Health Organization: *Global tuberculosis report 2018* [Online]. Available: https://www.who.int/tb/publications/global_report/en/ [Accessed November 2020].
- WHO. 2020. World Health Organization: *Global tuberculosis report 2020* [Online]. Available: https://www.who.int/tb/publications/global_report/en/ [Accessed November 2020].
- Wittwer, C. T. & Garling, D. J. 1991. Rapid cycle DNA amplification: time and temperature optimization. *Biotechniques*, 10, 76-83.
- Yim, K. H., Nahm, F. S., Han, K. A. & Park, S. Y. 2010. Analysis of statistical methods and errors in the articles published in the Korean journal of pain. *The Korean Journal of Pain*, 23, 35.
- Youm, J. & Saier Jr, M. H. 2012. Comparative analyses of transport proteins encoded within the genomes of *Mycobacterium tuberculosis* and *Mycobacterium leprae*. *Biochimica et Biophysica Acta (BBA)-Biomembranes*, 1818, 776-797.
- Young, D. B., Comas, I. & de Carvalho, L. P. 2015. Phylogenetic analysis of vitamin B12-related metabolism in *Mycobacterium tuberculosis*. *Frontiers in Molecular Biosciences*, 2, 6.

Chapter 2 investigated the role of MTP and HBHA in regulation of respiration and metabolism, cell wall biosynthesis, membrane transport, and virulence pathways. The absence of MTP was implicated with altered cell wall biosynthesis and decreased virulence whilst the absence of HBHA resulted in decreased virulence due to the significant down-regulation of virulence associated proteins (Vap) BC toxin-antitoxin (TA) systems. The data suggested that the absence of both MTP and HBHA resulted in attempts to increase ATP production via ATP synthase, transport of proteins and adhesion components to the cell wall and membrane, and decreased virulence. Observations point toward a potential increased energy requirement for transport of proteins to the cell wall and an altered cell wall or a decreased ATP generation via PMF. Chapter 3 synthesizes the important findings from the previous chapter with limitations and future recommendations.

Chapter 3: Synthesis of research findings, conclusions, and recommendations

Tuberculosis (TB), caused by *Mycobacterium tuberculosis*, remains the foremost cause of death from a single infectious agent (World Health Organization, WHO, 2020). The ongoing challenges such as increased drug resistance, growing HIV epidemic (Karim et al., 2009), lack of effective point of care (POC) diagnostics, effective vaccines and efficacious drugs (Andersen and Doherty, 2005), warrant more attention being directed toward early detection and prevention of TB (Stones and Krachler, 2015). Research focusing on *M. tuberculosis* pathogenicity during early infection stages may aid in the search for novel accurate biomarkers for the development of improved diagnostics and treatment. Hence, bacterial adhesins are a promising target as they have immunogenic characteristics and are easily accessible (Stones and Krachler, 2015). Recent studies suggest that the surface located, heparin-binding hemagglutinin adhesin (HBHA) and *M. tuberculosis* curli pili (MTP), show great promise as potential biomarkers and vaccine candidates.

The HBHA (*Rv0475*) adhesin is a virulence factor present during the early stages of TB infection (Pethe et al., 2001). Infection studies, using A549 pneumocytes, reported a significant reduction in adhesion and invasion by a *M. tuberculosis* HBHA-deficient strain, relative to the wild-type (WT). Additionally, antibody response to HBHA may provide further immune protection against *M. tuberculosis* (Pethe et al., 2001). Moreover, it was suggested that HBHA induces epithelial transcytosis, which could represent a macrophage-independent extrapulmonary dissemination mechanism, leading to *M. tuberculosis* infection (Menozzi et al., 2006). Furthermore, as a diagnostic antigen, the presence or absence of HBHA is capable of distinguishing between active and latent TB infection (LTBI) in humans, due to the ability of the adhesin to induce a higher level of interferon- γ in LTBI (Hougardy et al., 2007). Hence, HBHA may pose a promising target in the development of TB diagnostics, vaccines and therapeutics (Esposito et al., 2012).

The MTP (*Rv3312A*) adhesin binds to laminin and reacts with IgG antibodies in patients' sera (Alteri et al., 2007). Additionally, MTP plays a role in biofilm production (Ramsugit et al., 2013), and is unique to the *M. tuberculosis* complex (MTBC) pathogens (Naidoo et al., 2014). Infection studies, using THP-1 macrophages (Ramsugit and Pillay, 2014) and A549 epithelial cells (Ramsugit et al., 2016), elucidated the role MTP played in adhesion and invasion. The MTP adhesin may reduce chemokine/cytokine induction in A549 epithelial cells as a survival

mechanism (Ramsugit et al., 2016). Thus, MTP shows great promise as a suitable biomarker for the development of a POC TB test, therapeutic intervention, and a potential vaccine candidate.

Despite the growing research efforts elucidating the influence of MTP and HBHA in *M. tuberculosis* pathogenesis, their individual and dual role in regulation of the *M. tuberculosis* transcriptome has not been explored. Therefore, in this study, the effect of *mtp* and *hbhA* deletion on the *M. tuberculosis* transcriptome was assessed by RNA extraction and sequencing of *M. tuberculosis* strains [*M. tuberculosis* V9124 (WT), MTP-deficient (Δmtp), MTP-proficient (*mtp*-complement), HBHA-deficient ($\Delta hbhA$), HBHA-proficient (*hbhA*-complement), MTP-HBHA-deficient ($\Delta mtp-hbhA$), MTP-HBHA-proficient (*mtp-hbhA*-complement)], global transcriptomics, genotypic confirmation of selected pathway genes by real-time quantitative PCR (RT-qPCR), and phenotypic confirmation by a bioluminescence cell viability assay. The data demonstrated perturbations in central carbon metabolism (CCM), adenosine triphosphate (ATP) synthesis, cell wall biosynthesis, membrane transport and virulence in the absence of MTP and HBHA.

3.1 MTP and HBHA influence central carbon metabolism (CCM) and the tricarboxylic acid (TCA) cycle in *Mycobacterium tuberculosis*

In the present study, perturbations in several CCM pathways were observed in the absence of MTP and HBHA. Increased expression of genes responsible for the breakdown of fructose and the reversible conversion of phosphoenolpyruvate (PEP) into pyruvate and adenosine 5'-monophosphate (AMP), suggest an increase of precursors feeding into the CCM pathway and an increase in the initial reactions in the TCA cycle, in the absence of MTP. Moreover, a decreased expression of genes responsible for conversion of inosine monophosphate (IMP) to ATP in the CCM indicates alterations in this pathway in the absence of HBHA, thus potentially decreasing ATP generation.

Significant alterations in the citric acid cycle, were observed in the absence of MTP. The perturbations observed suggest an increased flux through this pathway, and the stimulation of alarmones via increased expression of branched-chain amino acids (BCAAs), valine and isoleucine. Stimulation of alarmones decreases replication, resulting a general decreased synthesis of amino acids such as serine and methionine.

3.2 MTP and HBHA play a role in regulation of ATP synthesis in *Mycobacterium tuberculosis*

Mycobacterial ATP synthases show promise as targets for antimicrobial drugs (Cook et al., 2009, Bald and Koul, 2010, Lu et al., 2014). Perturbations resulting in increased expression of genes involved in complex IV (cytochrome *c* oxidase) and V (ATP synthase) of the oxidative phosphorylation (OPP) were observed in Δmtp , while $\Delta hbhA$ and $\Delta mtp-hbhA$ showed a non-significant up-regulation of few ATP synthase genes. This was validated by genotypic (RT-qPCR) and phenotypic (bioluminescence assay) assays. The increased expression of the ATP synthase is suggestive of a potential decreased proton motive gradient (Bald and Koul, 2010), which is postulated to be perturbed by the absence of the surface located adhesins. The perturbations in the proton gradient may subsequently decrease ATP generation via proton motive force (PMF), potentially signalling the increased expression of ATP synthases. Future bioenergetics studies may elucidate the percentage of ATP generated by each cellular pathway (PMF, OPP, glycolysis) to identify the perturbed pathways. Furthermore, with the deletion of the surface located adhesin and increased expression of the ATP synthase, it is postulated that the proton gradient may be altered, potentially resulting in a decreased ATP production via this pathway. Subsequently, this decrease may signal increased ATP synthesis via ATP synthase.

It was therefore postulated that there is either an increased consumption of ATP in the deletion mutants which may be sequestered into cell wall biogenesis and ATP dependant ABC-cell wall transporters, or a decrease in ATP generation via the proton motive gradient. Future bioenergetic studies could be used to determine the percentage of ATP generation by each cellular pathway to elucidate which pathway is perturbed in the absence of the adhesins.

3.3 MTP influences cell wall biosynthesis in *Mycobacterium tuberculosis*

The highly impermeable lipid-rich outer layer of *M. tuberculosis* cell wall aids in its success as a pathogen (Minnikin, 1982). Perturbations reported in this study, suggest a disruption in the mycobacterial cell wall biosynthesis in the absence of MTP and HBHA. Deletion of the adhesins, alone or in combination, resulted in perturbations in membrane lipoprotein synthesis resulting in an increased expression of membrane lipoproteins, to potentially compensate for the lack of adhesins. Moreover, the deletion of *hbhA* resulted in alterations in regulation of genes associated

with immune response, potentially resulting in an increase in the pathogen's susceptibility to killing by the host.

3.4 MTP and HBHA influence transport across the cell wall and cell membrane

M. tuberculosis has several cell wall transport proteins aiding in its survival and persistence (Youm and Saier Jr, 2012). Up-regulation of several ATP-binding cassette (ABC) transporters (Petthe et al., 2004, Rosas-Magallanes et al., 2006), were observed in all deletion mutants (Δmtp , $\Delta hbhA$, and $\Delta mtp-hbhA$). These transporters are involved in active transport of adhesion components (Kapopoulou et al., 2011), mycobacterial translocation with a high ATPase activity (Daniel et al., 2018), and translocation of proteins (Sharma et al., 2003). This was genotypically validated by RT-qPCR, thus potentially explaining the increased requirement of ATP for transport and translocation of proteins and adhesion components in the absence of MTP and HBHA.

3.5 MTP and HBHA play a role in transport and regulation

Alterations resulting in a decrease in molybdenum cofactor biosynthesis and transposition of insertion sequence element IS6110 were observed in the absence of both MTP and HBHA. These perturbations suggest a potential role of both MTP and HBHA in the regulation of these pathways.

The absence of HBHA resulted in a significant up-regulation of genes involved in iron and copper regulation. The up-regulation of the copper sensitive operon (*csoR*) could potentially be attributed to the increased expression of copper-dependant metalloenzyme *ctaC* (Liu et al., 2007, Marcus et al., 2016), which may lead to an increased expression of the ATP synthase (complex V of the OPP). Increased expression of ferredoxin iron-sulphur protein suggests an increase in electron transfer, and possible involvement in the electron transfer chain. Collectively, these perturbations suggest a potential role of HBHA in regulation of electron transfer and copper-dependant metalloenzymes. Moreover, increased expression of only *devS* and *devR*, in the absence of HBHA, suggest overexpression of *devR* under aerobic conditions. Therefore, these perturbations suggest a potential role for HBHA in DevR regulation.

3.6 MTP and HBHA influence virulence

Down-regulation of virulence associated proteins (VapBC), involved in maintenance of virulence factors (Arcus et al., 2005), as well as chaperonin proteins that prevent misfolding and promote refolding (Kong et al., 1993, Hu et al., 2008, Kapopoulou et al., 2011) was reported in the absence of HBHA. This suggests a disruption in overall mRNA cleavage and maintenance of stress induced peptides and attenuation of efficient macrophage binding rendering the pathogen more susceptible to environmental stressors and disrupt efficient macrophage binding. The deletion of *mtp* resulted in alterations in tryptophan biosynthesis potentially resulting in decreased virulence. Furthermore, perturbations in the regulation of an inducer of cell-mediated response by interleukin-1 and interferon gamma (Al-Attayah and Mustafa, 2008), was reported in the absence of MTP-HBHA. This suggests a potential decrease of the T-cell mediated response, thus making the pathogen more susceptible to killing by the host. Collectively, these findings are suggestive of the role that MTP and HBHA play in modulation of the host immune response as a survival mechanism.

3.7 Conclusion

In the absence of MTP and HBHA, alterations in expression of specific genes led to perturbations in important pathways, underlining the significant effect of each adhesin. A total of 43 genes was significantly differentially expressed among the Δmtp , $\Delta hbhA$, and $\Delta mtp-hbhA$ strains, relative to the WT strain. The significant perturbations to the related pathways indicate the relevance of MTP and HBHA in *M. tuberculosis* pathogenicity. The absence of MTP alone, was associated with decreased virulence, and perturbations in cell wall biosynthesis, ATP synthesis and the CCM. The lack of HBHA suggested decreased virulence, perturbations in iron and copper regulation, DevR regulation, and the CCM. The absence of both adhesins, MTP and HBHA, resulted in an increased ATP synthesis, and cell wall transporters, decreased virulence, and alterations in regulation of insertion elements. Thus, the double knockout deletion mutant displayed the most significant effect on the mentioned pathways, substantiating the use of MTP and HBHA, in combination, as notable virulence factors with potential as accurate biomarkers for the development of novel TB diagnostics and therapeutic interventions.

3.8 Limitations

Although the global transcriptomics approach used is advantageous in the discovery of novel accurate biomarkers, it is limited to a bacterial transcriptome model and therefore, cannot be extrapolated to an *in vitro* or *in vivo* infection model. Furthermore, since a single representative of the F15/LAM4/KZN strain was used in this study, the findings cannot be extrapolated to other clinical strains of the same family, or other strain families of *M. tuberculosis*. A comparison of bacterial transcriptomic findings with an *in vitro* infection model would provide a more holistic view of the roles these adhesins play during infection. Additionally, it was not possible to perform further functional genotypic and phenotypic studies of all the interesting up- and down-regulated pathway genes that may have provided better insight into the role of these adhesins and their influence on *M. tuberculosis* transcriptome. Furthermore, only one housekeeping gene was included for normalization. The bioluminescence assay measured the total ATP concentration within the cell, but did not determine the cellular pathway (PMF, OPP, glycolysis) by which the ATP was generated. Lastly, only alterations in the ATP synthase were further investigated via RT-qPCR and a functional assay, thus leaving the CCM to be investigated in more detail. Despite these limitations, this novel study has produced new knowledge and increased the understanding of the contributions of two important adhesins in TB pathogenesis and their potential role in regulation of the *M. tuberculosis* transcriptome.

3.9 Recommendations for future research

The impact of MTP and HBHA on the host and bacterial transcriptome should be studied in infection models *in vitro* to understand the intertwined relationship. The successful application of dual RNA-sequencing in a host infection model using these deletion mutant strains will support the use of this technology in future infection models. A comparison between the two technologies revealed the differences in detection of gene expression. Holistically, the data obtained from this study point toward RT-qPCR being the more accurate technique to detect the more subtle changes in gene expression in the altered transcriptome. Therefore, future studies could include a second confirmatory technique to corroborate RNA sequencing data. Future studies could include the use of a second housekeeping gene, such as *recA* or *sigA*, to provide a stronger representation of differential gene expression in RT-qPCR. Additionally, *in vivo* investigations in mice analysing survival kinetics may be used to determine if the deletion of the MTP adhesin potentially attenuates

virulence of *M. tuberculosis*. Moreover, future bioenergetic studies could be used to elucidate the percentage of ATP generated by each cellular pathway (proton motive force, the OPP, glycolysis) to determine alterations in ATP generation. In addition, although there are studies (Patel, 2013, Herricks et al., 2020, Gani et al., 2021) that performed the bioluminescence assay as per manufacturer's instructions on various *M. tuberculosis* strains, future studies could include additional lysing steps to ensure the cells are exhaustively lysed, thus detecting the most accurate levels of ATP. Future studies could also investigate the perturbations observed in the CCM through genotypic and functional assays, to determine the altered pathways in the absence of MTP and HBHA. Functional confirmation of the disruption of cell wall polymers, in the absence of MTP, could be confirmed by measurement of galactose-1-phosphate concentration.

3.10 References

- Al-Attayah, R. & Mustafa, A. 2008. Characterization of human cellular immune responses to novel *Mycobacterium tuberculosis* antigens encoded by genomic regions absent in *Mycobacterium bovis* BCG. *Infection and Immunity*, 76, 4190-4198.
- Alteri, C. J., Xicohtencatl-Cortes, J., Hess, S., Caballero-Olín, G., Girón, J. A. & Friedman, R. L. 2007. *Mycobacterium tuberculosis* produces pili during human infection. *Proceedings of the National Academy of Sciences*, 104, 5145-5150.
- Andersen, P. & Doherty, T. M. 2005. The success and failure of BCG—implications for a novel tuberculosis vaccine. *Nature Reviews Microbiology*, 3, 656-662.
- Arcus, V. L., Rainey, P. B. & Turner, S. J. 2005. The PIN-domain toxin–antitoxin array in mycobacteria. *Trends in Microbiology*, 13, 360-365.
- Bald, D. & Koul, A. 2010. Respiratory ATP synthesis: the new generation of mycobacterial drug targets? *Federation of European Microbiological Societies, Microbiology Letters*, 308, 1-7.
- Cook, G. M., Berney, M., Gebhard, S., Heinemann, M., Cox, R. A., Danilchanka, O. & Niederweis, M. 2009. Physiology of mycobacteria. *Advances in Microbial Physiology*, 55, 81-319.
- Daniel, J., Abraham, L., Martin, A., Pablo, X. & Reyes, S. 2018. Rv2477c is an antibiotic-sensitive manganese-dependent ABC-F ATPase in *Mycobacterium tuberculosis*. *Biochemical and Biophysical Research Communications*, 495, 35-40.
- Ducati, R., Breda, A., A Basso, L. & S Santos, D. 2011. Purine salvage pathway in *Mycobacterium tuberculosis*. *Current medicinal chemistry*, 18, 1258-1275.
- Esposito, C., Cantisani, M., D'Auria, G., Falcigno, L., Pedone, E., Galdiero, S. & Berisio, R. 2012. Mapping key interactions in the dimerization process of HBHA from *Mycobacterium tuberculosis*, insights into bacterial agglutination. *Federation of European Biochemical Societies, Letters*, 586, 659-667.
- Gani, Z., Boradia, V. M., Kumar, A., Patidar, A., Talukdar, S., Choudhary, E., Singh, R., Agarwal, N., Raje, M. & Iyengar Raje, C. 2021. *Mycobacterium tuberculosis* glyceraldehyde-3-

- phosphate dehydrogenase plays a dual role—As an adhesin and as a receptor for plasmin (ogen). *Cellular Microbiology*, 23, e13311.
- Herrick, T., Donczew, M., Mast, F., Rustad, T., Morrison, R., Sterling, T. R., Sherman, D. & Aitchison, J. D. 2020. ODELAM: Rapid sequence-independent detection of drug resistance in clinical isolates of *Mycobacterium tuberculosis*. *Elife*, 9, p.e56613.v.
- Hougardy, J.-M., Schepers, K., Place, S., Drowart, A., Lechevin, V., Verscheure, V., Debie, A.-S., Doherty, T. M., Van Vooren, J.-P. & Loch, C. 2007. Heparin-binding-hemagglutinin - induced IFN- γ release as a diagnostic tool for latent tuberculosis. *PLoS One*, 2, e926.
- Hu, Y., Henderson, B., Lund, P. A., Tormay, P., Ahmed, M. T., Gurcha, S. S., Besra, G. S. & Coates, A. R. 2008. A *Mycobacterium tuberculosis* mutant lacking the groEL homologue cpn60. 1 is viable but fails to induce an inflammatory response in animal models of infection. *Infection and Immunity*, 76, 1535-1546.
- Kapopoulou, A., Lew, J. M. & Cole, S. T. 2011. The MycoBrowser portal: a comprehensive and manually annotated resource for mycobacterial genomes. *Tuberculosis*, 91, 8-13.
- Karim, S. S. A., Churchyard, G. J., Karim, Q. A. & Lawn, S. D. 2009. HIV infection and tuberculosis in South Africa: an urgent need to escalate the public health response. *The Lancet*, 374, 921-933.
- Kong, T. H., Coates, A., Butcher, P., Hickman, C. & Shinnick, T. 1993. *Mycobacterium tuberculosis* expresses two chaperonin-60 homologs. *Proceedings of the National Academy of Sciences*, 90, 2608-2612.
- Liu, T., Ramesh, A., Ma, Z., Ward, S. K., Zhang, L., George, G. N., Talaat, A. M., Sacchettini, J. C. & Giedroc, D. P. 2007. CsoR is a novel *Mycobacterium tuberculosis* copper-sensing transcriptional regulator. *Nature Chemical Biology*, 3, 60-68.
- Lu, P., Lill, H. & Bald, D. 2014. ATP synthase in mycobacteria: special features and implications for a function as drug target. *Biochimica et Biophysica Acta (BBA)-Bioenergetics*, 1837, 1208-1218.
- Marcus, S. A., Sidiropoulos, S. W., Steinberg, H. & Talaat, A. M. 2016. CsoR is essential for maintaining copper homeostasis in *Mycobacterium tuberculosis*. *PloS one*, 11, e0151816.
- Menozi, F. D., Reddy, V. M., Cayet, D., Raze, D., Debie, A.-S., Dehouck, M.-P., Cecchelli, R. & Loch, C. 2006. *Mycobacterium tuberculosis* heparin-binding hemagglutinin adhesin (HBHA) triggers receptor-mediated transcytosis without altering the integrity of tight junctions. *Microbes and Infection*, 8, 1-9.
- Minnikin, D. E. 1982. Complex lipids, their chemistry biosynthesis and roles. *The Biology of Mycobacteria*, 1, 95-184.
- Naidoo, N., Ramsugit, S. & Pillay, M. 2014. *Mycobacterium tuberculosis pili* (MTP), a putative biomarker for a tuberculosis diagnostic test. *Tuberculosis*, 94, 338-345.
- Patel, N. 2013. The Effects of Glutathione and Its Derivatives on the Survival of *Mycobacterium bovis*-BCG Vegetative and Persistent Organisms. Honors College Thesis, Pace University, United States of America.
- Pethe, K., Alonso, S., Biet, F., Delogu, G., Brennan, M. J., Loch, C. & Menozzi, F. D. 2001. The heparin-binding hemagglutinin of *M. tuberculosis* is required for extrapulmonary dissemination. *Nature*, 412, 190-194.
- Pethe, K., Swenson, D. L., Alonso, S., Anderson, J., Wang, C. & Russell, D. G. 2004. Isolation of *Mycobacterium tuberculosis* mutants defective in the arrest of phagosome maturation. *Proceedings of the National Academy of Sciences*, 101, 13642-13647.

- Ramsugit, S., Guma, S., Pillay, B., Jain, P., Larsen, M. H., Danaviah, S. & Pillay, M. 2013. Pili contribute to biofilm formation in vitro in *Mycobacterium tuberculosis*. *Antonie Van Leeuwenhoek*, 104, 725-735.
- Ramsugit, S. & Pillay, M. 2014. *Mycobacterium tuberculosis* pili promote adhesion to and invasion of THP-1 macrophages. *Japanese Journal of Infectious Diseases*, 67, 476-478.
- Ramsugit, S., Pillay, B. & Pillay, M. 2016. Evaluation of the role of *Mycobacterium tuberculosis* pili (MTP) as an adhesin, invasin, and cytokine inducer of epithelial cells. *The Brazilian Journal of Infectious Diseases*, 20, 160-165.
- Rosas-Magallanes, V., Deschavanne, P., Quintana-Murci, L., Brosch, R., Gicquel, B. & Neyrolles, O. 2006. Horizontal transfer of a virulence operon to the ancestor of *Mycobacterium tuberculosis*. *Molecular Biology and Evolution*, 23, 1129-1135.
- Sharma, V., Arockiasamy, A., Ronning, D. R., Savva, C. G., Holzenburg, A., Braunstein, M., Jacobs, W. R. & Sacchettini, J. C. 2003. Crystal structure of *Mycobacterium tuberculosis* SecA, a preprotein translocating ATPase. *Proceedings of the National Academy of Sciences*, 100, 2243-2248.
- Stones, D. H. & Krachler, A.-M. 2015. Fatal attraction: how bacterial adhesins affect host signaling and what we can learn from them. *International Journal of Molecular Sciences*, 16, 2626-2640.
- WHO. 2020. *Global tuberculosis report 2020* [Online]. Available: [Accessed November 2020].
- Youm, J. & Saier Jr, M. H. 2012. Comparative analyses of transport proteins encoded within the genomes of *Mycobacterium tuberculosis* and *Mycobacterium leprae*. *Biochimica et Biophysica Acta (BBA)-Biomembranes*, 1818, 776-797.

APPENDICES

Appendix A: BREC Approval



04 August 2020

Ms TJ Naidoo (214582706)
School of Laboratory Medicine and Medical Sciences
College of Health Sciences
214582706@stu.ukzn.ac.za

Dear Ms Naidoo

Protocol: The role of Mycobacterium tuberculosis curli pili (MTP) and heparin-binding hemagglutinin adhesin (HBHA) on global in vitro bacterial transcriptions.
Degree: MMedSc
BREC Ref No: BE383/18

We wish to advise you that your correspondence received on 27 July 2020 submitting an application for amendments listed below for the above study has been **noted and approved** by a subcommittee of the Biomedical Research Ethics Committee.

List of Amendments approved:

1. Remove entire objective 3
2. Objective 4
3. Objective 7
4. Objective 8
5. Methodology 4.1
6. Methodology 4.5
7. Methodology 4.7

The committee will be notified of the above at its next meeting to be held on 08 September 2020.

Yours sincerely

A handwritten signature in black ink, appearing to read "A Marimuthu".

Ms A Marimuthu
(for) Prof D Wassenaar
Chair: Biomedical Research Ethics Committee

Appendix B: Media, solutions and reagents

1. Middlebrook 7H9 broth (1 L) (BD Difico)

4.7 g Middlebrook 7H9 powder

900 mL distilled water

10 mL 50% (w/v) glycerol

100 mL OADC

2.5 mL 20% Tween-80

Middlebrook 7H9 powder was dissolved in distilled water and autoclaved at 121 °C for 15 min. Glycerol, OADC and Tween-80 were added aseptically after cooling at 56 °C in a water bath. Media was mixed well and stored at 4 °C.

2. 4 M G guanidine thiocyanate (GTC) (200 mL)

25 g GTC (4 M GTC) in 50 mL autoclaved water

0.25 g Sodium N-laurylsarcosine (0.5%) in 50 mL autoclaved water

0.5g Trisodium citrate (25 mM) in 50 mL autoclaved water

0.375 2-mercaptoethanol (0.1 M) in 50 mL autoclaved water

Dissolve all components individually in the respective volumes of autoclaved water to dissolve. Once all components are dissolved combine GTC, Sodium N-laurylsarcosine and Trisodium citrate. Only add the diluted 2-mercaptoethanol solution prior to RNA extraction.

3. Diethylpyrocarbonate (DEPC)

1 mL 0.1% DEPC

1 L distilled water

DEPC was added to the distilled water, mixed well and left at room temperature ($25^{\circ}\text{C} \pm 5^{\circ}\text{C}$) overnight. Thereafter, the water was autoclaved at 121 °C for 15 min and allowed to cool prior to use.

4. 0.5 M EDTA

9.305 g EDTA

40 mL DEPC water

EDTA was dissolved in DEPC water and brought to 50 mL volume with DEPC water. Thereafter, the solution was autoclaved 121 °C for 15 min and allowed to cool prior to use.

5. 37% Formaldehyde

1.85 g paraformaldehyde

3.5 mL H₂O

90 µL 1 N NaOH.

Water was added to paraformaldehyde and heated in a boiling water bath. NaOH was added and the mixture was agitated for ~1 min. Thereafter, it was cooled and sterilized by filtration through a 0.22 µm membrane

6. 10 X MOPS Buffer (1 L)

41.9 g MOPS

8.2 g Sodium acetate. 3H₂O

3.72 g EDTA

DEPC-treated water

The MOPS, Sodium acetate and EDTA were dissolved in 800 mL DEPC-treated water, and the volume made up to 1 L with DEPC-treated water. Thereafter, the solution was autoclaved for 121 °C for 15 min and aliquoted in 200 mL amounts.

7. MOPS gel (1.5%)

3 g agarose

144 mL DEPC-treated water

20 mL 10X MOPS buffer

36 mL 37% Formaldehyde

DEPC-treated water was added to the agarose and gently swirled to mix. The mixture was heated in a microwave until dissolved, and cooled to 60°C, after which the 10X MOPS buffer was added. Thereafter, formaldehyde was added to this mixture in a fume hood. The gel was poured into a casting tray, avoiding air bubbles, and allowed to set for 30 min.

Appendix C: Chapter 2 Supplementary Material

C1. PCR confirmation of bacterial strains

InstaGene Matrix (BioRad) was used to perform total DNA extraction for all strains. This method was selected based on standardizing the DNA extraction for the inclusion of both genomic and plasmid DNA given how the mutant and complemented strains were constructed. The crude DNA from each strain was used to perform conventional PCR reactions using the specific primers and their respective annealing temperatures reported in Table C1. The expected PCR product of 861 bp was observed in Figure 1a for the wild-type (Lane 2), *mtp*-complement (Lane 4), and *mtp-hbhA*-complement (Lane 6 and 7). These samples indicate the presence of the *mtp* gene which is absent in Δmtp (lane 3) and $\Delta mtp-hbhA$ (lane 5). The expected PCR product of 624 bp was observed in Figure 1b for the wild-type (Lane 5), *hbhA*-complement (Lane 7), and *mtp-hbhA*-complement (Lane 8). These samples indicate the presence of the *hbhA* gene which is absent in $\Delta hbhA$ (lane 5) and $\Delta mtp-hbhA$ (lane 7).

Table C1.1 PCR target and primer sequences used for confirmation of three strains

PCR target	Primers	Annealing temperature (°C)
Region of <i>hyg^R</i> cassette	Hyg-F: 5'-ACC CCC CAT TCC GAG GTC TT-3' Hyg-R: 5'-CCG GAA GGC GTT GAG ATG CA-3'	55
Upstream AES	Mtp-LL: 5' CCCGGCACTTGGATGCATTC 3' Universal uptag 5'GATGTCTCACTGAGGTCTCTs3'	50
<i>mtp</i> gene	Mtp-F: 5' CTCATGGGTCACAGCGAGTA 3' Mtp-R: 5' ATGACAGGTTCCCTTCAAGC 3'	60
<i>hbhA</i> gene	HbhA-F: 5' TTTTTTGAATTCATGGCTGAAAACCTCGAACAT 3' HbhA -R: 5' TTTTTTAAGCTTCTACTTCTGGGTGACCTTCT 3'	65

hyg^R: Hygromycin resistance; AES: allelic exchange substrate; *mtp*: gene encoding MTP; *hbhA*: gene encoding HBHA.

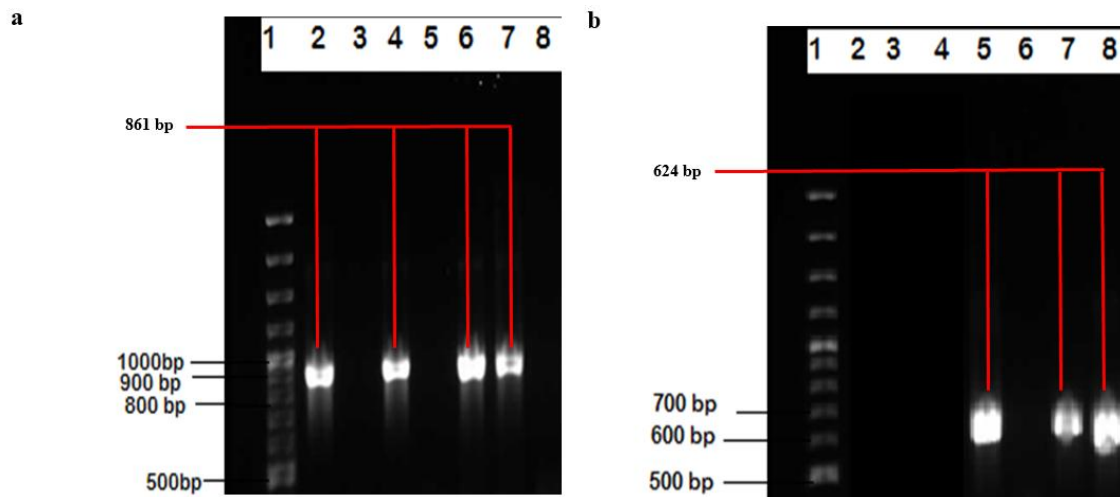


Figure C1.1 Gel electrophoresis images of PCR products confirming bacterial strains run at 70V for 3 hours on a 1.5% agarose gel using 100 bp (BioLabs) marker. (a) PCR targeting the *mtp* gene. (Lane 1) Molecular weight marker, (Lane 2) wild-type (V9124), (Lane 3) Δmtp , (Lane 4) *mtp*-complement, (Lane 5) Δmtp -*hbhA*, (Lane 6) *mtp*-*hbhA*-complement, (Lane 7) *mtp*-*hbhA*-complement, (Lane 8) negative control.(b) PCR targeting the *hbhA* gene. (Lane 1) Molecular weight marker, (Lane 2) negative control, (Lane 4) $\Delta hbhA$, (Lane 5) wild-type (V9124), (Lane 6) Δmtp -*hbhA*, (Lane 7) *hbhA* -complement, (Lane 8) *mtp*-*hbhA*-complement.

Selection of RNA samples for sequencing

The concentration (as per nanodrop reading), 260/280, 260/230 and the integrity of the RNA (as per MOPS gel analysis) were used as selection criteria. Samples that had concentrations ≥ 500 ng/ μ L, a 260/280 ratio that fell between 1.8-2, a 260/230 ratio closest to 1, and exhibited intact 16S and 23S rRNA (visualized on the MOPS gel) were selected.

Table C1.2. RNA concentrations and purity ratios obtained for all strains for biological assay 1

Sample	Replicate	Concentration	260/280	260/230
<i>Δmtp</i>	1	635.4	1.95	2.03
	2	852.5	1.99	1.89
	3	721.7	1.94	2.08
MTP complement	1	1293.5	1.99	2.04
	2	1313.1	1.98	2.00
	3	1480.9	2.02	2.07
<i>ΔhbhA</i>	1	347.7	1.90	1.99
	2	639.7	1.98	1.68
	3	471.3	1.89	2.03
HBHA complement	1	2136.3	2.01	1.93
	2	1343.2	2.01	2.22
	3	1351.9	2.01	2.18
Wildtype	1	839.9	1.95	2.18
	2	514.5	1.95	2.19
	3	20.5	1.68	0.23
<i>mtp-hbhA-complement</i>	1	80	1.85	1.03
	2	1155.6	1.98	2.14
	3	1036.4	1.98	2.24
<i>Δmtp-hbhA</i>	1	1378.2	2.03	2.27
	2	2151.9	2.01	2.17
	3	88.5	1.97	2.31

Samples selected for sequencing are highlighted in grey.

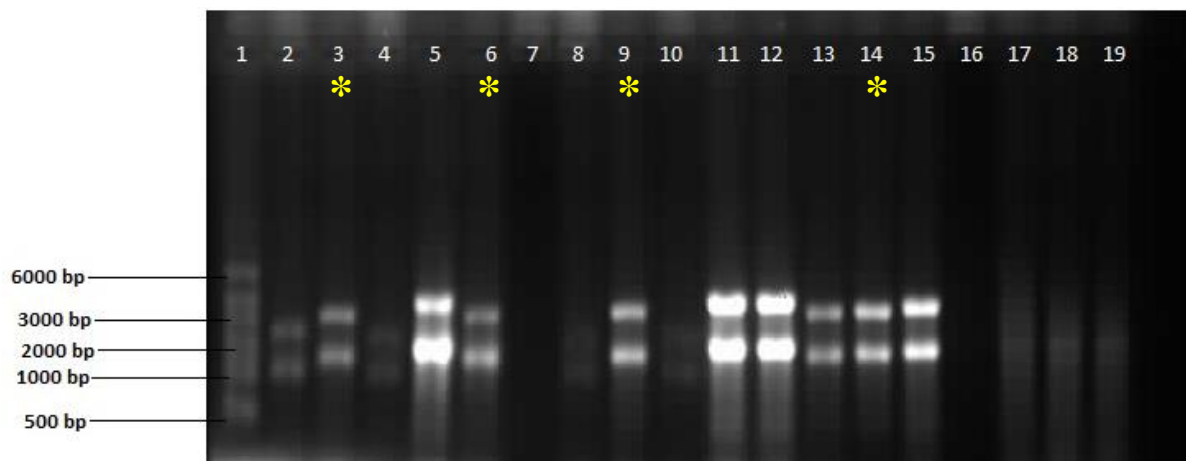


Figure C1.2. Gel electrophoresis images RNA extractions from *M. tuberculosis* strains (Biological Assay 1) run at 90V for 3 hours on a 1.5% MOPS gel using a molecular riboruler marker. (Lane 1) represents the molecular weight marker. Lanes 2-4 correspond to Δmtp sample (Replicates 1-3) from Table C2. Lanes 5-7 correspond to wild-type (Replicates 1-3). Lanes 8-10 correspond to $\Delta hbhA$ (Replicates 1-3). Lanes 11-13 correspond to *hbhA*-complement (Replicates 1-3). Lanes 14-16 correspond to Δmtp -*hbhA* (Replicates 1-3). Lanes 17-19 correspond to *mtp*-complement (Replicates 1-3). Samples that were selected for sequencing are indicated by a yellow asterisk.

Table C1.3. RNA concentrations and purity ratios obtained for all strains for biological assay**2**

Sample	Replicate	Concentration	260/280	260/230
<i>Δmtp</i>	1	588.6	1.96	2.08
	2	1333.9	1.97	2.32
	3	741.4	1.94	2.16
MTP complement	1	1252.1	1.95	2.27
	2	1308.8	1.95	2.22
	3	1003.9	1.93	2.23
<i>ΔhbhA</i>	1	2158.5	1.97	2.29
	2	838.4	1.92	2.28
	3	2748.4	2.02	2.24
HBHA complement	1	954.5	2.02	1.94
	2	1739.6	2.02	2.00
	3	2291.1	1.98	2.13
Wildtype	1	562.9	1.93	2.06
	2	590.7	1.90	2.14
	3	272.0	1.86	2.18
<i>mtp-hbhA-complement</i>	1	926.3	1.92	2.24
	2	1158.7	2.0	2.24
	3	397	1.92	2.14
<i>Δmtp-hbhA</i>	1	1542.4	1.98	2.17
	2	1340.5	1.94	2.19
	3	1087.8	2.01	1.50

Samples selected for sequencing are highlighted in grey.

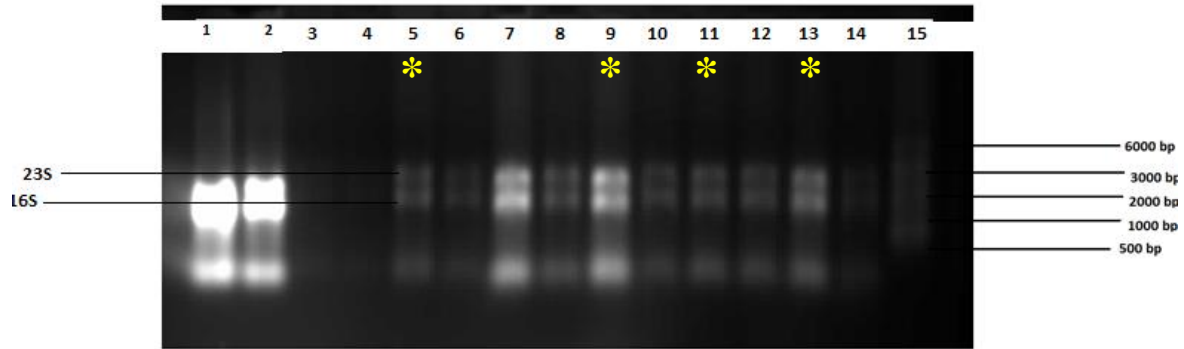


Figure C1.3. Gel electrophoresis images RNA extractions from *M. tuberculosis* strains (Biological Assay 2) run at 90V for 3 hours on a 1.5% MOPS gel using a molecular riboruler marker. Lanes 1-3 correspond to *mtp*-complement (Replicates 1-3). Lanes 4-6 correspond to $\Delta mtp-hbhA$ (Replicates 1-3). Lanes 7-9 corresponds to Δmtp sample (Replicates 1-3). Lanes 10-12 correspond to $\Delta hbhA$ (Replicates 1-3). Lanes 13-14 correspond to the wild-type (Replicates 1-3). Lane 15 represents the molecular maker. Samples that were selected for sequencing are indicated by a yellow asterisk.

Table C1.4. RNA concentrations and purity ratios obtained for all strains for biological assay**2**

Sample	Replicate	Concentration	260/280	260/230
<i>Δmtp</i>	1	436.1	1.88	2.13
	2	758.5	1.93	2.19
	3	816.6	1.96	2.12
MTP complement	1	3281.1	1.98	0.87
	2	3031.6	1.96	0.76
	3	3189.0	1.94	0.73
<i>ΔhbhA</i>	1	1519.2	1.97	2.13
	2	1122.5	1.95	2.29
	3	1120.8	1.95	2.34
HBHA complement	1	1626.6	1.96	2.18
	2	473.2	1.87	2.20
	3	1509.7	1.97	2.12
Wildtype	1	164.5	1.85	2.30
	2	499.8	1.91	2.25
	3	489.7	1.86	2.20
<i>mtp-hbhA-complement</i>	1	2612.9	2.06	2.23
	2	1898.8	2.02	2.18
	3	2404.2	1.97	2.07
<i>Δmtp-hbhA</i>	1	1163.9	1.97	2.22
	2	1758.3	1.96	2.17
	3	1266.3	1.98	2.05

Samples selected for sequencing are highlighted in grey.

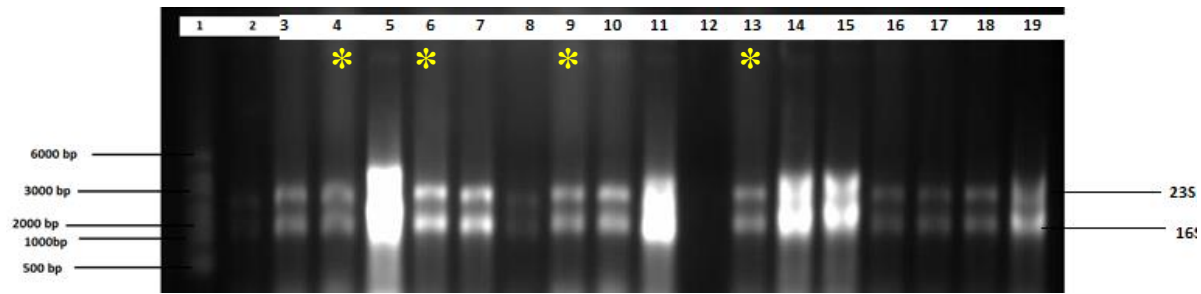


Figure C1.4. Gel electrophoresis images RNA extractions from *M. tuberculosis* strains (Biological Assay 3) run at 90V for 3 hours on a 1.5% MOPS gel using a molecular riboruler marker. (Lane 1) represents the molecular weight marker. Lanes 2-4 correspond to Δmtp sample (Replicates 1-3) from Table C2. Lanes 5-7 correspond to $\Delta hbhA$ (Replicates 1-3). Lanes 8-10 correspond to wild-type (V9124) (Replicates 1-3). Lanes 11-13 correspond $\Delta mtp-hbhA$ (Replicates 1-3). Lanes 14-16 correspond to *mtp*-complement (Replicates 1-3). Lanes 17-19 correspond to *hbhA*-complement (Replicates 1-3). Samples that were selected for sequencing are indicated by a yellow asterisk.

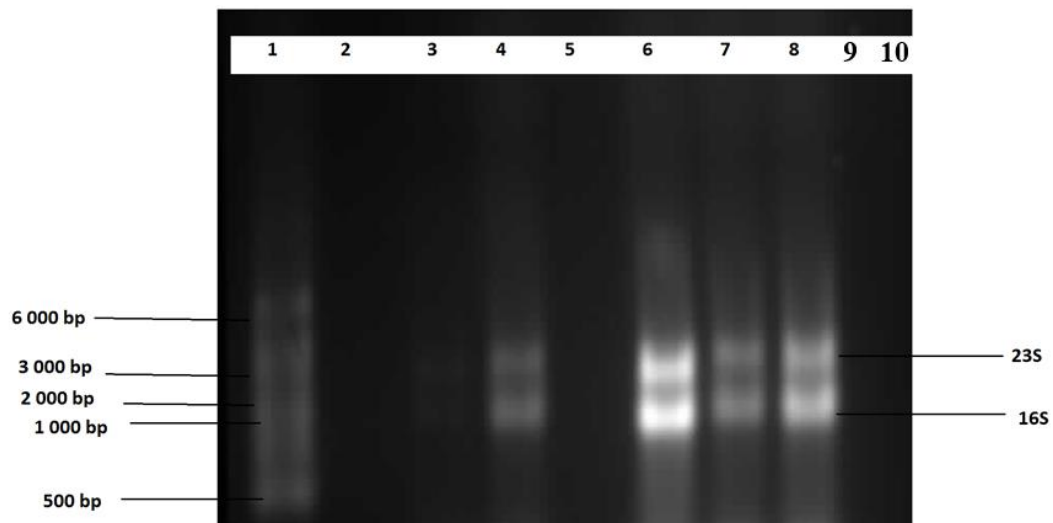


Figure C1.5. Gel electrophoresis images RNA extractions from *M. tuberculosis* strains (Biological Assay 1-3) run at 90V for 3 hours on a 1.5% MOPS gel using a molecular riboruler marker. (Lane 1) represents the molecular marker. Lanes 2-4 represent wild-type from (biological assay 2) (Replicates 1-3). Lanes 5-7 correspond to *mtp-hbhA*-complement (biological assay 1) (Replicates 1-3). Lanes 8-10 correspond to *mtp-hbhA*-complement (biological assay 3) (Replicates 1-3).

C2. Bioinformatic Analysis

The sequenced reads were analysed by FastQC (version 0.11.8). The reads were then trimmed and pre-processed using Trimmomatic (version 0.36) and analysed once again by *FastQC* (version 0.11.8). The FastQC report of the Δmtp , $\Delta hbhA$, $\Delta mtp-hbhA$ and the WT are depicted in Figures C5-C8. The trimmed reads passed the QC and was then mapped to a custom built *M. tuberculosis* H37Rv genome index using Hierarchical Indexing for Spliced Alignment of Transcripts (HISAT version 2.1.0). The mapping rates are shown in Table C5. The mapped reads were further analysed using Stringtie (version 1.2.1), and further annotated and assembled transcripts into known and novel categories by Gffcompare, located within Stringtie. The output files were annotated in R (version 1.2.1578) using the Ballgown package to generate the respective fold changes (FC) between the deletion mutants and the WT, and *q*-values and *p*-values for the differential expression. The extended table of generated up- and down-regulated genes are shown in Tables C6 and C7.

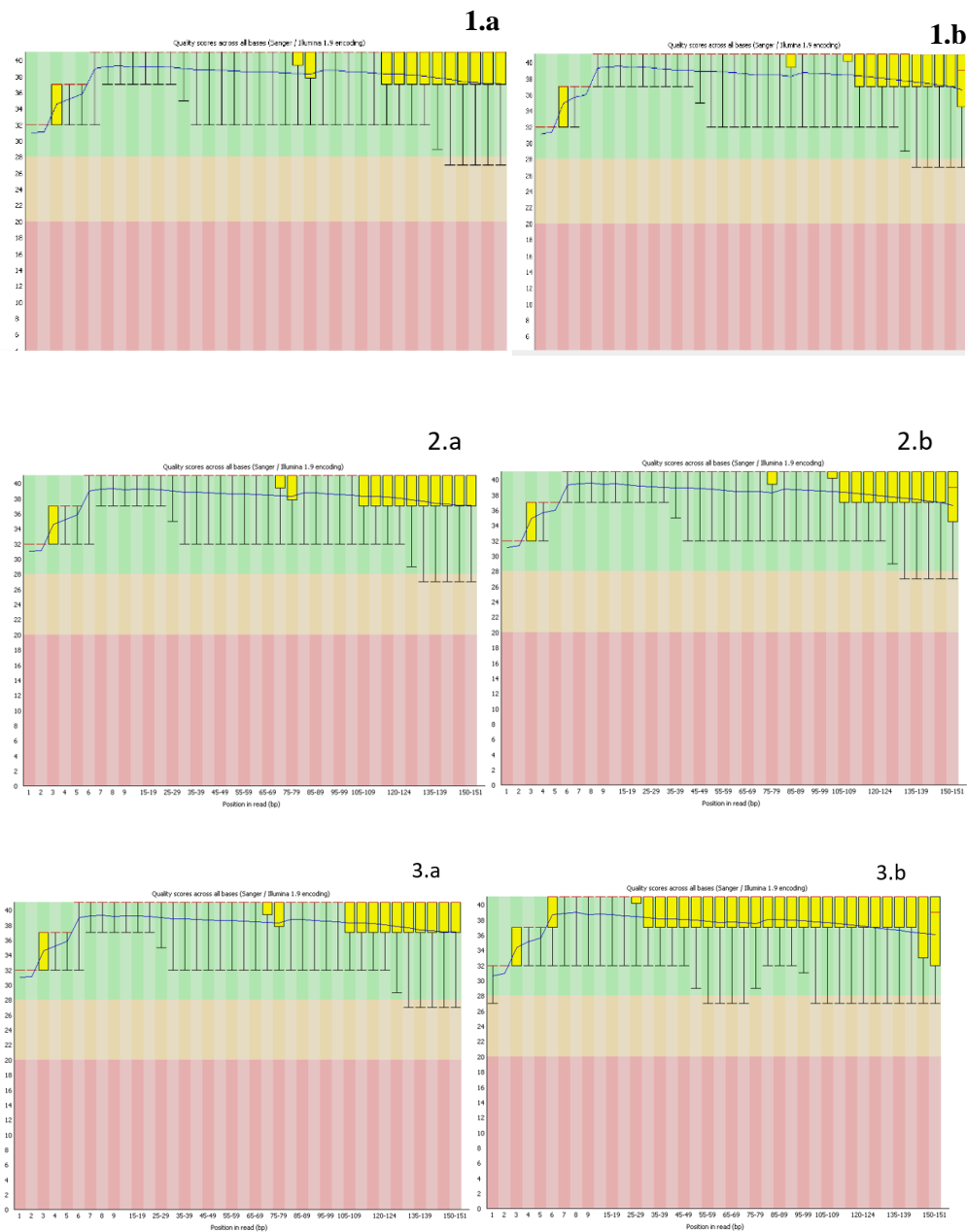


Figure C2.1. Summary analysis of FastQC report for the trimmed Δmtp . (1a) Δmtp Replicate 1 R1 (mapped in a 5'-3') and (1b) R2 (mapped 3'-5'). (2a) Δmtp Replicate 2 R1 (mapped in a 5'-3') and (2b) R2 (mapped 3'-5'). (3a) Δmtp Replicate 3 R1 (mapped in a 5'-3') and (3b) R2 (mapped 3'-5') Results indicated that Δmtp passed the overall QC, as the box-whisker plot remains in the green zone.

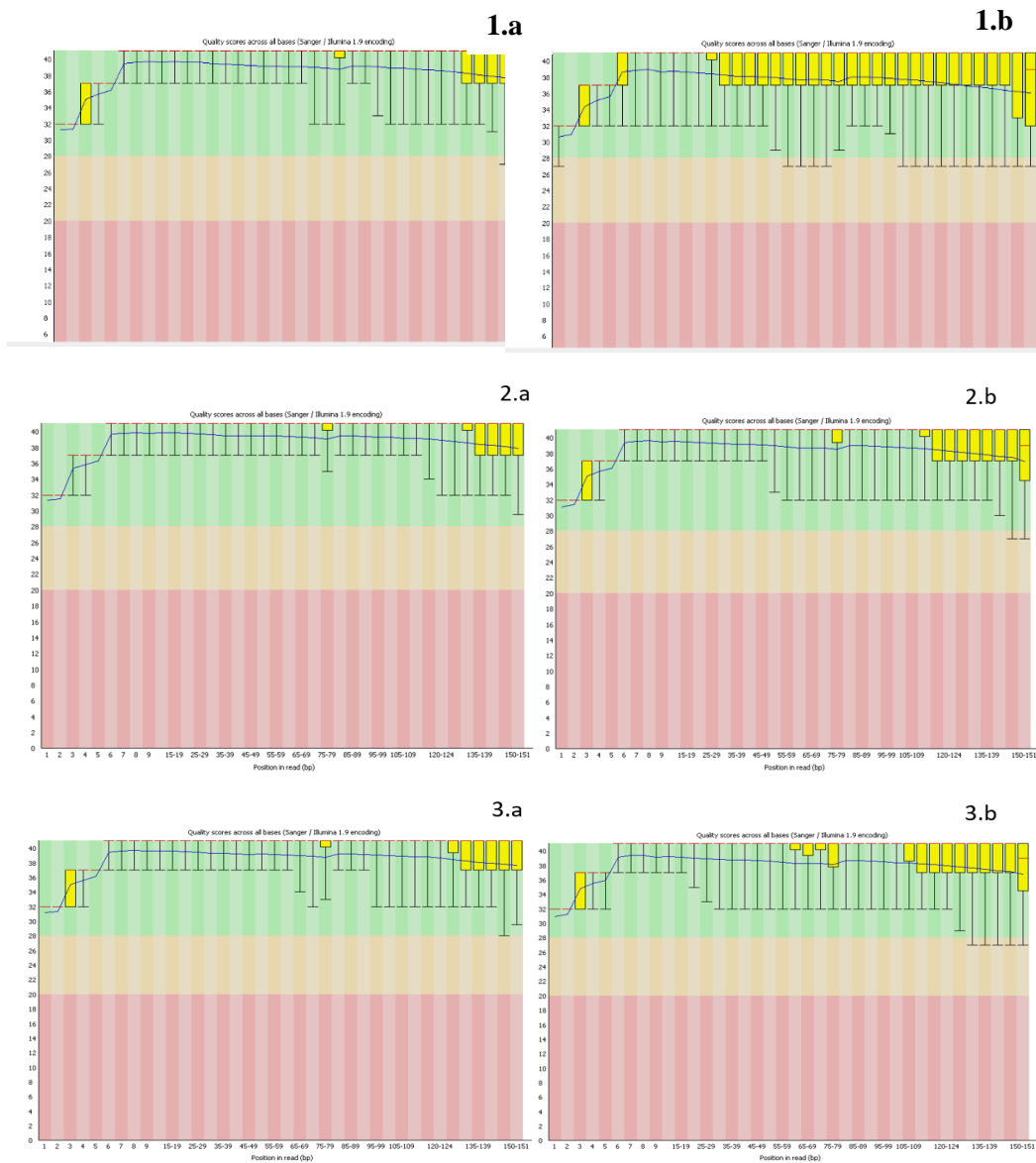


Figure C2.2. Summary analysis of FastQC report for the trimmed $\Delta hbhA$. (1a) $\Delta hbhA$ Replicate 1 R1 (mapped in a 5'-3') and (1b) R2 (mapped 3'-5'). (2a) $\Delta hbhA$ Replicate 2 R1 (mapped in a 5'-3') and (2b) R2 (mapped 3'-5'). (3a) $\Delta hbhA$ Replicate 3 R1 (mapped in a 5'-3') and (3b) R2 (mapped 3'-5'). Results indicated that $\Delta hbhA$ passed the overall QC, as the box-whisker plot remains in the green zone

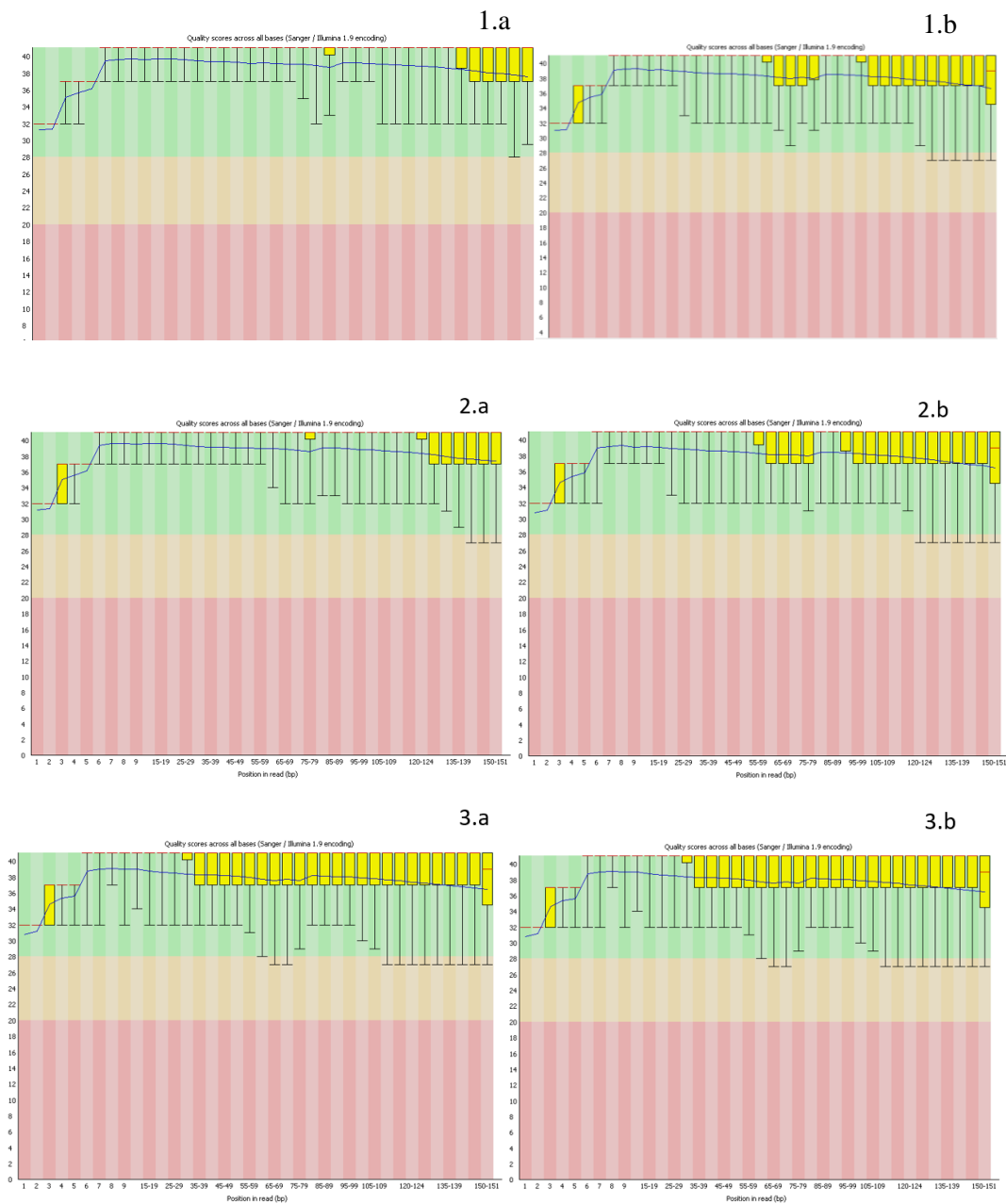


Figure C2.3. Summary analysis of FastQC report for trimmed $\Delta mtp-hbhA$. (1a) $\Delta mtp-hbhA$ Replicate 1 R1 (mapped in a 5'-3') and (1b) R2 (mapped 3'-5'). (2a) $\Delta mtp-hbhA$ Replicate 2 R1 (mapped in a 5'-3') and (2b) R2 (mapped 3'-5'). (3a) $\Delta mtp-hbhA$ Replicate 3 R1 (mapped in a 5'-3') and (3b) R2 (mapped 3'-5'). Results indicated that $\Delta mtp-hbhA$ passed the overall QC, as the box-whisker plot remains in the green zone.

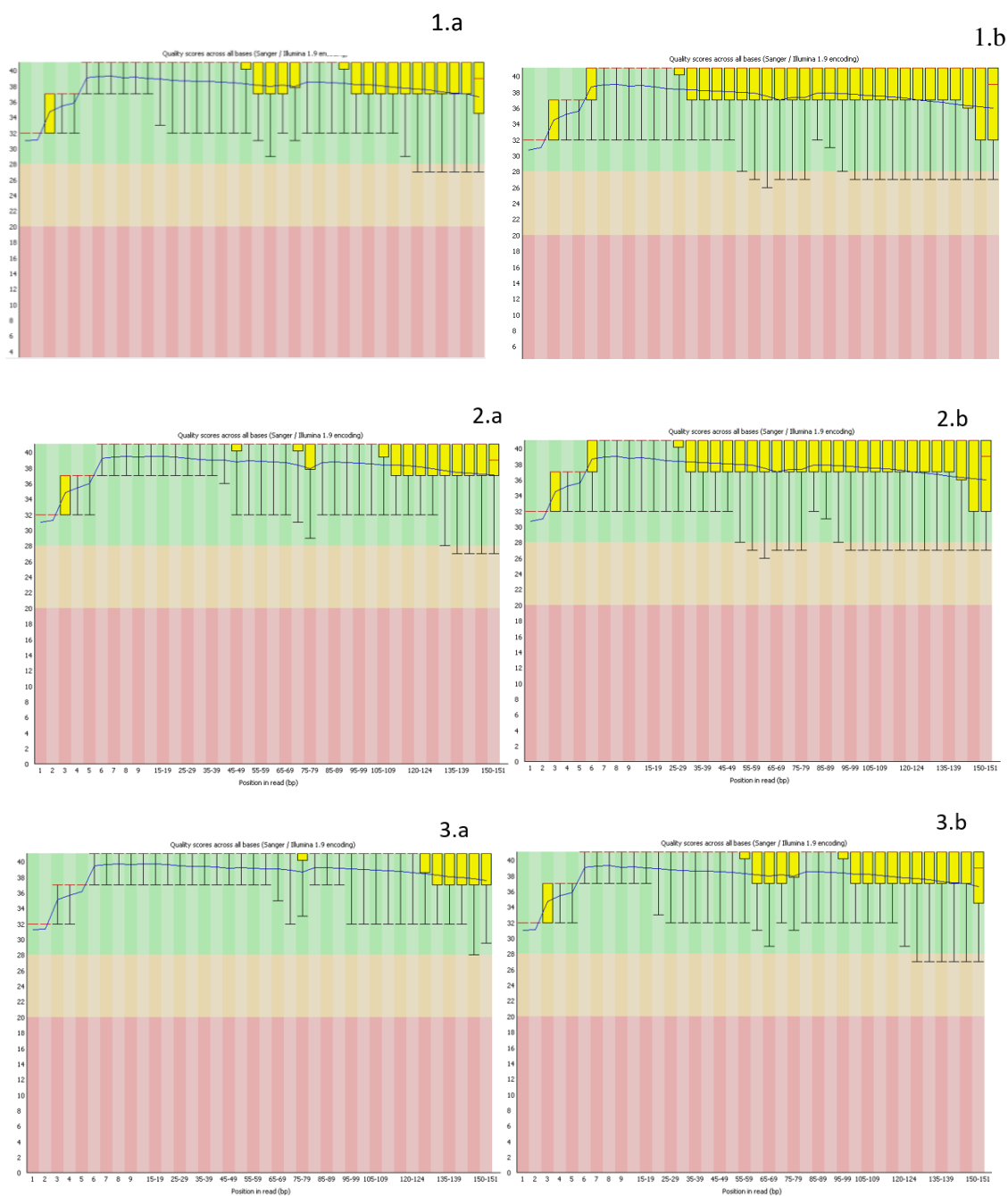


Figure C2.4. Summary analysis of FastQC report for the trimmed WT. (1a) WT Replicate 1 R1 (mapped in a 5'-3') and (b) R2 (mapped 3'-5'). (2a) WT Replicate 2 R1 (mapped in a 5'-3') and (2b) R2 (mapped 3'-5'). (3a) WT Replicate 3 R1 (mapped in a 5'-3') and (3b) R2 (mapped 3'-5'). Results indicated that the WT passed the overall QC, as the box-whisker plot remains in the green zone.

Table C2.1. Overall alignment percentages for each replicate for each strain, relative to *M. tuberculosis* H37Rv

Strain	Replicate	Overall alignment
<i>Δmtp-hbhA</i>	1	89.38%
	2	86.48%
	3	88.86%
<i>Δmtp</i>	1	90.79%
	2	86.01%
	3	92.52%
Wild-type (WT)	1	88.70%
	2	86.36%
	3	88.24%
<i>ΔhbhA</i>	1	90.55%
	2	90.72%
	3	89.21%

WT: wild-type; *Δmtp*: *mtp*-gene knockout mutant; *ΔhbhA*: *hbhA*-gene knockout mutant; *Δmtp-hbhA*: *mtp-hbhA* gene knockout mutant.

Subsequent to identification of novel transcripts, known transcripts were analysed and filtered using a fold-change (FC) FC cut-off value ≥ 1.3 (to indicate a 1.3-fold up-regulation) and ≤ 0.5 (to indicate a 2-fold down-regulation), between the deletion mutants and the WT. The extended table comprising FC and *p*-values of up- and down-regulated genes are listed below.

Table C2.2 Differentially expressed up- and down-regulate genes induced by the Δmtp deletion mutants relative to the wild-type.

Gene	Gene ID	FPKM <i>$\Delta mtp1$</i>	FPKM <i>$\Delta mtp2$</i>	FPKM <i>$\Delta mtp3$</i>	FPKM WT1	FPKM WT2	FPKM WT3	FC	<i>p-value</i>
Up-regulated genes									
<i>ilvC</i>	MSTRG.1993	174.3111	151.8738	181.4549	103.8889	144.3416	110.069	1.318103	0.000183
<i>PE_PGRS62</i>	MSTRG.2517	297.2071	238.2724	334.0728	168.8085	262.5674	166.8093	1.304867	0.00497
<i>Rv3126c</i>	MSTRG.2055	238.3167	219.9807	263.7231	133.4774	223.3391	142.6992	1.319902	0.005034
<i>Rv1303</i>	MSTRG.896	176.8377	182.0453	202.713	116.4416	149.6191	121.8141	1.37470742 3	0.00573457 5
<i>icd1</i>	MSTRG.2194	200.7752	163.3776	198.0125	120.9552	162.1805	117.4838	1.300575	0.005753
<i>Rv2477c</i>	MSTRG.1678	6,745447	3,280484	0,033402	1,533323	0,058227	1,104459	2.3400	0.2880

Table C2.2 Differentially expressed up- and down-regulate genes induced by the Δmtp deletion mutants relative to the wild-type.

Gene	Gene ID	FPKM $\Delta mtp1$	FPKM $\Delta mtp2$	FPKM $\Delta mtp3$	FPKM WT1	FPKM WT2	FPKM WT3	FC	<i>p-value</i>
<i>Rv0987</i>	MSTR G.691	15,35297	9,879573	15,27272	4,255792	5,419528	9,130246	1.9900	0.9400
<i>metE</i>	MSTRG.786	3,958146	2,374119	1,662446	1,623254	0,293548	2,247858	1.8888	0.0968
<i>gap</i>	MSTRG.958	2,2144	2,064136	0,004701	1,995149	0,013513	0,062759	1.7910	0.3359
<i>tesA</i>	MSTRG.193 7	0,76501	1,165443	1,455025	0,826464	0,044087	0,638361	1.5940	0.0658
<i>secE2</i>	MSTRG. 2681	177.9619	144.4083	177.8106	89.0626	148.2808	84.59483	1.4030	0.0058
<i>ctaC</i>	MSTRG.146 1	20.09757	22.25016	18.88117	11.27138	11.2156	13.67248	1.6900	0.0088
<i>PPE56</i>	MSTRG.219 7	24.86207	17.24185	25.02412	1.690388	2.109151	4.524411	6.424851	0.008765

Table C2.2 Differentially expressed up- and down-regulate genes induced by the Δmtp deletion mutants relative to the wild-type.

Gene	Gene ID	FPKM <i>$\Delta mtp1$</i>	FPKM <i>$\Delta mtp2$</i>	FPKM <i>$\Delta mtp3$</i>	FPKM WT1	FPKM WT2	FPKM WT3	FC	<i>p-value</i>
<i>atpE</i>	MSTRG.897	378.2178	388.4163	394.937	286.2736	312.7594	258.8344	1.320119	0.01006
<i>PPE67</i>	MSTRG.244 8	215.9785	197.4763	248.0787	127.0865	182.1322	146.5528	1.347423	0.010159
<i>lpqV</i>	MSTRG.753	2.26351	0.901948	2.753061	0.023385	0.822865	0.016766	1.927874	0.014122
<i>Rv1928c</i>	MSTRG.128 7	0.906623	0.610487	0.871895	0.204096	0.390482	0.357743	1.317304	0.019255
<i>ppdK</i>	MSTRG.217 9	1.14352	0.854585	1.179834	0.602121	0.149667	0.392017	1.374694	0.025655
<i>Rv3377c</i>	MSTRG.783	63.96148	74.92075	67.11469	44.44081	55.05516	44.21109	1.562306	0.028147
<i>Rv0988</i>	MSTRG.221 2	1.942971	1.500834	1.489486	0.583174	0.580481	1.083535	1.384304	0.032545
<i>atpF</i>	MSTRG.691	485.9854	413.2196	434.4684	338.9169	315.4052	264.3184	1.552266	0.039138

Table C2.2 Differentially expressed up- and down-regulate genes induced by the Δmtp deletion mutants relative to the wild-type.

Gene	Gene ID	FPKM <i>$\Delta mtp1$</i>	FPKM <i>$\Delta mtp2$</i>	FPKM <i>$\Delta mtp3$</i>	FPKM WT1	FPKM WT2	FPKM WT3	FC	<i>p-value</i>
<i>Rv3857c</i>	MSTRG.898	261.4347	255.8223	345.8023	179.2441	237.9914	182.8822	1.381781	0.043375
<i>PE25</i>	MSTRG.256 1	571.4044	418.9909	465.5733	311.348	376.6409	304.1723	3.84764	0.044147
<i>SecE2</i>	MSTRG. 281	177.9619	144.4083	177.8106	89.0626	148.2808	84.59483	1.403147	0.005828
<i>atpB</i>	MSTRG. 896	460.2688	484.7766	396.3477	275.7222	347.5646	243.7619	1.49262	0.049617
<i>atpH</i>	MSTRG. 899	417.9018	366.2022	372.9645	294.8143	274.8796	175.9374	1.530809	0.114219
<i>atpA</i>	MSTRG. 900	286.2702	246.4708	263.2965	214.0836	216.2528	175.4323	1.280266	0.061659

Table C2.2 Differentially expressed up- and down-regulate genes induced by the Δmtp deletion mutants relative to the wild-type.

Gene	Gene ID	FPKM <i>$\Delta mtp1$</i>	FPKM <i>$\Delta mtp2$</i>	FPKM <i>$\Delta mtp3$</i>	FPKM WT1	FPKM WT2	FPKM WT3	FC	<i>p-value</i>
<i>atpG</i>	MSTRG. 901	273.5947	264.8813	248.6554	215.4467	199.9504	134.0745	1.426541	0.138981
<i>atpD</i>	MSTRG. 902	245.5496	225.5711	243.0976	189.2383	185.6675	136.7313	1.363638	0.07986
<i>atpC</i>	MSTRG. 903	217.9742	222.4428	256.6363	202.9863	201.9573	128.5401	1.266942	0.26619
Down-regulated genes									
<i>mtp</i>	MSTRG.217 5	61.13174	64.62286	69.53075	117.9687	212.2222	110.8945	0.410205	0.004053
<i>Rv2814c</i>	MSTRG.187 1	2.633282	0.724852	2.850949	1.509956	6.106334	2.611971	0.558418	0.041403

Table C2.2 Differentially expressed up- and down-regulate genes induced by the Δmtp deletion mutants relative to the wild-type.

Gene	Gene ID	FPKM <i>$\Delta mtp1$</i>	FPKM <i>$\Delta mtp2$</i>	FPKM <i>$\Delta mtp3$</i>	FPKM WT1	FPKM WT2	FPKM WT3	FC	<i>p-value</i>
<i>serA2</i>	MSTRG.511	79.76093	64.57289	85.27908	77.23531	116.3066	97.00468	0.731102	0.02777
<i>trpD</i>	MSTRG.146 1	2.206974	1.881347	2.713622	2.699429	4.116653	2.527276	0.731415	0.005471
<i>ruvA</i>	MSTRG.174 7	112.8308	74.69458	114.819	98.76666	156.6116	106.9883	0.738218	0.037299
<i>mmuM</i>	MSTRG.166 2	107.4678	81.17094	134.2105	99.43321	174.6356	106.8598	0.739279	0.022163
<i>moeX</i>	MSTRG.112 3	83.75152	80.06928	105.3587	96.5335	146.609	88.44745	0.739879	0.027279
<i>Rv2026c</i>	MSTRG.136 8	35.00646	28.31617	42.55465	22.2387	27.66067	30.16794	0.3535	0.1940
<i>cobO</i>	MSTRG.	0.060095	0.293458	0.029485	1.82033	3.844659	0.16581	0.3770	0.1030

Table C2.2 Differentially expressed up- and down-regulate genes induced by the Δmtp deletion mutants relative to the wild-type.

Gene	Gene ID	FPKM $\Delta mtp1$	FPKM $\Delta mtp2$	FPKM $\Delta mtp3$	FPKM WT1	FPKM WT2	FPKM WT3	FC	<i>p-value</i>
<i>dxs1</i>	MSTRG.	0.00798	0.152956	0.939203	2.227821	4.026626	0.090908	0.4040	0.1439
<i>msrB</i>	MSTRG.	4.606488	2.352699	1.62033	2.609289	8.434713	10.99448	0.4536	0.2135
<i>aftC</i>	MSTRG.	24.20935	15.75667	20.0102	16.38443	59.8269	48.5135	0.4578	0.1182
<i>Rv3693</i>	MSTRG.240 2	110.4871	98.71408	128.5447	96.16892	143.6528	94.4115	0.5084	0.3060
<i>Rv1456c</i>	MSTRG.967	7.150163	0.390068	1.6742	0.978985	6.253993	5.724941	0.5310	0.4220
<i>gnd2</i>	MSTRG.778	0.022677	0.029967	0.022021	0.02331	0.447098	2.625268	0.6040	0.3557
<i>glgE</i>	MSTRG.921	0.086561	0.123215	0.109682	0.129642	0.213385	4.242808	0.6468	0.5208

Table C2.2 Differentially expressed up- and down-regulate genes induced by the Δmtp deletion mutants relative to the wild-type.

Gene	Gene ID	FPKM <i>$\Delta mtp1$</i>	FPKM <i>$\Delta mtp2$</i>	FPKM <i>$\Delta mtp3$</i>	FPKM WT1	FPKM WT2	FPKM WT3	FC	<i>p-value</i>
<i>mce2D</i>	MSTRG.427	4.677025	21.99951	5.80978	14.5262	27.84254	3.857115	0.6667	0.6580
<i>echA15</i>	MSTRG.181 2	1.247352	0.4642	0.820953	0.513409	1.905665	1.884415	0.7030	0.2421
<i>galTa</i>	MSTRG.448	87.38976	67.41986	65.36688	74.88635	118.3477	93.84309	0.7188	0.0909
<i>wag31</i>	MSTRG.143 7	0.015978	0.013567	0.012366	0.027221	0.184748	1.613364	0.7264	0.4186

WT: wild-type; Δmtp : *mtp*-gene knockout mutant; fold change (FC); Fragments per kilobase of transcript per million mapped reads (FPKM), $p \leq 0.05$ was considered significant.

Table C2.3 Differentially expressed up- and down-regulate genes induced by the $\Delta hbhA$ deletion mutants relative to the wild-type.

Gene	Gene ID	FPKM <i>$\Delta hbhA1$</i>	FPKM <i>$\Delta hbhA2$</i>	FPKM <i>$\Delta hbhA3$</i>	FPKM WT1	FPKM WT2	FPKM WT3	FC	<i>p-value</i>
Up-regulated genes									
<i>hspX</i>	MSTRG .1224	39.33716	1472.034	1862.074	101.5714	1119.784	793.4222	6.0139	0.1005
<i>Rv2030c</i>	MSTRG .1223	22.5371	463.7529	541.5175	90.91164	441.7668	216.1086	3.610667918	0.025677926
<i>fdxA</i>	MSTRG .1207	64.57011	748.399	1052.281	184.5936	697.0797	461.0035	3.15175812	0.04475168
<i>hrp1</i>	MSTRG .1891	27.50744	299.6852	515.6089	95.00924	370.4746	197.4117	2.923359645	0.031725129
<i>Rv3134c</i>	MSTRG .2378	38.389187	247.97406	405.370361	110.127777	297.03717	190.038986	2.252538507	0.040043161
<i>TB31.7</i>	MSTRG .1888	29.23027	262.4276	373.4244	122.833	332.1042	162.2937	2.247760832	0.006439429
<i>devS</i>	MSTRG .2377	54.8864	237.3781	324.0018	111.2764	257.3765	135.7297	2.224354974	0.002141911

Table C2.3 Differentially expressed up- and down-regulate genes induced by the $\Delta hbhA$ deletion mutants relative to the wild-type.

Gene	Gene ID	FPKM <i>ΔhbhA1</i>	FPKM <i>ΔhbhA2</i>	FPKM <i>ΔhbhA3</i>	FPKM WT1	FPKM WT2	FPKM WT3	FC	<i>p-value</i>
<i>devR</i>	MSTRG .2377	62.85395	276.2814	384.5554	128.8909	370.3603	167.6869	2.130182373	0.009860649
<i>pfkB</i>	MSTRG .1222	22.15677	201.56	209.1792	91.64476	223.4125	105.0169	2.088419114	0.004453102
<i>PPE57</i>	MSTRG .2535	0.762887	2.070162	4.550397	1.074833	2.21355	1.284409	1.909289475	0.049836143
<i>PE12</i>	MSTRG .618	0.067747	0.123852	0.632654	0.645222	0.005189	0.032721	1.84385648	0.041301726
<i>Rv0482</i>	MSTRG .1421	11.21626	55.60949	93.16769	34.72536	77.17987	45.52669	1.828513237	0.035718914
<i>secE2</i>	MSTRG .1336	24.25459	147.9241	146.6986	89.67889	149.4047	85.59721	1.708454881	0.028609752

Table C2.3 Differentially expressed up- and down-regulate genes induced by the $\Delta hbhA$ deletion mutants relative to the wild-type.

Gene	Gene ID	FPKM <i>ΔhbhA1</i>	FPKM <i>ΔhbhA2</i>	FPKM <i>ΔhbhA3</i>	FPKM WT1	FPKM WT2	FPKM WT3	FC	<i>p-value</i>
<i>Rv2028c</i>	MSTRG .1222	24.55163	176.5223	189.1088	106.3481	206.683	123.2315	1.635933997	0.033434856
<i>Rv3128c</i>	MSTRG .2373	58.41698	319.693	426.4213	204.2645	399.3027	267.7664	1.633664424	0.045521753
<i>serT</i>	MSTRG .2797	39.51354	209.1746	187.2323	125.1723	235.6404	118.3144	1.599436328	0.027393344
<i>mpr17</i>	MSTRG .2596	88.50262	266.924	211.1838	142.8192	234.986	148.6242	1.587783245	0.039190237
<i>Rv2005c</i>	MSTRG .1205	52.81059	215.9812	332.3335	146.4234	343.468	193.5525	1.585895928	0.043185903
<i>csoR</i>	MSTRG .484	83.52833	284.5811	254.0524	158.5629	276.4202	195.7747	1.518881601	0.034415785

Table C2.3 Differentially expressed up- and down-regulate genes induced by the $\Delta hbhA$ deletion mutants relative to the wild-type.

Gene	Gene ID	FPKM <i>ΔhbhA1</i>	FPKM <i>ΔhbhA2</i>	FPKM <i>ΔhbhA3</i>	FPKM WT1	FPKM WT2	FPKM WT3	FC	<i>p-value</i>
<i>Rv2004c</i>	MSTRG .1204	40.55251	152.9136	210.4625	105.3865	240.1092	128.959	1.511244598	0.020554131
<i>phoH2</i>	MSTRG .560	37.69875	3.331741	12.36124	3.564123	3.394532	0.326391	2.6035	0.3528
<i>rpmG1</i>	MSTRG .1237	69.12332	441.5842	184.5275	110.2679	154.4569	159.5765	2.2300	0.1774
<i>rpmB2</i>	MSTRG .1237	44.26603	290.4057	149.5706	91.70711	125.8018	111.1051	2.1400	0.1339
<i>glnU</i>	MSTRG .2208	49.11441	495.3003	219.8441	193.0665	409.825	166.4166	1.7589	0.2557
<i>Rv2477c</i>	MSTRG .1850	13.44296	2.113231	3.662921	1.543982	0.058668	1.117584	1.7339	0.1003

Table C2.3 Differentially expressed up- and down-regulate genes induced by the $\Delta hbhA$ deletion mutants relative to the wild-type.

Gene	Gene ID	FPKM <i>ΔhbhA1</i>	FPKM <i>ΔhbhA2</i>	FPKM <i>ΔhbhA3</i>	FPKM WT1	FPKM WT2	FPKM WT3	FC	<i>p-value</i>
<i>eccA5</i>	MSTRG .1019	0.335099	1.886061	2.125872	0.533836	0.645787	1.278151	1.7330	0.1299
<i>Rv1461</i>	MSTRG .841	20.75254	20.71076	20.39624	9.74939	19.93507	12.64938	1.6300	0.1429
<i>glpQ1</i>	MSTRG .2863	406.8954	349.825	428.1983	178.7321	442.3802	251.6407	1.6320	0.2558
<i>rpmJ</i>	MSTRG .2522	6109.842	2990.484	2441.201	1991.121	1336.892	1605.301	1.4946702	0.022748033
<i>PPE39</i>	MSTRG .1751	793.6209	727.949	611.8809	449.4208	393.1288	451.1813	1.490427218	0.009114777
<i>Rv2624c</i>	MSTRG .1889	19.6208	160.0454	213.4221	121.8138	254.5644	134.4763	1.48702405	0.052027566

Table C2.3 Differentially expressed up- and down-regulate genes induced by the $\Delta hbhA$ deletion mutants relative to the wild-type.

Gene	Gene ID	FPKM <i>ΔhbhA1</i>	FPKM <i>ΔhbhA2</i>	FPKM <i>ΔhbhA3</i>	FPKM WT1	FPKM WT2	FPKM WT3	FC	<i>p-value</i>
<i>Rv2885c</i>	MSTRG .2125	62.19757	233.532	217.1311	139.4542	246.0377	167.1307	1.472784632	0.030178335
<i>rsfB</i>	MSTRG .2699	96.6495	272.1294	240.7912	166.5467	293.4629	177.222	1.443466858	0.032812292
<i>infA</i>	MSTRG .2523	7975.321	3616.887	2862.066	2234.528	1638.354	2183.839	1.436645333	0.016130149
<i>Rv2628</i>	MSTRG .1906	45.72569	171.2548	203.7106	125.7012	226.4752	137.7727	1.420609359	0.002828234
<i>Rv3196A</i>	MSTRG .2292	62.60093	189.4726	188.2155	132.976	211.994	136.1313	1.391386003	0.00596255
<i>leuX</i>	MSTRG .534	62.60093	189.4726	188.2155	132.976	211.994	136.1313	1.348138578	0.009120602

Table C2.3 Differentially expressed up- and down-regulate genes induced by the $\Delta hbhA$ deletion mutants relative to the wild-type.

Gene	Gene ID	FPKM <i>ΔhbhA1</i>	FPKM <i>ΔhbhA2</i>	FPKM <i>ΔhbhA3</i>	FPKM WT1	FPKM WT2	FPKM WT3	FC	<i>p-value</i>
<i>Rv2625c</i>	MSTRG .1890	32.51238	154.4425	181.5053	123.2851	246.4574	127.6836	1.324546702	0.001144668
<i>atpB</i>	MSTRG .716	619.411316	280.931519	351.375488	277.630096	350.199005	246.65033	1.105901	0.736091
<i>atpC</i>	MSTRG .723	181.509201	158.908112	182.529129	204.390869	203.488022	130.063217	1.078707	0.990118
<i>ctaC</i>	MSTRG .1619	442.145142	402.893341	335.870758	271.135986	379.530823	288.634918	1.2327	0.3246
Down-regulated genes									
<i>mtp</i>	MSTRG .2411	13.81234	56.14729	67.49126	118.785	213.8307	112.2085	0.533492514	0.00109665

Table C2.3 Differentially expressed up- and down-regulate genes induced by the $\Delta hbhA$ deletion mutants relative to the wild-type.

Gene	Gene ID	FPKM <i>$\Delta hbhA1$</i>	FPKM <i>$\Delta hbhA2$</i>	FPKM <i>$\Delta hbhA3$</i>	FPKM WT1	FPKM WT2	FPKM WT3	FC	<i>p-value</i>
<i>hbhA</i>	MSTRG .1416	2.498533	10.17263	5.902902	133.6487	251.4865	133.4202	0.06153387	0.001504369
<i>cobO</i>	MSTRG .2135	0.014679	0.02538	0.015892	2.968723	4.615386	0.189638	0.3980	0.2375
<i>groEL2</i>	MSTRG .1384	86.53638	72.21209	86.00369	156.5173	144.9753	86.52316	0.6515	0.2059
<i>vapC38</i>	MSTRG .1831	135.5824	95.00311	106.8143	146.1758	186.3456	114.8229	0.7232	0.2565
<i>Rv2650c</i>	MSTRG .1959	0.645379	1.485734	3.49694	4.111334	2.673649	4.226442	0.7248	0.4257
<i>coaA</i>	MSTRG .562	1.025221	0.783057	1.726346	1.826245	3.56191	1.922438	0.7255	0.2712

Table C2.3 Differentially expressed up- and down-regulate genes induced by the $\Delta hbhA$ deletion mutants relative to the wild-type.

Gene	Gene ID	FPKM <i>ΔhbhA1</i>	FPKM <i>ΔhbhA2</i>	FPKM <i>ΔhbhA3</i>	FPKM WT1	FPKM WT2	FPKM WT3	FC	<i>p-value</i>
<i>vapB38</i>	MSTRG .18130	125.9363	89.61166	113.2298	123.6264	149.8421	145.1767	0.7371	0.1285
<i>Rv2928</i>	MSTRG .2192	13.13711	6.941485	6.181803	10.88956	10.31946	13.27747	0.570643	0.011792663
<i>purA</i>	MSTRG .1319	2.073925	5.111541	4.780717	8.325025	8.878793	8.38393	0.654165923	0.030224634
<i>Rv2642</i>	MSTRG .1955	22.97967	77.08738	63.46792	108.3547	180.6468	104.6858	0.643913258	0.037801337
<i>Rv1353c</i>	MSTRG .768	0.004063	0.008324	0.043649	0.893441	1.181884	0.465909	0.589387568	0.03920523
<i>Rv1082</i>	MSTRG .560	0.977851	0.012522	0.358866	1.804373	1.238027	0.929535	0.493709993	0.044102018

Table C2.3 Differentially expressed up- and down-regulate genes induced by the $\Delta hbhA$ deletion mutants relative to the wild-type.

Gene	Gene ID	FPKM <i>ΔhbhA1</i>	FPKM <i>ΔhbhA2</i>	FPKM <i>ΔhbhA3</i>	FPKM WT1	FPKM WT2	FPKM WT3	FC	<i>p-value</i>
<i>atpE</i>	MSTRG .717	497.453674	272.643188	292.051086	288.254486	315.129944	261.901459	0.982322	0.88
<i>atpF</i>	MSTRG .718	576.72583	239.177032	317.622101	341.262146	317.795868	267.450439	0.890928	0.582856
<i>atpH</i>	MSTRG .719	479.013641	183.472672	286.75174	296.85434	276.963074	178.022125	0.953372	0.856205
<i>atpA</i>	MSTRG .720	272.308136	151.063187	198.821594	215.564987	217.891846	177.511047	0.883165	0.465694
<i>atpG</i>	MSTRG .721	338.703644	156.746658	184.822205	216.937561	201.465927	135.663239	0.927565	0.803041
<i>atpD</i>	MSTRG .722	233,766907	130,505646	161,886475	190,547821	187,074738	138,351517	0.853589	0.512922

WT: wild-type; $\Delta hbhA$: *hbhA*-gene knockout mutant; fold change (FC); Fragments per kilobase of transcript per million mapped reads (FPKM), $p \leq 0.05$.

Table C2.4 Differentially expressed up- and down-regulate genes induced by the *Δamp-hbhA* deletion mutants relative to the wild-type.

Gene	Gene ID	FPKM <i>Δamp- hbhA1</i>	FPKM Δ <i>Δamp-hbhA 2</i>	FPKM Δ <i>Δamp-hbhA 3</i>	FPKM WT1	FPKM WT2	FPKM WT3	FC	<i>p-value</i>
Up-regulated genes									
<i>ASdes</i>	MSTRG. 592	8.499549	10.66415	8.09766	6.916006	4.436069	5.741576	1.7061	0.0153
<i>PPE59</i>	MSTRG. 2473	1.632053	1.875318	1.134236	0.488049	0.498046	0.423956	1.6938	0.0207
<i>moaA1</i>	MSTRG. 2244	1.090256	1.258118	1.298246	0.542891	0.403701	0.81757	1.5022	0.0099
<i>lpdA</i>	MSTRG. 2397	188.7717	182.7458	189.6203	83.53325	150.491	82.73969	1.4947	0.0223
<i>atpB</i>	MSTRG. 971	268.6685	433.0232	264.2791	276.4777	348.9817	244.4468	1.23843	0.928766
<i>atpH</i>	MSTRG. 974	269.8682	318.5572	216.8346	295.6222	276.0003	176.4317	1.031709	0.908862

Table C2.4 Differentially expressed up- and down-regulate genes induced by the *Δamp-hbhA* deletion mutants relative to the wild-type.

Gene	Gene ID	FPKM <i>Δamp- hbhA1</i>	FPKM Δ <i>Δamp-hbhA 2</i>	FPKM Δ <i>Δamp-hbhA 3</i>	FPKM WT1	FPKM WT2	FPKM WT3	FC	<i>p-value</i>
<i>atpC</i>	MSTRG. 978	195.2074	215.6235	172.436	203.5425	202.7807	128.9012	1.036397	0.870821
<i>secE2</i>	MSTRG. 283	240.226	145.5616	150.7794	89.30666	148.8853	84.83249	1.297687	0.116409
<i>Rv0986</i>	MSTRG. 731	2.48211	7.071077	2.942366	2.585641	2.233383	3.076322	1.506125	0.298005
<i>Rv0987</i>	MSTRG. 731	20.79475	61.92069	30.06477	19.24612	20.4594	24.75195	1.7552	0.2548
<i>iniB</i>	MSTRG. 240	4.744889	2.104063	0.023535	0.006332	0.009999	2.669574	1.7669	0.5627
<i>mas</i>	MSTRG. 2128	2.012033	1.925537	0.051068	0.015196	0.226519	0.012665	1.7009	0.3126
<i>efpA</i>	MSTRG. 2058	0.055832	6.956303	8.950564	0.051389	4.92113	0.213795	1.6689	0.6852

Table C2.4 Differentially expressed up- and down-regulate genes induced by the *Δmtp-hbhA* deletion mutants relative to the wild-type.

Gene	Gene ID	FPKM <i>Δmtp- hbhA1</i>	FPKM Δ <i>Δmtp-hbhA 2</i>	FPKM Δ <i>Δmtp-hbhA 3</i>	FPKM WT1	FPKM WT2	FPKM WT3	FC	<i>p-value</i>
<i>metE</i>	MSTRG. 840	7.53155	4.65986	1.212931	5.15886	1.272789	1.447414	1.6042	0.5309
<i>cysG</i>	MSTRG. 2058	0.812702	1.4511	0.017982	0.019014	0.026048	0.015262	1.5951	0.2642
<i>Rv2652c</i>	MSTRG. 1918	2.621811	1.224613	2.322058	1.12877	0.874918	1.139035	1.4688	0.1603
<i>Rv3256c</i>	MSTRG. 2360	191.015	130.4797	183.4209	85.56055	118.3392	103.8679	1.4514	0.0895
Down-regulated genes									
<i>hbhA</i>	MSTRG. 363	6.247754	7.03305	8.830567	133.094	250.6123	132.2282	0.0415	0.0005
<i>Rv3312A/mtp</i>	MSTRG. 2406	79.27003	70.95984	95.74751	118.2919	213.0874	111.2061	0.4706	0.0192
<i>Rv3326</i>	MSTRG. 2414	18.27863	14.8242	13.76989	13.62322	31.59735	19.01274	0.5989	0.0157

Table C2.4 Differentially expressed up- and down-regulate genes induced by the *Δamp-hbhA* deletion mutants relative to the wild-type.

Gene	Gene ID	FPKM <i>Δamp- hbhA1</i>	FPKM Δ <i>Δamp-hbhA 2</i>	FPKM Δ <i>Δamp-hbhA 3</i>	FPKM WT1	FPKM WT2	FPKM WT3	FC	<i>p-value</i>
<i>Rv2815c</i>	MSTRG. 2056	45.07672	39.23551	36.8853	34.08397	86.29191	40.31591	0.6002	0.0080
<i>Rv3475</i>	MSTRG. 2503	24.86111	18.7321	18.658	17.83681	37.47012	26.26255	0.6341	0.0356
<i>Rv2042c</i>	MSTRG. 1473	0.02874	0.00305	0.097335	0.036113	0.936653	0.186634	0.6424	0.0267
<i>mce2D</i>	MSTRG. 453	5.407008	4.322682	22.210196	14.566113	27.955986	3.867906	0.5149	0.4880
<i>PE_PGRS26</i>	MSTRG. 1046	0.430199	0.078672	0.292399	0.043776	1.175426	1.750476	0.5960	0.2540
<i>Rv1377c</i>	MSTRG. 1022	1.438699	0.591306	1.019056	1.696533	2.760498	0.928811	0.5979	0.0610

Table C2.4 Differentially expressed up- and down-regulate genes induced by the *Δmtp-hbhA* deletion mutants relative to the wild-type.

Gene	Gene ID	FPKM <i>Δmtp- hbhA1</i>	FPKM Δ <i>Δmtp-hbhA 2</i>	FPKM Δ <i>Δmtp-hbhA 3</i>	FPKM WT1	FPKM WT2	FPKM WT3	FC	<i>p-value</i>
<i>aprA</i>	MSTRG. 1736	3.246228	10.96353	0.467055	10.44725	7.882983	0.956195	0.6108	0.6755
<i>Rv0487</i>	MSTRG. 368	0.220625	3.992121	0.536228	1.03853	4.920024	0.15833	0.6253	0.5806
<i>Rv3475</i>	MSTRG. 2503	24.86111	18.7321	18.658	17.83681	37.47012	26.26255	0.6341	0.0356
<i>ncrMT1234</i>	MSTRG. 888	2669.317	1835.483	561.0939	3278.263	1789.627	1812.08	0.6352	0.5499
<i>Rv1096</i>	MSTRG. 810	0.0144	1.240411	0.104641	1.796884	1.233723	0.921231	0.6470	0.2996
<i>atpE</i>	MSTRG. 972	304.0207	370.4341	219.3473	287.058	314.0345	259.5616	0.96702	0.8807
<i>atpF</i>	MSTRG. 973	298.2995	369.4603	241.3163	339.8457	316.6912	265.061	0.967342	0.8717

Table C2.4 Differentially expressed up- and down-regulate genes induced by the *Δmtp-hbhA* deletion mutants relative to the wild-type.

Gene	Gene ID	FPKM <i>Δmtp- hbhA1</i>	FPKM Δ <i>Δmtp-hbhA 2</i>	FPKM Δ <i>Δmtp-hbhA 3</i>	FPKM WT1	FPKM WT2	FPKM WT3	FC	<i>p-value</i>
<i>atpA</i>	MSTRG. 975	196.2348	224.0662	162.2335	214.6702	217.1344	175.9252	0.961492	0.61665
<i>atpG</i>	MSTRG. 976	184.653	218.6242	152.6178	216.0371	200.7656	134.4512	0.973881	0.91618
<i>atpD</i>	MSTRG. 977	159.4179	187.3604	161.2693	189.7569	186.4244	137.1155	0.988502	0.845504

WT: wild-type; *Δmtp-hbhA*: *mtp-hbhA*-gene knockout mutant; fold change (FC); Fragments per kilobase of transcript per million mapped reads (FPKM), $p \leq 0.05$ was considered significant.

C3. Real time quantitative PCR (RT-qPCR) raw data

Conversion of cDNA

DNase treatment was performed using the DNase I, RNase-free kit, as per the manufacturer's instruction (Thermo Fisher Scientific, Massachusetts, USA). The RNA concentrations for each sample were standardized to 1 µg.

Table C3.1 DNase treatment mastermix

Reagent	Concentration
RNA	1 µg
10x reaction buffer with MgCl ₂	1 µL
DNase I, RNase free	1 µL (1U)
DEPC treated water	Up to 10 µL

The reagents were added into a RNase free tube and incubated at 37°C for 30 minutes. Thereafter, 1 µL of EDTA (50 mM) was added and the samples were incubated at 65°C for 10 minutes. The RNA was quantified using the nanodrop (Nanodrop 2000, Thermo Fisher Scientific, Massachusetts, USA).

The High-Capacity cDNA Reverse Transcription Kit (Roche Applied Sciences, Penzberg, Germany) was used to perform the cDNA conversion as per Manufacturer's instructions.

Table C3.2 cDNA synthesis mastermix

	1 reaction (10 µL)
10x RT Buffer	2
25x dNTP Mix (100 mM)	0.8
10x RT Random Primers	2
MultiScribe™ Reverse Transcriptase	1
RNase Inhibitor	1

The treated samples were placed on ice and mixed gently. The samples were briefly centrifuged (Heraeus Fresco™ 21, Thermo Fisher Scientific, Massachusetts, USA) at $27\,670 \times g$ for 30 seconds to spin down the contents and eliminate air bubbles. The samples were placed into the thermocycler to start the transcription run.

Conditions:

Step 1: 25°C for 10 min

Step 2: 37°C for 120 min

Step 3: 85°C for 5 min

Step 4: 4°C for ∞ min

Confirmation of cDNA

Conventional PCR was performed to confirm cDNA conversion. Each sample was used and a negative control (no template DNA). The run was performed using 16S primers.

Table C3.3. cDNA mastermix (10 μ L reaction) using cDNA Reverse Transcription Kit (Roche Applied Sciences, Penzberg, Germany)

Reagent	Volume (μL)
nfH₂O	5.75
dNTPs (100 mM)	0.2
10x Forward Primer	1
10x Reverse Primer	1
10x Buffer with MgCl₂	1
Taq	0.05
cDNA (1 μg/ 10 μL)	1
TOTAL	10

Conditions:

Initial denaturation @ 94°C for 2 min

30 cycles of 94°C for 30 s

60°C for 30 s

72°C for 1 min

Final extension @ 72°C for 7 minutes

The PCR products were then run on a 1.5% agarose gel at 70 V for 1 hour.

The PCR was successful and showed the RNA was converted to cDNA (Figure C9 and C10) as single bands were observed within the range.

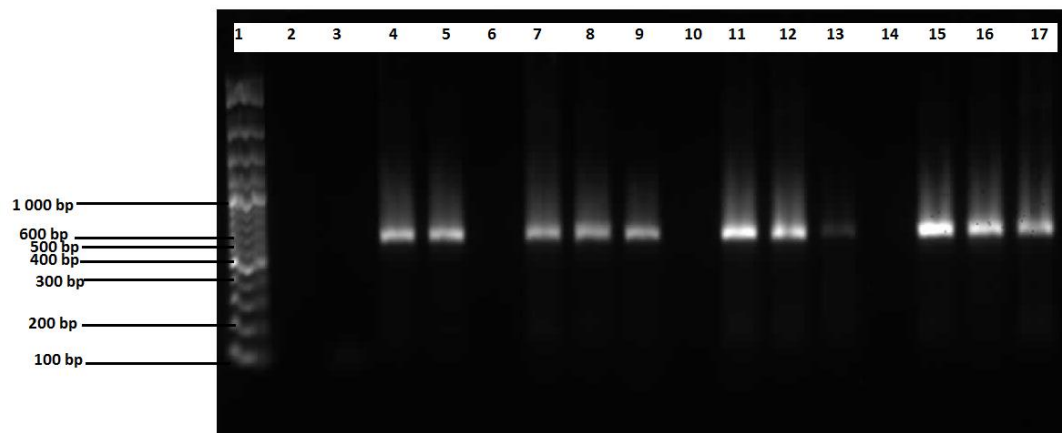


Figure C3.1. Gel electrophoresis images of cDNA confirmations from *M. tuberculosis* strains run at 70V for 3 hours on a 1.5% agarose gel using 100 bp (BioLabs) marker and 16S rRNA primers. (Lane 1) represents the molecular weight marker. Lane 2 represents the negative control. Lanes 3-5 correspond to Δmtp sample (Replicates 1-3). Lanes 7-9 correspond to $\Delta hbhA$ (Replicates 1-3). Lanes 11-13 correspond $\Delta mtp-hbhA$ (Replicates 1-3). Lanes 15-17 correspond to *mtp*-complement (Replicates 1-3).

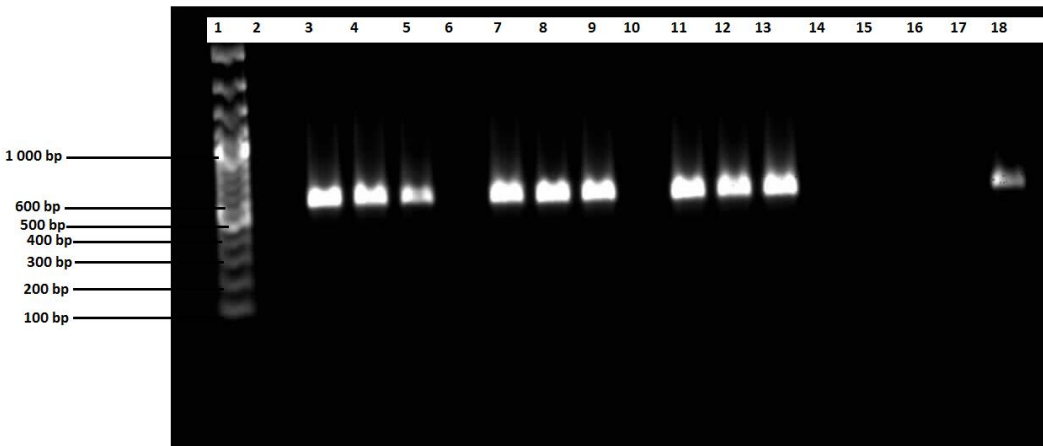


Figure C3.2. Gel electrophoresis images of cDNA confirmations from *M. tuberculosis* strains run at 70V for 3 hours on a 1.5% agarose gel using 100 bp (BioLabs) marker and 16S rRNA primers. (Lane 1) represents the molecular weight marker. Lanes 2 represents the negative control. Lanes 3-5 correspond to *hbhA*-complement samples (Replicates 1-3). Lanes 7-9 correspond *mtp-hbhA*-complement (Replicates 1-3). Lanes 11-13 correspond the wild-type (WT) (Replicates 1-3). Lane 18 represents Δmtp replicate 1.

Primer efficiency calculations and dilutions

Prior to RT-qPCR primer efficiency was determined for each of the primer sets using the following concentrations: 10 μ M, 5 μ M and 2.5 μ M concentrations and WT DNA with the following conditions.

Hold stage: 95 °C for 3 min

PCR stage (40 cycles of): 95°C for 30 s
 60°C for 30 s
 72°C for 30 s

Melt Curve: 95°C for 1 min
 60°C for 30 s
 95°C for 15 s

Analysis on the amplification plots and melt curve showed the cycling conditions used and following primer concentrations for each primer to be most desirable:

-atpB: 5 μ M

-atpD: 10 μ M

-atpE: 5 μM
 -atpH: 10 μM
 -SecE2: 10 μM
 -Rv0986: 2.5 μM

-atpF: 5 μM
 -lpqV: 10 μM
 -Rv2477c: 10 μM
 -Rv0987: 10 μM

The number of molecules/copies were calculated for each gene specific to its product size and concentration and used in the generation of the standard curve (Table C3.4). The dilution for the WT DNA for each standard curve for each gene was done using 5 standards: 10^{10} , 10^9 , 10^8 , 10^7 , 10^6 .

$$\text{Number of copies} = (\text{ng of DNA} \times 6.022 \times 10^{23}) / (\text{genome length} \times 1 \times 10^9 \times 650)$$

Table C3.4. Copy number and product sizes of selected RT-qPCR genes

Gene	Product Size (bp)	Copy Number
<i>atpB</i>	165	5.61×10^{10}
<i>atpD</i>	329	2.82×10^{10}
<i>atpE</i>	329	2.82×10^{10}
<i>atpF</i>	178	5.2×10^{10}
<i>atpH</i>	228	4.06×10^{10}
<i>lpqV</i>	185	5.01×10^{10}
<i>SecE2</i>	165	5.61×10^{10}
<i>Rv2477c</i>	250	3.71×10^{10}
<i>Rv0986</i>	226	4.1×10^{10}
<i>Rv0987</i>	270	3.43×10^{10}
<i>16S rRNA</i>	471	1.97×10^{10}

Table C3.5. RT- qPCR mastermix (10 μ L reaction) (Ssoadvanced Universal SYBR Green Supermix kit) (Bio-Rad Laboratories, Hercules, California, USA)

Reagent	1 rxn (μL)	120 rxns
1 X SYBR green	5	600
Foreword primer (2.5 , 5, 10 μM)	1	120
Reverse Primer (2.5 , 5, 10 μM)	1	120
cDNA (100 ng)	1	-
nfH2O	2	240
Total	10	1080

nfH2O: nuclease-free water.

Table C3.6. Transcriptome number obtained for each gene and sample generated after the RT-qPCR run

	<i>atpD</i>	<i>atpH</i>	<i>lpqV</i>	<i>secE2</i>	<i>Rv2477c</i>	<i>Rv0986</i>	<i>Rv0987</i>	<i>atpB</i>	<i>atpE</i>	<i>atpF</i>
Wild-type	0,6128	0,65	0,588	0,6324	0,61748	0,57683	0,56927	0,6769	0,6812	0,6688
	0,6024	0,7049	0,4398	0,6253	0,62238	0,58751	0,52398	0,6959	0,6565	0,6792
	0,6237	0,6658	0,5907	0,625	0,62969	0,59873	0,5647	0,6651	0,6874	0,6922
	0,6344	0,6714	0,6028	0,6225	0,59627	0,57994	0,5713	0,6886	0,6788	0,6942
	0,678	0,7207	0,6329	0,637	0,6498	0,58612	0,58625	0,6873	0,6928	0,6789
	0,6645	0,6818	0,6253	0,6224	0,62474	0,59447	0,55047	0,6948	0,6755	0,6889
Δmtp	0,7024	0,7339	0,6344	0,6706	0,6804	0,62187	0,60643	0,7525	0,7035	0,7517
	0,7036	0,7452	0,6066	0,6711	0,67749	0,62439	0,60929	0,7607	0,7322	0,7456
	0,6695	0,7317	0,6298	0,6666	0,68389	0,62574	0,60622	0,7544	0,8004	0,7475
	0,676	0,7236	0,6161	0,666	0,67262	0,61347	0,61011	0,7717	0,7435	0,7572
	0,6984	0,7453	0,6187	0,6666	0,66485	0,62437	0,61219	0,7733	0,7218	0,7395
	0,7272	0,7774	0,6142	0,6711	0,66654	0,62337	0,6037	0,7683	0,7334	0,7663
<i>mtp</i> -complement	0,6651	0,7367	0,6045	0,651	0,66001	0,6036	0,57023	0,6944	0,6925	0,7258
	0,6701	0,6942	0,5952	0,654	0,66555	0,60093	0,58282	0,6898	0,7206	0,7095
	0,6712	0,6906	0,6171	0,6446	0,61651	0,55957	0,56303	0,6869	0,7098	0,6554
	0,7057	0,6939	0,6059	0,6511	0,65164	0,66965	0,58275	0,699	0,7016	0,6887
	0,6689	0,6872	0,6251	0,6463	0,65024	0,57311	0,57698	0,6838	0,7064	0,6643
	0,6563	0,6764	0,611	0,6385	0,65266	0,56717	0,53921	0,6568	0,6925	0,7159
$\Delta hbhA$	0,7064	0,7437	0,6425	0,6616	0,67204	0,60866	0,59817	0,7634	0,7248	0,7208
	0,7012	0,7117	0,6301	0,6575	0,668	0,62952	0,5999	0,7278	0,7332	0,7268
	0,6578	0,812	0,6499	0,8004	0,68129	0,61944	0,59126	0,7662	0,7055	0,758
	0,673	0,9812	0,6469	0,79	0,67618	0,61719	0,59651	0,7885	0,7559	0,7717
	0,6763	0,7789	0,6415	0,8009	0,6831	0,61291	0,60585	1,0056	0,703	0,7768
	0,672	0,775	0,6393	0,7906	0,67383	0,61044	0,60325	0,8055	0,7638	0,7719
$\Delta hbhA$ - complement	0,6881	0,6858	0,6103	0,644	0,65762	0,55248	0,5697	0,696	0,6959	0,7071
	0,6648	0,6871	0,6082	0,6408	0,66504	0,57056	0,56438	0,6911	0,6789	0,6696
	0,6903	0,6964	0,6241	0,6436	0,66273	0,56509	0,57381	0,6997	0,6867	0,6052
	0,6967	0,6919	0,6017	0,6435	0,64325	0,56156	0,56214	0,6912	0,6808	0,6278
	0,6477	0,6796	0,5962	0,6363	0,63922	0,58402	0,5554	0,696	0,6728	0,6651
	0,6301	0,6938	0,6113	0,6386	0,66188	0,5697	0,56127	0,7183	0,7014	0,6687
Δmtp - <i>hbhA</i>	0,695	0,732	0,6268	0,6474	0,6809	0,80693	0,68359	0,7546	0,7397	0,7527
	0,6904	0,7624	0,6192	0,6479	0,66555	0,82826	0,6844	0,7296	0,7239	0,7469
	0,7061	0,7585	0,7141	0,7905	0,72318	0,89671	0,59292	0,8211	0,7641	0,7927
	0,7149	0,7645	0,7241	0,8101	0,73852	0,89553	0,81653	0,8381	0,7934	0,8185
	0,7985	0,8559	0,8038	0,902	0,78896	0,60901	0,90358	0,7869	0,8191	0,8427
	0,7774	0,8538	0,7957	0,8969	0,78243	0,71575	0,88639	0,861	0,8203	0,8466
Δmtp - <i>hbhA</i> - complement	0,7244	0,7564	0,6062	0,6312	0,66491	0,59561	0,58406	0,7228	0,6873	0,6894
	0,7967	0,84	0,5884	0,6368	0,62157	0,59973	0,58621	0,7201	0,6933	0,7068
	0,7019	0,743	0,6088	0,632	0,67421	0,60926	0,59864	0,7234	0,6642	0,6939
	0,7008	0,7438	0,6002	0,6236	0,6937	0,59417	0,59074	0,7104	0,701	0,6915
	0,6491	0,7087	0,61	0,6223	0,68021	0,60648	0,55943	0,7136	0,6895	0,7081
	0,6576	0,7694	0,6007	0,6201	0,65215	0,5926	0,59484	0,6912	0,6967	0,6949

Table C3.7 The Cycle threshold (Ct) values for each gene for the different *M. tuberculosis* deletion mutants and respective complemented strains

Sample	CT for each gene									
	<i>atpB</i>	<i>atpD</i>	<i>atpE</i>	<i>atpF</i>	<i>atpH</i>	<i>secE2</i>	<i>Rv0986</i>	<i>Rv0987</i>	<i>lpqV</i>	<i>16S rRNA</i>
<i>Δmtp</i>	14.128	15.682	13.846	14.539	15.014	20.680	18.401	18.571	20.258	4.597
<i>Δmtp</i>	13.817	16.016	14.166	14.699	14.835	20.883	19.635	19.276	21.457	4.663
<i>Δmtp</i>	13.906	15.489	16.081	16.399	14.593	20.577	18.340	18.488	20.347	4.456
<i>Δmtp</i>	13.118	16.012	15.052	15.173	13.995	20.733	19.394	18.335	20.916	4.453
<i>Δmtp</i>	13.113	15.623	11.673	14.623	14.126	22.502	19.776	19.849	20.856	4.522
<i>Δmtp</i>	13.609	15.301	13.736	14.340	13.809	22.211	19.783	20.345	21.240	4.800
<i>Δmtp</i>	15.390	14.883	14.893	14.322	14.456	21.946	20.830	19.784	20.849	4.486
<i>Δmtp</i>	14.001	14.901	13.731	14.657	14.033	22.979	19.646	20.198	21.427	4.569
<i>Δmtp</i>	14.302	16.184	10.566	14.346	14.401	22.189	18.299	18.237	21.264	4.313
<i>Δmtp</i>	14.118	15.923	13.051	13.958	14.787	22.656	18.213	18.450	21.705	4.343
<i>Δmtp</i>	15.777	15.175	14.229	14.965	14.083	21.609	18.364	18.254	20.133	4.627
<i>Δmtp</i>	15.577	14.795	14.601	14.723	13.613	23.806	19.610	20.662	21.384	5.623
<i>ΔhvhA</i>	13.904	11.546	13.628	14.096	13.598	21.366	19.594	20.144	20.132	5.325
<i>ΔhvhA</i>	12.726	14.603	13.396	14.291	13.922	22.344	20.802	19.195	27.544	Undetermined
<i>ΔhvhA</i>	14.506	14.879	15.087	14.389	14.209	21.373	18.962	22.137	19.988	4.689
<i>ΔhvhA</i>	14.546	15.433	12.840	14.060	14.415	22.478	18.942	19.863	20.782	5.076

<i>ΔhbhA</i>	16.728	17.183	15.459	16.013	15.525	22.029	19.129	20.221	19.853	4.919
<i>ΔhbhA</i>	16.525	16.529	15.500	16.392	16.672	21.788	19.100	19.250	19.982	4.927
<i>ΔhbhA</i>	13.771	16.236	15.412	15.859	15.658	22.008	19.641	18.930	20.067	4.743
<i>ΔhbhA</i>	15.208	16.273	15.121	15.445	16.336	21.852	24.137	24.043	20.024	4.558
<i>ΔhbhA</i>	19.686	22.659	20.947	19.908	17.495	27.637	24.734	23.907	27.187	11.040
<i>ΔhbhA</i>	18.500	22.545	19.304	19.097	10.945	27.205	25.163	23.945	28.387	10.679
<i>ΔhbhA</i>	10.893	22.703	19.387	19.317	18.764	27.544	24.813	23.618	27.789	11.117
<i>ΔhbhA</i>	17.943	22.032	20.059	19.164	18.569	28.640	16.108	15.537	28.248	10.760
<i>Δmtp-hbhA</i>	13.872	15.811	15.947	15.121	14.738	20.230	16.915	15.569	20.236	4.527
<i>Δmtp-hbhA</i>	14.932	16.129	14.518	14.920	14.656	20.609	19.017	19.059	19.975	4.614
<i>Δmtp-hbhA</i>	14.717	16.163	14.842	12.951	15.535	20.327	14.354	18.840	19.990	4.542
<i>Δmtp-hbhA</i>	14.615	15.748	14.358	15.535	13.134	19.902	15.981	15.821	20.115	4.420
<i>Δmtp-hbhA</i>	13.736	15.883	14.249	14.531	15.247	23.018	14.875	16.041	20.619	Undetermined
<i>Δmtp-hbhA</i>	15.252	15.778	13.544	14.757	14.636	22.709	19.323	19.324	20.648	4.651
<i>Δmtp-hbhA</i>	13.840	15.129	13.257	14.197	14.265	23.663	19.565	19.780	20.423	4.392
<i>Δmtp-hbhA</i>	15.030	15.381	13.993	14.499	14.293	22.612	16.739	16.662	20.787	4.455
<i>Δmtp-hbhA</i>	17.629	20.304	18.216	18.677	19.414	22.058	16.723	16.720	22.225	11.023
<i>Δmtp-hbhA</i>	17.784	20.635	17.889	18.495	19.898	21.913	17.531	16.898	22.507	11.772
<i>Δmtp-hbhA</i>	22.563	20.580	19.894	20.621	19.772	22.654	17.441	17.263	22.603	14.744
<i>Δmtp-hbhA</i>	20.026	21.128	19.742	20.382	19.716	22.402	18.913	19.757	22.735	14.625

<i>mtp-complement</i>	16.076	16.771	15.631	16.118	15.993	21.789	19.483	21.753	21.645	4.805
<i>mtp-complement</i>	15.690	16.717	14.605	15.361	15.232	21.856	19.140	18.965	22.167	5.004
<i>mtp-complement</i>	18.387	16.275	14.651	14.643	14.756	21.321	18.840	20.166	20.918	4.519
<i>mtp-complement</i>	15.237	15.104	15.336	15.625	14.720	21.717	20.573	19.540	21.663	4.916
<i>mtp-complement</i>	16.831	16.511	14.938	15.588	16.380	23.131	18.775	20.062	20.706	4.687
<i>mtp-complement</i>	16.691	16.745	15.206	15.257	16.200	23.021	19.255	19.458	21.012	4.287
<i>mtp-complement</i>	17.054	16.722	14.891	16.177	16.277	23.087	19.174	19.513	20.898	4.552
<i>mtp-complement</i>	16.267	16.610	16.157	18.273	16.343	23.026	21.410	21.384	21.204	4.278
<i>mtp-complement</i>	17.550	17.473	16.662	17.400	17.396	24.139	21.788	21.551	21.543	4.968
<i>mtp-complement</i>	17.750	17.884	13.931	18.077	17.797	24.133	20.759	21.022	21.678	11.322
<i>mtp-complement</i>	17.405	16.600	14.791	18.340	19.708	24.374	20.769	30.354	21.716	4.852

<i>mtp-complement</i>	16.708	17.741	14.099	14.718	18.632	24.633	19.356	19.713	22.033	4.491
<i>hbhA-complement</i>	16.201	15.810	13.984	15.099	14.932	22.598	19.372	20.710	20.390	4.848
<i>hbhA-complement</i>	16.279	16.706	11.851	14.584	15.338	22.703	19.327	19.440	20.701	4.707
<i>hbhA-complement</i>	14.769	15.757	15.563	15.728	15.313	22.383	19.347	19.351	20.608	4.902
<i>hbhA-complement</i>	14.268	15.507	16.309	16.491	12.255	23.238	20.377	19.966	20.570	4.930
<i>hbhA-complement</i>	16.364	17.341	15.679	15.944	16.646	23.186	20.000	20.072	21.262	4.563
<i>hbhA-complement</i>	16.448	18.236	16.067	16.823	16.730	23.186	21.473	20.202	21.194	4.730
<i>hbhA-complement</i>	16.688	17.810	16.309	16.838	16.217	23.060	20.750	19.882	21.264	4.606
<i>hbhA-complement</i>	16.973	17.012	15.145	16.319	16.475	23.198	20.966	20.316	21.402	4.678
<i>hbhA-complement</i>	16.561	13.227	15.286	15.998	16.991	23.142	21.299	20.740	20.722	4.652
<i>hbhA-complement</i>	17.180	17.360	15.074	15.771	16.603	23.397	20.282	20.457	21.844	4.927

<i>hbhA-complement</i>	16.880	17.538	15.492	16.038	16.373	23.174	21.616	21.571	22.004	4.829
<i>hbhA-complement</i>	16.852	17.088	13.103	14.960	16.352	23.437	20.822	20.848	22.141	5.910
<i>mtp-hbhA-complement</i>	15.569	15.638	14.420	14.603	15.272	23.280	19.909	19.686	21.540	6.448
<i>mtp-hbhA-complement</i>	13.747	15.695	13.921	14.948	15.025	23.516	19.973	19.815	21.448	9.618
<i>mtp-hbhA-complement</i>	15.223	15.340	12.842	14.215	14.516	23.027	19.387	19.177	21.222	4.997
<i>mtp-hbhA-complement</i>	16.529	15.670	15.487	16.348	14.789	23.478	19.800	19.278	21.526	5.333
<i>mtp-hbhA-complement</i>	16.492	17.679	15.716	15.838	16.075	22.455	19.526	20.691	21.761	5.072
<i>mtp-hbhA-complement</i>	15.611	17.058	15.696	16.277	13.139	23.240	19.949	19.195	22.277	4.755
<i>mtp-hbhA-complement</i>	16.046	17.519	13.436	15.373	16.509	22.719	19.856	20.673	21.673	5.103
<i>mtp-hbhA-complement</i>	15.692	17.200	14.816	12.024	16.491	22.873	21.012	19.869	21.869	4.873
<i>mtp-hbhA-complement</i>	15.877	16.641	15.507	16.899	16.189	23.318	19.533	19.814	21.151	4.428

<i>mtp-hbhA-complement</i>	15.694	17.224	15.179	16.080	15.987	23.935	20.181	19.388	21.511	4.386
<i>mtp-hbhA-complement</i>	16.636	15.712	16.419	16.617	16.586	23.190	19.413	20.303	20.435	4.296
<i>mtp-hbhA-complement</i>	15.937	15.526	16.332	18.328	16.932	23.088	16.916	21.822	20.708	4.277
WT	19.180	19.251	17.091	17.598	18.633	23.987	19.951	20.267	22.514	5.081
WT	16.535	19.428	15.787	17.062	15.931	24.257	19.885	19.947	28.406	4.711
WT	17.188	18.518	16.068	16.888	17.666	23.648	19.614	19.908	22.164	4.733
WT	16.759	17.968	14.044	16.044	17.331	23.614	19.792	20.793	21.589	4.625
WT	13.560	16.771	9.783	15.445	15.919	22.758	20.672	19.598	20.963	5.484
WT	13.830	16.711	14.446	14.991	16.931	22.789	20.115	19.770	20.706	4.696
WT	13.990	16.765	14.537	15.566	Undetermined	22.698	19.680	20.339	20.842	4.955
WT	14.674	16.510	15.231	16.674	Undetermined	22.726	20.176	20.757	20.528	4.801
WT	17.765	16.919	15.302	16.852	17.213	23.392	20.159	20.154	21.006	4.859
WT	16.532	14.498	16.334	17.664	17.051	23.524	19.464	20.142	20.892	4.422
WT	18.229	17.228	15.880	16.845	15.899	23.467	11.182	12.204	21.026	4.781
WT	16.753	17.616	12.759	13.297	15.732	23.133	11.669	11.754	20.582	4.295

Table C3.8 The RT-qPCR expression means and standard deviations for each gene for the *M. tuberculosis* WT, deletion mutants, and their respective complements

Gene	Wild-type		Δmtp		<i>mtp</i> -complement		$\Delta hbhA$		<i>hbhA</i> -complement		$\Delta mtp-hbhA$		<i>mtp-hbhA</i> complement	
	Mean	SD	Mean	SD	Mean	SD	Mean	SD	Mean	SD	Mean	SD	Mean	SD
<i>atpB</i>	0.668	0.012	0.764	0.009	0.685	0.015	0.78	0.02	0.699	0.010	0.799	0.051	0.714	0.012
<i>atpD</i>	0.621	0.024	0.705	0.018	0.673	0.017	0.69	0.01	0.670	0.027	0.730	0.046	0.693	0.054
<i>atpE</i>	0.679	0.013	0.739	0.033	0.704	0.011	0.73	0.03	0.686	0.011	0.777	0.041	0.689	0.013
<i>atpF</i>	0.669	0.006	0.751	0.009	0.693	0.029	0.75	0.02	0.672	0.018	0.800	0.044	0.697	0.008
<i>atpH</i>	0.644	0.029	0.743	0.019	0.697	0.021	0.77	0.04	0.689	0.006	0.788	0.053	0.760	0.044
<i>lpqV</i>	0.580	0.071	0.635	0.016	0.610	0.010	0.64	0.01	0.609	0.010	0.714	0.079	0.602	0.008
<i>secE2</i>	0.627	0.006	0.669	0.003	0.648	0.006	0.75	0.05	0.641	0.003	0.759	0.063	0.628	0.007
<i>Rv0986</i>	0.587	0.008	0.627	0.015	0.596	0.040	0.62	0.01	0.587	0.002	0.784	0.048	0.600	0.007
<i>Rv0987</i>	0.561	0.021	0.611	0.006	0.569	0.017	0.61	0.01	0.564	0.007	0.765	0.072	0.586	0.014

WT: wild-type; Δmtp : *mtp*-gene knockout mutant; $\Delta hbhA$: *hbhA*-gene knockout mutant; $\Delta mtp-hbhA$: *mtp-hbhA*-gene knockout mutant.
SD: standard deviation.

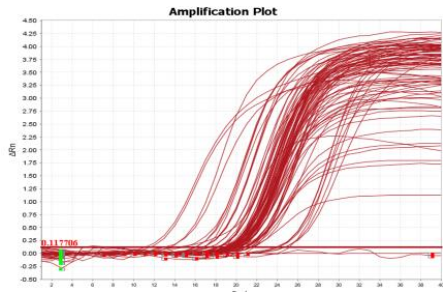
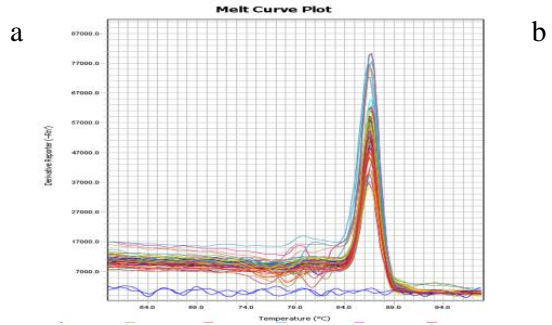
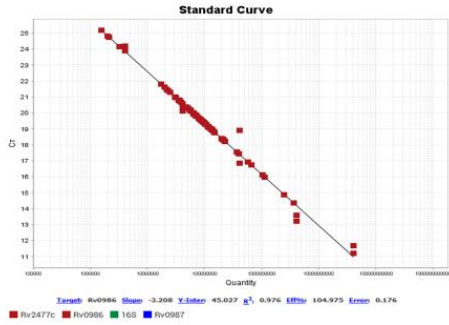
A dilution series of the WT DNA and each gene amplicon were used as a standard template for the individual standard curves and ranged from 10^{10} - 10^6 copies per PCR reaction.

Cycle threshold (Ct value) refers to the number of cycles required for the fluorescence signals to cross the threshold (background noise). Ct levels are inversely proportional to target nucleic acid in the sample; therefore, a lower Ct value correlates to a higher concentration of nucleic acid. A Ct value less than 29 are strong positive reactions indicative of abundant target nucleic acid. The Ct values of all genes were below 29, indicating a strong positive reaction.

The Ct values are used to plot the standard curve. In the standard curve the Y-intercept is the expected CT value for a 1 ng/ μ L sample. The R^2 measures how well the regression line fits the data values. An R^2 value of 1 equates to a perfect regression. A lower R^2 value is indicative of scattered data. In this study, all R^2 values ranges from 0.976-0.997 (Figures C13-C23 in appendix) and majority of the data points for each standard curve fall on the regression line. This indicates a high-quality standard curve. Slope measures the efficiency of the RT-qPCR reaction. A slope of -3.3 indicates a perfect reaction. The slope for all genes tested in the RT-qPCR were approximately -3.2 (Figures in appendix), indicating a strong reaction.

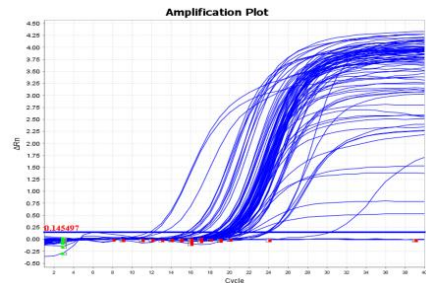
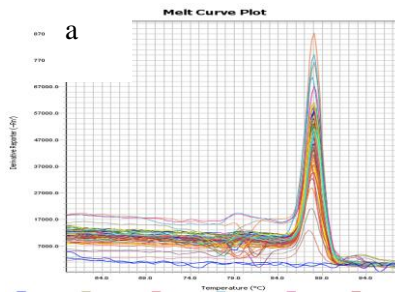
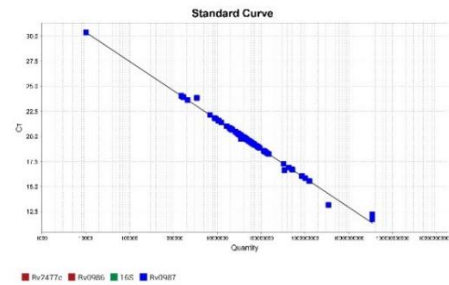
Efficiency of 100% represents a doubling of the template after each cycle. Efficiency between 90-120% is acceptable. The efficiency percentages for all genes tested ranged from 96.972-116.568%.

Melt curves are used to determine the presence of any nonspecific products. The melt curves for all genes display a single peak (Figures in appendix) indicating that there are no nonspecific products in the reaction.



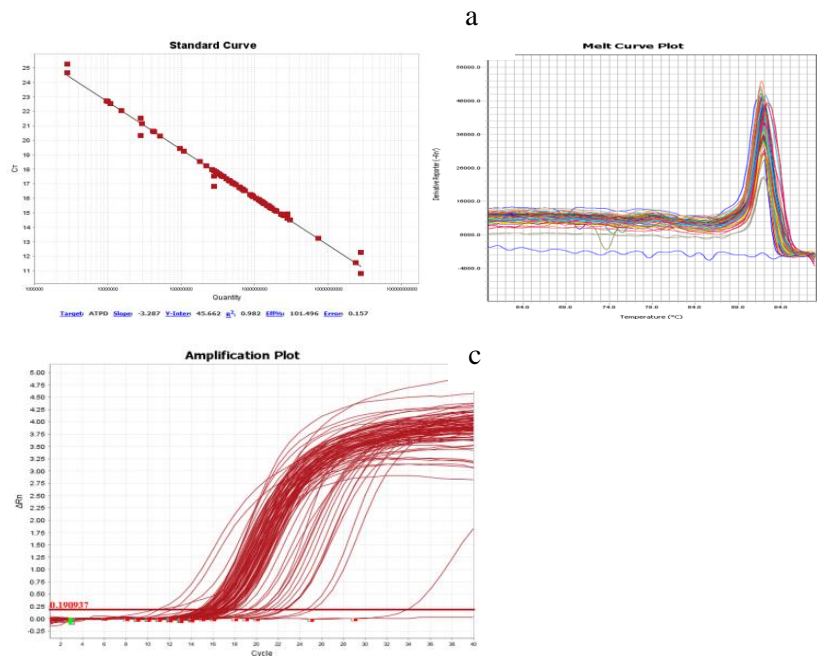
C

C3.3. RT-qPCR analysis for *Rv0986*. Results generated a slope = -3.208, $R^2 = 0.976$, efficacy= 104.975%, error = 0.176 and Y-intercept = 45.027, depicted by the standard curve (a), melt curve (b) and amplification plot (c).

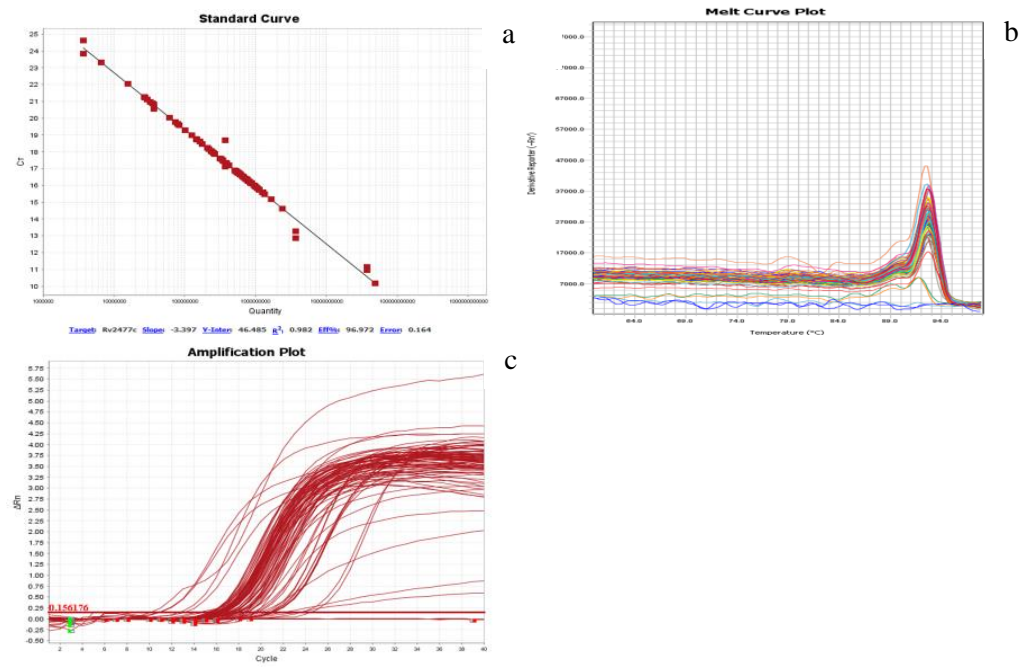


C

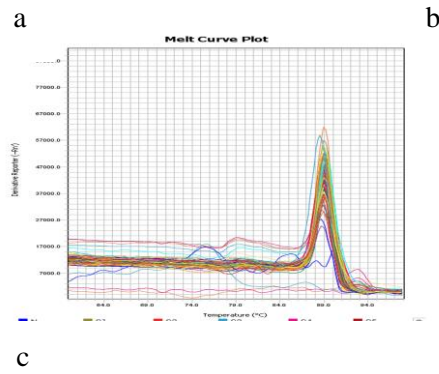
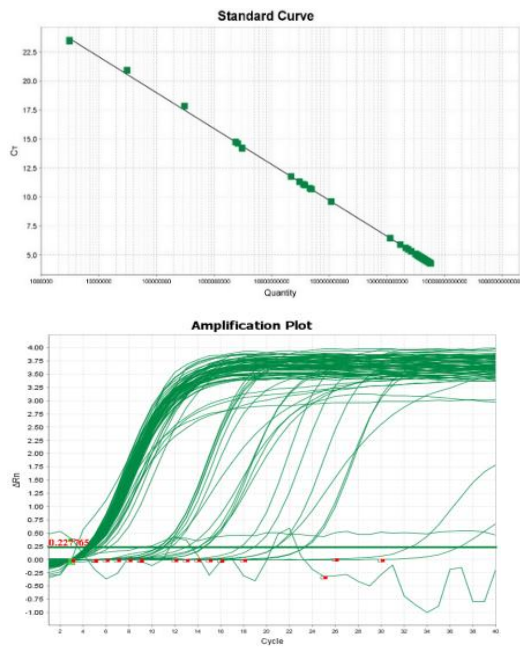
C3.4. RT-qPCR analysis for *Rv0987*. Results generated a slope = -2.671, $R^2 = 0.976$, efficacy= 116.569%, error = 0.192 and Y-intercept = 39.55, depicted by the standard curve (a), melt curve (b) and amplification plot (c).



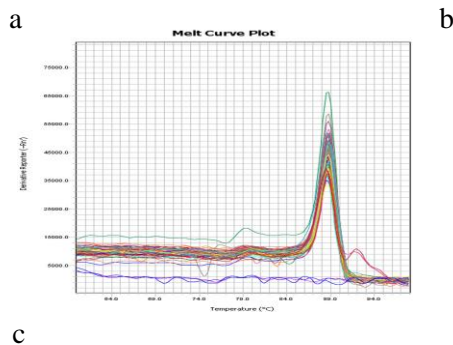
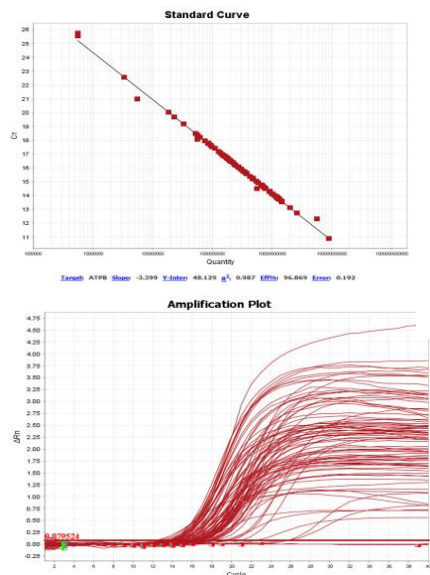
C3.5. RT-qPCR analysis for *atpD*. Results generated a slope = -3.287, $R^2 = 0.982$, efficacy= 101.496%, error = 0.157 and Y-intercept = 45.662, depicted by the standard curve (a), melt curve (b) and amplification plot (c).



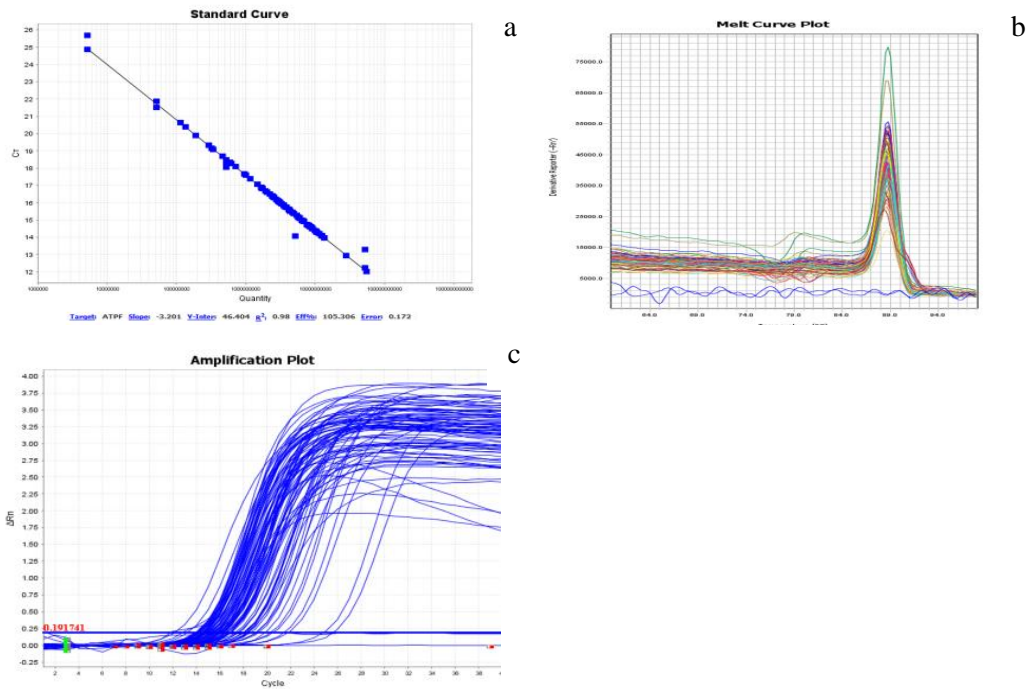
C3.6. RT-qPCR analysis for *Rv2477c*. Results generated a slope = -3.397, $R^2 = 0.982$, efficacy= 96.972%, error = 0.164 and Y-intercept = 46.485, depicted by the standard curve (a), melt curve (b) and amplification plot (c).



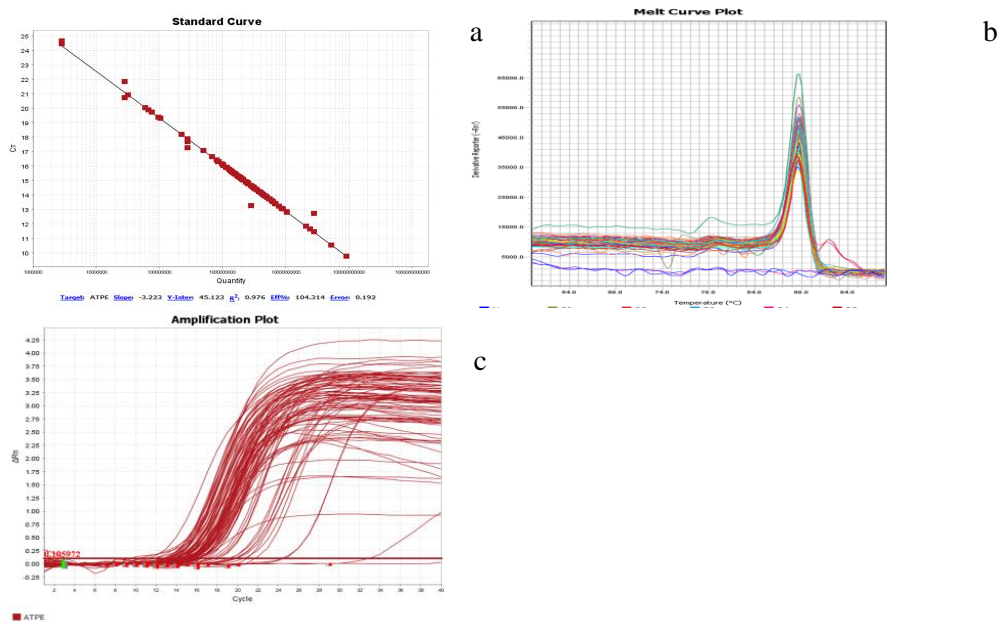
C3.7. RT-qPCR analysis for *16S*. Results generated a slope = -3.286, $R^2 = 0.987$, efficacy= 98.689%, error = 0.156 and Y-intercept = 46.829, depicted by the standard curve (a), melt curve (b) and amplification plot (c).



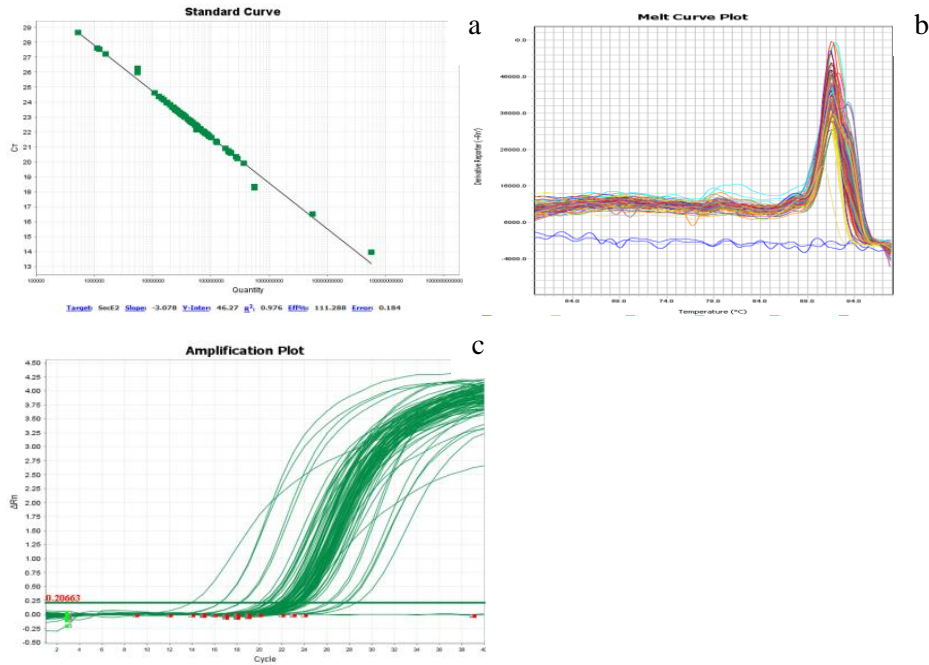
C3.8. RT-qPCR analysis for *atpB*. Results generated a slope = -3.399, $R^2 = 0.987$, efficacy= 98.869%, error = 0.192 and Y-intercept = 48.129, depicted by the standard curve (a), melt curve (b) and amplification plot (c).



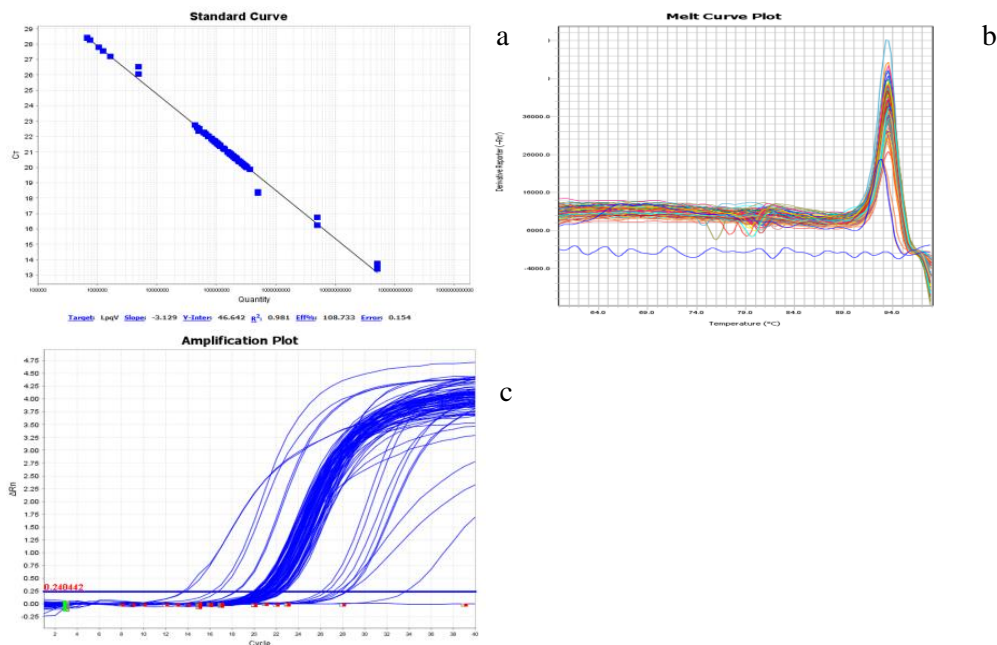
C3.9. RT-qPCR analysis for *atpF*. Results generated a slope = -3.201, $R^2 = 0.9800$, efficacy= 103.306%, error = 0.172 and Y-intercept = 46.404, depicted by the standard curve (a), melt curve (b) and amplification plot (c).



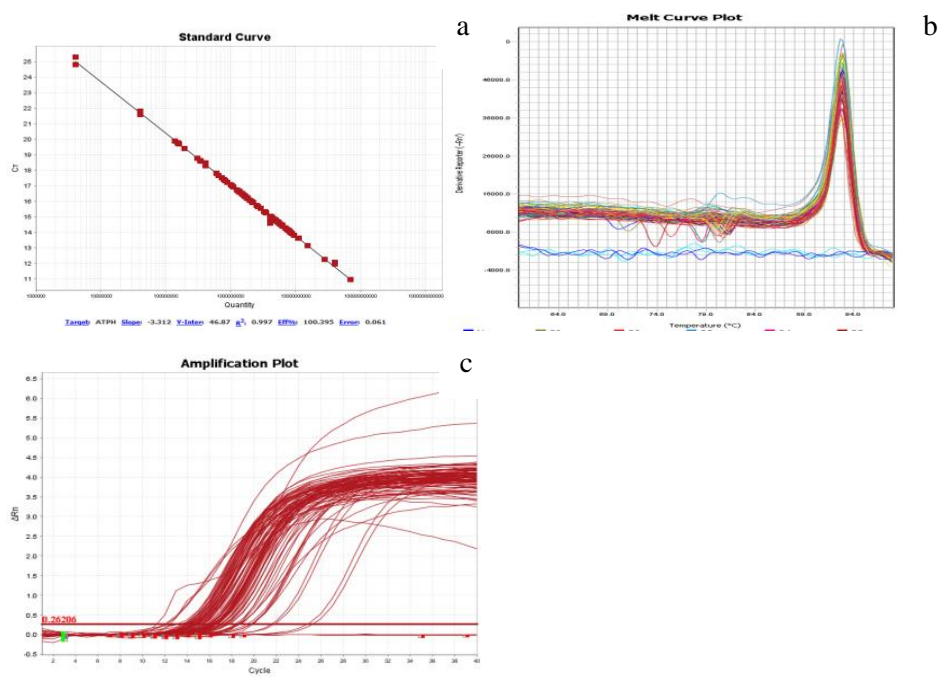
C3.10. RT-qPCR analysis for *atpE*. Results generated a slope = -3.223, $R^2 = 0.9876$, efficacy= 104.314%, error = 0.192 and Y-intercept = 45.123, depicted by the standard curve (a), melt curve (b) and amplification plot (c).



C3.11. RT-qPCR analysis for *secE2*. Results generated a slope = -3.078, $R^2 = 0.9760$, efficacy = 111.288%, error = 0.184 and Y-intercept = 46.27 depicted, by the standard curve (a), melt curve (b) and amplification plot (c).



C3.12. RT-qPCR analysis for *lpqV*. Results generated a slope = -3.129, $R^2 = 0.981$, efficacy = 108.733%, error = 0.154 and Y-intercept = 46.462, depicted by the standard curve (a), melt curve (b) and amplification plot (c).



C3.13. RT-qPCR analysis for *atpH*. Results generated a slope = -3.312, $R^2 = 0.997$, efficacy= 100.395%, error = 0.061 and Y-intercept = 46.87, depicted by the standard curve (a), melt curve (b) and amplification plot (c).

C4. ATP synthase genes used in a comparison of RNA sequencing to RT-qPCR

RNA-sequencing data was further validated by comparing the calculated FC to RT-qPCR, relative to the WT. Graphpad prism was then used to calculate the respective *p*-values.

Table C4.1. RNA- sequencing fold changes for each mutant compared to RT-qPCR fold change, relative to the WT, for ATP synthase genes.

	Δmtp RNA sequencing FC	Δmtp RT-qPCR FC	$\Delta hbhA$ RNA sequencing FC	$\Delta hbhA$ RT-qPCR FC	$\Delta mtp-hbhA$ RNA sequencing FC	$\Delta mtp-hbhA$ RT-qPCR FC
<i>atpH</i>	1,53	1,154	0,933	1,120	0,9333	1,224
<i>atpB</i>	1,492	1,143	1,1059	1,169	1,02	1,195
<i>atpF</i>	1,4339	1,123	0,8709	1,128	0,9673	1,196
<i>atpD</i>	1,343	1,135	0,8535	1,112	0,96	1,760
<i>atpE</i>	1,32	1,089	0,9723	1,077	0,9723	1,144

WT: wild-type; Δmtp : *mtp*-gene knockout mutant; $\Delta hbhA$: *hbhA*-gene knockout mutant; $\Delta mtp-hbhA$: *mtp-hbhA* gene knockout mutant

C5. Bioluminescence raw data

The bioluminescence assay was performed for three biological assays (BA) in triplicate. The average for each sample per BA is shown in Table C13. The average for the three biological assays was calculated for each sample. A control comprising BacTiter-Glo™ Reagent and no sample was used to record the baseline luminescence. Expression levels were recorded in relative light units (RLU), relative to the control, and are shown in Table C13.

Table C5.1. The average bioluminescence absorbance values of three biological assays and the respective expression level (RLU)

	Biological Assay 1	Biological Assay 2	Biological Assay 3	Average	Expression level (RLU)
Control	2.06E+03	2.27E+03	5.16E+03	3.16E+03	
WT	3.99E+06	3.81E+06	3.99E+06	3.93E+06	3.93E+06
<i>Δmtp</i>	2.08E+06	2.14E+06	2.16E+06	2.13E+06	2.12E+06
<i>ΔhbhA</i>	2.03E+06	2.05E+06	2.01E+06	2.03E+06	2.03E+06
<i>Δmtp-hbhA</i>	3.46E+06	3.51E+06	3.21E+06	3.39E+06	3.39E+06
<i>Mtp-complement</i>	2.72E+07	2.69E+07	2.70E+07	2.71E+07	2.71E+07
<i>hbhA-complement</i>	4.90E+06	4.93E+06	5.01E+06	4.95E+06	4.94E+06
<i>Mtp-hbhA-complement</i>	2.58E+07	2.69E+07	2.64E+07	2.64E+07	2.64E+07

Appendix D: Turnitin Reports

Literature Review

ORIGINALITY REPORT

2 %	1 %	1 %	1 %
SIMILARITY INDEX	INTERNET SOURCES	PUBLICATIONS	STUDENT PAPERS

MATCH ALL SOURCES (ONLY SELECTED SOURCE PRINTED)

1%

★ Submitted to University of KwaZulu-Natal

Student Paper

Exclude quotes	Off	Exclude matches	Off
Exclude bibliography	On		

Manuscript, Synthesis, Appendix

ORIGINALITY REPORT

13 %	9 %	10 %	6 %
SIMILARITY INDEX	INTERNET SOURCES	PUBLICATIONS	STUDENT PAPERS

PRIMARY SOURCES

1	Submitted to University of KwaZulu-Natal Student Paper	3 %
2	link.springer.com Internet Source	1 %
3	S. Ashokcoomar, K. S. Reedy, S. Senzani, D. T. Loots, D. Beukes, M. van Reenen, B. Pillay, M. Pillay. "Mycobacterium tuberculosis curli pili (MTP) deficiency is associated with alterations in cell wall biogenesis, fatty acid metabolism and amino acid synthesis", <i>Metabolomics</i> , 2020	<1 %

4	www.mdpi.com Internet Source	<1 %
5	hdl.handle.net Internet Source	<1 %
6	dx.doi.org Internet Source	<1 %
7	mcf.gsfc.nasa.gov Internet Source	<1 %
8	www.repository.cam.ac.uk Internet Source	<1 %
9	V. L. Arcus, J. L. McKenzie, J. Robson, G. M. Cook. "The PIN-domain ribonucleases and the prokaryotic VapBC toxin-antitoxin array", Protein Engineering Design and Selection, 2010 Publication	<1 %
10	Methods in Molecular Biology, 2015. Publication	<1 %
11	journals.lww.com Internet Source	<1 %
12	Anna Kovalchuk, Lilit Nersisyan, Rupasri Mandal, David Wishart, Maria Mancini, David Sidransky, Bryan Kolb, Olga Kovalchuk. "Growth of Malignant Non-CNS Tumors Alters Brain Metabolome", Frontiers in Genetics, 2018 Publication	<1 %
13	orca.cf.ac.uk Internet Source	<1 %
14	K. S. Reedy, D. T. Loots, D. Beukes, M. van Reenen, B. Pillay, M. Pillay. "Mycobacterium tuberculosis curli pili (MTP) is associated with significant host metabolic pathways in an A549 epithelial cell infection model and contributes to the pathogenicity of Mycobacterium tuberculosis", Metabolomics, 2020	<1 %

15	Saiyur Ramsugit, Balakrishna Pillay, Manormoney Pillay. "Evaluation of the role of Mycobacterium tuberculosis pili (MTP) as an adhesin, invasin, and cytokine inducer of epithelial cells", The Brazilian Journal of Infectious Diseases, 2016 Publication	<1%
16	Phuong Chi Nguyen, Van Son Nguyen, Benjamin P. Martin, Patrick Fourquet et al. "Biochemical and Structural Characterization of TesA, a Major Thioesterase Required for Outer-Envelope Lipid Biosynthesis in Mycobacterium tuberculosis", Journal of Molecular Biology, 2018 Publication	<1%
17	www.jneurosci.org Internet Source	<1%
18	Submitted to University of Melbourne Student Paper	<1%
19	www.nature.com Internet Source	<1%
20	parishudh.org Internet Source	<1%
21	Submitted to The University of the West of Scotland	<1%

22	krishikosh.egranth.ac.in Internet Source	<1%
23	Alex Chao, Paul J. Sieminski, Cedric P. Owens, Celia W. Goulding. "Iron Acquisition in ", Chemical Reviews, 2018 Publication	<1%
24	Methods in Molecular Biology, 2014. Publication	<1%
25	Nandakumar, Madhumitha, Carl Nathan, and Kyu Y. Rhee. "Isocitrate lyase mediates broad antibiotic tolerance in Mycobacterium tuberculosis", Nature Communications, 2014. Publication	<1%
26	www.krisp.org.za Internet Source	<1%
27	Elena Silvestri, Federica Cioffi, Daniela Glinni, Michele Ceccarelli et al. "Pathways affected by 3,5-diiodo-L-thyronine in liver of high fat-fed rats: Evidence from two-dimensional electrophoresis, blue-native PAGE, and mass spectrometry", Molecular BioSystems, 2010 Publication	<1%
28	Hironori Mitsuyoshi. "Analysis of hepatic genes involved in the metabolism of fatty acids and iron in nonalcoholic fatty liver disease",	<1%
29	Submitted to Quest International University Perak Student Paper	<1%
30	ro.ecu.edu.au Internet Source	<1%
31	Hai-Feng Huo, Shuai-Jun Dang, Yu-Ning Li. "Stability of a Two-Strain Tuberculosis Model with General Contact Rate", Abstract and Applied Analysis, 2010 Publication	<1%
32	Danielle D. Barnes, Mimmi L. E. Lundahl, Ed C. Lavelle, Eoin M. Scanlan. "The Emergence of Phenolic Glycans as Virulence Factors in ", ACS Chemical Biology, 2017 Publication	<1%

33	Ariany Rosa Gonçalves, Luciana Oliveira Barateli, Ueric José Borges de Souza, Ana Maria Soares Pereira et al. "Development and characterization of microsatellite markers in <i>Stryphnodendron adstringens</i> (Leguminosae)", <i>Physiology and Molecular Biology of Plants</i> , 2020 Publication	<1%
34	academic.oup.com Internet Source	<1%
35	Senthilvelan Manohar, Francesca Yoshie Russo, Gail M. Seigel, Richard Salvi. "Dynamic Changes in Synaptic Plasticity Genes in Ipsilateral and Contralateral Inferior Colliculus Following Unilateral Noise-induced Hearing Loss", <i>Neuroscience</i> , 2020 Publication	<1%
36	spandidos-publications.com Internet Source	<1%
37	Heinz Rupp, Angel Zarain-Herzberg, Bernhard Maisch. "The Use of Partial Fatty Acid Oxidation Inhibitors for Metabolic Therapy of Angina Pectoris and Heart Failure", <i>Herz</i> , 2002 Publication	<1%
38	Elena Faioni, Cristina Razzari, Aida Zulueta, Eti Femia et al. "Bleeding diathesis and gastro-duodenal ulcers in inherited cytosolic phospholipase-A2 alpha deficiency", <i>Thrombosis and Haemostasis</i> , 2017 Publication	<1%
39	theses.gla.ac.uk Internet Source	<1%
40	patents.justia.com Internet Source	<1%
41	Zhuo Fang, Samantha Leigh Sampson, Robin Mark Warren, Nicolaas Claudius Gey van	<1%

42	Submitted to Queensland University of Technology Student Paper	<1 %
43	Submitted to Universiti Sains Malaysia Student Paper	<1 %
44	Taiz, Lincoln. "Plant Physiology & Development", Oxford University Press Publication	<1 %
45	Submitted to KYUNG HEE UNIVERSITY Student Paper	<1 %
46	digital.library.adelaide.edu.au Internet Source	<1 %
47	www.ncbi.nlm.nih.gov Internet Source	<1 %
48	archive.epa.gov Internet Source	<1 %
49	Gopal Ganesh, Thallampuranam Krishnaswamy S Kumar, Shanmugiah Thevar Karutha Pandian, Chin Yu. "Rapid staining of proteins on polyacrylamide gels and nitrocellulose membranes using a mixture of fluorescent dyes", Journal of Biochemical and Biophysical	<1 %
50	ujcontent.uj.ac.za Internet Source	<1 %
51	actaneurocomms.biomedcentral.com Internet Source	<1 %
52	www.frontiersin.org Internet Source	<1 %
53	journals.tubitak.gov.tr Internet Source	<1 %
54	"Laboratory Procedures in Clinical Microbiology", Springer Science and Business Media LLC, 1981 Publication	<1 %
55	pub.epsilon.slu.se Internet Source	<1 %
56	koofers.com Internet Source	<1 %

57	Elena G. Salina, Artem Grigorov, Yulia Skvortsova, Konstantin Majorov et al. " MTS1338, a small RNA, regulates transcriptional shifts consistent with bacterial adaptation for entering into dormancy and survival within host macrophages ", Cold Spring Harbor Laboratory, 2019 Publication	<1%
58	Submitted to Glasgow Caledonian University Student Paper	<1%
59	Flavia Squeglia, Alessia Ruggiero, Alfonso De Simone, Rita Berisio. "A structural overview of mycobacterial adhesins: Key biomarkers for diagnostics and therapeutics", Protein Science, 2018 Publication	<1%
60	biotechnologyforbiofuels.biomedcentral.com Internet Source	<1%
61	"Laboratory Procedures in Clinical Microbiology", Springer Science and Business Media LLC, 1985 Publication	<1%
62	freidok.uni-freiburg.de Internet Source	<1%
63	Xinhua Huang, Hui Wang, Lu Meng, Qinglan Wang, Jia Yu, Qian Gao, Decheng Wang. "Role of eosinophils and apoptosis in PDIMs/PGLs deficient mycobacterium elimination in adult zebrafish", Developmental & Comparative Immunology, 2016 Publication	<1%
64	www.researchsquare.com Internet Source	<1%

65	epdf.pub Internet Source	<1%
66	"Posters", <i>Clinical Microbiology and Infection</i> , 5/2008 Publication	<1%
67	Perlin, D.S.. "Resistance to echinocandin-class antifungal drugs", <i>Drug Resistance Updates</i> , 200706 Publication	<1%
68	doi.org Internet Source	<1%
69	ueaeprints.uea.ac.uk Internet Source	<1%
70	Kap Lim, Randy J. Read, Celia C. H. Chen, Aleksandra Tempczyk et al. " Swiveling Domain Mechanism in Pyruvate Phosphate Dikinase ", <i>Biochemistry</i> , 2007 Publication	<1%
71	onlinelibrary.wiley.com Internet Source	<1%
72	core.ac.uk Internet Source	<1%
73	www.dovepress.com Internet Source	<1%
	denniskunkel.com	
74	Internet Source	<1%
75	Melissa S. Pischke, Edward L. Huttlin, Adrian D. Hegeman, Michael R. Sussman. "A Transcriptome-Based Characterization of Habituation in Plant Tissue Culture", <i>Plant Physiology</i> , 2006 Publication	<1%
76	Srivastava, V.. "Selection of genes of <i>Mycobacterium tuberculosis</i> upregulated during residence in lungs of infected mice", <i>Tuberculosis</i> , 200805 Publication	<1%
77	Mihaela Pertea, Daehwan Kim, Geo M Pertea, Jeffrey T Leek, Steven L Salzberg. "Transcript-level expression analysis of RNA-seq experiments with HISAT, StringTie and Ballgown", <i>Nature Protocols</i> , 2016 Publication	<1%